THE TRANSCRIPTIONAL REGULATION OF CELL DEFENCE AND ITS ROLE IN PROTECTION AGAINST DRUG-INDUCED LIVER INJURY

Thesis submitted in accordance with the requirements of the University of Liverpool for the degree of Doctor of Philosophy

Ian Mathew Copple

February 2008

DECLARATION

This thesis is the result of my own work. The material contained within this thesis has not been presented, nor is currently being presented, either wholly or in part for any other degree or qualification.

Ian Mathew Copple.

This research was carried out in the Department of Pharmacology and Therapeutics, School of Biological Science, at The University of Liverpool.

CONTENTS

ABSTRACT

Adverse drug reactions constitute a major cause of patient morbidity and mortality, and are important factors in drug attrition within the pharmaceutical industry. Some adverse drug reactions are inextricably linked to the process of drug metabolism, through the generation of chemically reactive intermediates. The hepatotoxicity associated with overdose of paracetamol is a pertinent example of an adverse drug reaction that is linked to the generation of an electrophilic metabolite, N-acetyl-*p*-benzoquinoneimine (NAPQI). This molecule binds covalently to specific hepatic proteins and inhibits their function, contributing to liver failure. Mammalian cells have evolved a multi-faceted, highly regulated defence system, which affords protection against chemical and oxidative stress. By far the most important regulator of inducible cell defence is the transcription factor Nrf2, which controls the expression of numerous genes involved in the detoxification of electrophiles and reactive oxygen species, the maintenance of cellular redox balance, and the degradation of damaged/misfolded proteins. In the absence of cellular stress, Nrf2 is restrained in the cytosol and repressed by the cysteine-rich protein Keap1. The main aims of the studies presented in this thesis were to further our understanding of the means by which the Nrf2 pathway is regulated, and to explore its role in the protection against drug-induced liver injury (DILI).

Previous work in this laboratory has demonstrated that the Nrf2 pathway is activated in mouse liver following administration of hepatotoxic and non-hepatotoxic doses of paracetamol. It has been proposed that the molecular trigger for activation of Nrf2 by electrophiles is the modification of cysteine residues within Keap1, which inhibits the repressive activity of Keap1 towards Nrf2. In order to test the hypothesis that the modification of Keap1 by NAPQI may play a role in the activation of Nrf2 observed in mouse liver following administration of paracetamol, a series of experiments were performed using the mouse hepatoma cell line Hepa-1c1c7. RNA interference (RNAi), directed against Nrf2 and Keap1, was used to validate Hepa-1c1c7 as a suitable model for studying the Nrf2 pathway. Using immunofluorescence confocal microscopy and luciferase reporter transgene analysis, NAPQI was shown to directly activate the Nrf2 pathway in Hepa-1c1c7 cells. Activation of the Nrf2 pathway was shown to correlate with the induction of cell defence, as demonstrated by a time-dependent increase in levels of glutathione (GSH). By using a combination of RNAi and quantitative real-time PCR, the increase in GSH was shown to be caused by an Nrf2-dependent induction of Gclc, the Nrf2-regulated rate-limiting enzyme in the synthesis of GSH. In order to explore the importance of cysteine reactivity in the activation of Nrf2 by NAPQI, the activity of the transcription factor was assessed following exposure of Hepa-1c1c7 cells to the model cysteine-reactive electrophiles 2,4-dinitrochlorobenzene (DNCB) and 15-deoxy-Δ-$^{(12,14)}$-prostaglandin J_2 (15d-PGJ_2), and the lysine-reactive molecule trimellitic anhydride (TMA). Both DNCB and 15d-PGJ_2 invoked a concentration-dependent increase in nuclear levels of Nrf2, as measured by Western blot. In contrast, TMA had no effect on the nuclear level of Nrf2, indicating that cysteine reactivity is an important property of Nrf2-activating molecules, and that this may underlie the ability of NAPQI to induce Nrf2-dependent cell defence. Although Nrf2 activation was observed

concomitantly with the depletion of GSH for NAPQI and DNCB, this was not a prerequisite for activation of the transcription factor, as 15d-PGJ_2 stimulated the nuclear accumulation of Nrf2 without having any apparent effect on cellular GSH levels.

In order to further explore the possibility that NAPQI activates the Nrf2 pathway through direct modification of cysteine residues in Keap1, an *in vitro* test system was developed, based on the expression and purification of recombinant Keap1 protein, and the analysis of residue-specific modification(s) by liquid chromatography electrospray ionization tandem mass spectrometry (LC-ESI-MS/MS). All three Nrf2-activating molecules, NAPQI, DNCB and 15d-PGJ_2, selectively modified cysteine residues in Keap1 *in vitro*. TMA, which did not activate Nrf2, modified lysines, but not cysteines, within Keap1. Although no single cysteine residue was found to be preferentially modified by NAPQI, DNCB and 15d-PGJ_2, all three molecules did modify one or more cysteines within the central intervening region (IVR) of Keap1. A cell-based method for analysing Keap1 modification was then developed, so as to enable the examination of Keap1 modification, in tandem with Nrf2 activation, within a more biologically-relevant cellular context. Immunoprecipitation of endogenous Keap1 was attempted, however the levels of Keap1 that were purified were too low to enable reliable LC-ESI-MS/MS analysis. Therefore, HEK293T cells were transfected with an expression vector for Keap1 tagged with a V5 epitope. The ectopic expression of Keap1-V5 was shown not to compromise the responsiveness of the Nrf2 pathway to electrophiles. By using a combination of immunoaffinity purification and LC-ESI-MS/MS analysis, the residue-selective modification of Keap1-V5 was demonstrated following exposure of HEK293T cells to NAPQI, DNCB and 15d-PGJ_2. No single cysteine residue was universally modified, although, as in the *in vitro* experiments, all three Nrf2-activating molecules modified one or more cysteines within the IVR domain of Keap1-V5.

In summary, the results presented in this thesis have demonstrated that NAPQI can directly activate the Nrf2-ARE cell defence pathway in mouse liver cells, and selectively modifies cysteines residues within Keap1, both in the recombinant protein *in vitro* and in a cell-based model. This work has also identified a potential unifying mechanism by which Nrf2 activation is triggered; through the direct modification of one or more cysteines within the IVR domain of Keap1. In future studies, it will be important to determine whether this mechanism applies to all Nrf2-activating molecules, and to explain how the modification of cysteines in Keap1 is translated into the activation of Nrf2.

ACKNOWLEDGEMENTS

First and foremost, I would like to thank my supervisors Prof. Kevin Park and Dr. Chris Goldring for their steady guidance and support over the course of this PhD. I have learnt an immense amount over the past three years, about science and myself, and a great deal of this is due to your much-valued input. Thank you.

I am also very grateful to Dr. Neil Kitteringham for his continual advice and interest in my work, Alvin Chia for his help in setting up the RNAi experiments, and Dr. Roz Jenkins; your expert assistance with all things proteomic (particularly the somewhat temperamental QSTAR!) is very much appreciated. Thank you also to Jan Lampard, Pete Metcalfe and Phill Roberts for technical, and sometimes non-technical, assistance.

To all of the members of the Drug Safety Research Group, particularly Adam, Alvin, Amy, Charlotte, Dan, Dean, Emma, Jayne, Haiyi, Laura, Luke, Rachel, Rowena, Rym, Sam, Sophie and Vicki, many thanks for your collaboration, help, advice, friendship, and, perhaps most importantly, for lending me endless numbers of reagents. I cannot guarantee that I will return all of them! I would also like to acknowledge the financial support of The University of Liverpool, the Wellcome Trust and Pfizer Ltd.

Finally, I would like to thank my friends and family, particularly Mum, Dad and Alex, for their constant encouragement and support, not only over the past three years, but throughout my life. And yes, this does mean I'll be getting a proper job now!

PUBLICATIONS

Papers

Copple, I.M., Goldring, C.E., Jenkins, R.E., Chia, A.J., Randle, L.E., Kitteringham, N.R., Hayes, J.D. & Park, B.K. The hepatotoxic metabolite of acetaminophen directly activates the Keap1-Nrf2-ARE cell defence system. *Manuscript in preparation.*

Copple, I.M., Goldring, C.E., Kitteringham, N.R. & Park, B.K. The Nrf2-Keap1 defence pathway: role in protection against drug-induced toxicity (2008). *Toxicology,* 246, 24-33.

Liu, X.P., Goldring, C.E., Wang, H.Y., **Copple, I.M.**, Kitteringham, N.R., Park, B.K. & Wei, W. Extract of Ginkgo biloba induces glutamate cysteine ligase catalytic subunit (GCLC) (2008). *Phytother. Res.*, 22, 367-371.

Liu, X.P., Goldring, C.E., **Copple, I.M.**, Wang, H.Y., Wei, W., Kitteringham, N.R. & Park, B.K. (2007) Extract of Ginkgo biloba induces phase 2 genes through Keap1-Nrf2-ARE signaling pathway. *Life Sci.,* 80, 1586-1591.

Goldring, C.E., Kitteringham, N.R., Jenkins, R.E., **Copple, I.M.,** Jeannin, J-F. & Park, B.K. (2006) Plasticity in cell defense: access to and relative reactivity of critical protein residues and DNA response elements. *J. Exp. Biol.,* 209, 2337-2343.

Abstracts

Copple, I., Goldring, C., Jenkins, R., Kitteringham, N. & Park, K. (2006). Activation of the Nrf2/ARE antioxidant pathway by N-acetyl-*p*-benzoquinoneimine (NAPQI). *Drug Metab. Rev.,* 38 Suppl. 1, 49.

ABBREVIATIONS

αCHCA;	α-cyano-4-hydroxy-cinnamic acid
ACN;	acetonitrile
AKR;	aldo-keto reductase
amu;	atomic mass units
ANOVA;	analysis of variance
AP-1;	activator protein 1
APAF-1;	apoptotic protease activating factor 1
ARE;	antioxidant response element
ASK1;	apoptosis signal-regulating kinase 1
ATF;	activating transcription factor
β_2M;	β_2-microglobulin
BACH1;	BTB and CNC homolog 1
BCA;	bicinchoninic acid
BLAST;	basic local alignment search tool
bp;	base pair
BSA;	bovine serum albumin
BTB;	bric-a-brac/tram-track/broad complex
bZip;	basic leucine zipper
cAMP;	cyclic adenosine monophosphate
CBP;	CREB-binding protein
cDNA;	complementary DNA
CMV;	cytomegalovirus
CNC;	cap 'n' collar
CO_2;	carbon dioxide
COOH;	carboxyl
COX2;	cyclooxygenase 2
CRE;	cAMP-responsive element
CREB;	cAMP responsive element binding protein
Cu;	copper
CUL3;	Cullin 3
CYP450;	cytochrome P450
Cys;	cysteine
dex-mes;	dexamethasone 21-mesylate
DGR;	double glycine repeat
dH_2O;	distilled H_2O
DILI;	drug-induced liver injury
DMEM;	Dulbecco's modified Eagle's medium
DMSO;	dimethyl sulphoxide
DNA;	deoxyribonucleic acid
DNCB;	2,4-dinitrochlorobenzene
DNFB;	2,4-dinitrofluorobenzene

dNTP;	deoxyribonucleotide triphosphate
15d-PGJ$_2$;	15-deoxy-$\Delta^{12,14}$-prostaglandin J$_2$
DPP3;	dipeptidyl-peptidase 3
dsRNA;	double stranded RNA
DTNB;	5,5′-dithiobis(2-nitrobenzoic acid)
DTT;	dithiothrietol
ECH;	erythroid cell-derived protein with CNC homology
EDTA;	ethylenediaminetetraacetic acid
ERK-1;	extracellular signal-regulated kinase 1
FasL;	Fas ligand
FBS;	fetal bovine serum
GCL;	γ-glutamylcysteine ligase
GCLC;	GCL, catalytic subunit
GCLM;	GCL, regulatory subunit
GPX;	GSH peroxidase
GS;	GSH synthetase
GSH;	glutathione
GSR;	GSH reductase
GSSG;	oxidised GSH
GST;	GSH S-transferase
GSTP1-1;	GST subunit P1-1
H_2O;	water
H_2O_2;	hydrogen peroxide
HAT;	histone acetyltransferase
HEPES;	4-(2-hydroxyethyl)-1-piperazineethanesulfonic acid
HIF-1;	hypoxia-inducible factor 1
6xHis;	polyhistidine
HIV;	human immunodeficiency virus
HO-1;	heme oxygenase 1
HRP;	horseradish peroxidase
HSF;	heat shock factor
HSP;	heat shock protein
ICAD;	inhibitor of caspase-activated DNAse
IκB;	inhibitor of κB
IKK;	IκB kinase
IL;	interleukin
iNOS;	inducible nitric oxide synthase
IPTG;	isopropyl-β-D-thiogalactopyranoside
IVR;	intervening region
kDa;	kiloDalton
Keap1;	Kelch-like ECH-associated protein 1

LC-ESI-MS/MS;	liquid chromatography electrospray ionisation MS/MS
LDH;	lactate dehydrogenase
Lys;	lysine
MALDI-TOF MS;	matrix-assisted laser desorption ionisation time-of-flight mass spectrometry
MAPK;	mitogen-activated protein kinase
MEH;	microsomal epoxide hydrolase
Mn;	manganese
MOPS;	3-(N-morpholino)propanesulfonic acid
mRNA;	messenger RNA
MS/MS;	tandem mass spectrometry
m/z;	mass-to-charge ratio
NADPH;	nicotinamide adenine dinucleotide phosphate
NAPQI;	N-acetyl-*p*-benzoquinoneimine
Neh;	Nrf2-ECH homology
NEM;	N-ethylmaleimide
NES;	nuclear export signal
NF-E2;	nuclear factor erythroid 2
NF-κB;	nuclear factor κB
NH_2;	amine
NHS;	National Health Service
Ni^{2+};	nickel
NLS;	nuclear localisation signal
NQO1;	NAD(P)H:quinone oxidoreductase 1
Nrf2;	NF-E2 -related factor 2
NSAID;	non-steroidal anti-inflammatory drug
OD_{600nm};	optical density at 600 nm
OH;	hydroxyl
O_2;	molecular oxygen
$O_2^{\cdot-}$;	superoxide anion radical
PAPS;	phosphoadenosine phosphosulphate
PARP;	poly (adenosine diphosphate-ribose) polymerase
PBS;	phosphate-buffered saline
PCR;	polymerase chain reaction
PERK;	protein kinase R-like endoplasmic reticulum kinase
pI;	isoelectric point
PI3K;	phosphatidyl inositol 3-kinase
pKa;	acid dissociation constant
PKC;	protein kinase C
PMA;	phorbol 12-myristate-13-acetate
PRX;	peroxiredoxin
REF-1;	redox effector factor 1

RIPA;	radioimmunoprecipitation assay
RNA;	ribonucleic acid
RNAi;	RNA interference
ROS;	reactive oxygen species
rpm;	revolutions per minute
S^-;	thiolate
SD;	standard deviation of the mean
SH;	sulphydryl
siRNA;	short interfering RNA
S_N2;	bimolecular nucleophilic substitution
SNO;	S-nitrosothiol
SNO_2;	S-nitrothiol
SOD;	superoxide dismutase
SOH;	sulphenic acid
SO_2H;	sulphinic acid
SO_3H;	sulphonic acid
S-S;	disulphide
ST;	sulphotransferase
Std;	standard
SV40;	simian virus 40
tBHQ;	*tert*-butylhydroquinone
TBS;	tris-buffered saline
TFA;	trifluoroacetic acid
TMA;	trimellitic anhydride
TNB;	5-thio-2-nitrobenzoic acid
TNF-α;	tumour necrosis factor α
TNF-R;	TNF receptor
TPA;	12-O-tetradecanoate-13-acetate
TRE;	TPA-responsive element
TRX;	thioredoxin
TRX-R;	TRX reductase
Tyr;	tyrosine
U;	unit
UDPGA;	uridine diphosphate glucuronic acid
UGT;	UDP-glucuronosyltransferases
UK;	United Kingdom
USA;	United States of America
UV;	ultraviolet
v/v;	volume/volume
w/v;	weight/volume
Zn;	zinc

CHAPTER 1

General Introduction

CONTENTS

1.1 INTRODUCTION

Adverse drug reactions, i.e. any undesirable effect of a drug outside of its intended therapeutic action (Pirmohamed *et al.*, 1998), constitute a major cause of patient morbidity and mortality, and are important factors in drug attrition within the pharmaceutical industry (Park *et al.*, 2005b). It is, therefore, imperative that advances in our understanding of the chemical, biochemical and molecular mechanisms that underlie specific adverse reactions translate into the 'designing out' of toxicity and the development of safer, more effective medicines.

From a mechanistic perspective, at least, adverse drug reactions can be considered as pharmacological, immunological and/or chemical in nature. Although generally beneficial, drug metabolism, the physiological process by which a foreign chemical (xenobiotic) is biotransformed and eliminated from the body, can, in some cases, be inextricably linked to toxicity, through the generation of chemically reactive intermediates (for a review, see Park, 1986); the hepatotoxicity associated with overdose of paracetamol being a pertinent example. Paracetamol is bioactivated to an electrophilic metabolite, N-acetyl-*p*-benzoquinoneimine (NAPQI), which binds covalently to specific hepatic proteins and inhibits their function, contributing to liver failure (for a review, see Zhou *et al.*, 2005).

The liver, as the major site of drug metabolism, is at relatively high risk of exposure to toxic species generated through metabolic bioactivation, and thus is a major target for tissue-specific toxicity, or drug-induced liver injury (DILI) (Park *et al.*, 1995). However, as with other mammalian tissues, the liver has evolved a multi-faceted, highly regulated cell defence system. At the forefront of this system is a group of specialised proteins, known as transcription factors. Through their ability to 'sense' cellular stress and induce adaptive responses, characterised by the upregulated expression of a multitude of genes encoding detoxification enzymes and antioxidants (Prestera *et al.*, 1993b; Primiano *et al.*, 1997), transcription factors play a major role in governing the protection against drug-induced toxicity. By far the most important regulator of inducible, and perhaps

basal, cell defence is the transcription factor Nrf2 (for a review, see Jaiswal, 2004). Through a pathway that also involves the thiol-rich cytosolic repressor protein Keap1, Nrf2 controls the expression of numerous genes involved in the detoxification of electrophiles and reactive oxygen species, the maintenance of cellular redox balance, and the degradation of damaged/misfolded proteins (Jaiswal, 2004).

An appreciation of the molecular mechanisms that underlie the adaptive response to cellular stress, primarily regulated by the Nrf2 pathway, is vital to gain insights into the signalling events that determine the progression, and outcome, of adverse drug reactions such as DILI. Therefore, this thesis aims to further our understanding of the means by which the Nrf2 pathway is regulated, and to elucidate its role in the protection against DILI.

1.2 ADVERSE DRUG REACTIONS

Adverse drug reactions constitute a major cause of patient morbidity and mortality (Park *et al.*, 2005a). Indeed, in a recent prospective analysis of 18,820 hospital admissions across two Merseyside National Health Service (NHS) Trusts, during a six month period between 2002 and 2003, adverse drug reactions, or related incidents, accounted for 1225 (6.5 %) admissions, with 72 % of these incidents classified as 'avoidable' by clinicians (Pirmohamed *et al.*, 2004). Of patients admitted with an adverse reaction during this study, 28 (2.3 %) died as a direct result of the reaction (Pirmohamed *et al.*, 2004). Due to the time and cost associated with treating patients, adverse drug reactions place an estimated £466 million burden on the NHS per year (Pirmohamed *et al.*, 2004). Furthermore, adverse drug reactions have been responsible for the withdrawal of 4 % of all drugs licensed in the United Kingdom (UK) between 1974 and 1994 (Jefferys *et al.*, 1998). Hence, adverse drug reactions pose a significant public health problem.

From a clinical perspective, adverse drug reactions can be grouped into five main categories (Table 1.1), although these are not mutually exclusive, and a particular

reaction may have characteristics of more than one subtype (Park *et al.*, 1995). From a chemico-pharmacological point of view, adverse drug reactions can simply be regarded as on-target, i.e. those that are predictable from the known primary or secondary pharmacology of the drug, or off-target, i.e. those that are not predictable from a knowledge of the basic pharmacology of the drug, often exhibiting marked inter-individual variability in the degree of susceptibility (Liebler *et al.*, 2005).

Type	Features	Example
A	*Augmented;* predictable from the known pharmacology of the drug, often represent an exaggeration of the pharmacological effect, usually dose-dependent	Hypotension with anti-hypertensives, haemorrhage with anti-coagulants
B	*Bizarre;* idiosyncratic, not predictable from the basic pharmacology of the drug, no simple dose-response relationship, host-dependent metabolic/immunological factors may contribute to, and determine, individual susceptibility	Hepatitis with halothane, hypersensitivity with anti-convulsants
C	*Chemical;* can be predicted or rationalised from the chemical structure of the drug or metabolite	Hepatotoxicity with paracetamol
D	*Delayed;* occur some time, even years, after treatment, include teratogenic effects seen in children following drug intake by the mother during pregnancy	Foetal hydantoin syndrome with phenytoin, phocomelia with thalidomide
E	*End-of-treatment;* occur upon drug withdrawal, especially when treatment is stopped suddenly	Withdrawal syndrome upon stopping paroxetine, withdrawal seizures upon stopping phenytoin

Table 1.1 - Clinical classification of adverse drug reactions. Features and examples of type A-E adverse drug reactions. Adapted from Park *et al.* (1998).

1.3 DRUG METABOLISM

In general terms, drug metabolism is the process by which a xenobiotic undergoes enzymatic conversion from a non-polar, lipophilic compound that is readily absorbed via the gastrointestinal tract, to a polar, hydrophilic species (Hodgson *et al.*, 2001). Typically, the net result of this process is the elimination of the molecule from the body

in urine, and thus an eventual loss of pharmacological activity. Conventionally, drug metabolism is divided into two phases; functionalisation (phase I) and conjugation (phase II) (Williams, 1959). Typically phase I and II metabolic reactions occur sequentially. However, phase I metabolism is not a pre-requisite for phase II conjugation, providing a suitable functional group is present in the parent compound (Timbrell, 2002).

1.3.1 Phase I metabolism

Phase I metabolic reactions generally involve oxidation, reduction, hydrolysis or hydration of the parent molecule, and result in the exposure or introduction of a functional group (Gibson *et al.*, 2001). The majority of oxidative phase I reactions are catalysed by the cytochrome P450 (CYP450) monooxygenase system, which comprises a superfamily of enzymes located predominantly in the smooth endoplasmic reticulum (Timbrell, 2002). The CYP450 enzymes evolved 400-500 million years ago, to enable animals to detoxify foreign chemicals ingested through plant matter (Gonzalez *et al.*, 1994). Of the numerous sub-families, CYP1, CYP2 and CYP3 are predominantly involved in xenobiotic metabolism (Gibson *et al.*, 2001). Although CYP450-catalysed oxidation involves a complex biochemical cycle, the overall outcome is straightforward; the transfer of one atom of oxygen (from molecular oxygen, O_2) to the drug to form a hydroxyl group (-OH), with the remaining oxygen atom converted to water (H_2O) (Gibson *et al.*, 2001). Other enzymes that catalyse oxidative reactions include flavin-containing monooxygenases, alcohol dehydrogenase and monoamine oxidase, which metabolise nicotine, ethanol and noradrenaline, respectively (Hodgson *et al.*, 2001). Of the less common non-oxidative phase I reactions, reduction, an important route of metabolism for azo- and nitro-compounds, epoxides and quinones, is catalysed by reductases (Gibson *et al.*, 2001). Esterases and amidases catalyse the hydrolysis of esters and amides, respectively, and the hydration of epoxides is catalysed by epoxide hydrolase (Gibson *et al.*, 2001). Individuals that are deficient in phase I metabolising capacities may be susceptible to 'on-target' adverse drug reaction, where diminished

clearance of the parent drug may lead to augmentation of the intended pharmacological effect. For example, patients carrying polymorphisms in the gene encoding CYP2C9, which is responsible for the phase I hydroxylation of the *S*-enantiomer of the anticoagulant warfarin, demonstrate a reduced ability to metabolise the parent drug, and thus are at high risk of haemorrhage should they receive a 'normal' dose (Wadelius *et al.*, 2007). As a result, patients with variant genotypes require a reduction in the prescribed dose in order to benefit from the anti-coagulant effects of warfarin without an increased risk of bleeding (Wadelius *et al.*, 2007).

1.3.2 Phase II metabolism

Phase II reactions are characterised by the conjugation of a substituent polar group onto a functionalised molecule. Such groups include glucuronyl, sulphate, acetyl, and glutathione (GSH). Glucuronylation, a major route of metabolism for alcohols, phenols, carboxylic acids, amines and thiols, involves the transfer of uridine diphosphate glucuronic acid (UDPGA) to a nucleophilic group, such as hydroxyl, carboxyl (-COOH), amine ($-NH_2$) or sulphydryl (-SH) (Gibson *et al.*, 2001). Catalysed by glucuronosyl transferases (UGT), the glucuronylation pathway has a relatively high capacity, due to the high tissue abundance of the co-factor UDPGA (Gibson *et al.*, 2001). Sulphation, catalysed by sulphotransferases (ST), involves the transfer of phosphoadenosine phosphosulphate (PAPS) to nucleophilic hydroxyl and amine groups, particularly in phenols and alcohols (Gibson *et al.*, 2001). Due to the relative low abundance of PAPS, sulphation is a low-capacity phase II pathway (Gibson *et al.*, 2001). The N-acetyl transferase family catalyses acetylation, the transfer of acetyl coenzyme A to amine groups (Gibson *et al.*, 2001). Acetylation is an important metabolic pathway for aromatic amines, sulphonamides and hydrazines (Timbrell, 2002). Conjugation with GSH is an important route of metabolism for a number of xenobiotics, including epoxides, alkenes and aromatic nitro-compounds (Timbrell, 2002). In addition to its physiological role in xenobiotic metabolism, GSH, as the most abundant non-protein thiol, present at millimolar concentrations in most cells, also acts as a major antioxidant

(for a review, see Kaplowitz *et al.*, 1985). The conjugation of GSH to reactive species, which can proceed non-enzymatically or via a glutathione S-transferase (GST) - catalysed reaction, is an important means of detoxifying electrophilic molecules. The nucleophilic cysteine thiol of GSH attacks an electrophilic moiety, forming a thioether bond between the two molecules (Timbrell, 2002). The resulting polar conjugate is then excreted in bile (Timbrell, 2002). Section 1.5.1.2 further details the role of GSH in cell defence.

1.3.3 The role of drug metabolism in adverse drug reactions

In general, the functionalisation of a xenobiotic, via phase I metabolic biotransformation, provides a handle for phase II conjugation reactions. However, this process may also result in bioactivation to yield an intermediate species that is more reactive towards cellular macromolecules and, in turn, is more toxic than the parent compound (Park, 1986). The propensity of a parent drug to form a reactive intermediate is a function of its chemistry, with structural 'alerts' now well defined; examples include epoxides, quinones, hydroxylamines and furans (Park *et al.*, 2005a). The balance between bioactivation and detoxification is a critical determinant of the risk of reactive intermediate-induced toxicity (Fig. 1.1).

Phase II conjugation reactions and other intrinsic bioinactivation pathways provide a means of detoxifying reactive phase I products. However, saturation of these detoxification pathways may enable the concentration of reactive intermediates, which consequently may interact with, and damage, critical macromolecules, such as proteins and nucleic acids. In this regard, the process of drug metabolism can be inextricably linked to certain adverse drug reactions (Park, 1986; Zhou *et al.*, 2005). For instance, compounds that inhibit the CYP450-mediated bioactivation of the non-steroidal anti-inflammatory drug (NSAID) paracetamol to its electrophilic metabolite NAPQI prevent its hepatotoxicity (Brady *et al.*, 1988; Mitchell *et al.*, 1973; Roberts *et al.*, 1986). Furthermore, CYP2E1 knockout mice are protected against (Lee *et al.*, 1996), whereas

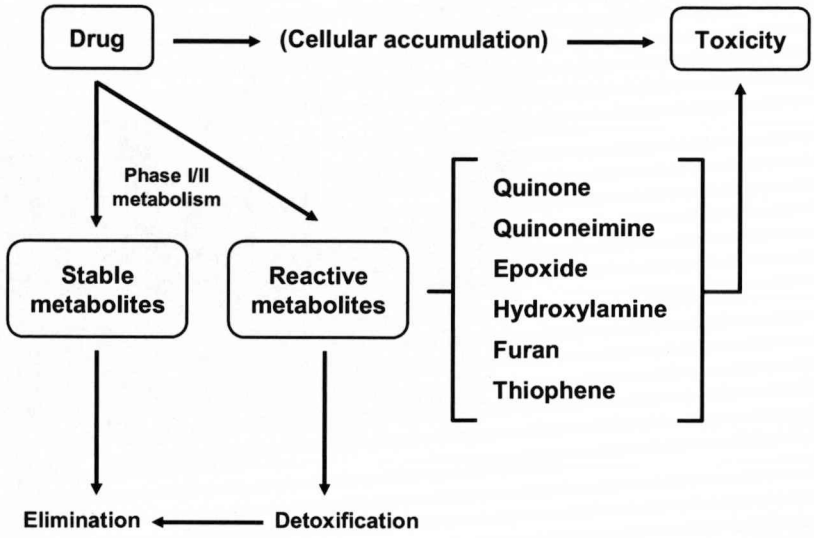

Figure 1.1 - The role of drug metabolism in adverse drug reactions. The metabolic biotransformation of drugs can, in some instances, lead to the formation of chemically reactive intermediates including quinones, epoxides and thiophenes. Unless detoxified, these intermediates may cause toxicity, often via the process of covalent binding to critical macromolecules, such as DNA and proteins.

induction of CYP2E1 increases susceptibility to (Burk *et al.*, 1990; Chien *et al.*, 1997; Thummel *et al.*, 2000), paracetamol-induced liver injury. Hence, the hepatotoxicity associated with overdose of paracetamol is a pertinent example of a bioactivation-related adverse drug reaction. A more detailed discussion of paracetamol-induced hepatotoxicity is presented in section 1.4.1. Phase II biotransformations, although typically regarded as bioinactivation reactions, may themselves yield toxic intermediates (Zhou *et al.*, 2005). For example, glucuronosyl transferases catalyse the conversion of carboxylic acid drugs, including certain NSAIDs, to electrophilic acyl glucuronides, that bind covalently to plasma and hepatic proteins (Ritter, 2000). Thus, drug metabolism can represent a double-edged sword; although generally a favourable process responsible for the elimination of foreign chemicals from the body, in certain circumstances, metabolic biotransformations may generate reactive species that pose a significant threat to cellular homeostasis.

1.4 DRUG-INDUCED LIVER INJURY (DILI)

Adverse drug reactions can have many different pathological manifestations, affecting any part of the body. However, as the liver is quantitatively the most important site of drug metabolism and, thus, bioactivation, it is a major target for tissue-specific toxicity, or DILI (Park *et al.*, 1995). In fact, DILI is the most common reason for the withdrawal of a drug from the market following initial regulatory approval (Temple *et al.*, 2002), with more than 600 drugs having been linked to hepatotoxicity (Park *et al.*, 2005a). Furthermore, DILI accounts for more than half of all cases of acute liver failure (Lee, 2003). As DILI mimics natural disease, an increased understanding of the pathogenesis of DILI will enable advances in both drug safety and the treatment of natural liver disorders, such as cirrhosis and hepatitis (Park *et al.*, 2005a).

1.4.1 Paracetamol hepatotoxicity

Paracetamol is a commonly-used analgesic and antipyretic, the pharmacological activity of which is thought to stem from the inhibition of cyclooxygenase activity and consequent reduction of prostaglandin synthesis (Botting, 2000a; Botting, 2000b; Boutaud *et al.*, 2002; Greco *et al.*, 2003; Hinz *et al.*, 2008; Sciulli *et al.*, 2003). The hepatotoxicity associated with overdose of paracetamol is the single biggest cause of acute liver failure in both the UK (Davern *et al.*, 2006) and United States of America (USA) (Larson *et al.*, 2005). Furthermore, within the field of toxicology, paracetamol-induced hepatotoxicity represents one of the most widely used models of DILI (for a review, see Newsome *et al.*, 2000). Three major pathways determine the metabolic fate of paracetamol; glucuronylation, sulphation and oxidation (Fig. 1.2). At well-tolerated therapeutic doses (4 g per day) (Thomas, 1993), around 55 % and 30 % of renally-excreted metabolites are non-toxic glucuronide and sulphate conjugates, respectively (Howie *et al.*, 1977; Tone *et al.*, 1990). A small proportion (5-10 %) of a therapeutic dose of paracetamol is bioactivated, mainly via CYP2E1, and less so CYP3A4 and CYP1A2, -mediated oxidations, to yield the electrophilic metabolite NAPQI (Dahlin *et*

al., 1984; Manyike *et al.*, 2000; Raucy *et al.*, 1989; Thummel *et al.*, 1993). The exact chemistry that underlies the oxidation of paracetamol to NAPQI has yet to be fully elucidated. NAPQI is quenched via spontaneous or GST-mediated conjugation with GSH and excreted in urine as a cysteine conjugate and mercapturic acid breakdown products (Coles *et al.*, 1988; Howie *et al.*, 1977; Prescott, 1980).

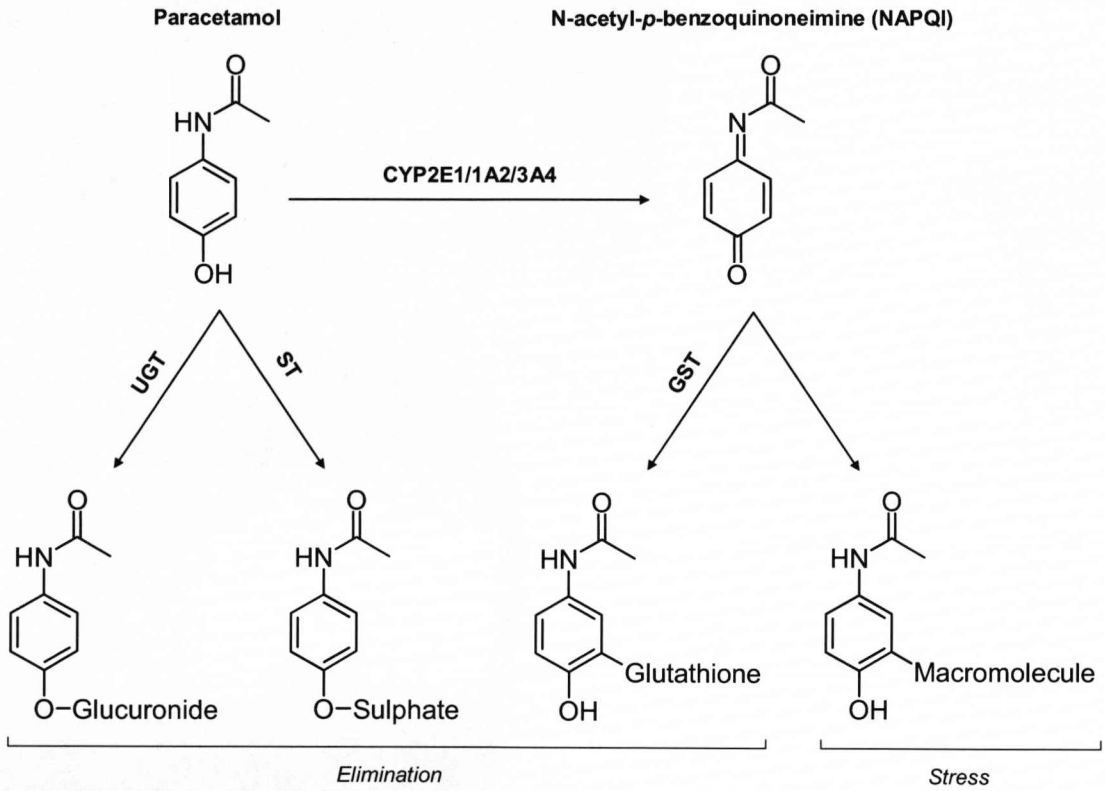

Figure 1.2 - Metabolic fate of paracetamol. The majority of a therapeutic dose of paracetamol is eliminated via the formation of glucuronide and sulphate conjugates, reactions catalysed by uridine diphosphate glucuronosyl transferases (UGT) and sulphotransferases (ST), respectively. A small proportion of a paracetamol dose is bioactivated, via CYP2E1, 1A2 and 3A4 -catalysed oxidations, to the electrophilic metabolite N-acetyl-*p*-benzoquinoneimine (NAPQI). At therapeutic doses, NAPQI is efficiently detoxified through glutathione S-transferase (GST) -catalysed conjugation with glutathione (GSH). Following an overdose, the saturation of conjugation pathways enables the accumulation of NAPQI and subsequent depletion of GSH stores. This facilitates the covalent binding of NAPQI to critical macromolecules, a process that is thought to contribute to the hepatocellular necrosis typically observed following paracetamol overdose. Adapted from Zhou *et al.* (2005).

Following paracetamol overdose, or the induction of specific CYP450 isoenzymes, the relatively low-capacity sulphation pathway becomes saturated, such that a greater fraction of the dose undergoes glucuronylation and oxidation, the latter resulting in the accumulation of NAPQI (Bessems *et al.*, 2001). Indeed, the different sensitivities of laboratory animal species to paracetamol-induced hepatotoxicity (generally, mice and hamsters are more sensitive than rats, rabbits and guinea pigs) are thought to be determined by the differential rates of bioactivation and detoxification (Gregus *et al.*, 1988; Ioannides *et al.*, 1983; Tee *et al.*, 1987). Under conditions of NAPQI accumulation, cellular GSH stores become depleted due to a shift in the balance between NAPQI formation and GSH synthesis (Potter *et al.*, 1974), and this is an obligatory step for paracetamol-induced hepatotoxicity (Davis *et al.*, 1974). As such, rapid therapeutic intervention with N-acetyl-L-cysteine, which replenishes GSH stores (Hazelton *et al.*, 1986), is the current treatment of choice for patients who present following an intentional or accidental paracetamol overdose (Smilkstein *et al.*, 1991).

The depletion of hepatic GSH enables NAPQI to covalently modify and inhibit at least 17 enzymes in various hepatocellular compartments in rodents (for a review, see Park *et al.*, 2005a), including γ-glutamylcysteine ligase, catalytic subunit (Gclc) (Kitteringham *et al.*, 2000), glyceraldehyde-3-phosphate dehydrogenase (Dietze *et al.*, 1997), aldehyde dehydrogenase (Landin *et al.*, 1996) and Ca^{2+}/Mg^{2+} ATPase (Tsokos-Kuhn *et al.*, 1988). Covalent modification of these proteins, and the oxidation of protein sulphydryls (Birge *et al.*, 1988; Tirmenstein *et al.*, 1990), by NAPQI has been hypothesised to contribute to mitochondrial dysfunction and the disruption of intracellular calcium homeostasis (for a review, see Jaeschke *et al.*, 2003) and, as such, is thought to be a critical step in the development of the centrilobular hepatic necrosis typically observed following paracetamol overdose (McJunkin *et al.*, 1976; Mitchell *et al.*, 1973). The centrilobular region is a primary target for paracetamol-induced toxicity due to the relatively high zonal expression of bioactivating CYP450s {Oinonen, 1998 #727}. The importance of mitochondrial protein binding in the toxicity of paracetamol is demonstrated by the observation that, despite both paracetamol and its non-toxic regioisomer 3-hydroxyacetanilide showing a similar overall degree of covalent binding, the reactive

metabolite of paracetamol binds to substantially more mitochondrial proteins than the metabolite of 3-hydroxyacetanilide (Myers *et al.*, 1995; Qiu *et al.*, 2001; Tirmenstein *et al.*, 1989). Therefore, it is likely that the extent of modification to specific macromolecules, and not covalent binding *per se*, is the major factor underlying paracetamol-induced hepatotoxicity. Furthermore, the early signs of paracetamol-induced hepatocellular damage, both *in vivo* and *in vitro*, can be reversed by the reducing agent dithiothreitol (Albano *et al.*, 1985; Rafeiro *et al.*, 1994; Tee *et al.*, 1986), implying that the reversible oxidation of thiols to disulphides is also an important step in the progression of paracetamol-induced toxicity. The identification of critical protein targets for specific hepatotoxins, and the molecular mechanisms that underlie DILI, therefore, are major goals of current toxicological research.

1.4.2 Other drugs associated with hepatotoxicity

Other drugs associated with DILI, via discrete mechanisms, include; isoniazid, the first-line treatment for tuberculosis (Yew *et al.*, 2006); troglitazone (Chojkier, 2005), an anti-diabetic withdrawn from the marketplace in 2000; nevirapine and efavirenz (Rivero *et al.*, 2007), non-nucleoside reverse transcriptase inhibitors commonly used in combination regimens for the treatment of patients with human immunodeficiency virus (HIV); the anesthetic halothane (Kenna, 1997); and the NSAID diclofenac (Boelsterli, 2003). Hence, DILI is associated with multiple drugs and represents a significant health concern, both for patients and the pharmaceutical industry.

1.5 MECHANISMS OF DEFENCE AGAINST DILI

Although the liver is a rich source of enzymes capable of bioactivating xenobiotics, and thus is at high risk of reactive intermediate-induced toxicity, it also possesses many bioinactivation pathways that are, in general, tightly coupled to bioactivation, and hence provide an intrinsic means of detoxifying reactive species. Such protective pathways

take various forms, and can be grouped into three 'tiers' of cell defence (Fig. 1.3); a) constitutive, relatively low levels of detoxification enzymes and antioxidants, b) the enhancement of these basal defences through transcription factor-mediated, upregulated expression of cytoprotective genes, and c) orchestrated cell suicide, in a final attempt to prevent the spread of damage to neighbouring cells.

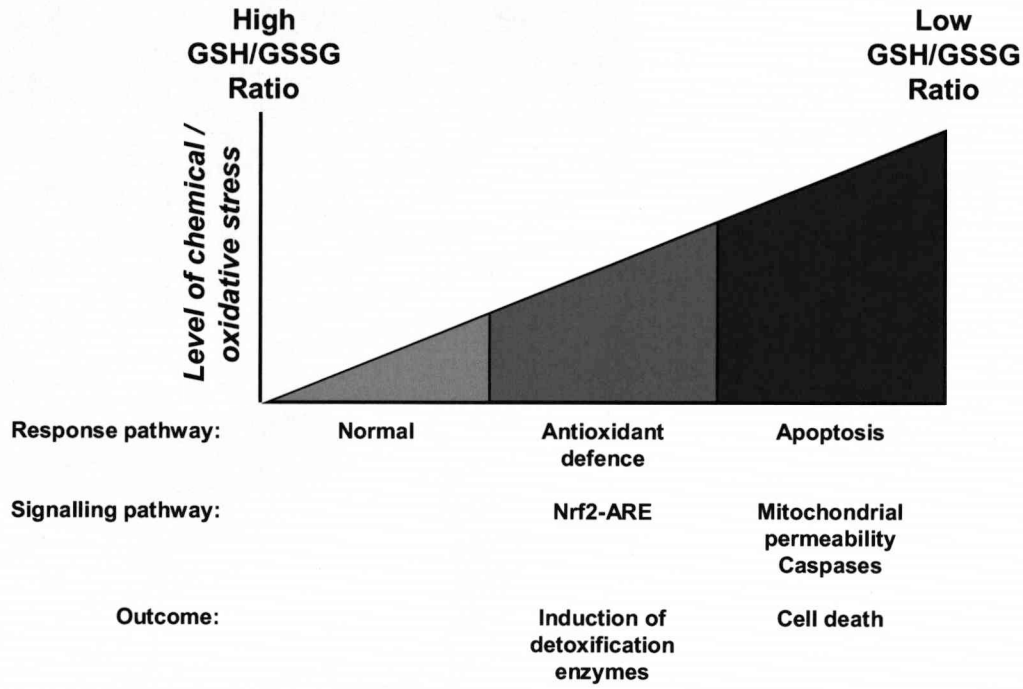

Figure 1.3 - The three major tiers of cell defence. Cells are equipped with three major 'tiers' of defence, the relative contributions of which are primarily determined by the levels of chemical/oxidative stress within a given cell. The first tier encompasses constitutive levels of non-protein antioxidants and detoxification enzymes. Transcription factors regulate the transition to the second tier of defence; the upregulated expression of detoxification enzymes. Should these initial attempts to defend the cell prove futile, programmed cell death (apoptosis) may ensue, in order to limit the spread of damage to neighbouring cells. The major features of the three tiers are discussed in section 1.5. Adapted from Nel *et al.* (2006).

1.5.1 Tiers of cell defence – Basal antioxidants and detoxification enzymes

The first defensive barrier comprises constitutive levels of antioxidant compounds and enzymes capable of detoxifying a broad range of reactive species, particularly electrophiles and free radicals, the latter generated through various aerobic metabolic transformations (Yu, 1994).

1.5.1.1 Non-protein antioxidants

α-Tocopherol (vitamin E; Fig. 1.4) is a potent, lipid-soluble antioxidant, that has a primary role in breaking chain reactions involving oxygen and lipid peroxyl free radicals (Yu, 1994). Ascorbic acid (vitamin C; Fig. 1.4) is a hydrophilic antioxidant that directly scavenges reactive oxygen species (ROS), byproducts of mitochondrial aerobic respiration (Yu, 1994). In addition, ascorbic acid has the capacity to recycle oxidised α-tocopherol, restoring its antioxidant properties following radical scavenging (Yu, 1994). Other radical-trapping antioxidants include β-carotene (Fig. 1.4), a metabolic precursor of retinol (vitamin A), and bilirubin (Fig. 1.4), a breakdown product of heme catabolism (Yu, 1994). In general, the scavenging actions of the above-mentioned antioxidants are 'suicidal' in nature; by donating an electron to a radical, and thus generating a non-radical species, the antioxidant is inactivated, but, in doing so, provides an alternative to critical macromolecules as targets for reactive species (Davies, 2000).

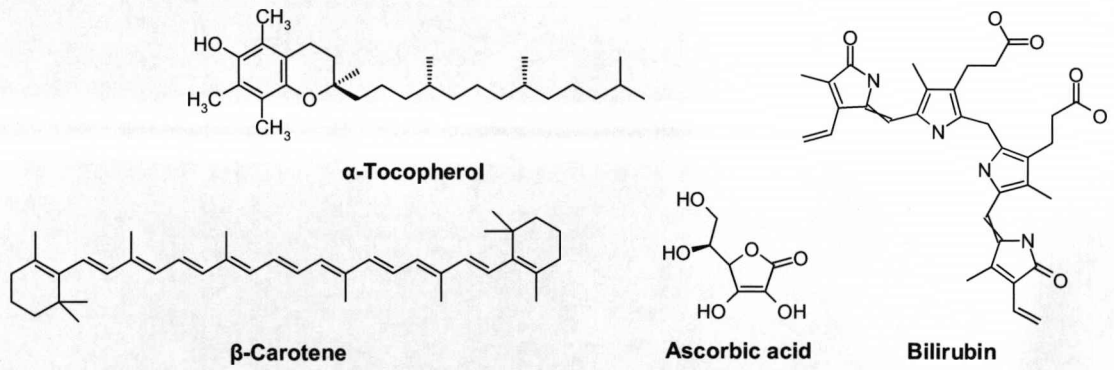

Figure 1.4 - Chemical structures of the major non-protein antioxidants.

1.5.1.2 Glutathione

GSH is the most abundant non-protein thiol, and is at the forefront of cell defence, providing a redox buffer for chemical and oxidative stress (DeLeve *et al.*, 1991). The two-step synthesis of GSH involves; a) the rate-limiting conjugation of L-glutamate and cysteine, via γ-glutamylcysteine ligase (GCL), to yield γ-glutamylcysteine, and b) the conjugation of glycine to γ-glutamylcysteine, via glutathione synthetase (GS), to yield γ-glutamylcysteinylglycine (GSH) (Kaplowitz *et al.*, 1985). The cysteine thiol of GSH endows it with a powerful nucleophilic group that facilitates the major functions of GSH, namely the conjugation of electrophiles, detoxification of ROS and thiol-disulphide exchange (DeLeve *et al.*, 1991). The reaction of GSH with electrophilic species to yield thioether conjugates may proceed spontaneously, particularly with highly reactive 'soft' electrophiles, or enzymatically, the latter being catalysed by the GST family (DeLeve *et al.*, 1991). GSH conjugates are cleaved by γ-glutamyltranspeptidase, which removes the γ-glutamyl moiety (DeLeve *et al.*, 1991). The remaining cysteinyl-glycine conjugate is then cleaved by dipeptidase, yielding a cysteinyl conjugate, which in turn is acetylated to form a mercapturic acid (DeLeve *et al.*, 1991). Ultimately, the various breakdown products of GSH-conjugate metabolism are recycled or excreted (DeLeve *et al.*, 1991).

In contrast to its role in the detoxification of electrophiles, the antioxidant capacity of GSH does not stem from its ability to react with ROS directly, but from its function as a substrate for GSH peroxidases (GPX), which catalyse the reduction of hydrogen peroxide (H_2O_2) and lipid hydroperoxides (DeLeve *et al.*, 1991). These reactions yield GSH disulphide (GSSG), which is reduced back to GSH via a nicotinamide adenine dinucleotide phosphate (NADPH) -dependent, GSH reductase-mediated reaction, a cycle that serves to maintain essential redox balance (DeLeve *et al.*, 1991). Due to the relatively high acid dissociation constant (pKa 9.2) of GSH (Jung *et al.*, 1972) and its cellular abundance, factors that disfavour disulphide formation, GSSG is normally maintained at less than 1 % of total cellular glutathione, though under conditions of oxidative stress, when GSSG levels may increase, GSSG can be actively transported out

of cells, in order to protect against redox imbalance (DeLeve *et al.*, 1991). GSH also serves an important function in thiol-disulphide exchange reactions, whereby the favourable redox state of a given cysteine residue is maintained through bidirectional reaction with GSH, mediated by thiol-transferases (DeLeve *et al.*, 1991). The preservation of cysteine redox state is particularly important for the function of certain enzymes whose catalytic activity is dependent upon the integrity of a sulphydryl or disulphide moiety. Examples of such enzymes include protein tyrosine phosphatases, and the peroxiredoxin (PRX) and thioredoxin (TRX) protein families (Dickinson *et al.*, 2002). The PRX and TRX families, in their own right, serve as important antioxidant defence proteins, as discussed in section 1.5.1.3.

1.5.1.3 Detoxification enzymes

The superoxide dismutase (SOD) family, members of which utilise the transition metals copper and zinc (Cu,Zn-SOD) or manganese (Mn-SOD) at their active sites, catalyse the dismutation of two superoxide anion radicals ($O_2^{\cdot-}$) to H_2O_2 and O_2 (Nordberg *et al.*, 2001). The cytotoxic product of this reaction, H_2O_2, is detoxified via reduction to H_2O and O_2 by GPX, catalase, and/or PRX (Nordberg *et al.*, 2001). The heme-containing catalase family constitutes an important antioxidant defence found predominantly within peroxisomes, organelles involved in the oxidative metabolism of fatty acids (Nordberg *et al.*, 2001). Catalases also function to detoxify phenols and alcohols, via a coupled reaction with H_2O_2 (Nordberg *et al.*, 2001). Within the PRX family of peroxidases, a conserved cysteine residue is utilised to enable the reduction of H_2O_2 and other peroxides (Ishii *et al.*, 2007; Wood *et al.*, 2003). In members of the PRX family that contain two thiols (2-Cys), the resulting cysteine sulphenic acid (-SOH) reacts with a second 'resolving' cysteine, either in the second subunit of a homodimer, or within the same subunit in monomeric atypical 2-Cys enzymes, resulting in the formation of an intermolecular/intersubunit disulphide bond, respectively, rendering PRX inactive (Ishii *et al.*, 2007; Wood *et al.*, 2003). PRX function is reestablished through reduction of this disulphide by thiol-containing electron donors, including GSH and the TRX family

(Ishii *et al.*, 2007; Wood *et al.*, 2003). Oxidised TRX is reactivated by TRX reductase (TRX-R) (Ishii *et al.*, 2007; Wood *et al.*, 2003). Hence, numerous inter-related and highly regulated processes enable the maintenance of steady-state levels of chemical and protein -based antioxidants, providing the cell with a degree of basal protection against low-level chemical/oxidative stressors.

1.5.2 Tiers of cell defence – Upregulation of antioxidants and detoxification enzymes

The second tier of cell defence involves the induction of cytoprotective genes, an adaptive response that increases the cell's capacity to nullify reactive species, through the increased expression of enzymes that catalyse detoxification reactions or the synthesis of antioxidants (Prestera *et al.*, 1993b; Primiano *et al.*, 1997). The induction of cell defence genes is mediated by certain transcription factors, proteins that recognise specific deoxyribonucleic acid (DNA) sequences, bind to these sequences, and recruit the co-activators and ribonucleic acid (RNA) polymerase required to enable transcription and translation of target genes (Latchman, 1997). At the forefront of the adaptive response to cellular stress are the transcription factors nuclear factor-erythroid 2 (NF-E2) -related factor 2 (Nrf2), nuclear factor κB (NF-κB), activator protein 1 (AP-1), hypoxia-inducible factor 1 (HIF-1) and members of the heat-shock factor (HSF) family. A detailed evaluation of the role of transcription factors in the adaptive response to cellular stress is presented in section 1.7.

1.5.3 Tiers of cell defence – Programmed cell death (apoptosis)

Should initial efforts to detoxify and eliminate a cellular stressor prove futile, a last-ditch attempt is made to halt the spread of damage to neighbouring cells, through programmed cell death (apoptosis). Membrane blebbing, cell shrinkage, chromatin condensation and DNA fragmentation are the hallmarks of apoptotic cell death (Robertson *et al.*, 2000).

These orchestrated events culminate in the cell being engulfed by macrophages, thus preventing the insult from spreading to neighboring cells (Robertson *et al.*, 2000). In this regard, apoptosis is distinct from necrosis, which can be regarded simply as a failure of cellular homeostasis, resulting from a sudden, lethal insult (Raffray *et al.*, 1997). Necrosis promotes an inflammatory response via the uncontrollable release of cellular contents into the local environment, leading to the damage of nearby cells (Robertson *et al.*, 2000). Although there appears to be a degree of overlap between the biochemical signaling mechanisms that regulate the apoptotic and necrotic pathways {for a review, see \Nicotera, 2004 #722}, various factors determine the balance between the two types of cell death, including the nature of the toxic insult, the dose and/or time of exposure to the insult, and the relative thresholds for apoptosis and necrosis within a given cell type (Raffray *et al.*, 1997).

1.5.3.1 Regulation of apoptosis

Apoptosis may be triggered via two distinct pathways, prompted by extrinsic or intrinsic signals, and involves the sequential activation of caspases, a family of cysteine proteases that act as both initiators and effectors of cell death (Thornberry *et al.*, 1998). In the extrinsic pathway, cell surface transmembrane death receptors, such as Fas and tumour necrosis factor receptor (TNF-R), recognise specific extracellular ligands, such as Fas ligand (FasL) or TNF-α, respectively, an event that induces receptor trimerisation (Budihardjo *et al.*, 1999). The subsequent formation of a death-inducing signalling complex between clustered receptors, intracellular 'death-domain' -containing proteins and procaspase-8 triggers the activation of downstream effector caspases (Budihardjo *et al.*, 1999). Perhaps more relevant to xenobiotic-induced chemical/oxidative stress, the intrinsic apoptotic pathway is triggered via an increase in mitochondrial membrane permeability, though a consensus has yet to be reached on the molecular events that cause such permeation (Blank *et al.*, 2007). A variety of intracellular stress signals can stimulate the intrinsic pathway, including DNA and cytoskeletal damage, oxidative and endoplasmic reticulum stress, and the misfolding of proteins (Blank *et al.*, 2007;

Chandra *et al.*, 2000). These and other stress signals promote the leakage of proteins, normally resident within the mitochondrial inter-membrane space, into the cytosol (Hengartner, 2000). Amongst the proteins released, cytochrome c, a component of the electron transport chain, associates with apoptotic protease activating factor 1 (APAF-1) to form the 'apoptosome' complex, which then binds to, and activates, procaspase-9 (Riedl *et al.*, 2007). As with activation of procaspase-8 in the extrinsic pathway, activation of procaspase-9 triggers downstream effector caspases, particularly caspases -3 and -7 (Blank *et al.*, 2007). Notable caspase substrates include cytoskeletal proteins such as actin (Mashima *et al.*, 1999) and lamin A (Rao *et al.*, 1996), degradation of which causes loss of membrane integrity, the inhibitor of caspase-activated DNAse (ICAD) (Enari *et al.*, 1998), inactivation of which promotes DNA fragmentation, the DNA repair enzyme poly (adenosine diphosphate-ribose) polymerase (PARP) (Lazebnik *et al.*, 1994), and components of various cell division/survival signalling cascades (Blank *et al.*, 2007). Apoptosis is partly regulated by the cellular redox balance, and thus is sensitive to oxidative stress (Chandra *et al.*, 2000; Davis *et al.*, 2001), which in turn is both a trigger and a target for the basal and inducible defence machinery discussed above. Hence, cells employ an integrated three-pronged defence strategy to coordinate protection against cytotoxic reactive species and other stressors.

1.6 REDOX REGULATION OF CELL DEFENCE

As with other cellular processes, cell defence is subject to redox regulation. The sulphydryl group of the amino acid cysteine represents a versatile moiety that facilitates the regulation of protein function, via reversible and irreversible redox reactions, i.e. those involving the loss (oxidation) or gain (reduction) of electrons at the sulphydryl group (Cooper *et al.*, 2002). The various oxidation states of cysteine sulphydryls are summarised in Figure 1.5. Some cysteines are stabilised in the thiolate form ($-S^-$) via structural interactions with basic amino acids, namely arginine, lysine or histidine (Snyder *et al.*, 1981). The deprotonated thiolate is more nucleophilic, and thus reacts more readily with oxidants, than the protonated thiol (–SH; **a**), which is relatively

unreactive (Netto *et al.*, 2007). Nevertheless, the thiol is capable of partaking in various reactions; sequential oxidations yield sulphenic acid (–SOH; **b**), which is generally unstable and reacts further to the more stable sulphinic (–SO_2H; **c**) and sulphonic acids (–SO_3H; **d**) (Paget *et al.*, 2003). Oxidation to sulphenic acid may also lead to the formation of a disulphide (S–S), either within a single protein (**e**), between separate proteins (**f**), or with a small, non-protein thiol such as GSH (S-glutathionylation) (**g**) (Paget *et al.*, 2003). Other important redox reactions include thiol-disulphide exchange reactions between a thiol and disulphide (**h**), and modifications by reactive nitrogen species such as nitric oxide, to yield S-nitrosothiol (–SNO; **i**), or peroxynitrite, to yield S-nitrothiol (–SNO_2; **j**) (Cooper *et al.*, 2002).

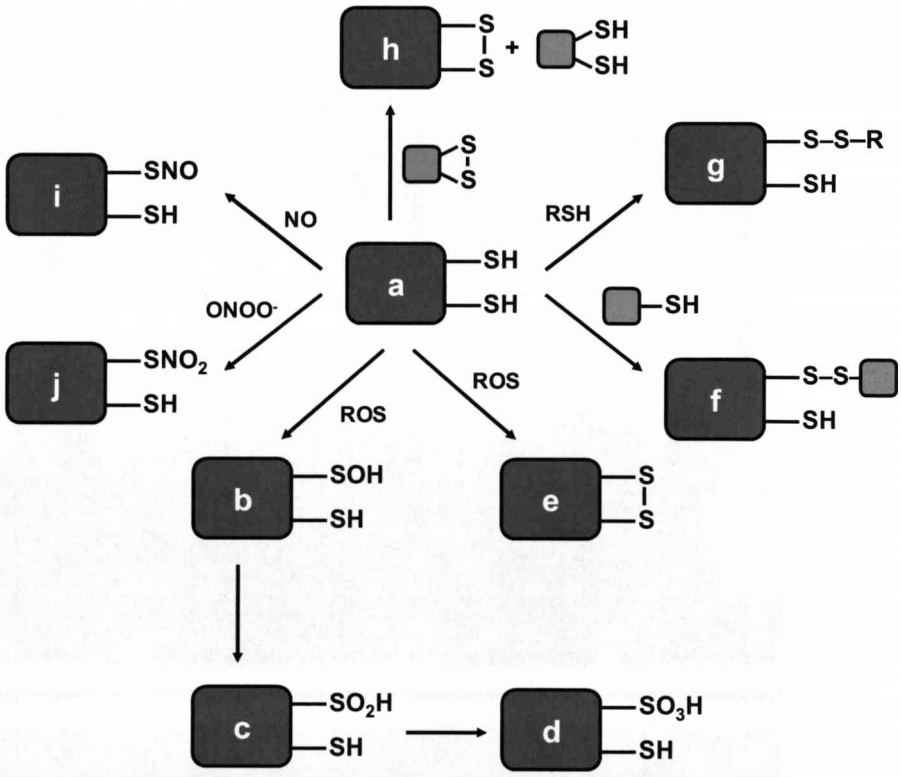

Figure 1.5 - Schematic overview of the various cysteine oxidations states. Letters representing each oxidation state refer to descriptions given in the main text. Adapted from Paget *et al.* (2003).

The oxidation state of certain cysteines is often critical to the function of a given protein and, as such, changes in the cellular redox environment can affect protein activity, either positively or negatively. A well-characterised redox-sensitive protein is the prokaryotic transcription factor OxyR, a major regulator of bacterial cell defence genes including *katG* (a hydrogen peroxidase), *gorZ* (a GSH reductase) and *oxyS* (a small RNA involved in DNA repair) (Paget *et al.*, 2003). OxyR 'senses' oxidative stress through a reactive cysteine (Cys-199) that, in a non-oxidative environment, is stabilised in the thiolate form via interaction with a basic arginine residue (Choi *et al.*, 2001). Oxidation of this cysteine results in a conformational change that activates OxyR, enabling the transcription factor to recognise specific response elements in the promoter regions of target genes (Paget *et al.*, 2003). Until recently, this conformational change was thought to be dependent upon the formation of an intramolecular disulphide bond (Storz *et al.*, 1990). However, evidence has emerged to suggest that, rather than acting as a simple 'on/off' switch, cysteine oxidation regulates OxyR in a graded manner, dependent upon the specific oxidation state of Cys-199, which may be modified to yield sulphenic acid, S-nitrosothiol or a mixed disulphide (Kim *et al.*, 2002).

The concept that a protein's function may be modulated through simple chemical changes within a single amino acid represents an important paradigm in cellular redox signalling. Redox-sensitive transcription factors that have major roles in regulating the eukaryotic cytoprotective response include Nrf2, NF-κB and AP-1. A more detailed discussion of the role of these transcription factors in cell defence is presented in section 1.7.

1.7 TRANSCRIPTIONAL REGULATION OF CELL DEFENCE

As discussed in section 1.5.2, one of the major tiers of cell defence involves the upregulated expression of cytoprotective genes, a process mediated by certain transcription factors. In working to nullify electrophiles and free radicals, these transcription factors play a critical role in maintaining cellular homeostasis. It is

noteworthy that the activity of these regulatory proteins themselves is particularly sensitive to changes in cellular redox balance. The ability of cytoprotective pathways to 'sense' and respond to chemical/oxidative stress has an important influence on the balance between bioactivation and detoxification, which ultimately determines the fate of a cell exposed to a potentially toxic species.

1.7.1 Nuclear Factor κB

NF-κB is a major regulator of the innate and adaptive immune response, cell proliferation and apoptosis, and thus serves an important function in the response to cellular stress. Under basal conditions, NF-κB is localised within the cytosol as a dimeric complex, usually comprising p50 and p65 subunits (Hayden *et al.*, 2004). The subcellular distribution of NF-κB is regulated by members of the inhibitor of κB (IκB) family; the association between the two molecules masks the nuclear localisation signal (NLS) in the NF-κB complex, thus inhibiting its nuclear translocation (Hayden *et al.*, 2004). Activation of NF-κB, in response to a variety of stimuli, including bacterial and viral infection, oxidative and endoplasmic reticulum stress, proinflammatory cytokines, and certain chemical agents (Pahl, 1999), involves the stimulation of a protein kinase cascade that promotes activation of IκB kinase (IKK), which subsequently phosphorylates critical serine residues within IκB, resulting in the latter's ubiquitination and proteasomal degradation (Hayden *et al.*, 2004). Consequently, the NLS of NF-κB is unmasked, facilitating its nuclear translocation and the transactivation of target genes, through binding to specific DNA sequences, known as κB elements (Hayden *et al.*, 2004). Notable NF-κB targets include the stress-response genes cyclooxygenase 2 (COX2) and inducible nitric oxide synthase (iNOS), the detoxification enzymes GST subunit P1-1 (GSTP1-1), GCL and SOD, and the apoptotic regulators p53, Bcl-xL and FasL (Pahl, 1999). Notably, exposure of mice to hepatotoxic doses of paracetamol causes the NF-κB -dependent upregulation of pro-inflammatory mediators, including interleukin-1β (IL-1β) and TNFα, and the anti-inflammatory cytokine IL-10 (Dambach *et al.*, 2006), indicating the role of NF-κB in regulating the cellular stress response.

The activity of NF-κB is subject to direct and indirect redox modulation (Kabe *et al.*, 2005; Pantano *et al.*, 2006). A rise in the levels of ROS in response to various stimuli, including TNF-α, IL-1 and lipopolysaccharide (LPS), augments NF-κB activation through induction of upstream protein kinases (Pantano *et al.*, 2006). Changes in the cellular GSH:GSSG balance have also been associated with repression of IκB and activation of NF-κB (Mihm *et al.*, 1995). Based on this evidence, therefore, it would appear that NF-κB is stimulated under oxidising conditions. However, recent reports that specific chemical entities can attenuate the DNA-binding activity of NF-κB, through chemical modification of Cys-62 within the p50 subunit (Cernuda-Morollon *et al.*, 2001; Lee *et al.*, 2002; Mahon *et al.*, 1995; Xia *et al.*, 2004), appear to conflict with this view. Furthermore, covalent modification of IKK at Cys-179, by electrophiles including cyclopentenone prostaglandins (Rossi *et al.*, 2000), 4-hydroxynonenal (Ji *et al.*, 2001) and acrolein (Valacchi *et al.*, 2005), inhibits its kinase activity and thus perturbs transactivation of target genes by NF-κB. In addition, NAPQI, the electrophilic metabolite of paracetamol, perturbs NF-κB activity in Hepa 1-6 mouse hepatoma cells, by inhibiting the degradation of IκB (Boulares *et al.*, 1999).

The balance between cytoplasmic and nuclear redox events, and their effects on NF-κB activity, is particularly evident in the case of TRX. Over-expression of TRX, which localises predominantly in the cytoplasm, represses activation of NF-κB, by reversing oxidation events promoted by NF-κB-stimulating ROS (Meyer *et al.*, 1993). However, in response to phorbol 12-myristate-13-acetate (PMA), TNF-α, or ionising radiation, TRX translocates to the nucleus, and enhances the DNA-binding activity of NF-κB, by maintaining Cys-62 of p50 in a reduced state (Hirota *et al.*, 1999). In a further demonstration of its redox regulation, NF-κB-dependent gene expression is suppressed by the quinone derivative E3330, but this inhibitory effect does not involve changes in the degradation of IκB or the nuclear translocation of NF-κB (Hiramoto *et al.*, 1998). Indeed, E3330 modifies and inhibits redox effector factor 1 (REF-1) (Hiramoto *et al.*, 1998), a nuclear protein that mediates the redox regulation of several transcription factors (Evans *et al.*, 2000), and can reduce the oxidised Cys-62 of p50, thus restoring the DNA-binding activity of NF-κB (Nishi *et al.*, 2002). Thus, by perturbing the activity

of REF-1, E3330 indirectly inhibits the binding of NF-κB to DNA (Hiramoto *et al.*, 1998). In summary, NF-κB is a redox-sensitive transcription factor with important functions in the cellular stress-response, although the redox regulation of NF-κB is particularly dependent on its subcellular localisation, and may involve a variety of signalling pathways.

1.7.2 Activator Protein 1

The transcription factor AP-1 plays an important role in various cellular processes, including proliferation, differentiation, survival and death (Shaulian *et al.*, 2002). AP-1 exists as a dimer, comprising members of the Jun, Fos and/or activating transcription factor (ATF) protein families (Karin *et al.*, 1997). Jun homodimers and Jun-Fos heterodimers, typically c-Jun and c-Fos, bind to the 12-O-tetradecanoate-13-acetate (TPA) -responsive element (TRE), whereas ATF homodimers and Jun-ATF heterodimers bind to the cyclic adenosine monophosphate (cAMP) -responsive element (CRE) (Karin *et al.*, 1997). Activation of AP-1, by stimuli including cytokines, bacterial and viral infection, and certain cellular and chemical stresses, is mediated predominantly via the mitogen-activated protein kinase (MAPK) pathway (Shaulian *et al.*, 2002). Activation of AP-1 involves the upregulation of immediate early genes that encode e.g. c-Jun and c-Fos, with subsequent dimerisation and binding to recognition elements resulting in the transactivation of genes including GSTs, GCL, COX2, iNOS and various apoptotic regulators (Karin *et al.*, 1997). AP-1 is known to be redox-sensitive (Schenk *et al.*, 1994), to such a degree that oxidation of a single cysteine residue within c-Jun and c-Fos can influence their DNA-binding capacities (Abate *et al.*, 1990). Previous work has demonstrated a reduction in AP-1 DNA-binding following adduction of c-Jun by reactive chemical species (Biswal *et al.*, 2002; Perez-Sala *et al.*, 2003). Furthermore, in a similar manner to NF-κB, the DNA binding activity of AP-1 is subject to redox regulation by REF-1 (Xanthoudakis *et al.*, 1992).

1.7.3 Hypoxia-Inducible Factor 1 and Heat Shock Factors

Other transcription factors with important roles in the adaptive response to cellular stress include HIF-1 and members of the HSF family. Under circumstances of low cellular oxygen levels (hypoxia), activation of HIF-1 enables induction of genes that facilitate short and long-term adaptation to hypoxia, including growth factors involved in cell survival and proliferation, regulators of erythropoiesis and angiogenesis, and components of various metabolic pathways (Semenza, 2003). In response to elevated temperature and other stresses, the HSF family of transcription factors mediate the induction of heat-shock proteins (HSP), which function to solubilise denatured protein aggregates, facilitate the restoration of protein function, and direct irreversibly damaged proteins to the cellular degradation machinery (Kiang *et al.*, 1998). In general terms, therefore, the heat-shock response represents a defence against protein damage (Wu, 1995).

1.7.4 The antioxidant response pathway

Mammalian cells have evolved an inducible line of cell defence, termed the antioxidant response pathway, that facilitates the enhanced bioinactivation and clearance of oxidants and electrophilic molecules, via the transcriptional upregulation of an array of detoxification and antioxidant enzymes (Primiano *et al.*, 1997). The three regulatory components of the antioxidant response pathway are a) the antioxidant response element (ARE) DNA motif, found within the promoter regions of numerous cytoprotective genes, b) Nrf2, the redox-sensitive transcription factor that binds to the ARE, and c) Keap1, the cysteine-rich cytosolic repressor of Nrf2.

1.7.4.1 Nuclear Factor Erythroid 2 (NF-E2) -Related Factor 2 (Nrf2)

Nrf2 was first isolated during a screen for Nuclear factor erythroid 2 (NF-E2) -regulating proteins in a complementary DNA (cDNA) expression library derived from hemin-induced erythroleukemia cells (Moi *et al.*, 1994). Unlike NF-E2, which regulates globin gene expression in developing erythroid cells (Igarashi *et al.*, 1994), Nrf2 is expressed in many tissues (Moi *et al.*, 1994), particularly those associated with detoxification (liver and kidney) and those that are exposed to the external environment (skin, lung and gastrointestinal tract) (Motohashi *et al.*, 2002). As with other members of the CNC family of transcription factors (Itoh *et al.*, 1995), so named because of structural similarities with the *Drosophila* protein cap 'n' collar (CNC), Nrf2 contains a C-terminal basic leucine zipper (bZip) structure that facilitates dimerisation and DNA binding (Moi *et al.*, 1994).

Through reporter transgene (Venugopal *et al.*, 1996) and electrophoretic mobility shift assay (Nguyen *et al.*, 2000) experiments, Nrf2 was shown to bind to the ARE and upregulate the expression of target genes. The ARE, a *cis*-acting DNA enhancer motif with a consensus sequence defined as 5'-gagTcACa**GTgAGtCggC**Aaaatt-3' (where essential nucleotides are in capitals and the core is in bold) (Nioi et al., 2003),, was originally identified within a 41 base-pair section from the 5'-flanking region of the rat GSTA2 gene that was responsive to the phenolic antioxidant β-naphthoflavone (Rushmore *et al.*, 1990). Although Nrf2 is by far the most potent transcriptional activator of the ARE amongst members of the CNC family (Kobayashi *et al.*, 1999; Papaiahgari *et al.*, 2006), Nrf1 also appears to play a role, albeit limited, in the regulation of ARE gene expression, at least at the basal level (Kwong *et al.*, 1999; Myhrstad *et al.*, 2001; Venugopal *et al.*, 1996; Xu *et al.*, 2005). Furthermore, Nrf1 is important for embryonic development, as Nrf1 knockout ($Nrf1^{-/-}$) embryos die within 17-18 days of gestation (Chan *et al.*, 1998). Evidence also exists, however, to suggest that Nrf1 (Wang *et al.*, 2007), in addition to the remaining members of the CNC family, Nrf3 (Sankaranarayanan *et al.*, 2004), bric-a-brac/tram-track/broad complex (BTB) and CNC homolog 1 (BACH1) (Dhakshinamoorthy *et al.*, 2005; Reichard *et al.*, 2007; Sun

et al., 2002) and BACH2 (Muto *et al.*, 2002), may act as negative regulators of Nrf2-mediated ARE gene expression, in part by competing with Nrf2 for binding to the ARE.

Nrf2 only binds with high affinity to the ARE as a heterodimer with small Maf proteins (Itoh *et al.*, 1997). Members of the small Maf family, comprising MafF, MafK and MafG, possess a bZip domain, facilitating their dimerisation with other bZip proteins (Kataoka *et al.*, 1993). However, small Maf proteins lack transactivation domains, and thus the ability of the Nrf2-Maf heterodimer to promote transcription is reliant on the transactivation faculty of Nrf2 (Motohashi *et al.*, 2002). Indeed, over-expression of small Maf proteins represses Nrf2-mediated transactivation of cell defence genes (Dhakshinamoorthy *et al.*, 2002; Dhakshinamoorthy *et al.*, 2000; Nguyen *et al.*, 2000), through binding of small Maf homodimers, which lack intrinsic transcriptional activity, to the ARE (Dhakshinamoorthy *et al.*, 2000).

Structural comparison of the chicken homologue of Nrf2 (erythroid cell-derived protein with CNC homology; ECH) (Itoh et al. 1995) with the human and mouse proteins enabled the identification of six highly-conserved regions, termed Nrf2-ECH homology (Neh) domains (Itoh *et al.*, 1997) (Fig. 1.6 and Table 1.2). The binding of Nrf2 to the ARE, which involves a highly conserved cysteine residue (Cys-506) within the Neh1 domain of the transcription factor (Bloom *et al.*, 2002), stimulates transcription of downstream genes, in part, by recruiting transcriptional co-activators (Lin *et al.*, 2006), particularly cAMP responsive element binding protein (CREB) -binding protein (CBP) through its Neh4 and Neh5 domains (Katoh *et al.*, 2001; Zhu *et al.*, 2001). CBP promotes transcription via a) its intrinsic histone acetyltransferase (HAT) activity, b) interaction with other proteins possessing HAT activity, and c) bridging to components of the general transcriptional machinery (Bannister *et al.*, 1996; Kalkhoven, 2004). Histones form the core of nucleosomes, around which DNA is wound into a condensed structure that represses transcription, but that can be unfolded to increase accessibility to general transcription factors and RNA polymerase II, and thus promote gene transcription (Grunstein, 1990; Kuo *et al.*, 1998).

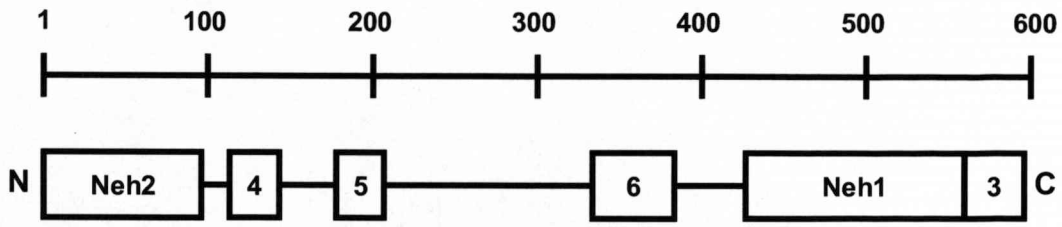

Figure 1.6 - Nrf2 functional domains. Schematic overview of the six Neh functional domains in Nrf2, drawn to scale, with each domain labelled. The line at the top of the panel indicates 100 amino acid sections of the protein. See Table 1.2 for functional characteristics of each domain.

Domain	Location (in mouse protein)	Function(s) and Features	Reference(s)
Neh2	1-96	Contains DLG and ETGE motifs (points of interaction with Keap1) Contains lysine-rich region (target for ubiquitination) Contains DIDLID element (regulation of Nrf2 turnover under homeostatic conditions)	Itoh *et al.* (1999) Katoh *et al.* (2005) McMahon *et al.* (2004) McMahon *et al.* (2006) Tong *et al.* (2006a)
Neh4	111-141	Transactivation Interaction with co-activator CBP	Katoh *et al.* (2001)
Neh5	172-201	Transactivation Interaction with co-activator CBP Contains nuclear export signal (#175-186)	Katoh *et al.* (2001) Li *et al.* (2006) Zhang *et al.* (2007b)
Neh6	330-380	Regulation of Nrf2 turnover under stressed conditions	McMahon *et al.* (2004)
Neh1	427-560	Contains CNC and bZip regions ARE binding Dimerisation with other bZip proteins (small Mafs) Contains nuclear localisation (#494-511) and export (#545-554) signals	Bloom *et al.* (2002) Itoh *et al.* (1999) Jain *et al.* (2005)
Neh3	561-597	Transactivation Interaction with putative co-activator proteins	Nioi *et al.* (2005)

Table 1.2 - Nrf2 functional domains.

Hence, the interaction with transcriptional co-activators such as CBP enables Nrf2 to regulate the basal and inducible expression of numerous cytoprotective genes, as summarised in Table 1.3. Therefore, activation of Nrf2 promotes cell survival through the detoxification and/or elimination of chemical/oxidative stressors (Fig. 1.7).

Protein	**Function**	**Reference(s)**
Aldo-keto reductases (AKR)	Reduce aldehydes and ketones to yield primary and secondary alcohols	Lou *et al.* (2006) Nishinaka *et al.* (2005)
Glutamate cysteine ligase, catalytic subunit (GCLC)	Catalyses the conjugation of cysteine with L-glutamate, to form γ-glutamylcysteine	Chan *et al.* (2000b) Jeyapaul *et al.* (2000) {Wild, 1999 #8}
Glutamate cysteine ligase, regulatory subunit (GCLM)	Lowers the K_m of GCLC for glutamate and raises the K_i for GSH	Moinova *et al.* (1999) Wild *et al.* (1999) Chan *et al.* (2000b)
Glutathione peroxidases (GPX)	Catalyse the reduction of H_2O_2 and other peroxides, using GSH as a substrate	Banning *et al.* (2005) Singh *et al.* (2006b)
Glutathione reductase (GSR)	Catalyses the reduction of oxidized glutathione (GSSG) to GSH	Thimmulappa *et al.* (2002)
Glutathione synthetase (GS)	Catalyses the conjugation of glycine with γ-glutamylcysteine	Lee *et al.* (2005)
Glutathione S-transferases (GST)	Reduces pK_a of GSH, catalysing its conjugation to electrophiles	Chanas *et al.* (2002) Hayes *et al.* (2000) McMahon *et al.* (2001)
Heme-oxygenase 1 (HO-1)	Catabolises heme to yield biliverdin, carbon monoxide and free iron	Alam *et al.* (1999); Ishii *et al.* (2000)
Microsomal epoxide hydrolase (MEH)	Hydrates simple epoxides and arene oxides to more polar vicinal diols and *trans*-dihydrodiols	Ramos-Gomez *et al.* (2001); Slitt *et al.* (2006); Thimmulappa *et al.* (2002)
NAD(P)H:quinone oxidoreductases (NQO)	Catalyse two-electron reduction and detoxification of quinones	Venugopal *et al.* (1996) Wang *et al.* (2006)
Peroxiredoxin 1 (Prx1)	Reduces H_2O_2, peroxynitrite and other organic hydroperoxides	Kim *et al.* (2007)
Superoxide dismutases (SOD)	Catalyse the dismutation of superoxide radicals to O_2 and H_2O_2	Park *et al.* (2002)
Thioredoxins (TRX)	Catalyse the reversible reduction of disulfides to sulphydryls	Kim *et al.* (2001) Kim *et al.* (2003)
UDP-Glucuronosyltransf-erases (UGT)	Catalyse conjugation of UDPGA to lipophilic substrates	Shelby *et al.* (2006) Yueh *et al.* (2007)

Table 1.3 - Cell defence proteins encoded by Nrf2-regulated genes.

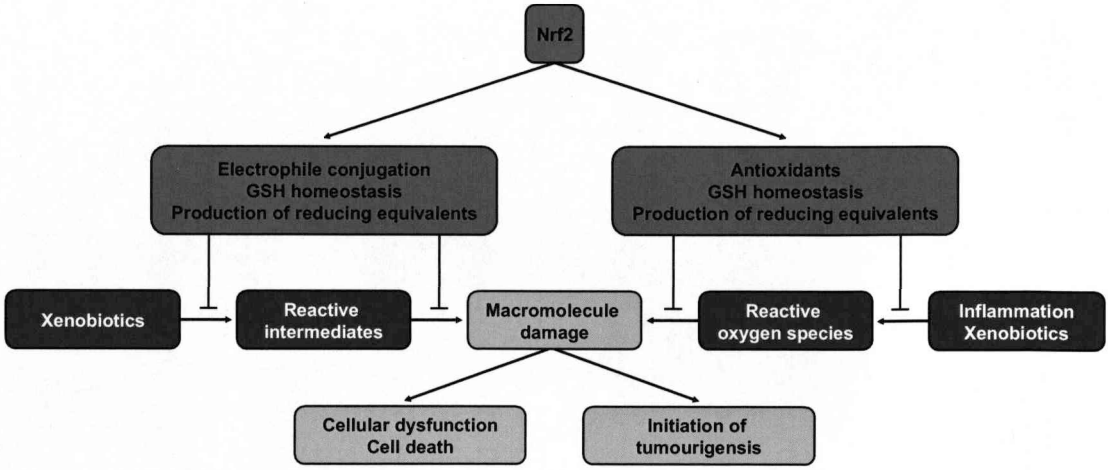

Fig. 1.7 - The inhibitory effects of Nrf2 activation on the progression of cellular injury. Through regulating the expression of genes encoding proteins that serve to detoxify reactive chemical species and maintain redox homeostasis, Nrf2 protects against the potential deleterious effects of chemically reactive intermediates and reactive oxygen species, and thus promotes cell survival. Adapted from Osburn *et al.* (2007).

1.7.4.1.1 Insights into Nrf2 function from transgenic knockout mice

Although *Nrf2* knockout (*Nrf2*$^{-/-}$) animals exhibit no significant developmental phenotype (Chan *et al.*, 1996), they do develop vacuolar leukoencephalopathy (the abnormal development of cavities in the brain and deterioration of the myelin sheaths that cover neurons) (Hubbs *et al.*, 2007) and lupus-like autoimmune symptoms, including multiorgan inflammation, oxidative lesions, deposition of immunoglobulin complexes in blood vessels, and nephritis (Vargas *et al.*, 2006; Yoh *et al.*, 2001). Two notable characteristics demonstrate the severely compromised defence systems in *Nrf2* knockout mice; a) lower basal and/or inducible expression of detoxification/antioxidant genes in a variety of tissues, including liver (Chan *et al.*, 2000; Chanas *et al.*, 2002; Iida *et al.*, 2004; Itoh *et al.*, 1997; Kwak *et al.*, 2001; Ramos-Gomez *et al.*, 2001), lung (Chan *et al.*, 1999; Cho *et al.*, 2002; Ishii *et al.*, 2005; Rangasamy *et al.*, 2005), gastrointestinal tract (Itoh *et al.*, 1997; Khor *et al.*, 2006; McMahon *et al.*, 2001; Ramos-Gomez *et al.*, 2001), brain (Kraft *et al.*, 2006; Lee *et al.*, 2003; Shih *et al.*, 2005), skin (Xu *et al.*, 2006) and bladder (Iida *et al.*, 2004), and b) enhanced susceptibility to the toxicities associated with various xenobiotics and environmental stresses (for a review, see Copple *et al.*,

2008). Furthermore, the chemopreventative actions of oltipraz (Iida *et al.*, 2004; Ramos-Gomez *et al.*, 2003; Ramos-Gomez *et al.*, 2001) and sulforaphane (Xu *et al.*, 2006) are abolished in *Nrf2*$^{-/-}$ mice. Taken together, these findings demonstrate the importance of Nrf2 for cellular defence.

1.7.4.2 Kelch-like ECH-associated Protein 1 (Keap1)

In the absence of cellular stress, Nrf2 is tethered within the cytosol by an inhibitory partner, which binds to Nrf2 via the Neh2 domain of the transcription factor (Itoh *et al.*, 1999). Due to similarities with sequence motifs found in the *Drosophila* cytoskeleton-binding protein Kelch (Xue *et al.*, 1993), the repressor of Nrf2 was named Kelch-like ECH-associated protein 1 (Keap1). Keap1 resides within the cytosol of mammalian cells, where it interacts with the actin cytoskeleton (Kang *et al.*, 2004) and, in the absence of chemical/oxidative stress, associates with Nrf2 (Dhakshinamoorthy *et al.*, 2001; Itoh *et al.*, 1999). Over-expression of Keap1 reduces Nrf2-mediated transactivation of ARE-regulated genes (Dhakshinamoorthy *et al.*, 2001; Itoh *et al.*, 1999; Wakabayashi *et al.*, 2004). Exposure to chemical/oxidative stress enables Nrf2 to evade Keap1-mediated repression, accumulate within the nucleus via a NLS located within the Neh1 domain (Jain *et al.*, 2005) and transactivate ARE target genes (Dhakshinamoorthy *et al.*, 2001; Itoh *et al.*, 1999). A detailed discussion of the molecular mechanisms thought to underlie the liberation of Nrf2 from Keap1-mediated repression is presented in section 1.7.4.6. The features of the three major functional domains of Keap1 are summarised in Figure 1.8 and Table 1.4.

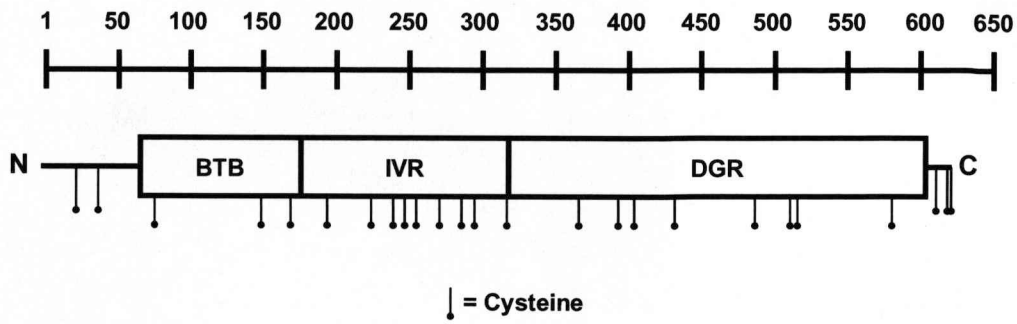

Figure 1.8 - Keap1 functional domains. Schematic overview of the three major functional domains in Keap1, drawn to scale, with each domain labelled. BTB, bric-a-brac/tram-track/broad complex; IVR, intervening region; DGR, double glycine repeat. The line at the top of the panel indicates 50 amino acid sections of the protein. The position of each cysteine in the mouse Keap1 protein is indicated. See Table 1.4 for functional characteristics of each domain.

Domain	Location	Function(s) and Comments	Reference(s)
BTB	67-178	Bric-a-brac/tram-track/broad complex Heterodimerisation Interaction with CUL3	Zipper *et al.* (2002)
IVR	179-321	Intervening region Cysteine-rich (6.3 % of amino acids)	
DGR	322-608	Double-glycine (kelch) repeat Interaction with Nrf2 Interaction with actin cytoskeleton	Dhakshinamoorthy *et al.* (2001) Itoh *et al.* (1999) Kang *et al.* (2004) Li *et al.* (2004) McMahon *et al.* (2006) Tong *et al.* (2006a)

Table 1.4 - Keap1 functional domains.

1.7.4.2.1 Insights into Keap1 function from transgenic knockout mice

Attempts to investigate the role of Keap1 in regulating Nrf2-mediated cell defence *in vivo* were initially hindered due to the retarded growth and death of *Keap1* knockout (*Keap1*$^{-/-}$) mice within 21 days of birth, due in part to malnutrition resulting from hyperkeratotic lesions in the eosophagus and forestomach, which obstruct the upper digestive tract (Wakabayashi *et al.*, 2003). Co-knockout of *Nrf2* (*Keap1*$^{-/-}$*::Nrf2*$^{-/-}$) rescued this phenotype, indicating that Nrf2 is the central downstream target of Keap1 *in vivo* (Wakabayashi *et al.*, 2003). Recently, however, hepatocyte-specific knockout of *Keap1* has been achieved using the Cre-loxP system, which facilitates tissue-specific gene knockout (Okawa *et al.*, 2006). Briefly, an *Alb-Cre* mouse, expressing a Cre recombinase transgene under the control of the liver-specific albumin promoter, is crossed with a *Keap1-loxP* mouse, in which exons 4-6 of the *Keap1* gene are flanked by loxP sites. In the double-transgenic *Alb-Cre::Keap1-loxP* mouse, Cre catalyses recombination between target loxP sites, resulting in excision of the flanked segment (exons 4-6) within *Keap1* and thus translation of a truncated form of the protein, lacking the double glycine repeat (DGR) domain that interacts with Nrf2 (Nagy, 2000; Okawa *et al.*, 2006). Without the growth retardation and malnutrition observed in *Keap1*$^{-/-}$ animals, hepatocyte-specific knockout of *Keap1* results in an increase in basal expression of numerous ARE-driven genes in the liver, including *Nqo1*, *Gclc*, *Gpx* and carbonyl reductase (Okawa *et al.*, 2006). Moreover, *Alb-Cre::Keap1-loxP* mice are highly resistant to doses of paracetamol that are hepatotoxic and lethal in wild-type mice (Okawa *et al.*, 2006). Therefore, Keap1 is a major regulator of cell defence, due to its repressive influence over Nrf2.

1.7.4.3 The role of ubiquitination in the regulation of Nrf2 activity

Although the physical restriction of Nrf2 is an important aspect of its repression by Keap1, this cannot fully account for the relatively short-half life of the transcription factor (10-30 minutes) in the absence of cellular stress (Alam *et al.*, 2003; Furukawa *et*

al., 2005; He *et al.*, 2006; Itoh *et al.*, 2003; McMahon *et al.*, 2003; Stewart *et al.*, 2003; Zhang *et al.*, 2003a). Notably, proteasome inhibition causes the stabilisation and nuclear accumulation of Nrf2, which in turn leads to an increase in ARE-driven gene transactivation (Alam *et al.*, 2003; Chen *et al.*, 2005a; Furukawa *et al.*, 2005; Itoh *et al.*, 2003; McMahon *et al.*, 2003; Nguyen *et al.*, 2003; Sekhar *et al.*, 2000; Stewart *et al.*, 2003; Usami *et al.*, 2005; Yamamoto *et al.*, 2007). Furthermore, ubiquitinated Nrf2 has been detected under such conditions (Cullinan *et al.*, 2004; Kobayashi *et al.*, 2004; Nguyen *et al.*, 2003; Stewart *et al.*, 2003; Zhang *et al.*, 2003a). This evidence suggests that Nrf2 is rapidly degraded by the ubiquitin-proteasome pathway, thus accounting for its relatively short half-life and the well-known difficulties associated with its detection in unstressed cells/tissues.

Recent evidence has demonstrated that, similar to other BTB family proteins (Pintard *et al.*, 2004), Keap1 functions as a substrate adaptor for a Cullin-dependent E3 ubiquitin ligase complex (Cullinan *et al.*, 2004; Furukawa *et al.*, 2005; Kobayashi *et al.*, 2004; Zhang *et al.*, 2004). Cullin proteins (in this case CUL3) act as molecular bridges, bringing together a substrate adaptor protein and substrate (in this case Keap1 and Nrf2, respectively) and the ring-box protein ROC1/RBX1, which recruits a ubiquitin-charged E2 protein (Pickart, 2001). Immunoprecipitation of Keap1 from established cell lines reveals association with CUL3 (Cullinan *et al.*, 2004; Furukawa *et al.*, 2005; Kobayashi *et al.*, 2004; Zhang *et al.*, 2004; Zhang *et al.*, 2005) and RBX1 (Furukawa *et al.*, 2005; Zhang *et al.*, 2004; Zhang *et al.*, 2005), and this association appears to occur via the BTB domain of Keap1 (Cullinan *et al.*, 2004; Furukawa *et al.*, 2005). Inhibition of CUL3 function, through expression of a dominant negative CUL3 mutant or targeted depletion by RNA interference (RNAi), results in a decrease in Nrf2 turnover, a concomitant increase in the basal levels of Nrf2 (Cullinan *et al.*, 2004; Furukawa *et al.*, 2005; Zhang *et al.*, 2004), and induction of an ARE-driven reporter transgene (Cullinan *et al.*, 2004). CUL3 associates with Nrf2, and promotes its ubiquitination (Cullinan *et al.*, 2004; Zhang *et al.*, 2004), but only through interaction with Keap1 (Cullinan *et al.*, 2004). Despite Nrf2 containing 39 lysines, compound mutation of the seven residues found within the Neh2 domain effectively abrogates Keap1-directed ubiquitination of

Nrf2 and increases its steady-state half-life threefold (Zhang *et al.*, 2004). Reversion of individual mutant residues back to lysines facilitates Nrf2 ubiquitination (Zhang *et al.*, 2004), indicating that the targeting of this subset of lysines within the Neh2 domain is critical for Keap1-mediated repression of Nrf2.

1.7.4.4 The role of Keap1 cysteine residues in the regulation of Nrf2 activity

The human and mouse Keap1 proteins contain 27 and 25 cysteines respectively, representing 4.3 and 4.0 % of the 624 total amino acids. This compares to the average occurrence of cysteine of 2.3 % across all human and mouse proteins (Miseta *et al.*, 2000). In light of this high cysteine content, and given its inhibitory influence over Nrf2, Keap1 was suggested as a putative 'sensor' for chemical/oxidative stress. Such a view was based on the following observations; a) although the array of phase II enzyme-inducing molecules is structurally diverse (Table 1.5), almost all are electrophilic (Prestera *et al.*, 1993a; Talalay *et al.*, 1988) and share a common capacity for modification of sulphydryl groups via alkylation, oxidation or reduction (Dinkova-Kostova *et al.*, 2001); b) the potency of benzylidene-alkanone and -cycloalkanone Michael acceptors (Dinkova-Kostova *et al.*, 2001) and heavy metals (Prestera *et al.*, 1993a) as inducers of phase II enzymes is related to their reactivity towards sulphydryl groups; c) the potency of isothiocyanate compounds as inducers of phase II enzymes mirrors their non-enzymatic second-order rate constants of conjugation with GSH (Prestera *et al.*, 1993a; Zhang, 2001); d) many of the cysteine residues in Keap1 have low predicted pKa values, and thus high relative reactivities, as they are flanked by one or more basic amino acid (arginine, lysine, histidine; Fig. 1.9), which stabilise cysteine in the more nucleophilic thiolate form ($-S^-$) (Snyder *et al.*, 1981). Notably, both Cys-273 and -297 are immediately preceded and followed by basic amino acids, and Cys-151, -257, -434 and -613 have two or more basic residues nearby in the primary structure (Fig. 1.9). Therefore, these residues are anticipated to be highly reactive towards electrophiles. This body of evidence implies that Keap1 functions as a 'sensor' for chemical/oxidative stress, and thus governs the adaptive cellular response to such stress.

Category	Example	Reference(s)
Alkenes	4-Hydroxynonenal	Chen *et al.* (2005b) Ishii *et al.* (2004) Zhang *et al.* (2006) Zhang *et al.* (2007a)
Arsenicals	Arsenite / arsenate	Aono *et al.* (2003) Gong *et al.* (2002) He *et al.* (2006) Pi *et al.* (2003)
Dithiolethiones	Oltipraz	Petzer *et al.* (2003) Ramos-Gomez *et al.* (2001)
Enones	Acrolein	Kwak *et al.* (2003) Tirumalai *et al.* (2002)
Isothiocyanates	Sulforaphane	Fahey *et al.* (2002) Jakubikova *et al.* (2006) Shinkai *et al.* (2006) Thimmulappa *et al.* (2002)
Mercaptans / disulphides	Diallyl disulphide	Chen *et al.* (2004) Fisher *et al.* (2007)
Michael acceptors	Diethylmaleate	Itoh *et al.* (1999)
Diphenols / quinones	*tert*-Butylhydroquinone	Lee *et al.* (2001b) Li *et al.* (2005)
Reactive oxygen / nitrogen species	Nitric oxide	Buckley *et al.* (2003) Dhakshinamoorthy *et al.* (2004) Liu *et al.* (2007)

Table 1.6 - Common classes of Nrf2-activating molecules.

```
                                 23                 38
  1 MQPEPKLSGA PRSSQFLPLW SKCPEGAGDA VMYASTECKA EVTPSQDGNR TFSYTLEDHT

 61 KQAFGVMNEL RLSQQLCDVT LQVKYEDIPA AQFMAHKVVL ASSSPVFKAM FTNGLREQGM

                                         151                     171
121 EVVSIEGIHP KVMERLIEFA YTASISVGEK CVLKVMNGAV MYQIDSVVKA CSDFLVQQLD

                                                             226
181 PSNAIGIANF AEQIGCTELH QRAREYIYMH FGEVAKQEEF FNLSHCQLAT LISRDDLNVR

    241      249       257                 273               288       297
241 CESEVFKACI DWVKYDCPQK RFYVQALLRA VRCHALTPRF LQTQLQKCEI LQADAKCKDY

                         319
301 LVQIFQELTL HKPTQAVPCK APKVGRLIYT AGGYFRQSLS YLEAYNPSNG SWLRLADLQV

361 PRSGLAGCVV GGLLYAVGGR NNSPDGNTDS SALDCYNPMT NQWSPCASMS VPRNRIGVGV

                   434
421 IDGHIYAVGG SKGCIHHSSV ERYEPERDEW HLVAPMLTRR IGVGVAVLNR LLYAVGGFDG

                                         513  518
481 TNRLNSAECY YPERNEWRMI TPMNTIRSGA GVCVLHNCIY AAGGYDGQDQ LNSVERYDVE

541 TETWTFVAPM RHHRSALGIT VHQGKIYVLG GYDGHTFLDS VECYDPDSDT WSEVTRMTSG

                  613
601 RSGVGVAVTM EPCRHQIDQQ NCTC
```

Fig. 1.9 - Mouse Keap1 cysteine residues with low predicted pKa values. The full-length mouse Keap1 protein sequence is shown. Cysteines are highlighted in blue. Basic amino acids flanking cysteine residues are highlighted in red. The residue numbers of cysteines flanked by basic amino acids are indicated.

1.7.4.4.1 Insights from site-directed mutagenesis studies

The extensive use of site-directed mutagenesis has served to highlight the critical roles of certain cysteine residues, particularly Cys-151, -273 and -288, in the function of Keap1 (Kobayashi *et al.*, 2006; Levonen *et al.*, 2004; Wakabayashi *et al.*, 2004; Zhang *et al.*, 2003a). Cys-151, which resides within the BTB domain of Keap1, appears to be important for the loss of Nrf2 repression and ubiquitination stimulated by chemical/oxidative stress (Zhang *et al.*, 2003a; Zhang *et al.*, 2004). As such, it would appear that Cys-151 is not integral to the function of Keap1 in the absence of chemical/oxidative stress, but is critical to its ability to respond to such conditions. In contrast, Cys-273 and -288, both located within the intervening region (IVR) of Keap1,

are essential for the repressive activity of the protein under basal conditions (Kobayashi *et al.*, 2006; Levonen *et al.*, 2004; Wakabayashi *et al.*, 2004; Zhang *et al.*, 2003a). Although mutation of Cys-273 and/or -288 to serine or alanine does not affect the association between Keap1 and CUL3 (Kobayashi *et al.*, 2004), it does render Keap1 unable to direct ubiquitination of Nrf2, inhibit the nuclear accumulation of the transcription factor, or repress transactivation of an ARE-driven reporter transgene (Kobayashi *et al.*, 2006; Levonen *et al.*, 2004; Wakabayashi *et al.*, 2004; Zhang *et al.*, 2003a). Furthermore, the responsiveness of Nrf2 to known activating molecules is diminished or abolished in cells expressing Keap1 Cys-273/288 mutants (Levonen *et al.*, 2004; Zhang *et al.*, 2003a). Notably, the mutation of other cysteines within the IVR, N-terminal and C-terminal domains has essentially no effect on Keap1 function (Wakabayashi *et al.*, 2004; Zhang *et al.*, 2003a). Interestingly, phylogenetic comparison of 34 Keap1-like proteins reveals that residues 273 and 288 are cysteines only in the six homologues (human, mouse, rat, zebrafish, *Drosophila* and mosquito) that are regarded as the stress 'sensing' sub-family of Keap1-related proteins (Zhang *et al.*, 2003b). Therefore, in light of the evidence discussed, the integrities of Cys-151, -273 and -288 are important for the function of Keap1, and these residues represent plausible targets for electrophilic inducers of Nrf2.

1.7.4.4.2 Evidence for the chemical modification of Keap1 cysteines

Compelling evidence for the chemical modification of Keap1 has been provided through the use of biotinylated analogues of Nrf2-activating molecules (Itoh *et al.*, 2004; Levonen *et al.*, 2004), spectroscopic binding experiments (Dinkova-Kostova *et al.*, 2002) and mass spectrometry (Dinkova-Kostova *et al.*, 2002). Exposure of HepG2 cells to the Nrf2-activating NSAID indomethacin alters the thiol oxidation state of ectopically-expressed FLAG-tagged Keap1, as demonstrated by a change in isoelectric point (pI) of FLAG-Keap1 subjected to isoelectric focussing, following reaction with iodoacetamide, which introduces a negative charge via alkylation of sulphydryl groups (Sekhar *et al.*, 2003). Furthermore, exposure of cells to low micromolar concentrations

of a biotinylated form of 15-deoxy-$\Delta^{12,14}$-prostaglandin J_2 (15d-PGJ_2), an endogenous cyclopentenone molecule with two electrophilic α,β-unsaturated carbonyl moieties, leads to the formation of adducts with Keap1 and an associated activation of Nrf2 (Itoh *et al.*, 2004; Levonen *et al.*, 2004).

In the only previous investigation to employ tandem mass spectrometry (MS/MS) as a tool to identify the residues in Keap1 targeted by a model electrophile, the thiol-reactive steroid dexamethasone 21-mesylate (dex-mes) was shown to preferentially modify Cys-257, -273, -288 and -297, located within the IVR domain, and the C-terminal Cys-613, of recombinant mouse Keap1 (Dinkova-Kostova *et al.*, 2002). It is important to note that this study used bacterially-expressed, purified Keap1 protein in which all cysteines were free for adduction, due to prior incubation with the reducing agent dithiothreitol (DTT). Hence, this study actually assessed the relative reactivities of Keap1 cysteines towards different electrophiles, and such *in vitro* observations cannot be directly extrapolated to a cellular context, particularly as it has yet to be demonstrated that, in its native environment, all cysteines in Keap1 are free sulphydryls. Nevertheless, a Keap1 protein in which Cys-257, -273, -288 and -297 are mutated to alanine binds dex-mes at 50 % of the rate of the wild-type protein *in vitro* (Wakabayashi *et al.*, 2004). Hence, although the current body of evidence suggests that modification of Keap1 cysteines may be an important triggering event in the activation of Nrf2, further characterisation of the residue selectivities of Nrf2-activating molecules, both *in vitro* and in a cellular context, is required to fully elucidate the role of Keap1 cysteine modification in the induction of adaptive cell defence.

1.7.4.5 The role of phosphorylation in the regulation of Nrf2 activity

Although the modification of, or at least the potential to modify, cysteine residues appears to be a common characteristic amongst Nrf2-activating molecules, the stimulation of phosphorylation signalling pathways may also underlie the ability of some molecules to induce Nrf2-dependent cell defence. Notably, the phosphatase inhibitor

okadaic acid, which promotes hyperphosphorylation (Cohen *et al.*, 1990), stimulates Nrf2 accumulation and ARE reporter transgene activation in HepG2 cells (Nguyen *et al.*, 2003). Although the majority of studies that have implicated phosphorylation as a regulatory influence on Nrf2 function have done so through the use of pharmacological inhibitors of specific protein kinases, which attenuate Nrf2 induction by known activating molecules, disparate studies have demonstrated direct phosphorylation of Nrf2 by protein kinase C (PKC) (Bloom *et al.*, 2003; Huang *et al.*, 2002; Nguyen *et al.*, 2000), extracellular signal-regulated kinase 1 (ERK-1) (Papaiahgari *et al.*, 2006) and protein kinase R-like endoplasmic reticulum kinase (PERK) (Cullinan *et al.*, 2003). In addition, several recent reports have described the phosphorylation of Nrf2, at Tyr-568, by the tyrosine kinase Fyn, an event that is required for the nuclear export of the transcription factor (Jain *et al.*, 2007; Jain *et al.*, 2006; Kannan *et al.*, 2006; Salazar *et al.*, 2006). Chemical inhibition or RNAi depletion of Fyn, or its upstream regulator glycogen synthase kinase 3β, appears to attenuate nuclear export of Nrf2 and augment ARE-driven gene transactivation (Jain *et al.*, 2007; Jain *et al.*, 2006; Kannan *et al.*, 2006; Salazar *et al.*, 2006). Hence, phosphorylation may be an important signalling event in both the activation and deactivation of Nrf2, through promotion of both nuclear accumulation and export, respectively.

At present, the general importance of phosphorylation in the regulation of Nrf2 activity is unclear. For instance, it is not known whether specific inducers stimulate specific kinase pathways, perhaps in a cell or species -dependent manner, or whether the simultaneous induction of numerous pathways is characteristic of all Nrf2-activating molecules. To demonstrate the ambiguity surrounding this issue, Table 1.7 provides a summary of protein kinases implicated in *tert*-butylhydroquinone (tBHQ) -induced Nrf2 activation. In light of these unresolved issues, current consensus regards the modification of cysteine residues within Keap1 as the most likely trigger for Nrf2-dependent cell defence.

Cell Type	Species	PKC	PI3K	p38	ERK	Reference
HepG2	Human	✓				Huang *et al.* (2000)
IMR-32	Human		✓		×	Lee *et al.* (2001a)
Neurons/glia	Mouse		✓			Johnson *et al.* (2002)
H4IIE	Rat		✓			Kang *et al.* (2002)
HepG2	Human	×			✓	Nguyen *et al.* (2003)
HepG2	Human	✓	×	×	×	Bloom *et al.* (2003)
Neurons/glia	Mouse		✓			Kraft *et al.* (2004)
Hepatic stellate cells	Rat		✓		×	Reichard *et al.* (2006)
Hepa-1c1c7	Mouse	✓				Lee-Hilz *et al.* (2006)

Table 1.7 - Summary of protein kinases implicated in Nrf2 activation by tBHQ. PKC, protein kinase C; PI3K, phosphatidyl inositol 3-kinase; p38, p38 mitogen-activated protein kinase; ERK, extracellular signal-regulated kinase; ✓ inhibition affects tBHQ-induced activation of the Nrf2-ARE pathway; × inhibition does not affect tBHQ-induced activation of the Nrf2-ARE pathway.

1.7.4.6 The 'hinge and latch' model of Nrf2 regulation by Keap1

The recently proposed 'hinge and latch' mechanism (Tong *et al.*, 2006b) of Nrf2 regulation advocates the continuous degradation of Nrf2, via its association with Keap1-CUL3, under basal conditions. Evidence suggests that Keap1 exists as a dimer in mammalian cells (McMahon *et al.*, 2006) and binds to Nrf2 in this form (i.e. two molecules of Keap1 per molecule of Nrf2) (Lo *et al.*, 2006; Tong *et al.*, 2006a; Wakabayashi *et al.*, 2004; Zipper *et al.*, 2002). Binding via the high-affinity ETGE motif (Kobayashi *et al.*, 2002), within the Neh2 domain of Nrf2, provides the 'hinge' through which the transcription factor can move in space relatively freely (McMahon *et al.*, 2006). Concomitant binding via the lower affinity DLG motif, also located within the Neh2 domain of Nrf2, provides the 'latch' that tightly restricts Nrf2 to enable optimal positioning of target lysines for conjugation with ubiquitin (McMahon *et al.*, 2006; Tong *et al.*, 2006a). In keeping with this, deletion of the ETGE motif attenuates the interaction between Nrf2 and Keap1 (Furukawa *et al.*, 2005; Kobayashi *et al.*, 2004; Kobayashi *et al.*, 2002), resulting in the stabilisation of Nrf2 (Furukawa *et al.*, 2005; Kobayashi *et al.*, 2004). In contrast, deletion of the DLG motif, or mutation of residues within, has no

effect on the association of Nrf2 and Keap1, but renders the latter unable to direct Nrf2 for degradation (McMahon *et al.*, 2006; McMahon *et al.*, 2004), also causing an increase in the stability of the transcription factor.

Although chemical inducers are capable of promoting the stabilisation and nuclear accumulation of Nrf2, evidence suggests that they do not evoke its complete dissociation from, nor impair its ability to associate with, Keap1 (Eggler *et al.*, 2005; Kobayashi *et al.*, 2006; Zhang *et al.*, 2003a; Zhang *et al.*, 2004). In fact, such Nrf2-activating molecules may increase the association of the transcription factor with Keap1 (He *et al.*, 2006; Hong *et al.*, 2005; Kobayashi *et al.*, 2006), most probably due to diminished degradation of Keap1-bound Nrf2. Notably, when *de novo* protein synthesis is inhibited by cyclohexamide, Nrf2 does not accumulate within the nuclei of cells exposed to diethylmaleate (Itoh *et al.*, 2003) or tBHQ (Kobayashi *et al.*, 2006). In the 'hinge and latch' model, the ubiquitination of Nrf2 is attenuated under conditions of chemical/oxidative stress (He *et al.*, 2006; Kobayashi *et al.*, 2006; Zhang *et al.*, 2004), and this is thought to be the result of disruption of the Nrf2-Keap1-CUL3 complex. This destabilisation is postulated to occur through loss of DLG motif binding, via a local conformational change in the IVR domain provoked by modification of critical cysteines, which leads to the improper spatial positioning of target lysines (McMahon *et al.*, 2006); further evidence for this is required, however. As a result of the destabilisation of the Nrf2-Keap1-CUL3 complex, the transcription factor is not directed for degradation, but remains associated with Keap1 via the ETGE motif. This leads to the saturation of Keap1, such that any newly-synthesised Nrf2 can evade Keap1 and accumulate within the nucleus, leading to the transactivation of ARE target genes (Tong *et al.*, 2006b). An overview of the 'hinge and latch' model of Nrf2 regulation is presented in Figure 1.10. In summary, the antioxidant response pathway, regulated by the transcription factor Nrf2, represents a major component of the cellular defensive machinery that serves to protect against chemical/oxidative stress.

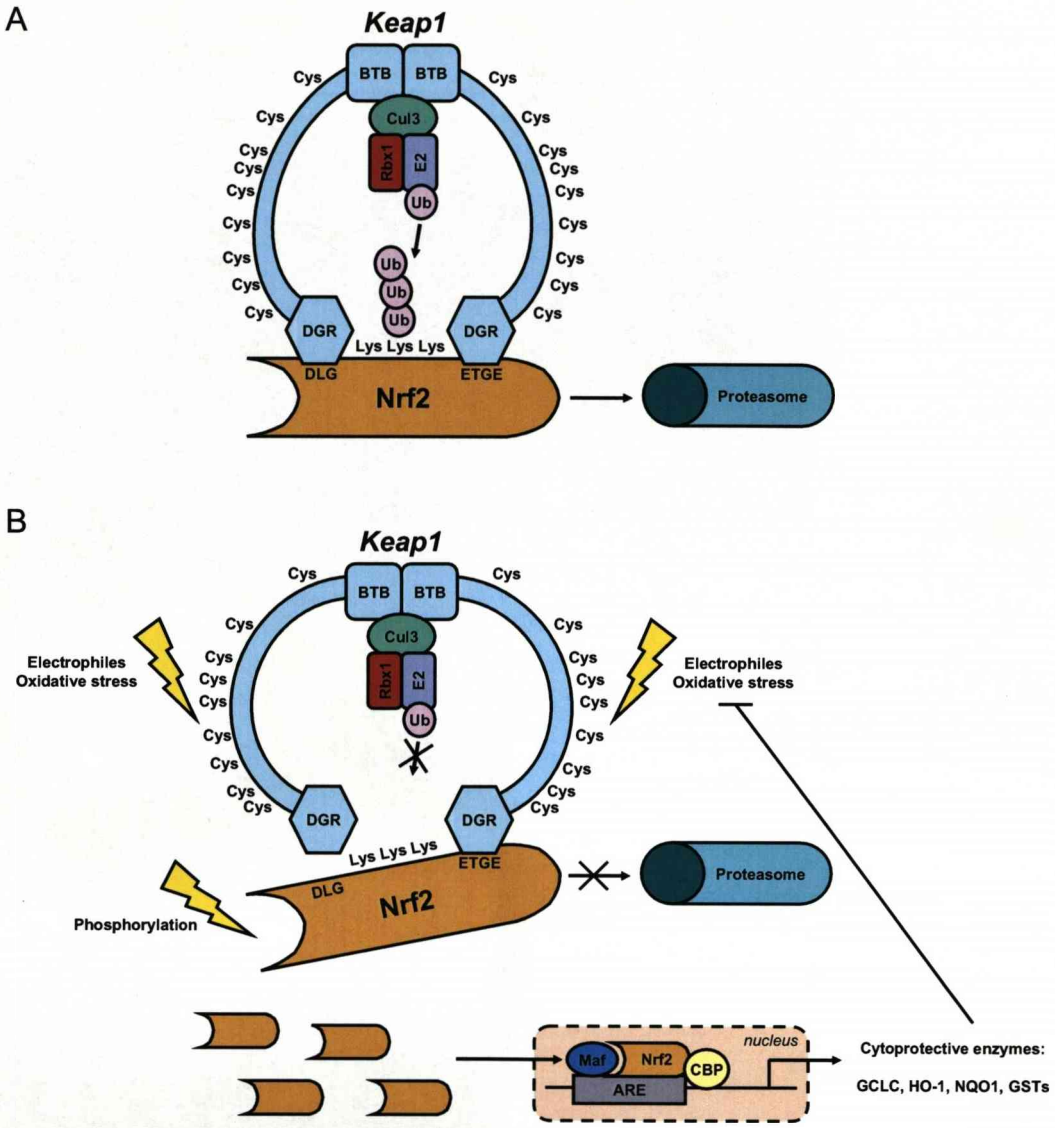

Figure 1.10 - Summary of the current 'hinge and latch' model of Nrf2 regulation. (A) In the absence of cellular stress, the Keap1 homodimer binds both the ETGE and DLG motifs of a single Nrf2 molecule, tightly positioning the transcription factor to enable the efficient transfer of ubiquitin, and thus directing Nrf2 for proteasomal degradation. (B) Under conditions of chemical/oxidative stress, binding through the low-affinity DLG 'latch' is perturbed, probably via a conformational change in Keap1 brought about through modification of one or more cysteine residues, whilst binding through the high-affinity ETGE 'hinge' is maintained. Although Nrf2 still associates with Keap1, the transcription factor is no longer held in the correct position to facilitate ubiquitin transfer, and thus Nrf2 is not directed for proteasomal degradation. As a result, Keap1 becomes saturated by Nrf2, and any newly-synthesised Nrf2 is able to accumulate within the nucleus and transactivate cytoprotective genes. Adapted from Tong *et al.* (2006b).

1.7.5 The coordinated regulation of transcription factor activity

Although the transcription factors highlighted in this section regulate the activity of discrete pathways in their own right, there is significant overlap between certain aspects of these pathways, particularly the signalling mechanisms that control their activation and the target genes that are induced as a result of an increase in transactivation. For example, GCL has been reported to be regulated by Nrf2, NF-κB and AP-1 (Lu, 1999). As such, the relative actions of several transcription factors may have a significant influence on the response, and eventual fate, of a cell following exposure to a given stimulus. Intriguingly, a number of transcription factors involved in the adaptive response to cellular stress appear to share a common means of control - the targeted ubiquitination, and consequent proteasomal degradation, of specific regulatory components, which represents a molecular switch that facilitates the rapid activation/inactivation of cytoprotective pathways (for a review, see Tong *et al.*, 2006b). For example, as discussed in section 1.7.4.3, Nrf2 is directed for proteasomal degradation in the absence of cellular stress, via association with its cytosolic repressor, Keap1. A similar mechanism inhibits the basal activity of HIF-1; the onset of hypoxia inhibits the O_2-dependent hydroxylation of HIF-1, perturbing recognition by its specific E3 ubiquitin ligase complex, and thus enabling an increase in its cytoprotective activity (Kallio *et al.*, 1999). On the other hand, the onset of ubiquitination signals the activation of the NF-κB pathway; upon the receipt of appropriate stimuli, NF-κB escapes repression following the ubiquitination and destruction of IκB (Hayden *et al.*, 2004). Hence, the transcriptional regulation of highly coordinated and, in some instances, overlapping signalling pathways endows cells with a multifaceted and inducible defence system.

1.8 THESIS AIMS

In light of the critical role played by transcription factors in the defence against toxic insult, an understanding of the molecular mechanisms that govern the adaptive response

to chemical/oxidative stress is vital to gain insights into the signalling events that determine the progression, and outcome, of adverse drug reactions such as DILI. The Nrf2-ARE pathway represents the major regulator of inducible cell defence, and deficiencies in this pathway may have a significant impact on the pathogenesis of DILI. As such, this thesis aims to investigate the role of the Nrf2-ARE pathway in DILI, by addressing key questions, namely; a) how important is the Nrf2-ARE pathway in the regulation of basal and inducible hepatic cell defence? b) is the Nrf2-ARE pathway activated by molecules that are known to cause DILI? c) do Nrf2 activators selectively modify cysteines within Keap1? d) does modification of Keap1 correlate with the activation of Nrf2 in cells? e) is there overlap between the Keap1 cysteine residues targeted by structurally-distinct Nrf2-activating molecules?

By increasing our appreciation of the role of the Nrf2-ARE pathway in the protection against DILI, it may be possible to develop a predictive toxicity screen, based on the activation of certain aspects of the pathway, for example, the adduction of Keap1 cysteines. In addition, the promise of manipulating the Nrf2-ARE pathway as a therapeutic strategy for the prevention and/or treatment of certain diseases is highly dependent upon advances in our understanding of the biochemistry that underlies this versatile cytoprotective system. Overall, therefore, this thesis aims to broaden our awareness of the role of the Nrf2-ARE pathway in the protection against DILI.

CHAPTER 2

Cell defence responses to N-acetyl-*p*-benzoquinoneimine and structurally distinct electrophiles

CONTENTS

2.1 INTRODUCTION

Mammalian cells can defend themselves against chemical and oxidative stress via the inducible expression of detoxification enzymes and antioxidant proteins (Prestera *et al.*, 1993b). A major regulator of this adaptive response is the transcription factor Nrf2, which controls the inducible expression of several cytoprotective genes (for a review, see Kensler *et al.*, 2007), through its action on the ARE regulatory motif (Wasserman *et al.*, 1997). Under non-stressed conditions, the activity of Nrf2 is repressed by Keap1 (Itoh *et al.*, 1999), a cysteine-rich protein which acts as a substrate adaptor for CUL3-dependent ubiquitination of Nrf2 (Kobayashi *et al.*, 2004), thereby directing the transcription factor for proteasomal degradation (McMahon *et al.*, 2003). Under conditions of chemical or oxidative stress, the negative regulation of Nrf2 is disrupted, enabling it to accumulate within the nucleus and transactivate target genes (Itoh *et al.*, 2003).

Research from this laboratory has previously shown that the Nrf2-ARE pathway is activated in mouse liver following administration of hepatotoxic and non-hepatotoxic doses of paracetamol, a model metabolism-dependent hepatotoxin (Goldring *et al.*, 2004). Paracetamol-induced hepatotoxicity, the single biggest cause of acute liver failure in both the UK (Davern *et al.*, 2006) and USA (Larson *et al.*, 2005), is inextricably linked to the formation of a chemically reactive metabolite, NAPQI (Fig. 2.1), which causes chemical and oxidative stress, and inhibits the function of critical proteins within hepatocytes (for a review, see Park *et al.*, 2005a). Whilst the molecular mechanisms underlying the activation of Nrf2 by chemical inducers are yet to be fully defined, it is clear that the Nrf2-ARE pathway is responsive to numerous chemicals that are all chemically reactive and capable of modifying sulphydryl groups (Dinkova-Kostova *et al.*, 2001). Given that NAPQI is known to react with cysteine thiols *in vitro* and *in vivo* (Hoffmann *et al.*, 1985a; Hoffmann *et al.*, 1985b), a plausible hypothesis to explain the activation of Nrf2 following paracetamol administration is that chemical modification of Keap1 cysteines by NAPQI perturbs its ability to repress the transcription factor.

The aims of the studies presented in this chapter were, firstly, to validate the Hepa-1c1c7 mouse liver cell line as a suitable model system for investigating the molecular regulation of the Nrf2-ARE pathway, using an RNAi approach to deplete cellular levels of Nrf2 or Keap1, and assess the effect of these changes on cell defence. Following the functional validation of Hepa-1c1c7, this cell line was used to examine the ability of the synthetic metabolite NAPQI to activate Nrf2 and stimulate adaptive cell defence; the latter was assessed by measuring levels of *Gclc* messenger RNA (mRNA) and GSH following direct exposure to the electrophile. The chemical, biochemical, and toxicological aspects of Nrf2 activation by NAPQI were further explored through the use of a panel of structurally distinct electrophiles. Specifically, two cysteine-reactive molecules were employed; 2,4-dinitrochlorobenzene (DNCB; Fig. 2.1), an aromatic electrophile that reacts with nucleophiles via bimolecular nucleophilic substitution (S_N2), leading to displacement of the halogen leaving group (chlorine), and 15-deoxy-$\Delta^{(12,14)}$-prostaglandin J_2 (15d-PGJ_2; Fig. 2.1), a cyclopentenone that reacts with nucleophiles via 1,4 addition. In order to explore the importance of cysteine reactivity and GSH depletion in the activation of Nrf2, these cysteine-reactive molecules were used in conjunction with trimellitic anhydride (TMA; Fig. 2.1), which acylates the amino group of lysine. As TMA lacks the *cis*-carbon-carbon double bond present in some anhydride molecules, the irreversible reaction with a sulphydryl group is not possible (de la Escalera *et al.*, 1989). Therefore, TMA is non-reactive towards cysteines in proteins and the sulphydryl group of GSH.

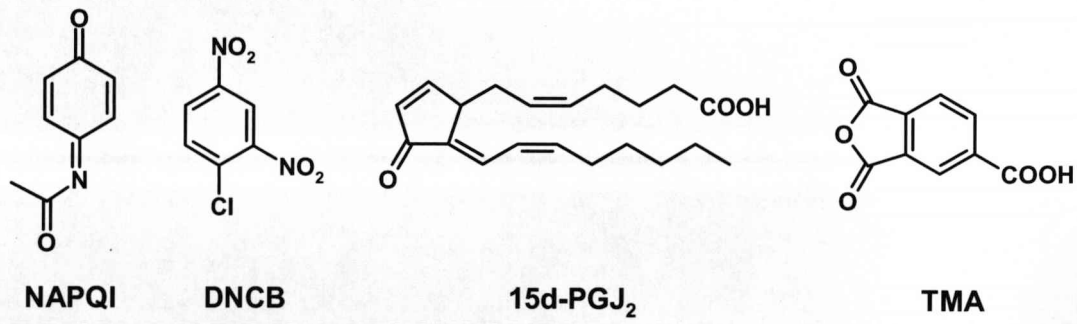

Fig. 2.1 - Chemical structures of NAPQI, DNCB, 15d-PGJ_2 and TMA.

2.2 METHODS

2.2.1 Materials and reagents

Nunclon Δ cell culture flasks, dishes and multi-well plates, and LabTek II chamber slides were from Nalge-Nunc International (c/o VWR International, Lutterworth, UK). DMEM and trypsin/versene were from Lonza Bioscience (Wokingham, UK). The Wilovert D6330 light microscope was from Will-Wetzlar (Wetzlar, Germany). 15d-PGJ_2 was from Alexis Biochemicals (Lausen, Switzerland). The rabbit anti-goat HRP-conjugated secondary antibody was from Dako (Ely, UK). The rabbit anti-sheep HRP-conjugated secondary antibody was from Calbiochem (Nottingham, UK). Protein assay dye reagent, Precision Plus protein Kaleidoscope standards, non-fat dry milk and the GS-710 calibrated imaging densitometer were from Bio-Rad (Hemel Hempstead, UK). FBS, NuPAGE Novex 4-12 % Bis-Tris gels, NuPAGE LDS sample buffer, sample reducing agent and antioxidant, the XCell Surelock mini-cell, the iBlot gel transfer device and transfer stacks, Alexa Fluor 594, Hoechst 33258, pCMV-SPORT β-galactosidase, Lipofectamine 2000 and RNasezap were from Invitrogen (Paisley, UK). TotalLab 100 software was from Nonlinear Dynamics (Newcastle, UK). Vectashield was from Vector Laboratories (Peterborough, UK). The SP2 AOBS confocal microscope was from Leica Microsystems (Milton Keynes, UK). The pGL3B-1016/*nqo*5'-*luc* reporter plasmids and rabbit anti-mouse Nrf2 primary antibody were kindly donated by Prof. John Hayes (Biomedical Research Centre, University of Dundee, UK). The sheep anti-Gclc primary antibody was kindly donated by Dr. Leslie McLellan (Biomedical Research Centre, University of Dundee, UK). GeneJuice was from Novagen (Nottingham, UK). Reporter lysis 5X buffer, the β-galactosidase Enzyme Assay System, the Bright-Glo Luciferase Assay System and QuantiLum recombinant luciferase were from Promega (Southampton, UK). The Cytotoxicity Detection Kit was from Roche Diagnostics (Burgess Hill, UK). The Nrf2, Keap1 and control siRNA duplexes were from Dharmacon (Lafayette, USA). The DU640 UV spectrophotometer was from Beckman Coulter (High Wycombe, UK). The TaqMan Reverse Transcription Kit, universal PCR master mix, and gene expression assay probes, MicroAmp optical

96-well reaction plates, the GeneAmp 9700 PCR system and the ABI PRISM 7000 sequence detection system were from Applied Biosystems (Warrington, UK). Absolute QPCR seals and the adhesive seal applicator were from ABgene (Epsom, UK). The FL600 fluorescence microplate reader was from BioTek Instruments (Winooski, USA). The MRX microplate reader was from Dynatech Laboratories (Billingshort, UK). The goat anti-Keap1 primary antibody was from Santa Cruz Biotechnology (Heidelberg, Germany). Western Lightening chemiluminescence reagents were from PerkinElmer, Beaconsfield, UK. Hyperfilm ECL was from Amersham (Little Chalfont, UK). Penicillin-streptomycin solution, Trypan Blue solution, NAPQI, DNCB, TMA, DMSO, Hank's balanced salt solution, BSA, spermidine, spermine, protease inhibitor cocktail, MOPS, the rabbit anti-actin primary antibody, the goat-anti rabbit HRP-conjugated secondary antibody, the Kodak BioMax MS intensifying screen, Kodak developer and fixer solutions, Ponceau S solution, Tween 20, PBS tablets, paraformaldehyde, DTNB, GSH, GSH reductase, NADPH, sulphosalicylic acid, chloroform DNase/RNase-free water and TRI reagent were from Sigma-Aldrich (Poole, UK). All other reagents were of analytical or molecular grade, and were from Sigma-Aldrich.

2.2.2 Cell culture

The mouse hepatoma cell line Hepa-1c1c7, which has been employed by others in previous studies of the Nrf2-ARE pathway (Jowsey *et al.*, 2003; McWalter *et al.*, 2004; Petzer *et al.*, 2003), was maintained in conventional growth medium (Dulbecco's modified Eagle's medium (DMEM) supplemented with 584 mg/L L-glutamine, 10 % fetal bovine serum (FBS), 100 U/mL penicillin and 100 μg/mL streptomycin). Cells were maintained in a humidified incubator, at 37 °C, in a 5 % carbon dioxide (CO_2) atmosphere. Cells were grown in 75 cm^2 Nunclon Δ culture flasks and routinely passaged every 3-4 days, at around 80 % confluency. Following a single wash with unsupplemented DMEM, cells were incubated for 1 min with 5 mL trypsin/versene at room temperature. Following the removal of the trypsin/versene, the cells were incubated for 5 min at 37 °C, sufficient time to enable the complete detachment of cells

from the flask surface. Detached cells were resuspended in 10 mL growth medium and passed three times through a 21-gauge needle, using a 10 mL syringe, to break up any cell clumps. For continuation, cells were re-seeded at a cells:growth medium ratio of 1:4.

For the analysis of nuclear Nrf2 content, cells were seeded onto 56.7 cm^2 Nunclon Δ culture dishes, at 5 x 10^6 cells/dish, in a total volume of 10 mL growth medium, and allowed to grow for 24 h. To ensure that an accurate number of cells were seeded, cells were counted using Trypan Blue solution (0.4 % w/v) and a haemocytometer. Briefly, cells were detached from the surface of a culture flask, as described above. A 45 μL aliquot of cells was combined with 5 μL Trypan Blue solution. 10 μL of this mixture was transferred to the edge of a haemocytometer and allowed to spread evenly across the surface by capillary action. Cells were visualised using the 20X objective of a Wilovert D6330 light microscope. Viable cells (those that did not take up the Trypan Blue dye) within the central 5 x 5 square (equivalent to 0.1 mm^3) were counted and the original cell density was calculated as follows:

Number of cells counted x 1.1 (to correct for dilution with Trypan Blue solution) = cells per 0.1 mm^3 x 10,000 = cells per 1 cm^3 = cells per 1 mL

2.2.3 Treatment of cells with electrophiles

Under sterile conditions, Hepa-1c1c7 cells, seeded onto 56.7 cm^2 Nunclon Δ culture dishes at 5 x 10^6 cells/dish the previous day, were washed once with unsupplemented DMEM, and then 9.95 mL unsupplemented DMEM was added to each dish. NAPQI, DNCB and TMA were dissolved, at 200x the required final concentration, in dimethyl sulphoxide (DMSO). As 15d-PGJ_2 was supplied pre-dissolved in methyl acetate, the solvent was removed by evaporation, under a gentle stream of nitrogen gas, immediately prior to each treatment. The solute was then reconstituted in DMSO, at 200x the required final concentration. To appropriate dishes of Hepa-1c1c7 cells, 50 μL DMSO

or electrophile were added (i.e. 1:200 dilution). The overall concentration of DMSO in the cell culture medium was 0.5 % (volume/volume; v/v). The cells were then returned to a humidified incubator (37 °C, 5 % CO_2) for the indicated period of time.

2.2.4 Preparation of cytosolic/nuclear fractions

Following treatment, cells were washed once with Hank's balanced salt solution, removed from the surface of the culture dish by scraping and resuspended in 1 mL buffer A (lysis; 50 mM NaCl, 10 mM 4-(2-hydroxyethyl)-1-piperazineethanesulfonic acid (HEPES), 1 mM ethylenediaminetetraacetic acid (EDTA), 0.5 mM sucrose, 0.5 mM spermidine, 0.15 mM spermine, 10 mM β-mercaptoethanol, 0.2 % (v/v) protease inhibitor cocktail, 0.2 % (v/v) Triton X-100). Lysates were clarified by centrifugation at 1150 g, 4 °C, for 5 min, and the supernatant retained as the cytosolic fraction. For the extraction of nuclear proteins, the pellet was washed in 0.5 mL buffer B (wash; 25 % (v/v) glycerol, 50 mM NaCl, 10 mM HEPES, 1 mM EDTA, 0.5 mM spermidine, 0.15 mM spermine, 10 mM β-mercaptoethanol, 0.2 % protease inhibitor cocktail) and centrifuged at 1150 g, 4 °C, for 5 min. Following removal of the supernatant, the pellet was resuspended in 0.1 mL buffer C (extraction; 0.35 M NaCl, 25 % (v/v) glycerol, 10 mM HEPES, 1 mM EDTA, 0.5 mM spermidine, 0.15 mM spermine, 10 mM β-mercaptoethanol, 0.2 % protease inhibitor cocktail) and incubated on ice for 30 min, to facilitate the osmotic extraction of nuclear proteins, which were isolated following a final centrifugation at 1150 g, 4 °C, for 5 min. All subcellular fractions were stored at -80 °C prior to analysis by Western blot.

2.2.5 Determination of protein content

The total protein content of subcellular fractions was determined using Protein Assay Dye Reagent, in accordance with the manufacturer's instructions. Based on the method of Bradford (1976), this assay relies on the binding of Coomassie Brilliant Blue G-250

dye to basic and aromatic amino acids, an event that results in a change in colour of the dye (red to blue), and a consequent change in absorbance maximum from 465 to 595 nm. Hence, the increase in absorbance at 570 nm, measured using a MRX microplate reader, is proportional to the amount of bound dye, and thus to the amount of protein present. A standard curve, ranging from 0.25-5 μg bovine serum albumin (BSA), was used to calculate sample protein content.

2.2.6 Western blot analysis

Nuclear (5 μg) or cytosolic (15 μg) protein fractions were denatured via the addition of 5 μL loading buffer (70 % (v/v) NuPAGE sample loading buffer, 30 % (v/v) NuPAGE reducing agent) and incubated at 80 °C for 5 min. Samples were loaded onto pre-cast 4-12 % NuPAGE Novex bis-tris polyacrylamide gels, alongside PrecisionPlus protein Kaleidoscope standards. Samples were resolved by electrophoresis in a XCell Surelock mini-cell, using a 3-(N-morpholino)propanesulphonic acid (MOPS) running buffer (50 mM MOPS, 50 mM Tris base, 3.5 mM sodium dodecyl sulphate, 1 mM EDTA, 0.25 % (v/v) NuPAGE antioxidant), at 90 V for 10 min, followed by 60 min at 170 V. Separated proteins were transferred to nitrocellulose membranes using the iBlot dry blotting system, in accordance with the manufacturer's instructions. To ensure the transfer process was successful, membranes were stained for 10 sec with Ponceau S solution. Membranes were blocked for 15 min, on an orbital shaker, in tris-buffered saline (TBS; 0.15 M NaCl, 25 mM Tris base, 3 mM KCl, pH 7.0) containing 0.1 % (v/v) Tween 20 and 10 % (weight/volume; w/v) non-fat dry milk. Blocked membranes were probed for 1 h with rabbit anti-mouse Nrf2 (1:5000 in TBS-Tween containing 2 % (w/v) BSA), goat anti-Keap1 (1:2000 in TBS-Tween containing 2 % (w/v) non-fat dry milk) or sheep anti-Gclc (1:5000 in TBS-Tween containing 2 % (w/v) non-fat dry milk) primary antisera. Following several washes in TBS-Tween, membranes were probed for 1 h with goat anti-rabbit (1:10,000 in TBS-Tween containing 2 % (w/v) BSA), rabbit anti-goat (1:3000 in TBS-Tween containing 2 % (w/v) non-fat dry milk) or rabbit anti-sheep (1:10,000 in TBS-Tween containing 2 % (w/v) non-fat dry milk) horseradish peroxidase

(HRP) -conjugated secondary antisera. Immunoblots were visualised with Western Lightening chemiluminescence reagents and exposed to Hyperfilm ECL under darkroom conditions, using a Kodak BioMax MS intensifying screen. Blots were developed using Kodak developer and fixer solutions. In order to ensure equal loading across gels, membranes were probed with rabbit anti-β-actin primary (1:5000 in TBS-Tween containing 2 % (w/v) BSA) and goat anti-rabbit HRP-conjugated secondary antisera. Recombinant mouse Nrf2 or mouse Keap1, or mouse liver lysate (Gclc standard), were loaded as standards to confirm antibody specificity. Films were scanned using a GS-710 calibrated imaging densitometer, immunoreactive band volumes were quantified using TotalLab 100 software, in accordance with the manufacturer's instructions, and normalised to β-actin.

2.2.7 Confocal microscopy

Hepa-1c1c7 cells were seeded onto Lab-TEK II chamber slides, at 2 x 10^5 cells/chamber, 24 h prior to treatment. Treatments were performed essentially as described in section 2.2.3. Following treatment, cells were washed via 2 x 3 min incubations with 0.5 mL of 1X phosphate-buffered saline (PBS; 0.137 M NaCl, 10 mM Na_2HPO_4, 1.8 mM KH_2PO_4, 2.7 mM KCl, pH 7.4). The removal of media from the chambers was achieved by inverting the slide and gently tapping onto a paper towel, to avoid dislodging cells through repeated pipetting. Cells were fixed in 0.5 mL fresh 4 % (w/v) paraformaldehyde at 4 °C for 30 min, followed by 4 x 3 min washes with 0.5 mL PBS. Fixed cells were permeabilised with 0.3 mL of 0.2 % (v/v) Triton X-100, quenched with 0.3 mL of 0.1 M glycine and blocked with 0.3 mL of 10 % (v/v) FBS, for 10 min each. Cells were then incubated with 0.2 mL of 2 % (v/v) FBS containing anti-mouse Nrf2 antiserum (1:500) at 37 °C for 1 h. Following 3 x 3 min washes with 0.5 mL PBS, cells were incubated with 0.2 mL of 2 % (v/v) FBS containing 8 μg/mL Alexa Fluor 594-conjugated goat anti-rabbit IgG, at 37 °C for 1 h. To prevent bleaching of the fluorescent signal, during this and subsequent steps, the chamber slide was wrapped in aluminium foil. Cells were washed for 3 x 3 min with 0.5 mL PBS and nuclear DNA

was counterstained at room temperature, for 10 min, with 0.2 mL PBS containing 2 μg/mL Hoechst 33258. Cells were washed with 0.5 mL PBS for 3 x 3 min. Chambers were carefully detached from slides, using the splitting tool provided by the manufacturer, and slides were allowed to dry at room temperature for 5 min. Coverslips were mounted using VectaShield hard-set medium, in accordance with the manufacturer's instructions. Slides were wrapped in aluminium foil and stored at 4 °C prior to confocal analysis. Immunofluoresence was visualised using a SP2 AOBS confocal microscope, with a 63X 1.4 oil objective. A total of five separate fields were evaluated for each treatment group (representative fields are presented).

2.2.8 Analysis of mouse *Nqo1* ARE reporter transgene activity

Hepa-1c1c7 cells were seeded onto 96-well plates, at 2 x 10^4 cells/well, 24 h prior to transfection. Cells were then transfected for 24 h with 100 ng of either pGL3B-1016/*nqo5'-luc* wild-type reporter plasmid or a mutant plasmid containing an entirely scrambled ARE sequence, as previously described by Nioi *et al.* (2005). pGL3B-1016/*nqo5'-luc* represents the pGL3 basic luciferase vector into which a 1016 bp 5'-upstream region of the mouse *Nqo1* gene has been subcloned, enabling ARE-mediated regulation of modified firefly luciferase gene expression. To control for any differences in the amount of reporter plasmid DNA transfected between wells, all cells were co-transfected with 100 ng of pCMV SPORT-β-galactosidase plasmid, in which the *E. coli* β-galactosidase gene is under the control of the upstream cytomegalovirus (CMV) promoter. Transfections were performed using GeneJuice reagent, in accordance with the manufacturer's instructions. For treatments, cells were washed once with unsupplemented DMEM, and then 199 μL unsupplemented DMEM was added to each well. NAPQI was dissolved, at 200x the required final concentration, in dimethyl sulphoxide (DMSO) and 1 μL was added to appropriate wells (i.e. 1:200 dilution). The overall concentration of DMSO in the cell culture medium was 0.5 % (v/v). The cells were then returned to a humidified incubator (37 °C, 5 % CO_2) for the indicated period of time. Following treatment, the media was removed and cells were lysed *in situ* with

0.1 mL of 1X Reporter Lysis Buffer. Lysates (20 μL) were transferred to a white 96-well plate and 20 μL Bright-Glo Luciferase Assay Reagent was added. 15 μg QuantiLum recombinant firefly luciferase was used as a positive control for the assay. Air bubbles were removed via brief centrifugation of the plate at 3000 revolutions per minute (rpm). Firefly luciferase activity was measured immediately on a FL600 fluorescence microplate reader, adapted to measure luminescence. Blank readings were obtained from wells containing 1X Reporter Lysis Buffer and Bright-Glo Reagent, and subtracted from sample readings. The β-Galactosidase Enzyme Assay System was used to measure β-galactosidase activity within the lysates; a separate 20 μL aliquot of each lysate was transferred to a clear 96-well plate, combined with 20 μL of 2X Assay Buffer, and incubated at 37 °C for 30 min. 1 unit (U) recombinant β-galactosidase was used as a positive control for the assay. The reaction was stopped by the addition of 60 μL of 1 M sodium carbonate. Air bubbles were removed via brief centrifugation of the plate at 3000 rpm. β-Galactosidase activity was measured at 405 nm, on a MRX microplate reader. Blank readings were obtained from wells containing 1X Reporter Lysis Buffer and 1X Assay Buffer, and subtracted from sample readings. Luciferase activity was normalised to β-galactosidase activity for all samples, to control for transfection efficiency.

2.2.9 Determination of total glutathione levels

Total GSH content was quantified using the 5,5′-dithiobis(2-nitrobenzoic acid) (DTNB) -GSH reductase recycling method, as previously described by Vandeputte *et al.* (1994), whereby:

1) $2GSH + DTNB \rightarrow GSSG + TNB$

2) $GSSG + NADPH + H^{+} \rightarrow 2GSH + NADP^{+}$ *(catalysed by GSH reductase)*

In this method, GSH is oxidised by DTNB to yield GSSG and the 5-thio-2-nitrobenzoic acid (TNB) chromophore, which has an absorbance maximum of 412 nm. Thus, the rate

of formation of TNB, as followed at 405 nm, is proportional to the sum of GSH and GSSG present in each sample. Briefly, cells in 24-well plates (seeded at 2 x 10^5 cells/well) were harvested by scraping in 0.125 mL of 10 mM HCl. Appropriate aliquots were taken to enable the determination of total protein content, as described in section 2.2.5. To the remaining samples, sulphosalicylic acid was added to a final concentration of 1.3 % (w/v), and protein precipitation was facilitated by incubating on ice for 10 min. Protein was pelleted by centrifugation at 18,000 g for 5 min. 20 μL supernatant was transferred to a clear 96-well plate, and combined with 20 μL assay buffer (0.143 M NaH_2PO_4, 6.3 mM EDTA, pH 7.4) to neutralise pH. Samples were incubated, at room temperature, with 0.2 mL assay reagent (1.0 mM DTNB, 0.34 mM NADPH, in 0.143 M NaH_2PO_4, 6.3 mM EDTA, pH 7.4) for 5 min. The enzymatic reaction was initiated by the addition of 0.35 U GSH reductase and followed kinetically at 405 nm for 5 min on a MRX microplate reader. The rate of TNB formation was calculated as the change in absorbance min^{-1}. Sample GSH concentrations were calculated via reference to a standard curve ranging from 1-50 nmol/mL GSH. The GSH concentration for each sample was normalised to total protein content.

2.2.10 Determination of lactate dehydrogenase leakage

Overt cytotoxicity was assessed by measuring the leakage of the cytoplasmic enzyme lactate dehydrogenase (LDH) into the cell culture media. LDH reduces NAD^+ to NADH + H^+, via the oxidation of lactate to pyruvate. The transfer of 2H from NADH + H^+ to the tetrazolium salt 2-[4-iodophenyl]-3-[4-nitrophenyl]-5-phenyltetrazolium chloride by a catalyst (diaphorose) yields a formazan dye with an absorbance maximum of 500 nm:

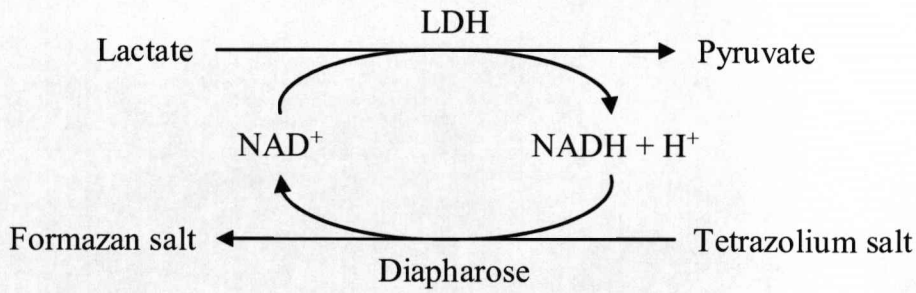

Thus, the amount of formazan formed over time is directly proportional to the LDH activity in the culture media, and therefore correlates to the degree of cell death. As the leakage of LDH is particularly indicative of the degree of membrane damage, it is typically used as a marker of cellular necrosis.

Hepa-1c1c7 cells were seeded onto 96-well plates at 1 x 10^4 cells/well and treated as described in section 2.2.3. Following treatment, the plate was briefly centrifuged at 3000 rpm to pellet cells, and the cell-free culture media was removed to a new 96-well plate. Cells were lysed via the addition of 40 μL DMEM containing 2 % (v/v) Triton X-100, followed by centrifugation at 3000 rpm for 5 min. 50 μL cell-free culture media (diluted 1:4 in DMEM) and cell lysate (diluted 1:20 in DMEM) were separately transferred to new 96-well plates. LDH leakage was measured using a Cytotoxicity Detection Kit; 50 μL assay reagent (1 μL catalyst per 45 μL dye solution) was then added to each well. Following incubation in the dark for 30 min, air bubbles were removed via brief centrifugation of the plates at 3000 rpm. Formazan salt formation was measured at 490 nm on a MRX microplate reader. Blank readings were obtained from wells containing 50 μL DMEM, and subtracted from sample readings. LDH leakage from cells into the culture media (extracellular) is expressed as a percentage of total LDH (intracellular plus extracellular).

2.2.11 RNA interference

Depletion of Nrf2 or Keap1 in Hepa-1c1c7 cells was achieved by RNAi, which exploits a natural cellular process that facilitates the post-transcriptional silencing of specific genes, through the targeted degradation of mRNA (for a review, see Novina *et al.*, 2004). RNAi is typically triggered when a cell encounters a long double-stranded RNA (dsRNA) molecule (Fig. 2.2) (Fire *et al.*, 1998). The dsRNA is cleaved into smaller fragments, called short interfering RNAs (siRNA), by the enzyme Dicer (Bernstein *et al.*, 2001). siRNA molecules are 21-23 nucleotide strands of dsRNA, with symmetric 3' overhangs of 2-3 nucleotides in length, and 5'-phosphate and 3'-hydroxyl groups

(Elbashir *et al.*, 2001b). The sense strand of the siRNA is degraded, whilst the antisense strand becomes incorporated into an RNA-induced silencing complex (RISC), which then targets complementary mRNA sequences for destruction (Fig. 2.2) (Hammond *et al.*, 2000). As a result of this mRNA destruction, no protein is translated. Hence, gene expression is effectively silenced in a post-transcriptional manner. As such, RNAi has proved to be a major advance in the field of biomedical research, and the targeted silencing of a large number of genes is now possible through the widespread availability of synthetic siRNA molecules (Elbashir *et al.*, 2001a).

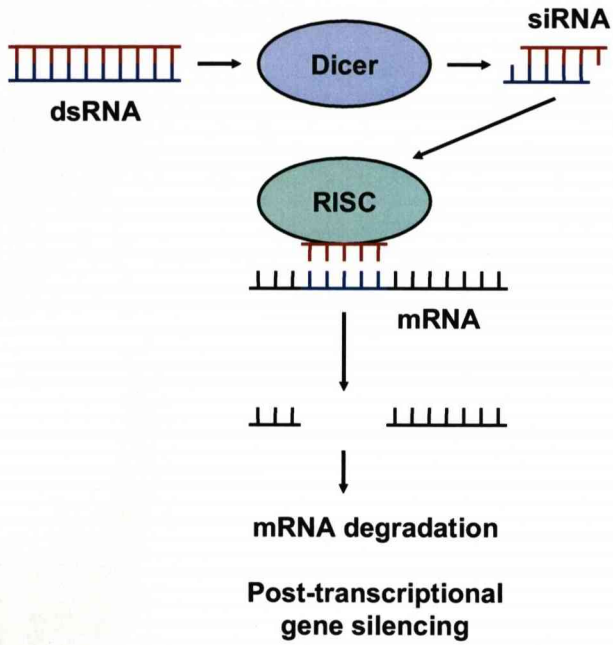

Fig. 2.2 - Overview of RNAi pathway. The endogenous RNAi pathway is typically triggered when a cell encounters a long double-stranded RNA (dsRNA) molecule. The dsRNA is cleaved into smaller short interfering RNAs (siRNA) by the enzyme Dicer. The sense strand of the siRNA is degraded, whilst the antisense strand becomes incorporated into an RNA-induced silencing complex (RISC), which then targets complementary mRNA sequences for destruction. As a result of this mRNA destruction, no protein is translated, and gene expression is effectively silenced in a post-transcriptional manner.

Predesigned siRNA duplexes targeted against mouse *Nrf2* (si-Nrf2) or *Keap1* (si-Keap1), and a scrambled, non-targeting control siRNA duplex (si-Con), were purchased from Dharmacon's siGENOME library. The siRNA duplex sequences were as follows;

si-Nrf2 #1 sense 5'-GCA AGA AGC CAG AUA CAA AUU-3', antisense 5'-P UUU GUA UCU GGC UUC UUG CUU-3'; si-Nrf2 #2 sense 5'-AGA CUC AAA UCC CAC CUU AUU-3', antisense 5'-P UAA GGU GGG AUU UGA GUC UUU-3'; si-Keap1 #1 sense 5'-GAA GCA AAU UGA UCA ACA AUU-3', antisense 5'-P UUG UUG AUC AAU UUG CUU CUU-3'; si-Keap1 #2 sense 5'-GCU AUG ACC CGG ACA GUG AUU-3', antisense 5'-P UCA CUG UCC GGG UCA UAG CUU-3', si-Con sense 5'-AUG UAU UGG CCU GUA UUA GUU-3', antisense 5'-P CUA AUA CAG GCC AAU ACA UUU-3'. Hepa-1c1c7 cells were seeded onto 12-well plates at 2.5 x 10^5 cells/well for RNA isolations, or 24-well plates at 1.25 x 10^5 cells/well for all other experiments, and allowed to grow for 6 h. Cells were transfected with 10 nM siRNA for 48 h, using Lipofectamine 2000, in accordance with the manufacturer's instructions.

2.2.12 RNA isolation

Total RNA was isolated from Hepa-1c1c7 cells using TRI reagent, an acidic solution containing guanidinium thiocyanate, sodium acetate, phenol and chloroform, which enables centrifugal separation of RNA from DNA and protein {Chomczynski, 1987 #724}. All surfaces and equipment were rendered RNase-free, by wiping with RNasezap, prior to the isolation of RNA. Briefly, cells in 12-well plates were harvested in 0.5 mL TRI reagent per well, transferred to RNase-free microcentrifuge tubes and incubated at room temperature for 5 min. Working inside a laminar flow cabinet, 0.1 mL chloroform was added to all samples, which were then vortexed for 15 sec and incubated at room temperature for 2 min. Following centrifugation at 12,000 g, 4 °C, for 15 min, the RNA-containing clear aqueous phase was removed to a new RNase-free microcentrifuge tube, combined with 0.25 mL isopropyl alcohol, and incubated at room temperature for 10 min, to precipitate RNA. Following centrifugation at 12,000 g, 4 °C, for 10 min, the RNA pellet was washed in 0.5 mL DNase/RNase-free water containing 75 % (v/v) ethanol. RNA was pelleted at 12,000 g, 4 °C, for 5 min; the supernatant was discarded and the pellet allowed to air-dry, at room temperature, for 10 min. The dried

RNA pellet was reconstituted in 25 μL DNase/RNase-free water and incubated at 55 °C for 2 min. RNA was stored at -80 °C until required.

2.2.13 Determination of RNA quantity and purity

RNA concentration and purity were assessed using a DU640 ultraviolet (UV) spectrophotometer. RNA was diluted 1:100 in 1X TE buffer (10 mM Tris base, 1 mM EDTA, pH 7.5); the latter was used to blank the spectrophotometer. From the average of triplicate measurements, and given that an absorbance of 1.0 at 260 nm equates to 40 μg/mL RNA, the concentration of RNA in each sample was determined as follows:

Absorbance at 260 nm x 100 (to correct for dilution) x 40 = RNA concentration (μg/mL)

The purity of RNA in each sample was determined via reference to the 260:280 nm ratio, as protein is detected at 280 nm. RNA samples with a 260:280 nm ratio of below 1.7 were rejected as impure.

2.2.14 cDNA synthesis

RNA was reverse-transcribed to cDNA using the TaqMan Reverse Transcription Kit. Reactions (20 μL) contained 2 μg RNA, 0.7X reverse transcription buffer, 3.6 mM $MgCl_2$, 2.9 mM deoxyribonucleotide triphosphate (dNTP), 1.8 μM random hexamers, 14.4 U RNase inhibitor and 36.0 U RTase multiscribe. Reverse-transcription was performed using the GeneAmp 9700 polymerase chain reaction (PCR) system, with reactions held for 10 min at 25 °C, followed by 30 min at 48 °C.

2.2.15 TaqMan real-time PCR

cDNA (1 μL, approximately 0.1 μg) was combined with 10 μL of 2X TaqMan Universal PCR Master Mix, 1 μL of the appropriate Gene Expression Kit, pre-optimised by Applied Biosystems for detection of mouse *Nrf2* (Mm00477784_m1), *Gclc* (Mm00802655_m1) or the housekeeping gene β_2 microglobulin (*β_2M*; Mm00437762_m1), and 8 μL DNase/RNase-free water, in a clear MicroAmp optical 96-well reaction plate. Plates were sealed with Absolute QPCR seals, using an adhesive seal applicator, and briefly centrifuged at 3000 rpm to remove air bubbles. Gene expression was analysed by quantitative real-time PCR on an ABI PRISM 7000 Sequence Detection System, in accordance with the manufacturer's instructions. Levels of *Nrf2* and *Gclc* gene expression were calculated via reference to standard curves ranging from 1-300 ng cDNA, and normalised to *β_2M*.

2.2.16 Data analysis

Where appropriate, experiments were performed at least in duplicate, and all experiments were replicated on separate occasions. Data are expressed as mean ± standard deviation of the mean (SD). One-way analysis of variance (ANOVA), with Dunnett's post-test applied, was used to assess the significance of any differences in the data compared to appropriate controls. A two-sided P value of ≤ 0.05 was considered to be statistically significant.

2.3 RESULTS

2.3.1 Validation of Hepa-1c1c7 as a model for studying the Nrf2-ARE pathway

In order to ascertain that the Hepa-1c1c7 cell line was a valid model for studying the Nrf2-ARE pathway, the functional operation of this pathway was determined using an RNAi approach. siRNA duplexes targeting two distinct regions of the mouse *Nrf2* (si-Nrf2 #1 and #2) or mouse *Keap1* (si-Keap1 #1 and #2) transcripts were designed. The introduction of a siRNA duplex into a cell can cause off-target effects, typically due to activation of non-specific innate immune responses, such as the interferon response (Bridge *et al.*, 2003; Sledz *et al.*, 2003), or because of inadvertent complementarity to non-target mRNA sequences. Aversion of the latter off-target effect is fairly straightforward; database search engines, such as BLAST (Basic local alignment search tool; http://www.ncbi.nlm.nih.gov/blast/Blast.cgi), can be used to examine all known mRNA sequences for complementarity to candidate siRNA target sequences. Such a procedure was performed for all of the siRNA duplexes used in this study; no complementarity with non-target mRNA sequences was found. Other off-target effects, such as activation of the interferon response, are typically observed following the introduction of siRNA into cells at relatively high concentrations, particularly $\geq$ 100 nM (Persengiev *et al.*, 2004; Semizarov *et al.*, 2003). Therefore, it is important to optimise the amount of siRNA transfected into cells in order to achieve a final concentration that enables maximal target gene depletion with minimal off-target effects. To this end, preliminary optimisation experiments were performed, using a range of siRNA concentrations between 1-100 nM, and it was determined that for each of the siRNA duplexes, transfecting Hepa-1c1c7 cells for 48 h with 10 nM siRNA provided considerable depletion of the respective target gene, without noticeably affecting the cellular mRNA level of the housekeeping gene β_2M (Nrf2 analysis; Fig. 2.3) or the protein level of the cytoskeletal protein β-actin (Keap1 analysis; data to be presented in Mr. Alvin Chia's thesis). Transfection of Hepa-1c1c7 cells with Nrf2 or Keap1 siRNA did not result in any major changes in cell viability or morphology, as determined by visual assessment using a light microscope (data not shown). Using siRNA at

concentrations below 20-30 nM is generally considered to be unlikely to stimulate non-specific innate immune responses and/or other off-target effects (Persengiev *et al.*, 2004; Semizarov *et al.*, 2003).

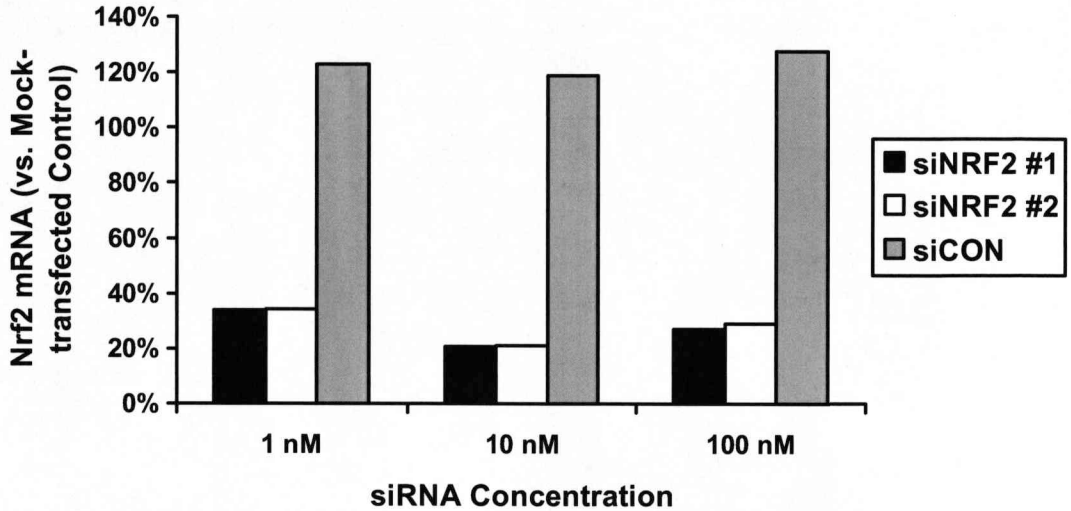

Fig. 2.3 - Preliminary analysis of *Nrf2* mRNA depletion by RNAi. Hepa-1c1c7 cells were mock-transfected, or transfected with 1, 10 or 100 nM of one of two Nrf2-targeting siRNA duplexes (si-Nrf2 #1 or #2), or a scrambled, non-targeting control siRNA duplex (si-Con), for 48 h. Total RNA was isolated, reverse-transcribed to cDNA and *Nrf2* gene expression was measured by TaqMan real-time PCR. Results are normalised to the housekeeping gene β_2 microglobulin, and are expressed relative to the mock-transfected *Nrf2* mRNA level, which was arbitrarily set at 100 %. Bars represent the mean mRNA level from duplicate transfections, n=1.

2.3.1.1 RNAi depletion of Nrf2 and Keap1

Due to the difficulties in detecting endogenous Nrf2 protein in the absence of cellular stress, RNAi depletion of the transcription factor was confirmed by measuring *Nrf2* mRNA. Transfection of Hepa-1c1c7 cells with the siRNA duplexes targeted against the *Nrf2* transcript resulted in a depletion of the transcription factor mRNA to 23.0 ± 3.0 % (si-Nrf2 #1) or 25.4 ± 2.3 % (si-Nrf2 #2) of the mock-transfected control level (Fig. 2.4). In contrast, a scrambled, non-targeting control siRNA duplex (si-Con) had no discernible effect on *Nrf2* mRNA (Fig. 2.4), demonstrating that the observed depletion of *Nrf2* mRNA was not simply due to activation of the RNAi pathway *per se*, but due to

sequence-specific targeting of the *Nrf2* transcript. Notably, none of the siRNA duplexes significantly affected the mRNA level of the housekeeping gene β_2M, demonstrating a lack of non-target effects.

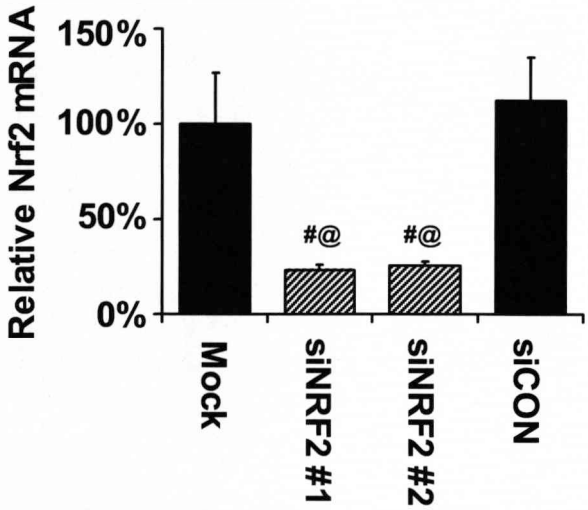

Fig. 2.4 - RNAi depletion of *Nrf2* mRNA. Hepa-1c1c7 cells were mock-transfected, or transfected with 10 nM of one of two *Nrf2*-targeting siRNA duplexes (si-Nrf2 #1 or #2), or a scrambled, non-targeting control siRNA duplex (si-Con), for 48 h. Total RNA was isolated, reverse-transcribed to cDNA and *Nrf2* gene expression was measured by TaqMan real-time PCR. Results are normalised to the housekeeping gene β_2 microglobulin, and are expressed relative to the mock-transfected *Nrf2* mRNA level, which was arbitrarily set at 100 %. One-way ANOVA, # P <0.001 versus mock, @ P <0.001 versus si-Con. Error bars = standard deviation of mean, n=3.

At the same time that RNAi depletion of *Nrf2* was confirmed in Hepa-1c1c7 cells, a laboratory colleague, Mr. Alvin Chia, successfully optimised the depletion of *Keap1* using targeted siRNA duplexes. At a concentration of 10 nM, both siRNA duplexes targeted against the *Keap1* transcript caused a considerable depletion of the protein to below 35 % of the levels in mock-transfected cells (data to be presented in Mr. Alvin Chia's thesis). The specificity of these changes was demonstrated by the fact that si-Con had no effect on Keap1 protein level, and that neither *Keap1*-targeting siRNA duplex had any discernible effect on levels of β-actin (data to be presented in Mr. Alvin Chia's thesis). Importantly, in light of the fact that Keap1 is known to repress the basal activity

of Nrf2, in part by tethering it within the cytosol, and therefore restricting the access of the transcription factor to the nucleus (Dhakshinamoorthy *et al.*, 2001; Itoh *et al.*, 1999), it was shown that RNAi depletion of *Keap1* resulted in a concomitant increase in the nuclear level of Nrf2 protein, compared with the mock-transfected control level (data to be presented in Mr. Alvin Chia's thesis). These results demonstrate that Keap1 serves as a functional repressor of Nrf2 in Hepa-1c1c7 cells.

2.3.1.2 Effect of RNAi depletion of Nrf2 or Keap1 on the basal expression of GCLC

In order to confirm that Nrf2 controls the expression of ARE-regulated genes in Hepa-1c1c7 cells, the effect of RNAi depletion of the transcription factor, or *Keap1*, on the expression of Gclc, a typical ARE-regulated cytoprotective enzyme (Chan *et al.*, 2000; Jeyapaul *et al.*, 2000; Sekhar *et al.*, 2000; Wild *et al.*, 1999), was assessed by Western blot. Targeted depletion of *Nrf2* decreased the basal protein level of Gclc by 20-30 % compared to mock-transfected cells (Fig. 2.5), whereas depletion of *Keap1*, which results in the nuclear accumulation of Nrf2 under resting conditions, increased Gclc protein level by 50-60 % (Fig. 2.5). These results demonstrate that Nrf2 regulates the expression of an important ARE-containing gene in Hepa-1c1c7, and that Keap1 antagonises this activity, probably through repression of the transcription factor.

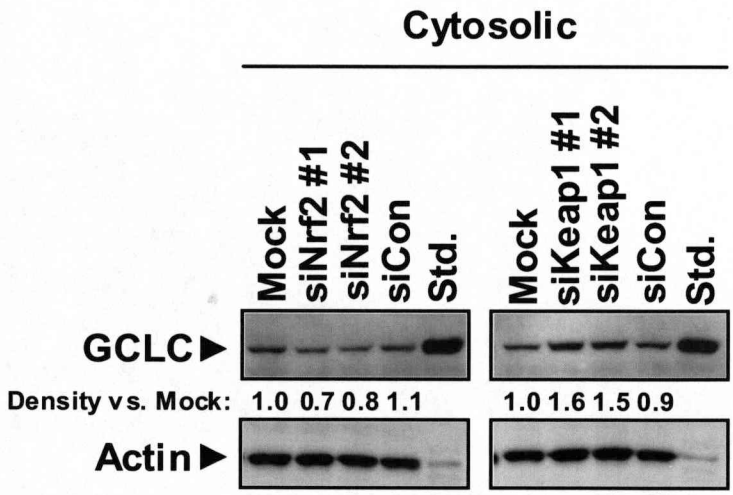

Fig. 2.5 - Effect of RNAi depletion of *Nrf2* or *Keap1* on the basal expression of Gclc. Hepa-1c1c7 cells were mock-transfected, or transfected with 10 nM Nrf2-targeting (si-Nrf2 #1 or #2) or Keap1-targeting (si-Keap1 #1 or #2) siRNA duplexes, or si-Con, for 48 h. Cytosolic fractions were prepared and the Gclc protein level was assessed by Western blot analysis. Gclc protein bands were quantified by densitometry and expressed relative to β-actin, to enable comparison with the mock-transfected Gclc level, which was arbitrarily set at 1. Mouse liver lysate was loaded onto the gel as a standard (Std). Representative gels from n=3 are presented.

2.3.1.3 Effect of RNAi depletion of *Nrf2* or *Keap1* on the basal level of GSH

Gclc is the rate-limiting enzyme in the GSH synthetic pathway (for a review, see Kaplowitz *et al.*, 1985). Therefore, the changes in expression of Gclc observed in response to RNAi depletion of *Nrf2* or *Keap1* should result in concomitant changes in the level of GSH in Hepa-1c1c7 cells. Indeed, *Nrf2*-targeting siRNA decreased, whereas *Keap1*-targeting siRNA increased, basal levels of GSH (Fig. 2.6), demonstrating that Nrf2-mediated induction of a typical ARE-regulated gene results in the upregulation of cell defence. In summary, the Nrf2-ARE pathway appears to be functional in Hepa-1c1c7 cells. As such, Hepa-1c1c7 is a valid model for investigating the molecular regulation of the Nrf2-ARE pathway.

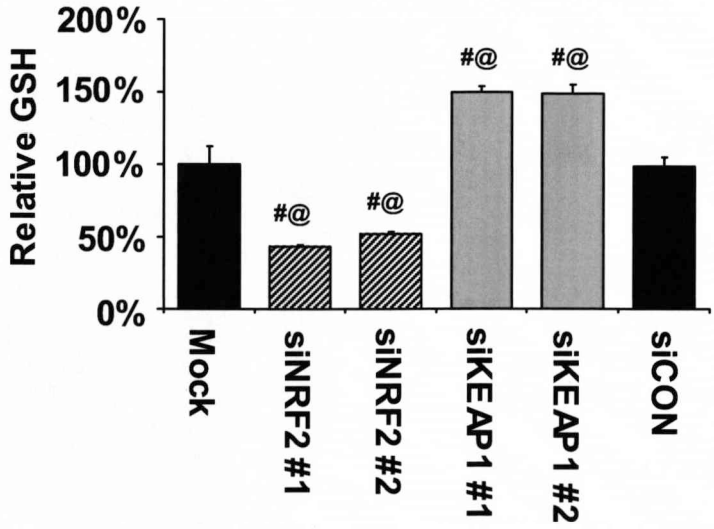

Fig. 2.6 - Effect of RNAi depletion of *Nrf2* or *Keap1* on the basal level of GSH. Hepa-1c1c7 cells were mock-transfected, or transfected with 10 nM Nrf2-targeting (si-Nrf2 #1 or #2) or Keap1-targeting (si-Keap1 #1 or #2) siRNA duplexes, or si-Con, for 48 h. Total GSH levels were quantified, using the DTNB-GSH reductase recycling method (Vandeputte *et al.*, 1994). The GSH concentration for each sample was normalised to total protein content. Results are expressed as the change in GSH relative to mock-transfected cells. The GSH content in mock-transfected cells was 35.8 ± 4.5 nmol/mg. One-way ANOVA, # P <0.001 versus mock, @ P <0.001 versus si-Con. Error bars = standard deviation of mean, n=3.

2.3.2 Activation of the Nrf2-ARE pathway by NAPQI

Activation of the Nrf2-ARE pathway has previously been observed in mouse liver following administration of paracetamol *in vivo* (Goldring *et al.*, 2004). In order to test the hypothesis that paracetamol may activate Nrf2 via the formation of the reactive metabolite NAPQI, Hepa-1c1c7 cells were directly exposed to NAPQI, and changes in the Nrf2-ARE pathway were assessed.

2.3.2.1 Effect of NAPQI on the subcellular distribution of Nrf2

Following exposure of Hepa-1c1c7 cells to NAPQI for 1 h, the subcellular distribution of Nrf2 was determined by immunocytochemistry and confocal microscopy. In the absence of NAPQI, Nrf2 appeared to be ubiquitously distributed throughout the cells, at low levels (Fig. 2.7). In contrast, Nrf2 accumulated within the nuclei of Hepa-1c1c7 cells, as demonstrated by co-localisation with Hoechst 33258 DNA staining, following direct exposure to NAPQI (Fig. 2.7).

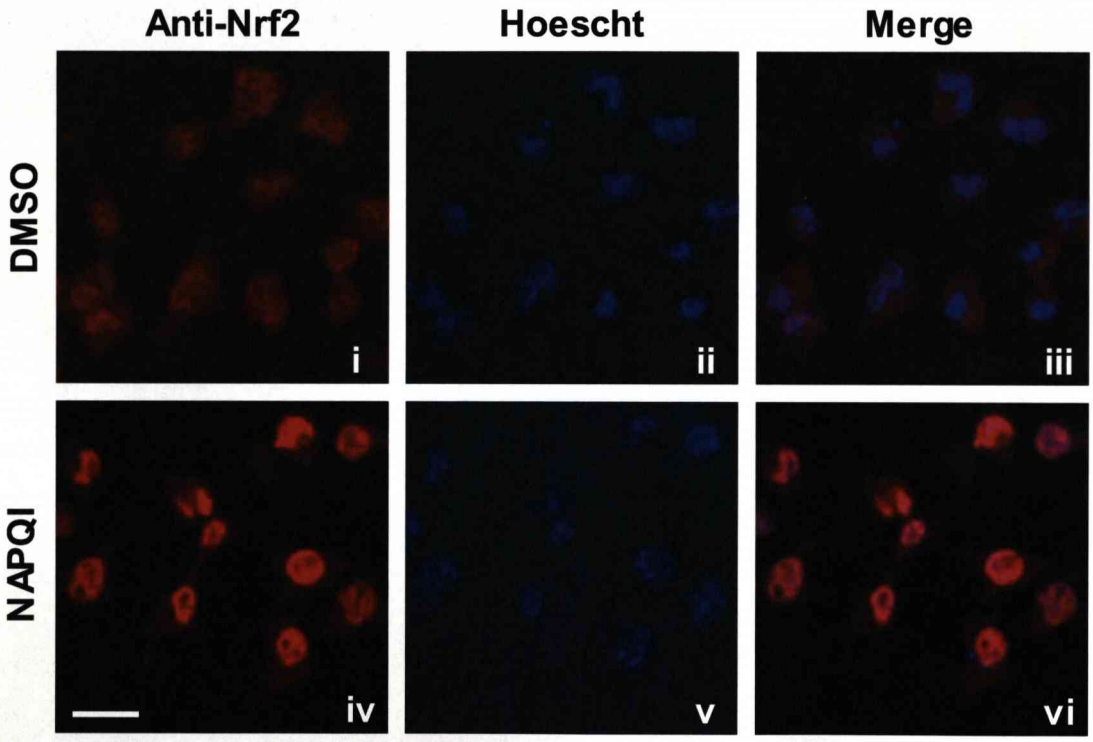

Fig. 2.7 - Effect of NAPQI on the subcellular distribution of Nrf2. Immunocytochemical analysis of subcellular Nrf2 localisation in Hepa-1c1c7 cells exposed to 0.5 % DMSO (*top panels*) or 50 μM NAPQI (*bottom panels*) for 1 h. Treated cells were fixed, permeabilised and incubated with a rabbit anti-mouse Nrf2 antibody, followed by Alexa Fluor 594-conjugated goat anti-rabbit IgG (i and iv). Nuclei were counterstained with Hoechst 33258 (ii and v). (iii and vi) Merged images of Nrf2 and Hoechst signals. Immunofluoresence was visualised by confocal microscopy. Representative fields are presented. Scale bar = 25 μm.

2.3.2.2 Effect of NAPQI on the activity of an ARE-regulated reporter transgene

In order to confirm that the observed increase in nuclear Nrf2 was functionally relevant, the activity of a reporter transgene controlled by the promoter region of the mouse *Nqo1* gene, which contains a functional ARE motif, was assessed. Hepa-1c1c7 cells were transfected for 24 h, exposed to NAPQI for 1 h, the medium was then exchanged for NAPQI-free DMEM, and the cells were incubated for a further 15 h. In the absence of NAPQI, activity of the wild-type ARE reporter transgene was more than double that of a scrambled, mutant ARE construct (Fig. 2.8), indicating the constitutive activity of factors that bind to the ARE under resting conditions. Compared with vehicle-treated cells, a 42 % increase in ARE-driven reporter transgene activity was observed following exposure to NAPQI (Fig. 2.8). However, NAPQI failed to augment the luciferase activity of the mutant reporter transgene (Fig, 2.8), indicating that the observed increase in luciferase activity was mediated by one or more ARE-binding factors, such as Nrf2.

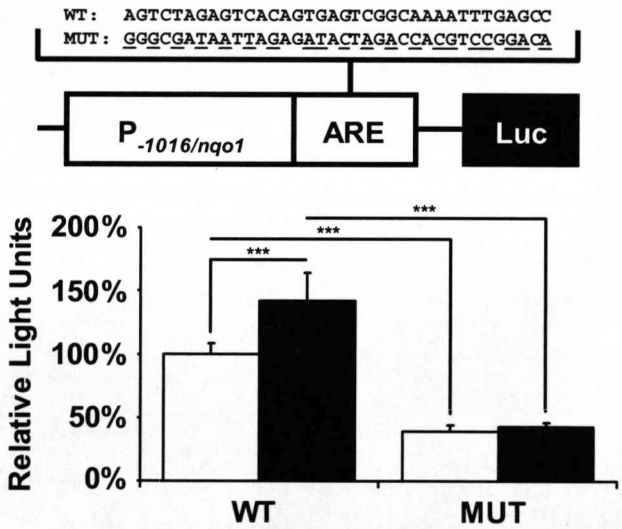

Fig. 2.8 - Effect of NAPQI on the activity of an ARE-regulated reporter transgene. Hepa-1c1c7 cells were co-transfected with pCMV SPORT-β-galactosidase and pGL3B-1016/*nqo5'-luc Nqo1* luciferase reporter plasmid containing a wild-type (WT) or a scrambled ARE sequence (Mut), as depicted in the top panel (mutated bases are underlined). Following 1 h exposure to 0.5 % DMSO (□) or 50 μM NAPQI (■), and a further 15 h incubation in drug-free medium, cells were lysed and luciferase activity was determined as described in 2.2.8. Results are normalised to β-galactosidase internal control activity and expressed as the change in relative light units compared to WT plasmid-transfected, vehicle-treated control cells. One-way ANOVA, *** P <0.001. Error bars = standard deviation of mean, n=3.

2.3.3 Induction of an adaptive defence response by NAPQI

Activation of Nrf2 and induction of ARE-regulated genes typically enhances cell defence. Therefore, the effect of NAPQI on markers of cell defence was assessed in Hepa-1c1c7 cells.

2.3.3.1 Time-dependent induction of GSH synthesis by NAPQI

Levels of GSH were measured over a period of 24 h, following exposure of Hepa-1c1c7 cells to NAPQI for 1 h. Consistent with its known reactivity with GSH (Albano *et al.*, 1985; Dahlin *et al.*, 1984; Potter *et al.*, 1986; Rosen *et al.*, 1984), NAPQI stimulated an initial depletion of GSH at 1 h, which was then followed by a time-dependent increase in GSH, which rose 2.1-fold, compared with the pre-treatment level, at the 24 h timepoint (Fig. 2.9). In contrast, vehicle-exposed cells experienced only a slight increase in GSH over the same time period (Fig. 2.9). These results indicate that NAPQI provokes an adaptive defence response, characterized by the induction of GSH synthesis.

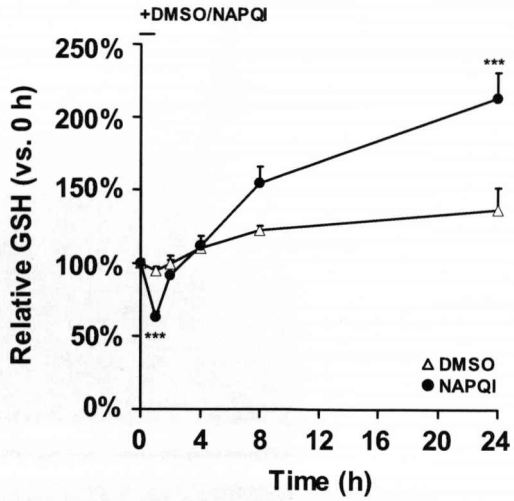

Fig. 2.9 - Induction of GSH synthesis by NAPQI. Hepa-1c1c7 cells were exposed to 0.5 % DMSO (Δ) or 25 μM NAPQI (●) for 1 h, followed by a further 23 h incubation in drug-free medium. Total GSH was measured at the indicated timepoints. The GSH concentration for each sample was normalised to total protein content. Results are expressed as the change in GSH relative to 0 h control cells. GSH content in 0 h control cells was 37.7 ± 2.5 nmol/mg. One-way ANOVA, *** P <0.001 versus DMSO. Error bars = standard deviation of mean, n=3.

2.3.3.2 Nrf2- and time-dependent induction of Gclc and GSH by NAPQI

In order to gain a mechanistic insight into the observed induction of GSH by NAPQI (Fig. 2.9), particularly in terms of the role of the Nrf2-ARE pathway in this adaptive response, Hepa-1c1c7 cells transfected with *Nrf2*-targeting siRNA were exposed to NAPQI for 1 h, and *Gclc* mRNA was measured over 8 h, by TaqMan real-time PCR. At 4 h, in mock-transfected cells, and cells transfected with control siRNA, *Gclc* mRNA increased 2.1-fold, compared with the pre-treatment level (Fig. 2.10). In cells transfected with *Nrf2*-targeting siRNA, basal *Gclc* mRNA was reduced to around 45 % of levels measured in mock-transfected cells (Fig. 2.10). *Nrf2*-targeting siRNA also antagonised the NAPQI-induced increase in *Gclc* mRNA at 4 h (Fig. 2.10). Furthermore, the NAPQI-induced, time-dependent increase in GSH was suppressed by *Nrf2*-targeting siRNA, but not control siRNA (Fig. 2.11). Therefore, the adaptive defence response to NAPQI, characterised by a time-dependent elevation of cellular GSH, involves an Nrf2-mediated induction of Gclc.

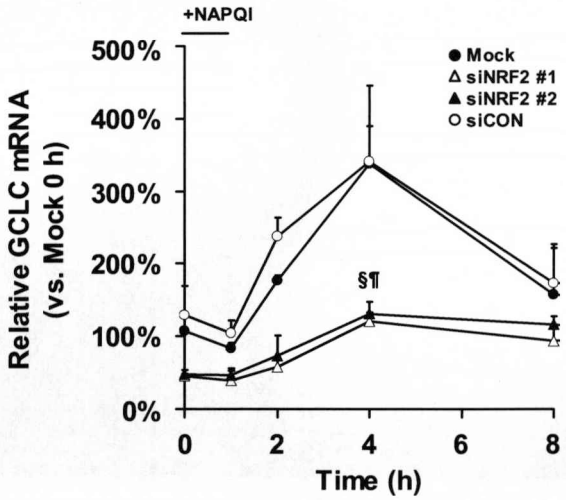

Fig. 2.10 - Nrf2- and time-dependent induction of Gclc by NAPQI. Hepa-1c1c7 cells were transfected with 10 nM *Nrf2*-targeting siRNA (si-Nrf2 #1 or #2) or a scrambled, non-targeting control siRNA duplex (si-Con) for 48 h. Cells were exposed to 25 μM NAPQI for 1 h, followed by a further 7 h incubation in drug-free medium. At the indicated timepoints, total RNA was isolated, reverse-transcribed to cDNA and *Gclc* gene expression was measured by TaqMan real-time PCR. Results are normalised to β_2 microglobulin, and expressed relative to mock-transfected *Gclc* mRNA level, which was arbitrarily set at 100 %. One-way ANOVA, § P <0.001 si-Nrf2 #1 versus mock, ¶ P <0.001 si-Nrf2 #2 versus mock. Error bars = standard deviation of mean, n=3.

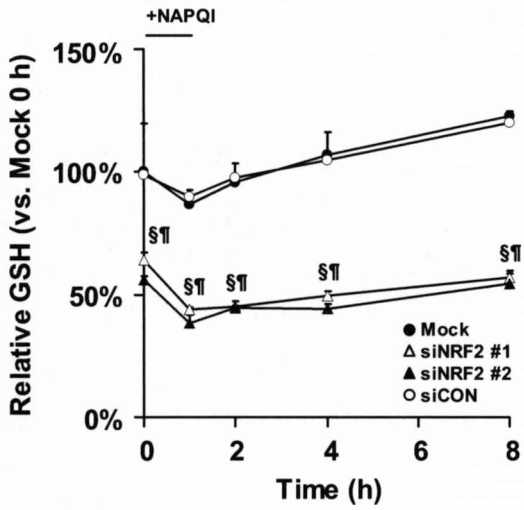

Fig. 2.11 - Nrf2- and time-dependent induction of GSH by NAPQI. Hepa-1c1c7 cells were transfected with 10 nM *Nrf2*-targeting siRNA (si-Nrf2 #1 or #2) or a scrambled, non-targeting control siRNA duplex (si-Con) for 48 h. Cells were exposed to 25 μM NAPQI for 1 h, followed by a further 7 h incubation in drug-free media. Total GSH was measured at the indicated timepoints. The GSH concentration for each sample was normalised to total protein content. Results are expressed as the change in GSH relative to 0 h mock-transfected cells, which was arbitrarily set at 100 %. The GSH content in 0 h mock-transfected cells was 51.1 ± 10.0 nmol/mg. One-way ANOVA, § P <0.001 si-Nrf2 #1 versus mock, ¶ P <0.001 si-Nrf2 #2 versus mock. Error bars = standard deviation of mean, n=3.

2.3.4 The role of cysteine reactivity in the activation of the Nrf2-ARE pathway by NAPQI

In an attempt to understand the chemical and biochemical aspects of the activation of the Nrf2-ARE pathway by NAPQI, the dose-dependency of Nrf2 nuclear accumulation was measured following exposure of cells to NAPQI, the model cysteine-reactive electrophiles DNCB and 15d-PGJ_2, and the lysine-reactive molecule TMA. NAPQI (Fig. 2.12a), DNCB (Fig. 2.12b) and 15d-PGJ_2 (Fig. 2.12c) stimulated Nrf2 nuclear accumulation in a dose-dependent manner, with maximum increases over vehicle control of 4-fold (250 μM NAPQI) and 3-fold (50 μM DNCB, 10 μM 15d-PGJ_2). In contrast, the lysine-reactive molecule TMA had no effect on nuclear Nrf2 content over the concentration range studied (Fig. 2.12d). These results are in agreement with the current

consensus that cysteine-reactivity is an important property of Nrf2-activating molecules, and suggest that modification of cysteine residues within Keap1 may be a plausible hypothesis to explain the ability of NAPQI to activate the Nrf2-ARE pathway.

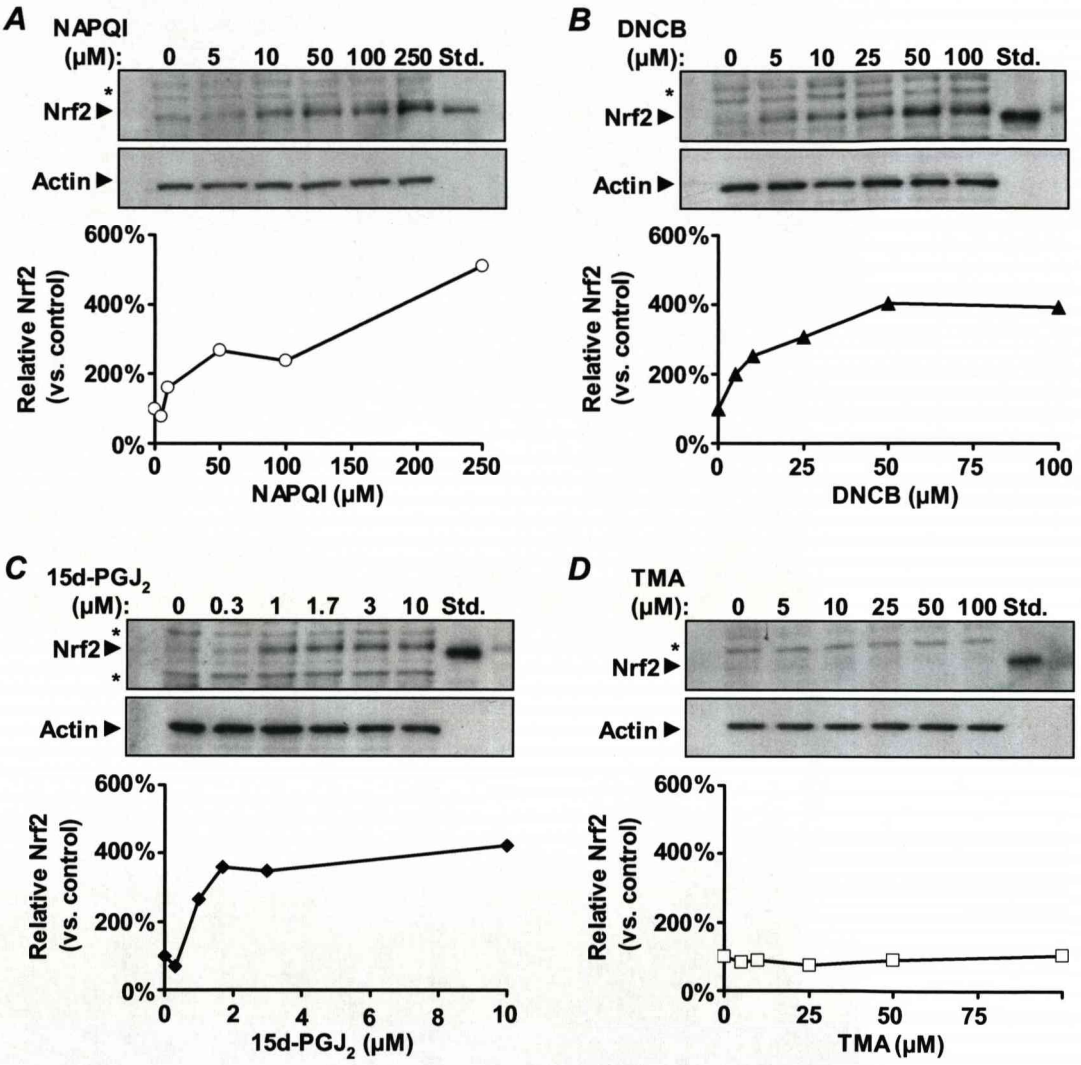

Fig. 2.12 - The role of cysteine reactivity in the activation of the Nrf2-ARE pathway by NAPQI and other model electrophiles. Hepa-1c1c7 cells were exposed to (A) NAPQI, (B) DNCB, (C) 15d-PGJ_2 or (D) TMA, at the indicated concentrations, for 1 h. Nuclear fractions were prepared and the Nrf2 protein level was assessed by Western blot analysis. Nrf2 bands were quantified by densitometry and expressed relative to β-actin, to enable comparison with vehicle-treated control (0 μM) Nrf2 levels, which were arbitrarily set at 100 %. Recombinant Nrf2-His, which runs slightly quicker than the endogenous protein, was loaded onto the gels as a standard (Std). Non-specific proteins that cross-react with the antibody are labeled *. Representative gels from n=3 are presented.

2.3.5 The role of GSH depletion in the activation of the Nrf2-ARE pathway by NAPQI

To assess the role of GSH depletion in the activation of Nrf2 by NAPQI and the model electrophiles, levels of GSH were measured in Hepa-1c1c7 cells following a 1 h exposure. NAPQI and DNCB both caused significant, dose-dependent depletion of GSH at, or above, 5 μM, whereas TMA had no significant effect on cellular GSH levels (Fig. 2.13a). Notably, 15d-PGJ_2 had no discernible effect on GSH over the same concentration range that induced Nrf2 nuclear accumulation (Fig. 2.13b), indicating that GSH depletion is not an absolute prerequisite for the activation of Nrf2.

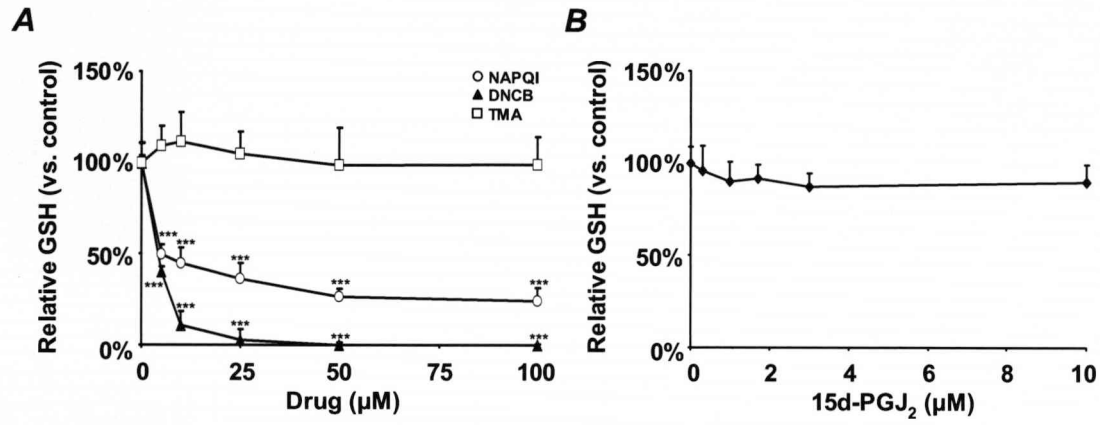

Fig. 2.13 - The role of GSH depletion in the activation of the Nrf2-ARE pathway by NAPQI and other model electrophiles. Hepa-1c1c7 cells were exposed to (A) NAPQI, DNCB or TMA, or (B) 15d-PGJ_2, at the indicated concentrations, for 1 h, and total GSH levels were quantified. The GSH concentration for each sample was normalised to total protein content. Results are expressed as the change in GSH relative to the vehicle-treated control (0 μM) GSH level. The GSH content in vehicle-treated control cells was 35.5 ± 1.5 nmol/mg. One-way ANOVA, *** P <0.001 versus vehicle-treated control. Error bars = standard deviation of mean, n=3.

2.3.6 The role of cytotoxicity in the activation of the Nrf2-ARE pathway by NAPQI

To examine the relationship between Nrf2 activation and cytotoxicity, LDH leakage from Hepa-1c1c7 cells was measured following exposure to the electrophiles. Notably,

none of the molecules caused significant cytotoxicity following a 1 h exposure (Fig. 2.14a-b), at which time point Nrf2 activation was observed at the concentrations studied (Fig. 2.12). At 24 h, however, NAPQI, DNCB and 15d-PGJ_2 (Fig. 2.14c-d) provoked dose-dependent increases in LDH leakage, compared to vehicle control. In contrast, TMA had no discernible effect on LDH leakage at 24 h (Fig. 2.14c).

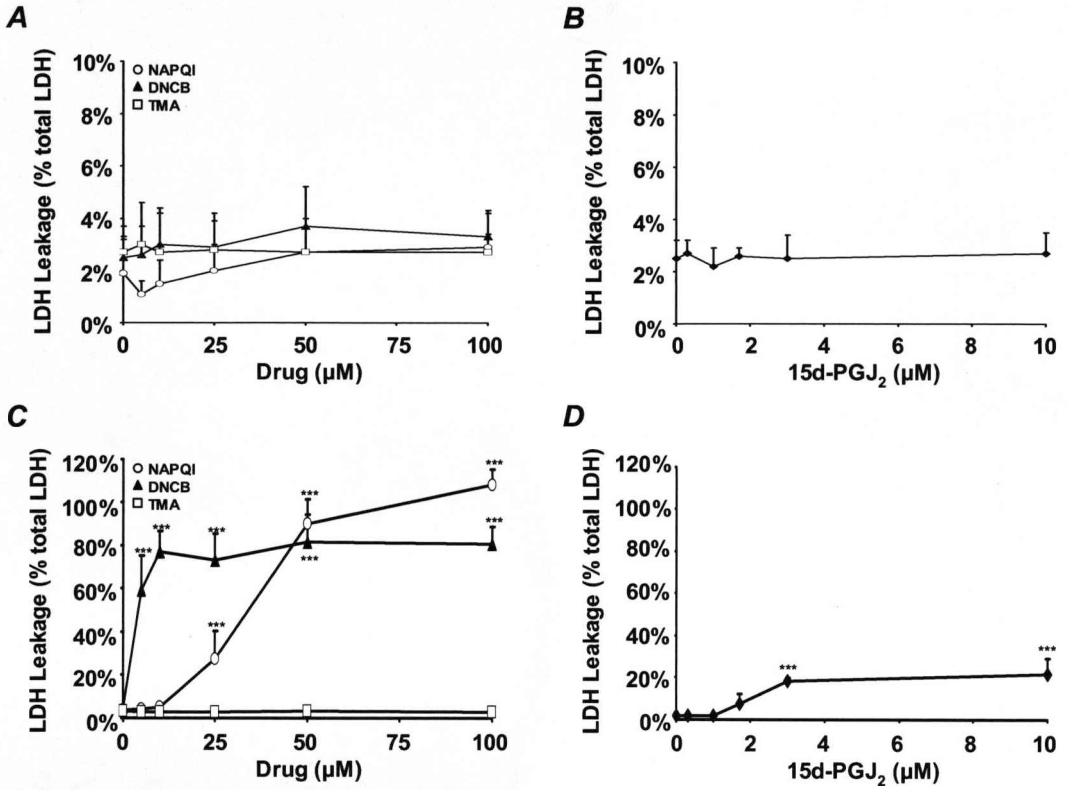

Fig. 2.14 - The role of cytotoxicity in the activation of the Nrf2-ARE pathway by NAPQI and other model electrophiles. Hepa-1c1c7 cells were exposed to (A and C) NAPQI, DNCB or TMA, or (B and D) 15d-PGJ_2, at the indicated concentrations, for 1 h (A and B) or 24 h (C and D). Cytotoxicity was assessed by measuring leakage of LDH into the culture medium. Extracellular LDH activity is expressed as a percentage of total (extracellular plus intracellular) LDH activity. One-way ANOVA, *** P <0.001 versus vehicle-treated control. Error bars = standard deviation of mean, n=3.

2.4 DISCUSSION

The Nrf2-ARE pathway represents an inducible defence mechanism that protects mammalian cells against the deleterious effects of chemical/oxidative stress (for a review, see Kensler *et al.*, 2007). Work in this research group has demonstrated that administration of paracetamol *in vivo* stimulates the Nrf2-ARE pathway in mouse liver, inducing an adaptive response characterised by the increased expression of cytoprotective enzymes (Goldring *et al.*, 2004). The over-arching hypothesis of the work described in this chapter is that the activation of the Nrf2-ARE pathway in mouse liver by paracetamol is linked to the formation of the reactive metabolite NAPQI, which has the potential to modify cysteine residues within Keap1, the cytosolic repressor of Nrf2. The main aim of the studies carried out in this chapter was to ascertain whether NAPQI was able to directly activate the Nrf2-ARE pathway in a mouse liver cell line, Hepa-1c1c7. The results presented in section 2.3.1 demonstrate that Hepa-1c1c7 is a functionally valid model for studying the Nrf2-ARE pathway, as has been shown previously by others (Jowsey *et al.*, 2003; McWalter *et al.*, 2004; Petzer *et al.*, 2003).

The results presented in section 2.3.2 demonstrate that NAPQI can directly activate the Nrf2-ARE pathway in Hepa-1c1c7 cells. NAPQI was used as a metabolite *per se*, to eliminate the potentially confounding effects of other paracetamol metabolites on Nrf2 activation. Due to the practical difficulties associated with measuring levels of unstable reactive intermediates, the threshold intracellular concentration of NAPQI that is associated with hepatotoxicity following paracetamol overdose is not precisely known. However, a reasonable, although somewhat simplistic, estimate can be made on the basis that the average liver (1.5 L volume) contains 6 mmol GSH (DeLeve *et al.*, 1991), and that paracetamol-induced hepatotoxicity is associated with the depletion of hepatic GSH to at least 70 % of basal levels (Mitchell *et al.*, 1973). Assuming the conjugation of GSH and NAPQI is stoichiometric, 4.2 mmol NAPQI (70 % of 6 mmol) would be required to cause the necessary degree of hepatic GSH depletion (Mitchell *et al.*, 1974; Rumack, 2002). This translates into a cellular concentration of 2.8 mM NAPQI (4.2 mmol per 1.5 L). Therefore, the concentrations of NAPQI used in this study (5-250 μM) are within the

range of concentrations that are estimated to occur in the liver following ingestion of a hepatotoxic.dose of paracetamol.

Although there is a general consensus that the direct exposure of cells to NAPQI can provide valuable information on the signaling pathways that are involved in the cellular response to this reactive intermediate (Albano *et al.*, 1985; Andersson *et al.*, 1990; Bender *et al.*, 2004; Dahlin *et al.*, 1984; Harman *et al.*, 1991; Holme *et al.*, 1984; Holme *et al.*, 1982a; Holme *et al.*, 1982b; Rundgren *et al.*, 1988), it is important to consider the physiological limitations of such an approach. Due to the predominant abundance of CYP450 enzymes on the cytoplasmic surface of the smooth endoplasmic reticulum (Guengerich, 1990), the majority of reactive intermediates are formed in or around this region *in vivo*. The direct application of NAPQI to cells may, therefore, not accurately represent the relative subcellular concentrations of NAPQI formed during the metabolic bioactivation of paracetamol *in vivo*. Indeed, the half-life of NAPQI is estimated to be less than 10 sec in the presence of nucleophiles and reductants (Miner *et al.*, 1979). Therefore, the direct exposure of cells to NAPQI most likely results in a 'short, sharp hit', with cell surface proteins bearing the greatest degree of exposure. In contrast, hepatocytes exposed to paracetamol generate the reactive metabolite at relatively low levels, over a longer period of time. Hence, it is important to consider the physiological site of NAPQI generation in any future attempts to dissect the mechanism(s) of Nrf2 activation by paracetamol *in vivo*. This issue should be addressed, initially, by employing metabolically competent cells that are capable of bioactivating paracetamol to NAPQI, and in which the Nrf2-ARE pathway is known to function. This would facilitate the direct application of the parent molecule, as opposed to the metabolite, and, through the pharmacological inhibition of CYP450 enzyme activity, would better enable the process of drug metabolism to be linked to the activation of Nrf2 by paracetamol. Interestingly, it has recently been demonstrated that, whilst localising predominantly within the perinuclear region of the cytoplasm, Keap1 is found to be present in the endoplasmic reticulum (Watai *et al.*, 2007). It is possible that such localisation enables Keap1 to 'sense' chemical stress at the initial point of generation.

Consistent with the observation that activation of Nrf2 by paracetamol induces cell defence in mouse liver *in vivo* (Goldring *et al.*, 2004), stimulation of the Nrf2-ARE pathway by NAPQI in Hepa-1c1c7 cells was associated with an adaptive defence response, characterised by the time-dependent induction of GSH synthesis. Such a response would augment the redox buffer within cells, and should enable the enhanced bioinactivation of NAPQI, therefore protecting cells against the toxic insult associated with this reactive intermediate. The adaptive response was shown to be mediated via an Nrf2-dependent induction of Gclc, the ARE-regulated rate-limiting enzyme in the synthesis of GSH (Wild *et al.*, 1999). The Nrf2-mediated adaptive response to NAPQI may serve as a critical determinant of the threshold for paracetamol toxicity, as separate studies have demonstrated that *Nrf2*$^{-/-}$ mice are more vulnerable to paracetamol-induced liver injury (Chan *et al.*, 2001; Enomoto *et al.*, 2001), whereas hepatocyte-specific knockout of the murine *Keap1* gene, which enhances Nrf2-dependent cell defence, confers protection against paracetamol hepatotoxicity (Okawa *et al.*, 2006). Therefore, it would be informative in future experiments to examine the effects of RNAi depletion of *Nrf2* or *Keap1* on the cytotoxic effects of NAPQI towards Hepa-1c1c7 cells.

The currently favoured model of Nrf2 regulation suggests that the transcription factor only accumulates within the nucleus in response to cellular stress (Dhakshinamoorthy *et al.*, 2001; Itoh *et al.*, 1999), since it is targeted for proteasomal degradation, via Keap1-directed ubiquitination, under resting conditions (Kobayashi *et al.*, 2004; McMahon *et al.*, 2003; Nguyen *et al.*, 2003; Stewart *et al.*, 2003; Zhang *et al.*, 2003a). Therefore, Nrf2 has primarily been regarded as a key regulator of inducible cell defence. However, the results presented in section 2.3.2.2 demonstrate the constitutive activity of factors, probably including Nrf2, that bind to the ARE in the absence of cellular stress, as indicated by the differences in basal activity of the *Nqo1* reporter transgenes containing wild-type and mutated AREs. Furthermore, this study has demonstrated a decrease in the basal expression of Gclc, and levels of GSH, following RNAi depletion of *Nrf2*. These findings are consistent with those of recent studies that have employed RNAi to demonstrate the importance of Nrf2 as a regulator of mammalian cell defence (Cao *et al.*, 2005; Chen *et al.*, 2005b; Dhakshinamoorthy *et al.*, 2004; Gong *et al.*, 2006b; So *et*

al., 2006; Warabi *et al.*, 2007; Zhang *et al.*, 2006b). A number of independent studies have also demonstrated the decreased basal expression of various ARE-regulated genes in mice lacking *Nrf2* (Chan *et al.*, 2000; Lee *et al.*, 2003; McMahon *et al.*, 2001; Ramos-Gomez *et al.*, 2001). It therefore appears that the activity of Nrf2 extends beyond that of mediating the adaptive response to cellular stress, by regulating the basal transcription of certain defence genes. As such, in addition to directing the response to cellular stress, Nrf2 may define the initial threshold for toxicity, by controlling, at least in part, the constitutive tier of cell defence. However, the current model of Nrf2 regulation does not fully address this latter point. It is possible that the expression of Nrf2 relative to Keap1 is tightly balanced, such that, in the absence of cellular stress, a small pool of Nrf2 is able to evade repression by Keap1, facilitating the basal transactivation of ARE-regulated genes. Thus, it is particularly interesting that putative ARE motifs have recently been identified in the promoter region of the mouse *Keap1* gene (Lee *et al.*, 2007). It is possible, therefore, that the expression of Keap1 is, at least partly, regulated by Nrf2 itself. Alternatively, background levels of oxidative stress, such as that caused by the generation of ROS as byproducts of mitochondrial aerobic respiration, may provide low-level stimulation of the Nrf2 pathway. In any case, this ambiguity in the current model of Nrf2 regulation has yet to be fully resolved.

Whilst the molecular mechanisms underlying the activation of Nrf2 by chemical inducers are yet to be fully defined, it is clear that the Nrf2-ARE pathway is responsive to a range of structurally diverse chemicals that are all electrophilic (Prestera *et al.*, 1993a; Talalay *et al.*, 1988) and capable of modifying sulphydryl groups (Dinkova-Kostova *et al.*, 2001). It has been postulated that the modification of critical cysteine residues within Keap1 represents a molecular 'sensing' mechanism that provides the trigger for activation of the Nrf2-dependent defence response (Dinkova-Kostova *et al.*, 2001). Nrf2-activating molecules can be broadly grouped into the following classes: alkenes, arsenicals, dithiolethiones, enones, isothiocyanates, mercaptans and disulphides, Michael acceptors, and diphenols and quinones. Given that NAPQI is a quinoneimine, which is known to react with cysteine thiols via 1,4-addition *in vitro* and *in vivo* (Hoffmann *et al.*, 1985a; Hoffmann *et al.*, 1985b; Streeter *et al.*, 1984), it is plausible

that NAPQI activates the Nrf2-ARE pathway through the modification of cysteine residues within Keap1, and this may form the molecular basis for the activation of the Nrf2-ARE pathway in mouse liver by paracetamol (Goldring *et al.*, 2004).

In order to test the role of cysteine reactivity in the activation of the Nrf2-ARE pathway by NAPQI, the responsiveness of Nrf2 to a panel of structurally distinct molecules, with different electrophilic chemistries, was assessed. Amongst the cysteine-reactive molecules employed, DNCB is a known Nrf2-dependent inducer of HO-1 in mouse primary macrophages (Ishii *et al.*, 2000), and 15d-PGJ_2 has been shown to activate Nrf2 in a number of cell types (Chen *et al.*, 2006; Hosoya *et al.*, 2005; Itoh *et al.*, 2004; Yu *et al.*, 2006). It can be seen in section 2.3.4 that the cysteine reactive molecules NAPQI, DNCB and 15d-PGJ_2 stimulated the nuclear accumulation of Nrf2 in a concentration-dependent manner, whereas the lysine-reactive hard electrophile TMA did not. DNCB, along with many other skin sensitizers, has recently been verified as a potent inducer of ARE-driven gene expression (Natsch *et al.*, 2007). The authors of this recent study hypothesised that the activation of Nrf2-dependent cell defence by some skin sensitizers may account for the lack of sensitivity observed in the majority of the population. As such, the idiosyncrasy associated with some sensitizations, and indeed other adverse drug reactions, may be partly determined by deficiencies in the Nrf2-ARE pathway. Therefore, it will be important to determine whether there is variability in the Nrf2-ARE pathway within the general population that may alter the inter-individual threshold for, and susceptibility to, drug-induced toxicity. The study by Natsch *et al.* (2007) also demonstrated that, similar to TMA, the lysine-reactive molecule phtalic anhydride is unable to activate the Nrf2-ARE pathway. Although TMA is incapable of reacting irreversibly with sulphydryl groups (de la Escalera *et al.*, 1989), related structures are capable of forming labile adducts with cysteine (Ahlfors *et al.*, 2005; Brinegar *et al.*, 1981; Palacian *et al.*, 1990). Therefore, it would be interesting to measure the response of the Nrf2-ARE pathway to TMA under conditions which may favour the modification of cysteine sulphydryls, for example following the depletion of cellular GSH. Indeed, molecules which can be classified as hard electrophiles have been shown to activate the Nrf2-ARE pathway, albeit by a redox-sensitive mechanism (Wang *et al.*, 2006c). Taken

together, these data support the notion that cysteine reactivity is an important chemical property of Nrf2-activating molecules, and indirectly support the hypothesis that the modification of cysteines within Keap1 may underlie the ability of NAPQI to activate the Nrf2-ARE pathway.

Through the use of several experimental approaches, the direct chemical modification of cysteine residues within Keap1 has gained support as a triggering mechanism for the activation of Nrf2 (Dinkova-Kostova *et al.*, 2002; Itoh *et al.*, 2004; Levonen *et al.*, 2004; Sekhar *et al.*, 2003). However, the common thiol reactivity of Nrf2-activating molecules also raises the possibility that the depletion of GSH, through conjugation at its nucleophilic sulphydryl group, may represent an indirect means of stimulating the transcription factor. Indeed, it is possible that, via the generation of an oxidising environment, the depletion of GSH may cause changes in the redox state of certain cysteines within Keap1, thus triggering Nrf2 activation. However, although it cannot be discounted that an alteration of the redox balance may contribute to the activation of Nrf2 by NAPQI and DNCB, the fact that 15d-PGJ_2 was able to induce the nuclear accumulation of the transcription factor without significantly affecting GSH levels indicates that depletion of GSH is not an absolute prerequisite for the stimulation of Nrf2.

Notably, components of the ubiquitin-proteasome pathway, which has a major role in regulating the basal activity of Nrf2 (Kobayashi *et al.*, 2004; McMahon *et al.*, 2003; Nguyen *et al.*, 2003; Stewart *et al.*, 2003; Zhang *et al.*, 2003a), are redox sensitive (Jahngen-Hodge *et al.*, 1997), and the function of this important cellular pathway is known to be inhibited by thiol-reactive molecules (Obin *et al.*, 1998), including 15d-PGJ_2 (Ishii *et al.*, 2005a; Mullally *et al.*, 2001; Shibata *et al.*, 2003). Cyclopentenone prostaglandins have also been shown to disrupt the actin cytoskeleton (Gayarre *et al.*, 2006), to which Keap1 is anchored (Kang *et al.*, 2004). Therefore, the ability of 15d-PGJ_2 to activate Nrf2 may be independent of the direct antagonism of Keap1 through chemical modification of critical cysteines. Further work is required to examine this hypothesis. Taken together, these results imply that biochemical mechanisms other than

the depletion of GSH, such as the modification of cysteine residues within Keap1, may have an important role in the activation of Nrf2 by certain molecules. Given that the mutual activation of multiple signaling pathways, in a chemical-specific manner, may contribute to the activation of the Nrf2-ARE pathway, further work, employing a broad panel of chemical inducers with well-characterised effects on cell signaling pathways, is required to fully elucidate the nature of the biochemical mechanisms that regulate Nrf2 activity.

Concentrations of NAPQI, DNCB and 15d-PGJ_2 that were not cytotoxic over 1h, but induced significant leakage of LDH over 24 h, stimulated the nuclear accumulation of Nrf2. These results, in keeping with our previous observation that Nrf2 is activated in murine liver by paracetamol at non-hepatotoxic, as well as hepatotoxic, doses (Goldring *et al.*, 2004), suggest that the Nrf2-ARE pathway is able to 'sense' and respond to chemical stress before the onset of overt cytotoxicity. However, it should also be noted that concentrations of NAPQI that caused almost complete cytotoxicity after 24 h incubations did so in spite of activating the Nrf2-ARE pathway. Therefore, it is clear that induction of Nrf2-dependent cell defence does not guarantee survival following exposure to cytotoxic chemicals. What is, perhaps, more important is the balance between the extent of the cytotoxic insult and the activation of Nrf2, and other cytoprotective signaling pathways. At lower levels of exposure, deleterious cytotoxic effects may be surmountable by the induction of cytoprotective systems. As the level of exposure increases, however, defensive barriers may simply be overwhelmed by the increasing scale of cellular stress. In keeping with this concept, the dose threshold of paracetamol required to induce hepatotoxicity is markedly reduced in *Nrf2*-null mice (Chan *et al.*, 2001; Enomoto *et al.*, 2001) and increased in hepatocyte-specific *Keap1* knockout animals (Okawa *et al.*, 2006). Thus, cytoprotective signaling pathways may enable cells, and indeed whole organisms, to withstand low-level exposure to toxic environments, but cannot provide complete protection against cytotoxic insults.

In summary, the results presented in this chapter demonstrate that NAPQI, the reactive metabolite of paracetamol, can directly activate the Nrf2-ARE pathway in a mouse liver

cell line, inducing an adaptive defence response characterised by the Nrf2-dependent induction of Gclc and GSH. Through the use of a panel of structurally distinct electrophiles, the activation of Nrf2 has been shown to be associated with the cysteine reactivity of a molecule, but not to be entirely dependent on the depletion of GSH. Therefore, it is possible that NAPQI activates the Nrf2-ARE pathway via the modification of cysteine residues within Keap1, and the subsequent chapters of this thesis are aimed towards investigating this potential signaling mechanism.

CHAPTER 3

Development of a cell-free *in vitro* system for investigating the chemical modification of Keap1 by Nrf2-activating electrophiles

CONTENTS

3.1 INTRODUCTION

The results presented in chapter 2, and the work of others (Dinkova-Kostova *et al.*, 2001; Prestera *et al.*, 1993a; Talalay *et al.*, 1988; Zhang, 2001), have demonstrated that cysteine reactivity is an important chemical property of Nrf2-activating molecules. Given that Keap1 is the major regulator of Nrf2 activity (Itoh *et al.*, 1999), and that Keap1 is a highly cysteine-rich protein, it has been proposed that the modification of one or more cysteine residues within Keap1 may evoke a conformational change in the protein, rendering it unable to efficiently repress Nrf2, and thus providing a trigger for activation of the transcription factor (Dinkova-Kostova *et al.*, 2002).

Site-directed mutagenesis has been employed to demonstrate the importance of certain cysteine residues, particularly Cys-151, -273 and -288, in the function of Keap1 (Kobayashi *et al.*, 2006; Levonen *et al.*, 2004; Wakabayashi *et al.*, 2004; Zhang *et al.*, 2003a). In addition, recent work has provided compelling evidence for the chemical modification of Keap1, through the use of biotinylated analogues of Nrf2-activating molecules (Itoh *et al.*, 2004; Levonen *et al.*, 2004), spectroscopic binding experiments (Dinkova-Kostova *et al.*, 2002) and mass spectrometry (Dinkova-Kostova *et al.*, 2002). Although it appears that other triggers for Nrf2 activation may exist, including direct phosphorylation of the transcription factor (Cullinan *et al.*, 2003; Huang *et al.*, 2002; Nguyen *et al.*, 2000), there is a far more substantial weight of evidence indicating that certain cysteines within Keap1 may be the targets of electrophiles, and that modification of Keap1 may underlie the ability of these molecules to induce Nrf2-dependent cell defence. The studies presented in this and subsequent chapters aim to explore the role of Keap1 modification in the regulation of Nrf2 activity.

The results presented in chapter 2 demonstrate that NAPQI, the electrophilic metabolite of paracetamol, directly activates the Nrf2-ARE pathway in a mouse liver cell line. Given that NAPQI is known to react with cysteine thiols *in vitro* and *in vivo* (Hoffmann *et al.*, 1985a; Hoffmann *et al.*, 1985b), a plausible hypothesis to explain the activation of the Nrf2-ARE pathway by paracetamol *in vivo* (Goldring *et al.*, 2004), and by NAPQI in

established cells, is that chemical modification of Keap1 by NAPQI perturbs its ability to repress the transcription factor. In order to explore this hypothesis, a cell-free *in vitro* test system has been developed, based on the expression and purification of recombinant polyhistidine-tagged mouse Keap1 protein, and its use in combination with mass spectrometry to enable the examination of Keap1 modification by NAPQI and other Nrf2-activating electrophiles. The work presented within this chapter describes the development and validation of this *in vitro* test system.

3.2 METHODS

3.2.1 Materials and reagents

The mouse *Keap1* I.M.A.G.E. cDNA clone was from Geneservice (Cambridge, UK). PCR and sequencing primers were custom-synthesised by Sigma-Genosys (Haverhill, UK). Expand High Fidelity PCR System and the 100 bp DNA ladder were from Roche Diagnostics (Burgess Hill, UK). pET-21a(+) was from Novagen (Nottingham, UK). *Ase*I was from New England Biolabs (Hitchin, UK). BL21 (DE3) competent *E. coli*, SOC media, UltraPure agarose and the SilverXpress silver staining kit were from Invitrogen (Paisley, UK). XL10-Gold ultracompetent *E. coli* were from Stratagene (Amsterdam, Netherlands). Isopropyl-β-D-thiogalactopyranoside and sequencing-grade modified trypsin were from Promega (Southampton, UK). The BCA Protein Assay Kit was from Pierce (Cramlington, UK). The Soniprep 150 ultrasonic disintegrator was from MSE (London, UK). αCHCA matrix was from Laserbio Labs (Valbonne, France). The GeneAmp 9700 PCR system, MALDI target plate, Voyager-DE PRO MALDI-TOF Biospectrometry Workstation, API QSTAR Pulsar i MS/MS spectrometer, and Analyst QS and ProteinPilot software packages were from Applied Biosystems (Warrington, UK). DTT was from USB Corporation (Cleveland, USA). Perfectprep gel cleanup kit was from Eppendorf (Cambridge, UK). ChromasPro software was from Technelysium (Tewantin, Australia). The integrated LCPackings System and C18 PepMap column were from Dionex (Camberley, UK). PicoTip emitters were from New Objective (Woburn, USA). Power Broth was from Athena Enzyme Systems (Baltimore, USA). Sex pheromone inhibitor peptide iPD1 was from Bachem (St Helens, UK). GenElute plasmid mini-prep kit, ethidium bromide, *Bgl*II, *Hind*III, *Nde*I, *Sac*I, *Xba*I, *Xho*I, the QuickLink DNA ligation kit, LB agar tablets, LB broth powder, ampicillin, imidazole, HIS-Select nickel-charged agarose beads, sepharose 6B beads, Iodoacetamide, N-ethylmaleimide, ProteoMass MALDI-MS standards (angiotensin II, ACTH fragment 18-39, oxidised insulin chain B), caesium iodide and the monoclonal anti-polyhistidine HRP-conjugated antibody were from Sigma-Aldrich (Poole, UK). All other reagents were of analytical or molecular grade, and were from Sigma-Aldrich.

3.2.2 Preparation of mouse *Keap1* coding sequence DNA template

An I.M.A.G.E. cDNA clone (# 6404252) for mouse *Keap1* was supplied streaked onto an agar slope; a small amount of this agar was used to inoculate 2 mL LB broth containing 50 μg/mL ampicillin, which was incubated overnight at 37 °C, 250 rpm. The clone vector was purified using a GenElute plasmid mini-prep kit, in accordance with the manufacturer's instructions.

3.2.3 Polymerase chain reaction

The purified vector, containing the mouse *Keap1* cDNA clone, was used as a template for hot-start PCR amplification of the mouse *Keap1* coding sequence. A forward primer (5'-TCGATTAATAGCATGCAGCCCGAACCCAA-3') was designed to introduce an *Ase*I restriction site, flanked on either side by three bases, at the start of the *Keap1* coding sequence. A reverse primer (5'-CGACTCGAGCTCGCAGGTACAGTTT TGTT-3') was designed to omit the stop codon (TGA) and to introduce a *Xho*I restriction site flanked on either side by three bases, at the end of the *Keap1* coding sequence. Hot-start PCR (see Table 3.1) was performed using the Expand High Fidelity PCR System. Reactions (50 μL) contained 1 μL purified vector, 1X Expand buffer, 2.5 mM $MgCl_2$, 0.2 mM dNTP mix and 0.2 nM forward and reverse primer. Reactions were heated to 80 °C in a GeneAmp 9700 PCR system and held at this temperature to allow the addition of 2.6 U Expand enzyme mix.

Step	Cycles	Denaturing	Annealing	Elongation
#1	1	2 min at 95 °C	–	–
#2	2	5 sec at 95 °C	30 sec at 68 °C	1.5 min at 72 °C
#3	2	5 sec at 95 °C	30 sec at 66 °C	1.5 min at 72 °C
#4	2	5 sec at 95 °C	30 sec at 64 °C	1.5 min at 72 °C
#5	2	5 sec at 95 °C	30 sec at 62 °C	1.5 min at 72 °C
#6	2	5 sec at 95 °C	30 sec at 60 °C	1.5 min at 72 °C
#7	2	5 sec at 95 °C	30 sec at 58 °C	1.5 min at 72 °C
#8	2	5 sec at 95 °C	30 sec at 56 °C	1.5 min at 72 °C
#9	2	5 sec at 95 °C	30 sec at 54 °C	1.5 min at 72 °C
#10	2	5 sec at 95 °C	30 sec at 52 °C	1.5 min at 72 °C
#11	24	5 sec at 95 °C	30 sec at 50 °C	1.5 min at 72 °C

Table 3.1 - Steps and cycles for hot-start PCR amplification of mouse *Keap1* coding sequence.

3.2.4 Sub-cloning of *Keap1* into pET-21a(+)

The pET-21a(+) vector was opened by restriction digest with *Nde*I and *Xho*I for 2 h at 37 °C. The digestion reaction (20 µL) contained 5 µL pET-21a(+), 10 U *Nde*I, 10 U *Xho*I and 1X buffer SH. The mouse *Keap1* PCR product from 3.2.3 was digested with *Ase*I and *Xho*I for 2 h at 37 °C. The digestion reaction (20 µL) contained 5 µL PCR product, 10 U *Ase*I, 10 U *Xho*I, and 1X buffer 3. As *Nde*I and *Ase*I yield compatible ends following restriction digest, it was possible to ligate *Ase*I/*Xho*I-digested *Keap1* into *Nde*I/*Xho*I-digested pET-21a(+). An *Ase*I restriction site, and not a *Nde*I restriction site, was introduced at the start of the *Keap1* coding sequence as the *Nde*I restriction site contains an ATG initiation codon, which would have resulted in premature translation of the construct. The pET-21a(+) and *Keap1* restriction products, alongside a 100 base pair (bp) DNA ladder, were resolved by electrophoresis on a 1 % agarose gel supplemented with 0.5 µg/mL ethidium bromide. The agarose gel was made by dissolving 0.5 g UltraPure agarose in 50 mL TBE buffer (89 mM Tris-base, 89 mM boric acid, 2 mM EDTA, pH 8.3) and heating the solution to boiling point. Ethidium bromide was added, and the solution was poured into a casting tray and allowed to set at room temperature. The resolved DNA fragments were purified using a Perfectprep gel cleanup kit, in

accordance with the manufacturer's instructions. The gel-purified restriction products were ligated using a QuickLink DNA ligation kit, in accordance with the manufacturer's instructions. XL10-Gold ultracompetent *E. coli* were immediately transformed with the ligated construct (0.6 μL per 30 μL bacteria), via a 30 sec heat-shock at 42 °C, and incubated in 0.25 mL nutrient-rich SOC media for 1 h, at 37 °C, 250 rpm. The bacteria were streaked onto a sterile LB-agar plate, made with LB-agar tablets, containing 50 μg/mL ampicillin, and incubated at 37 °C overnight. Antibiotic-resistant colonies were picked from the plate and used to inoculate 2 mL LB broth containing 50 μg/mL ampicillin; these cultures were incubated for 24 h at 37 °C, 250 rpm. The construct was purified by mini-prep. Diagnostic restriction digests were performed with *Bgl*II (5 μL PCR product, 10 U *Bgl*II, 1X buffer SM, 37 °C, 1 h), *Hind*III/*Xho*I (5 μL PCR product, 10 U *Hind*III, 10 U *Xho*I, 1X buffer SB, 37 °C, 1 h) and *Xba*I/*Sac*I (5 μL PCR product, 10 U *Xba*I, 10 U *Sac*I,1X buffer SA, 37 °C, 1 h). BL21 (DE3) competent *E. coli* were transformed with pET-21a(+)/Keap1, via a 30 sec heat-shock at 42 °C, and incubated in 0.25 mL SOC media for 1 h, at 37 °C, 250 rpm. The bacteria were streaked onto a sterile LB-agar plate, containing 50 μg/mL ampicillin, and incubated at 37 °C overnight. Antibiotic-resistant colonies were picked from the plate and used to inoculate 2 mL LB broth containing 50 μg/mL ampicillin; these cultures were incubated for 24 h at 37 °C, 250 rpm. The construct was purified by mini-prep, and diagnostic restriction digests were performed to confirm successful transformation with pET-21a(+)/Keap1, as described above. Glycerol stocks of a pET-21a(+)/Keap1-transformed BL21 (DE3) colony were made by supplementing a mid-log phase culture with 15 % (v/v) glycerol; these stocks were stored at -80 °C until required.

3.2.5 DNA two-strand sequencing

BL21 (DE3), transformed with pET-21a(+)/Keap1, and primers (at 3.2 μM) were sent to Geneservice for two-strand sequencing of pET-21a(+)/Keap1. Sequencing primers were custom-synthesised by Sigma-Genosys, in accordance with the requirements of Geneservice; external forward 5'-TAATACGACTCACTATAGGG-3', internal forward

5'-CCACCCTAAGGTCATGGAAA-3', external reverse 5'-GCTAGTTATTGCTCAG CGG-3', internal reverse 5'-GCTAGTTATTGCTCAGCGG-3'. Sequencing results were analysed using ChromasPro software.

3.2.6 Expression and purification of Keap1-His

LB broth (0.125 L), supplemented with 50 μg/mL ampicillin, was inoculated with 3 mL pET-21a(+)/Keap1-transformed BL21 (DE3) glycerol stock and incubated at 37 °C, 250 rpm, overnight. The culture was then diluted to 1.2 L in LB broth containing 50 μg/mL ampicillin, and incubated at 37 °C, 250 rpm, for 30 min. At this point, the optical density at 600 nm (OD_{600nm}) was measured using a spectrophotometer, to ensure that the culture was at early-log phase of growth (OD_{600nm} of approximately 0.4). Keap1-His protein expression was induced over 4 h, at 37 °C, 250 rpm, with 1 mM isopropyl-β-D-thiogalactopyranoside (IPTG). Following induction, bacteria were pelleted at 5000 g, for 5 min, and washed in 50 mL refolding buffer (0.5 M NaCl, 50 mM Tris base, 20 mM imidazole, pH 8.0). The washed pellet was resuspended in 50 mL ice-cold isolation buffer (2 M urea, 0.5 M NaCl, 50 mM Tris base, 2 % (v/v) Triton X-100, pH 8.0), divided into two equal aliquots in 50 mL tubes and disrupted in an ultrasonic disintegrator (10 sec, followed by 10 sec recovery, x 4 repeats). Disrupted bacteria were pelleted at 10,000 g for 5 min, resuspended in 30 mL binding buffer (6 M guanidine HCl, 0.5 M NaCl, 50 mM Tris base, 20 mM imidazole, 1 mM β-mercaptoethanol, pH 8.0) and shaken vigorously at 4 °C for 30 min. After making 1.5 mL aliquots of this solution, cell debris was pelleted at 18,000 g for 10 min; the supernatants were pooled and incubated with 0.6 mL (dry volume) HIS-Select nickel (Ni^{2+}) -charged agarose, or Sepharose 6B, beads at 4 °C for 30 min. Beads were pelleted by making 1.5 mL aliquots of the binding solution and centrifuging at 5000 g for 1 min. Beads were washed once with 1 mL binding buffer, three times with 1 mL wash buffer (6 M urea, 0.5 M NaCl, 50 mM Tris base, 20 mM imidazole, 1 mM β-mercaptoethanol, pH 8.0) and three times with 1 mL refolding buffer. Beads were finally resuspended in an equal volume of ice-cold phosphate buffer (13.08 mM KH_2PO_4, 67.27 mM Na_2HPO_4, pH 7.4).

3.2.7 Western blot analysis

Keap1-His expression and purification were determined by Western blot analysis, essentially as described in section 2.2.6. To assess Ni^{2+} purification of Keap1-His, proteins were eluted from agarose beads by resuspending in an equal volume of NuPAGE loading buffer. The slurry was heated at 80 °C for 5 min, the beads were pelleted by centrifugation at 5000 g for 5 min, and the supernatant loaded onto a pre-cast 4-12 % NuPAGE Novex bis-tris polyacrylamide gel. The anti-polyhistidine HRP-conjugated antibody was used at 1:10,000 in TBS-Tween containing 2 % (w/v) BSA.

3.2.8 Silver stain analysis

Keap1-His expression and purification were determined using a SilverXpress silver staining kit, in accordance with the manufacturer's instructions. Gels were scanned using a GS-710 calibrated imaging densitometer.

3.2.9 Determination of on-bead Keap1-His content

The on-bead content of Keap1-His was assessed with a bicinchoninic acid (BCA) Protein Assay Kit, with a slight modification of the method of Stich (1990). The BCA assay is based on the reduction of Cu^{2+} to Cu^{+} by protein in an alkaline environment (the biuret reaction). Each Cu^{+} formed reacts with two molecules of BCA to form a purple chromophore that has an absorbance maximum at 562 nm (Smith *et al.*, 1985). For the determination of protein immobilised on agarose beads, the BCA assay is preferred to a standard Bradford protein assay because the blue chromophore that forms when Coomassie Brilliant Blue G-250 reacts with immobilised protein remains associated with the agarose beads, which settle at the bottom of the plate/tube. Thus, constant stirring of the sample is required to enable spectrophotometric determination of protein content. The purple chromophore formed via the reaction of BCA with immobilised

protein is water-soluble, and thus does not remain associated with the agarose beads, enabling spectrophotometric determination of protein content without the need for constant stirring of the sample. Keap1-His -coupled Ni^{2+}-charged agarose beads (50 µL dry volume) were washed three times with 0.2 mL distilled H_2O (dH_2O). A standard curve ranging from 0.01-1 mg/mL BSA was prepared in separate tubes (50 µL each). Beads and standards were combined with 1 mL BCA assay reagent (0.98 mL reagent A, 20 µL reagent B) and incubated in a 37 °C water bath for 30 min. All tubes were vortexed every 10 min during this incubation period. Following the 30 min incubation, tubes were stored on ice to avoid further colour development. The beads were pelleted by centrifugation at 5000 g for 1 min. 0.2 mL supernatant, or standards, were transferred to a clear 96-well plate and the absorbance at 570 nm was read on a MRX microplate reader. A blank reading (dH_2O and BCA reagent) was subtracted from all sample and standard readings. A bead blank reading (uncoupled Ni^{2+}-charged agarose beads and BCA reagent) was subtracted from the sample reading. For the calculation of molar ratios, the concentration of Keap1-His (µg/µL) was converted to molarity using the following equation:

Protein concentration (µg/µL) x [1/protein molecular weight (µg)] = concentration (µM)

3.2.10 Determination of Keap1-His cysteine redox states

To determine whether Keap1-His cysteines were in sulphydryl or disulphide states, a differential chemical capping approach was developed. To cap free sulphydryls, Keap1-His -coupled Ni^{2+}-charged agarose beads (50 µL dry volume) were resuspended in 0.13 mL phosphate buffer and 20 µL of 0.55 M iodoacetamide, and incubated on a mechanical roller at 4 °C for 30 min. The beads were washed three times in 0.5 mL phosphate buffer to remove residual iodoacetamide. To reduce disulphides, the beads were resuspended in 0.148 mL phosphate buffer and 2 µL of 0.1 M DTT, and incubated on a mechanical roller at 4 °C for 30 min. The beads were washed three times in 0.5 mL phosphate buffer to remove residual DTT. In order to cap the sulphydryls formed from

the reduction of disulphides, the beads were resuspended in 0.13 mL phosphate buffer and 20 μL of 0.2 M N-ethylmaleimide (NEM), and incubated on a mechanical roller at 4 °C for 30 min. The beads were washed three times in 0.5 mL phosphate buffer to remove residual NEM. Prior to digestion with trypsin, the beads were washed once with 0.5 mL of 25 mM ammonium bicarbonate, and then resuspended in 25 μL of 25 mM ammonium bicarbonate. A 400 μg/mL stock solution of sequencing-grade modified trypsin was diluted 1:10, in 25 mM ammonium bicarbonate, and 6 μL (240 ng) was added to the bead slurry. Tryptic digestion was allowed to proceed overnight at 37 °C.

3.2.11 MALDI-TOF mass spectrometry

Following overnight tryptic digestion, peptide mixtures (0.5 μL) were combined with an equal volume of α-cyano-4-hydroxy-cinnamic acid (αCHCA) matrix (10 mg/mL αCHCA in 50 % (v/v) acetonitrile (ACN), 0.1 % (v/v) trifluoroacetic acid (TFA)) and spotted onto a matrix-assisted laser desorption ionization mass spectrometry (MALDI-MS) target plate alongside ProteoMass MALDI-MS standards (angiotensin II, adrenocorticotropic hormone fragment 18-39, oxidised insulin chain B, 0.5 pmol each), using the dried-droplet method. Peptide mass fingerprints were obtained on a Voyager DE Pro MALDI time-of-flight (TOF) Biospectrometry Workstation, in linear positive ion mode, and used in a MASCOT protein database search (http://www.matrixscience.com) to enable identification of proteins present within the sample.

3.2.12 LC-ESI-MS/MS mass spectrometry

Samples were delivered into an API QSTAR Pulsar i system by automated in-line reversed phase liquid chromatography (LC), using an integrated LCPackings System (Famos autosampler, Ultimate LC pump, Switchos microcolumn switching module) and 75 μm x 15 cm C18 PepMap column, via a nano-electrospray source head and 10 μm

inner diameter PicoTip emitter. A gradient of 5-48 % (v/v) ACN, 0.05 % (v/v) TFA over 60 min, followed by 10 min at 99 % (v/v) ACN, 0.05 % (v/v) TFA and 15 min at 5 % (v/v) ACN, 0.05 % (v/v) TFA, was applied to the column at a flow rate of 0.35 μL/min. Across a mass range of 300-2000 atomic mass units (amu), MS and MS/MS spectra were acquired automatically in positive ion mode using information-dependent acquisition powered by Analyst QS software. Above a threshold of 5 counts per sec, the three most intense ions in each MS spectrum were subjected to MS/MS analysis for 1.5 sec, and subsequently excluded from further analysis for 40 seconds. The instrument was routinely calibrated with 0.3 nmol caesium iodide ($M+H^+$ = 132.9) and 30 pmol sex pheromone inhibitor peptide iPD1 ($M+H^+$ = 829.5) in 50 % (v/v) methanol, 1 % (v/v) formic acid. Amino acid modifications were detected with ProteinPilot software v2.0 using the Paragon^{TM} algorithm (Shilov *et al.*, 2007) and the most recent version of the SwissProt database. Carboxyamidomethyl (+57.0 amu) or NEM (+125.0 amu) were selected as variable modifications. All adducts were confirmed by visual inspection of the MS/MS spectra.

3.3 RESULTS

3.3.1 PCR amplification of mouse *Keap1* coding sequence

The mouse *Keap1* coding sequence (1875 bp) was amplified by PCR. Primers were designed to enable amplification of the coding sequence without the TGA stop codon, to facilitate the translation of a polyhistidine-tagged Keap1 protein. The primers also permitted the introduction of an additional 12 bp at the 5' and 3' ends of the coding sequence. These inserts, containing *Ase*I (5') and *Xho*I (3') restriction digest sites (Fig. 3.1), were introduced to enable the ligation of the *Keap1* coding sequence into the *Nde*I and *Xho*I restriction sites of pET-21a(+). An *Ase*I restriction site, and not an *Nde*I site, was introduced into the *Keap1* coding sequence because the latter site contains an ATG initiation codon, which would have resulted in the premature translation of the construct.

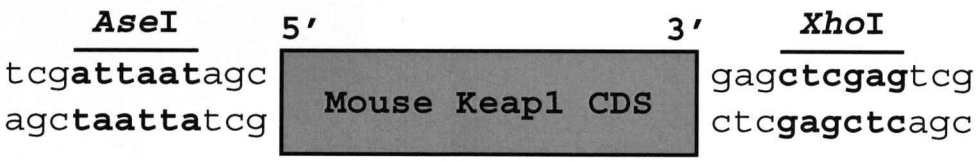

Fig. 3.1 - Schematic diagram showing insertion of *Ase*I and *Xho*I restriction digest sites at the 5' and 3' ends, respectively, of the mouse *Keap1* coding sequence (CDS). The restriction sites are shown in bold.

3.3.2 Ligation of mouse *Keap1* coding sequence into pET-21a(+)

The tagged *Keap1* PCR product was digested with *Ase*I and *Xho*I, whilst pET-21a(+) (Fig. 3.2) was digested with *Nde*I and *Xho*I; both restriction fragments were resolved by electrophoresis (Fig. 3.3). As digestion with *Ase*I and *Nde*I yields compatible ends, the *Ase*I/*Xho*I-digested *Keap1* fragment was ligated into *Nde*I/*Xho*I-digested pET-21a(+). XL10-Gold ultracompetent *E. coli* were transformed with the ligated construct. Successful transformation was confirmed by diagnostic restriction digests of construct DNA purified from selected bacterial colonies (Fig. 3.4). Specifically, fragments of the

expected size(s) were visualised following digestion with *Bgl*II (cuts at -106 and 1694 of *Keap1*; 1800 bp fragment), *Xba*I and *Sac*I (*Xba*I cuts at -40, *Sac*I cuts at 923; 963 bp fragment), and *Hind*III and *Xho*I (*Hind*III cuts at 16, *Xho*I cuts at 1879; 1863 fragment). These diagnostic restriction digests demonstrate that the *Keap1* coding sequence ligated into pET-21a(+) successfully, and in the correct orientation. In order to confirm that the PCR amplification process had not introduced mutations into the *Keap1* coding sequence, the pET-21a(+)/Keap1 construct was verified by two-strand sequencing. This process confirmed that no non-synonymous mutations, i.e. those that result in the translation of a different amino acid, were present in pET-21a(+)/Keap1. An example electropherogram, depicting the *Xho*I restriction site, polyhistidine tag and TGA stop codon of pET-21a(+)/Keap1, is presented in Fig. 3.5.

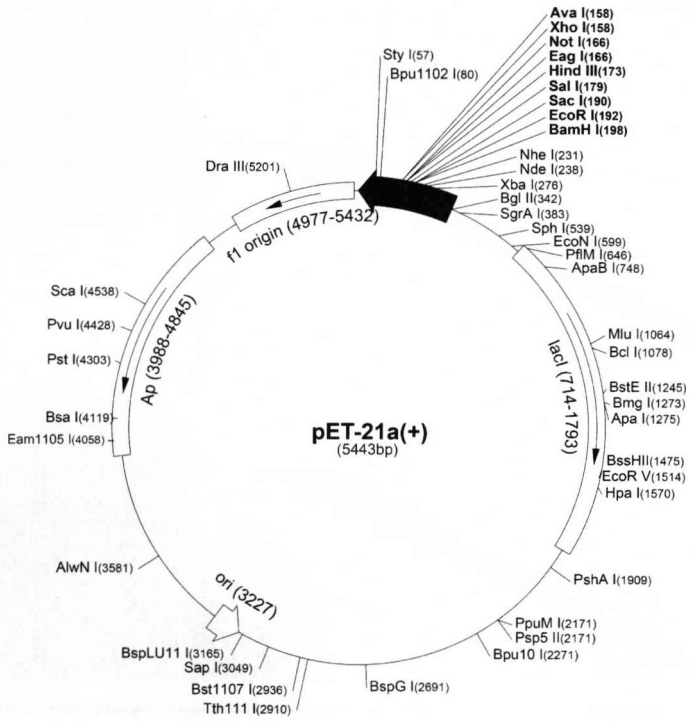

Fig. 3.2 - pET-21a(+) vector map. The tagged *Keap1* coding sequence was ligated into the *Nde*I and *Xho*I restriction sites of pET-21a(+). Image taken from Novagen on-line catalogue (http://www.merckbiosciences.co.uk/docs/NDIS/TB036-000.pdf).

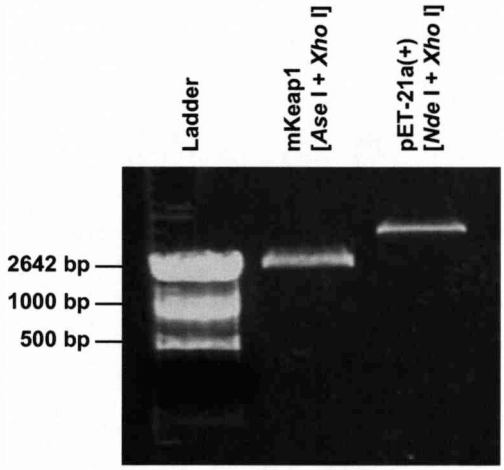

Fig. 3.3 - Restriction digested mouse *Keap1* coding sequence and pET-21a(+). The tagged mouse *Keap1* coding sequence was digested with *Ase*I and *Xho*I. pET-21a(+) was digested with *Nde*I and *Xho*I. Both restriction fragments, alongside a 100 bp DNA ladder, were resolved by electrophoresis on a 1 % (w/v) agarose gel, containing 0.5 μg/mL ethidium bromide. DNA fragments were visualised under UV illumination.

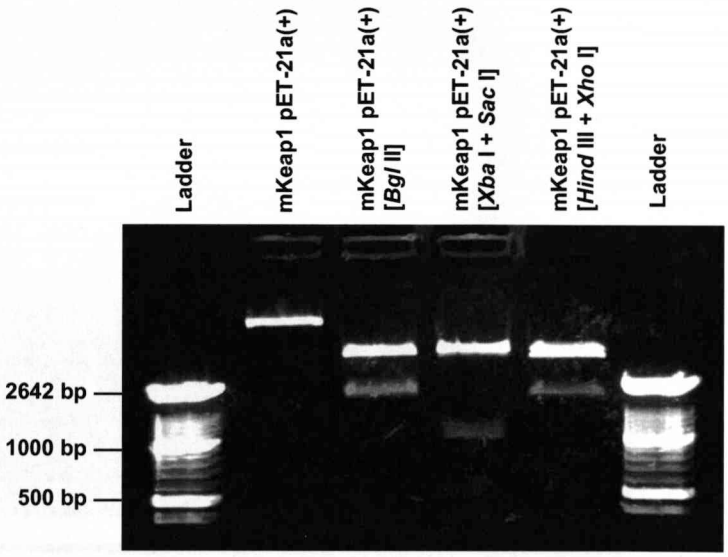

Fig. 3.4 - Diagnostic restriction digests of pET-21a(+)/Keap1 from putative transformed XL10-Gold *E. coli*. pET-21a(+)/Keap1 was purified from selected bacterial colonies by mini-prep. The construct was digested with *Bgl*II (cuts at -106 and 1694 of *Keap1*; 1800 bp fragment), *Xba*I and *Sac*I (*Xba*I cuts at -40, *Sac*I cuts at 923; 963 bp fragment), and *Hind*III and *Xho*I (*Hind*III cuts at 16, *Xho*I cuts at 1879; 1863 fragment). The restriction fragments, the undigested construct, and a 100 bp DNA ladder were resolved by electrophoresis on a 1 % (w/v) agarose gel, containing 0.5 μg/mL ethidium bromide. DNA fragments were visualised under UV illumination.

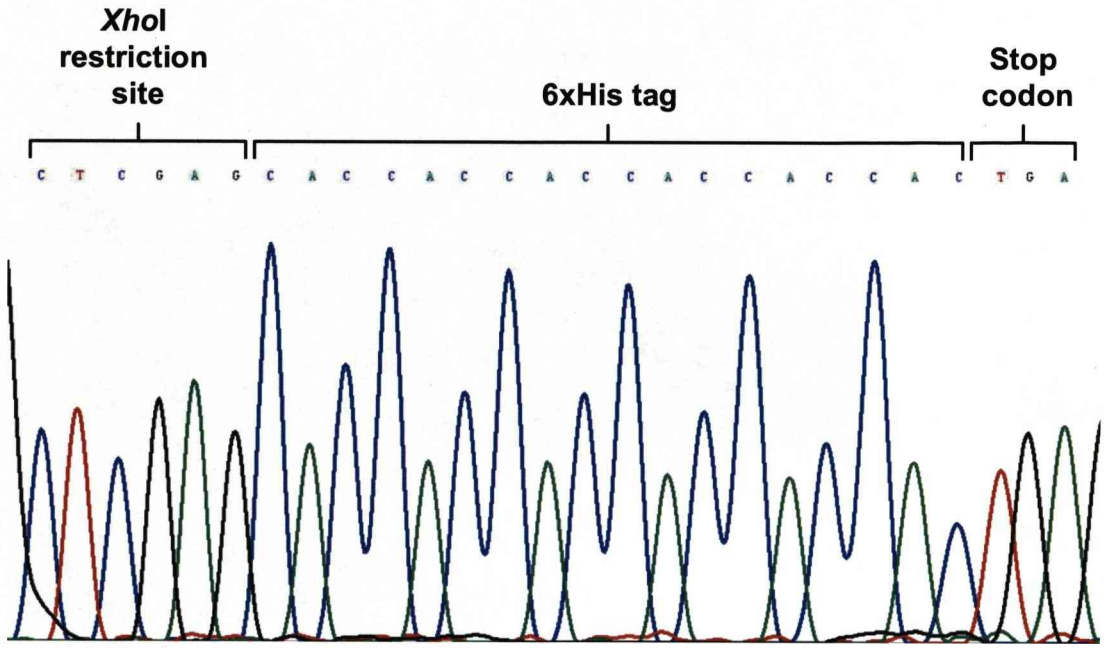

Fig. 3.5 - Sequencing electropherogram of pET-21a(+)/Keap1. pET-21a(+)/Keap1 was sequenced by Geneservice; the construct was amplified by PCR in the presence of the terminator nucleotides dideoxy -adenine (■), -thymine (■), -guanine (■) and -cytosine (■). The amplification products were resolved by electrophoresis, visualised under UV illumination, and recorded automatically. The region of electropherogram shown depicts the *Xho*I restriction site, polyhistidine (6xHis) tag and TGA stop codon of pET-21a(+)/Keap1.

3.3.3 Expression and purification of Keap1-His

BL21 (DE3) competent *E. coli* were transformed with the verified pET-21a(+)/Keap1 construct, and Keap1-His expression was induced via supplementation of the culture with IPTG. As an analogue of lactose, IPTG displaces the repressor from the *lac* operator of the BL21 (DE3) T7 polymerase gene (Dubendorff *et al.*, 1991; Studier *et al.*, 1986), allowing T7 polymerase to drive transcription of the gene of interest via the T7 promoter (Dubendorff *et al.*, 1991; Studier *et al.*, 1986). The inducible expression of Keap1-His was confirmed by Western blot analysis (Fig. 3.6). It was noted that the anti-Keap1 antibody consistently detected two protein bands of slightly different molecular weights (Fig. 3.6). As the exact nature of the two bands was not investigated during this work, the cause of this phenomenon is not clear. A large proportion of the recombinant

Keap1-His protein was insoluble following sonication of the bacterial pellet in 1X PBS (Fig. 3.6), and was thus unsuitable for purification of Keap1-His using Ni^{2+}-charged agarose beads, which could not have been separated from the insoluble pellet by centrifugation. Therefore, Keap1-His was purified under denaturing conditions, in order to enable maximal recovery of the recombinant protein in a soluble form. Denaturing purification of Keap1-His from the crude bacterial lysate was confirmed by silver stain, which showed a high degree of purity in the recovered fraction (Fig. 3.7). Western blot analysis also showed a high recovery of a polyhistidine-tagged protein that ran at the size anticipated for Keap1-His (70.8 kiloDalton; kDa) (Fig. 3.7).

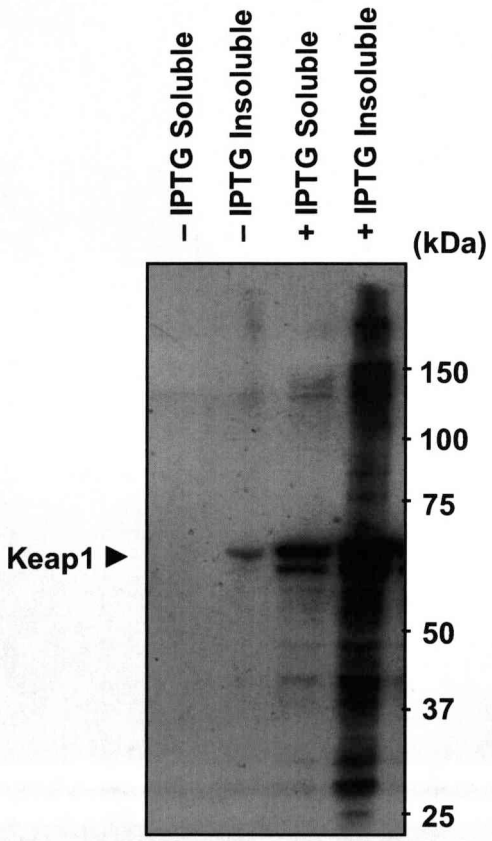

Fig. 3.6 - Inducible expression of Keap1-His in BL21 (DE3) *E. coli*. BL21 (DE3) transformed with pET-21a(+)/Keap1 were cultured in LB broth and, at an OD_{600nm} of 0.4, were not induced, or induced with 1 mM IPTG, for 4 h at 37 °C, 250 rpm. The bacterial pellets were resuspended in 1X PBS and disrupted by sonication. The soluble lysates and insoluble pellets were resolved by denaturing electrophoresis and Keap1 expression was assessed by Western blot analysis.

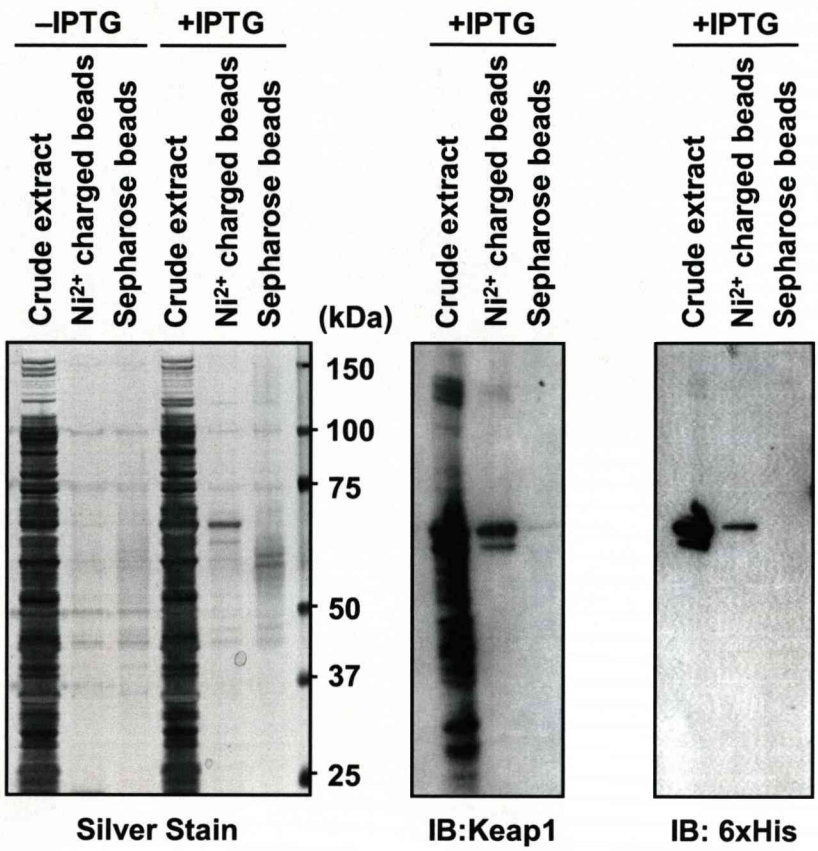

Fig. 3.7 - Denaturing purification of Keap1-His. Keap1-His expression was induced or not by the supplementation of a BL21 (DE3) culture with 1 mM IPTG. Following incubation for 4 h at 37 °C, 250 rpm, the bacterial pellets were lysed under denaturing conditions, and the soluble lysates were incubated for 30 min, at 4 °C, with HIS-Select Ni^{2+}-charged agarose, or Sepharose 6B, beads. The crude bacterial lysates and the proteins eluted from the respective beads were resolved by denaturing electrophoresis. Keap1-His expression and purification was confirmed by silver stain and Western blot analysis; the latter was performed separately with anti-Keap1 and anti-polyhistidine antisera.

MALDI-TOF MS analysis revealed that the polyhistidine-tagged protein recovered from pET-21a(+)/Keap1 -transformed BL21, using Ni^{2+}-charged agarose beads, was Keap1-His (Fig. 3.8). The peptide mass fingerprint obtained from this analysis was used in a MASCOT protein database search, which identified mouse Keap1 as the major constituent of the tryptic digest (Fig. 3.9). The amino acid coverage for mouse Keap1, from the MALDI-TOF MS analysis, was 82 %, and included Cys-151, -273 and -288,

which have been shown to be critical for the function of Keap1 (Kobayashi *et al.*, 2006; Levonen *et al.*, 2004; Wakabayashi *et al.*, 2004; Zhang *et al.*, 2003a). Of the 25 cysteines in Keap1-His, only Cys-622 and -624 were not routinely covered during MS analysis, as they were not released from the Ni^{2+}-charged agarose beads by tryptic digestion, due to their proximity to the polyhistidine tag of Keap1-His. Compound mutation of the three cysteines (Cys-613, -622, -624) located within the C-terminal domain of Keap1 has no effect on the repressive activity of Keap1 towards Nrf2 (Wakabayashi *et al.*, 2004), implying that Cys-622 and -624 are not essential for Keap1 function.

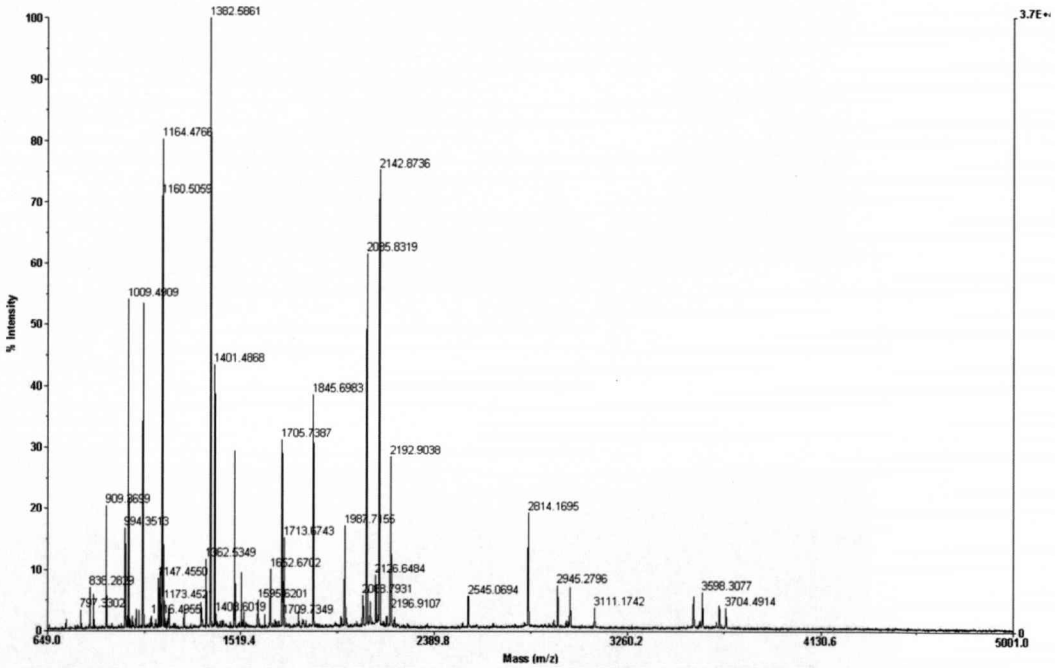

Fig. 3.8 - MALDI-TOF mass spectrum of the tryptic digest of protein(s) purified by Ni^{2+} affinity, under denaturing conditions, from pET-21a(+)/Keap1 -transformed BL21 (DE3). Keap1-His expression was induced via the supplementation of a BL21 (DE3) culture with 1 mM IPTG. Following incubation for 4 h at 37 °C, 250 rpm, the bacterial pellets were lysed under denaturing conditions and the soluble lysates were incubated for 30 min, at 4 °C, with HIS-Select Ni^{2+}-charged agarose beads. Bead-bound protein(s) were reduced with 1 mM DTT, alkylated with 55 mM iodoacetamide, and digested overnight with 240 ng trypsin. The resulting peptide mixture was visualised on a Voyager DE Pro MALDI-TOF Biospectrometry Workstation, in linear positive ion mode.

	Accession	Mass	Score	Description
1.	gi|33416964	69508	319	Kelch-like ECH-associated protein 1 [Mus musculus]
2.	gi|37359786	71015	309	mKIAA0132 protein [Mus musculus]
3.	gi|74207025	69492	301	unnamed protein product [Mus musculus]
4.	gi|26337871	69478	298	unnamed protein product [Mus musculus]
5.	gi|74219578	69482	274	unnamed protein product [Mus musculus]

Match to: **gi|33416964 Kelch-like ECH-associated protein 1 [Mus musculus]**
Sequence Coverage: **82%**

```
  1 MQPEPKLSGA PRSSQFLPLW SKCPEGAGDA VMYASTECKA EVTPSQDGNR
 51 TFSYTLEDHT KQAFGVMNEL RLSQQLCDVT LQVKYEDIPA AQFMAHKVVL
101 ASSSPVFKAM FTNGLREQGM EVVSIEGIHP KVMERLIEFA YTASISVGEK
151 CVLHVMNGAV MYQIDSVVRA CSDFLVQQLD PSNAIGIANF AEQIGCTELH
201 QRAREYIYMH FGEVAKQEEF FNLSHCQLAT LISRDDLNVR CESEVFHACI
251 DWVKYDCPQR RFYVQALLRA VRCHALTPRF LQTQLQKCEI LQADARCKDY
301 LVQIFQELTL HKPTQAVPCR APKVGRLIYT AGGYFRQSLS YLEAYNPSNG
351 SWLRLADLQV PRSGLAGCVV GGLLYAVGGR NNSPDGNTDS SALDCYNPMT
401 NQWSPCASMS VPRNRIGVGV IDGHIYAVGG SHGCIHHSSV ERYEPERDEW
451 HLVAPMLTRR IGVGVAVLNR LLYAVGGFDG TNRLNSAECY YPERNEWRMI
501 TPMNTIRSGA GVCVLHNCIY AAGGYDGQDQ LNSVERYDVE TETWTFVAPM
551 RHHRSALGIT VHQGKIYVLG GYDGHTFLDS VECYDPDSDT WSEVTRMTSG
601 RSGVGVAVTM EPCRKQIDQQ NCTC
```

Fig. 3.9 - MASCOT protein database search result for peptide mass fingerprint obtained from the MALDI-TOF MS analysis of protein(s) purified by Ni^{2+} affinity, under denaturing conditions, from pET-21a(+)/Keap1 -transformed BL21 (DE3). The peptide mass fingerprint shown in Fig. 3.8 was used in a MASCOT protein database search (http://www.matrixscience.com), which identified mouse Keap1 as the major constituent protein in the tryptic digest. The five proteins identified with the highest degree of confidence are shown (all are variant database entries for mouse Keap1). The amino acid sequence coverage for mouse Keap1 was 82 %. The specific amino acids covered by the MALDI-TOF MS analysis are underlined and in bold.

3.3.4 Determination of Keap1-His cysteine redox states

Although the denaturing purification process contained a refolding step, in which all denaturing and reducing agents were removed from the protein(s), it was not possible to determine if this step facilitated the reliable and correct folding of Keap1-His, partly because there is, at present, no point of reference for the whole protein, in that crystal structures have only been resolved for the DGR and C-terminal domains of mouse Keap1 (Padmanabhan *et al.*, 2005). Therefore, because the main application of the purified Keap1-His was to be in the analysis of Keap1 cysteine modification by Nrf2-activating molecules, the consistency of cysteine redox states in Keap1-His across

separate purifications was assessed using a differential chemical capping approach (Fig. 3.10). One of two procedures was followed: 1) Keap1-His was alkylated, or reduced and then alkylated; any cysteines that were alkylated without reduction were likely to be in a sulphydryl state, whilst those that were alkylated only following reduction were likely to be in a disulphide state, and 2) Keap1-His was exposed to iodoacetamide, then reduced with DTT, and exposed to NEM; any cysteines that were alkylated by iodoacetamide were likely to be in a sulphydryl state, whilst those that were only alkylated by N-ethylmaleimide were likely to be in a disulphide state. This approach, coupled with liquid chromatography electrospray ionization tandem mass spectrometry (LC-ESI-MS/MS), enabled the redox states of the cysteines in mouse Keap1-His to be determined, by detecting mass shifts (+57.0 amu for iodoacetamide, +125.0 amu for NEM) on each cysteine residue.

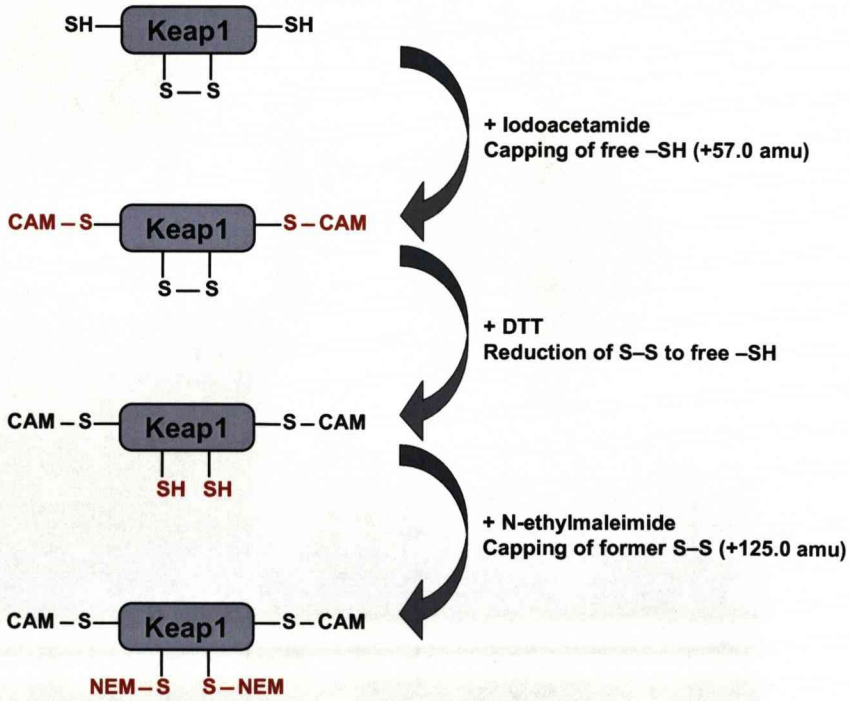

Fig. 3.10 - Differential chemical capping approach for determining the redox states of Keap1-His cysteines. Purified Keap1-His was alkylated with iodoacetamide, reduced with DTT and alkylated with N-ethylmaleimide. Cysteines in a -SH state were identified by an increase in mass of +57.0 amu (carboxamidomethylation; CAM) prior to reduction. Cysteines in a S-S state were identified by a lack of carboxamidomethylation prior to reduction and an increase in mass of +125.0 amu (N-ethylmaleimide; NEM) only following reduction.

Across three separate purifications, performed on individual bacterial pellets on the same day, inconsistencies in the redox states of Keap1-His cysteines were detected (Table 3.1). For example, certain residues were found to be in a sulphydryl state in one purification and a disulphide state in another. Some cysteine residues were also found to be in both sulphydryl and disulphide states within the same purification. Similar inconsistencies were also found across purifications performed on separate days (Table 3.1). These results indicate that the denaturing and refolding process employed to purify Keap1-His could not ensure a consistent redox state for Keap1-His cysteine residues, within or across purifications. Therefore, it would not be possible to assume that Keap1-His purified on separate occasions was structurally identical. Similarly, it was clearly not going to be possible to use the method described here to study the modification of Keap1 cysteines by Nrf2-activating molecules without first rendering all of the cysteines free for adduction (i.e. in a sulphydryl state). It was considered that such an approach would not render subsequent studies of Keap1 cysteine modification invalid, for the following reasons: 1) the native redox states of cysteines other than those residing within the DGR domain of human Keap1 (Li *et al.*, 2004b) have yet to be elucidated, and so it may transpire that many or all of the cysteines in Keap1 are naturally in a sulphydryl state, and, more importantly, 2) ensuring that all Keap1 cysteines were in a sulphydryl state would render all of them free for modification, thus enabling the examination of the relative reactivities of Keap1 cysteines towards chemically distinct Nrf2-activating molecules. In summary, then, these data describe the generation of recombinant mouse Keap1-His and validation of its use as an *in vitro* model for studying the modification of Keap1 cysteines by Nrf2-activating molecules, using LC-ESI-MS/MS.

		Day 1						Day 2				Day 3		
		Pellet 1		Pellet 2		Pellet 3		Pellet 1				Pellet 1		
Domain	Cys #	-DTT +Iodo	+DTT +Iodo	-DTT +Iodo	+DTT +Iodo	-DTT +Iodo	+DTT +Iodo	-DTT +Iodo	+DTT +Iodo	-DTT +NEM	+DTT +NEM	+Iodo +DTT +NEM	+Iodo +DTT +NEM	+Iodo +DTT +NEM
N-terminal	23	–	–	–	–	U	–	U	I	–	N	I N	I N	U I N
N-terminal	38	–	–	–	–	U	–	U	I	–	N	I N	I N	U I N
BTB	77	I	I	I	I	I	I	I	I	N	N	I N	I N	I N
BTB	151	–	–	–	–	I	–	–	I	–	–	N	N	N
BTB	171	–	I	I	I	I	I	–	I	–	–	N	N	U N
IVR	196	–	I	I	I	I	I	–	I	–	–	I N	I	U I N
IVR	226	I	I	I	I	I	I	I	–	N	N	I N	I N	I N
IVR	241	–	I	I	I	–	I	–	–	–	N	I N	N	I N
IVR	249	–	I	I	I	–	I	–	–	–	N	I N	I N	I N
IVR	257	–	–	–	–	–	–	–	–	–	N	I	I	I
IVR	273	–	–	–	–	–	–	–	–	N	N	U N	N	N
IVR	288	I	I	I	I	I	I	–	I	N	N	U I N	U I N	I N
IVR	297	–	I	–	I	–	I	–	–	–	–	I	I N	I
DGR	319	–	I	–	I	–	I	–	–	–	–	I	I	–
DGR	368	I	U I	U I	I	U I	I	I	I	–	–	I N	I N	I N
DGR	395	U	U I	U	U I	U	–	U	U	U	U N	U N	U	U
DGR	406	U	U I	U	U I	U	–	U	U	U	U N	U N	U	U I N
DGR	434	I	I	I	I	I	I	–	I	–	–	I N	I N	I N
DGR	489	–	I	I	I	I	I	I	I	N	N	I N	I N	I N
DGR	513	U I	U I	I	I	U	I	–	I	–	U N	N	N	I
DGR	518	U I	U I	I	I	U	I	–	I	–	U N	U I N	I N	N
DGR	583	I	I	I	I	I	I	I	I	N	N	I N	I N	U I
C-terminal	613	I	I	–	I	I	I	I	I	N	N	U I N	U I N	I N

Table 3.1 - Keap1-His cysteine redox states within and across purifications. A differential chemical capping approach was used to enable the determination of redox states of the 23 cysteines within mouse Keap1-His that were routinely covered by MS analysis. U = detected unmodified, I = detected alkylated by iodoacetamide (+57.0 amu), N = detected alkylated by NEM (+125.0 amu), – = not detected. Cysteines that were interpreted as sulphydryls, i.e. those that were alkylated prior to reduction, are labeled ■, whereas cysteines that were interpreted as disulphides, i.e. those that were alkylated only after reduction, are labeled ■.

3.3.5 Expression and purification of soluble Keap1-His under non-denaturing conditions

In the latter stages of this PhD, and with the technical assistance of Mr. Peter Metcalfe, the successful expression and purification of a soluble form of Keap1-His was achieved using non-denaturing conditions. LB broth was substituted with Power Broth, a nutrient-rich, proprietary formulation (Athena Enzyme Systems). pET-21a(+)/Keap1 -transformed BL21 (DE3) were grown in Power Broth and, at an OD_{600nm} of 0.4, were induced overnight at 20 °C, 250 rpm, via supplementation with 1 mM IPTG. The next morning, the pH of the culture was adjusted to 7.5 with 1 M Tris base, the bacteria were then pelleted and resuspended in binding buffer (0.5 M NaCl, 20 mM Na_2HPO_4, 20 mM imidazole, pH 7.4). The bacteria were disrupted by sonication (six bursts of 10 sec, interspersed with 10 sec recoveries) and clarified by centrifugation. Polyhistidine-tagged proteins were then purified from the soluble fraction using a HisTrap HP affinity column (Amersham, Little Chalfont, UK), in accordance with the manufacturer's instructions. Affinity-purified proteins were eluted from the column in elution buffer (0.5 M imidazole, 0.5 M NaCl, 20 mM Na_2HPO_4, pH 7.4), resolved by denaturing electrophoresis, and visualised by staining with Coomassie Brilliant Blue G-250. An abundant protein, at the anticipated size of Keap1-His (70.8 kDa) was detected in the lysate from induced, but not uninduced, pET-21a(+)/Keap1 -transformed BL21 (DE3) (Fig. 3.11). The successful purification of Keap1-His was confirmed by MALDI-TOF MS analysis of the trypsin-digested proteins eluted from the affinity column (Fig. 3.12). The peptide mass fingerprint obtained from this analysis was used in a MASCOT protein database search, which identified mouse Keap1 as the major constituent of the tryptic digest (Fig. 3.13). The amino acid coverage for mouse Keap1, from the MALDI-TOF MS analysis, was 45 %. The amino acid coverage from LC-ESI-MS/MS analysis, which affords greater resolution due to the chromatographic separation of peptides, was 85 %. Since this method was developed in the latter stages of the project, there was insufficient time to use the protein in further studies into the modification of Keap1 cysteines by Nrf2-activating molecules.

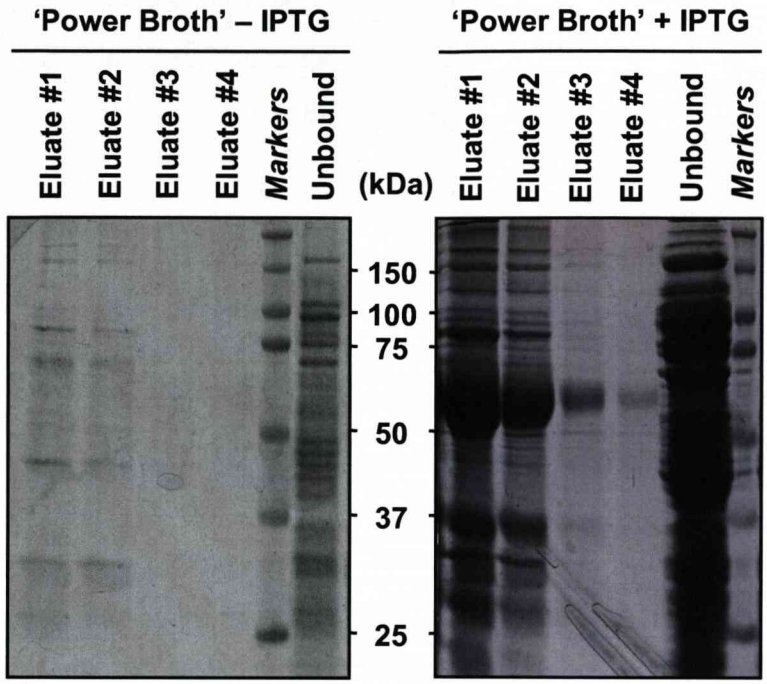

Fig. 3.11 - Coomassie Brilliant Blue stain of proteins eluted from a HisTrap HP affinity column, following non-denaturing expression of Keap1-His. Keap1-His expression was not induced or induced via the supplementation of a BL21 (DE3) Power Broth culture with 1 mM IPTG. Following overnight incubation at 20 °C, 250 rpm, the bacterial pellets were lysed under non-denaturing conditions and the soluble lysates were passed through a HisTrap HP affinity column. Proteins eluted from the column were resolved, alongside the flow-through fraction and protein molecular weight markers, by denaturing electrophoresis on a bis-tris polyacrylamide gel, which was subsequently stained with Coomassie Brilliant Blue G-250.

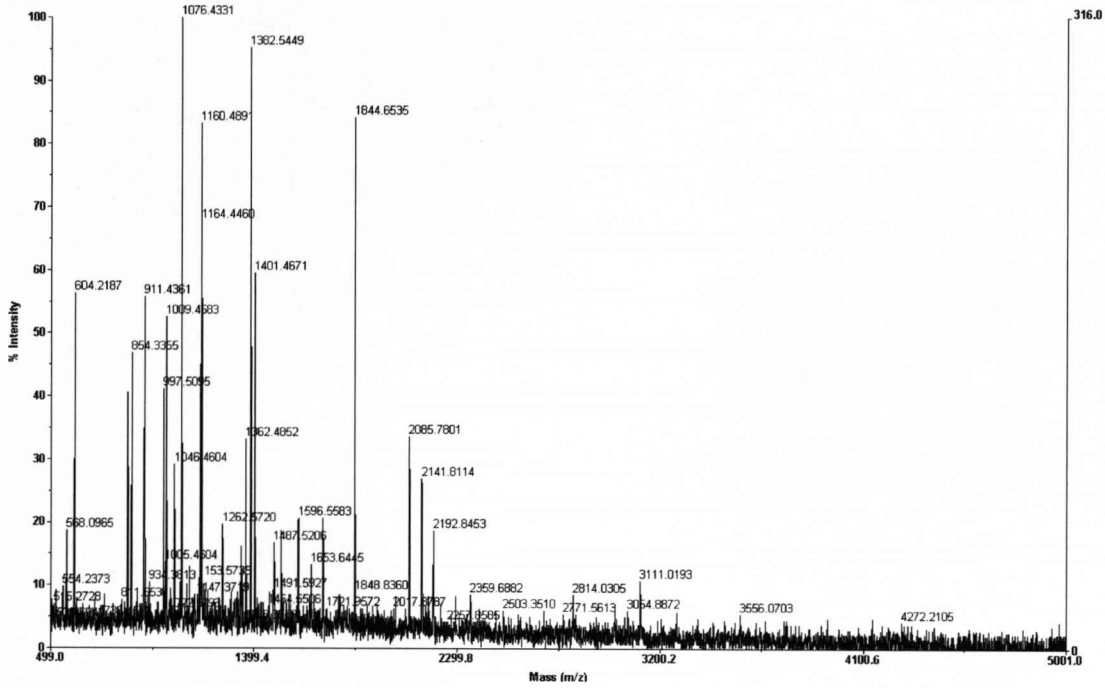

Fig. 3.12 - MALDI-TOF mass spectrum of the tryptic digest of protein(s) purified by Ni^{2+} affinity, under non-denaturing conditions, from pET-21a(+)/Keap1 - transformed BL21 (DE3). Keap1-His expression was induced via the supplementation of a BL21 (DE3) Power Broth culture with 1 mM IPTG. Following overnight incubation at 20 °C, 250 rpm, the bacterial pellets were lysed under non-denaturing conditions and the soluble lysates were passed through a HisTrap HP affinity column. Affinity purified protein(s) were reduced with 1 mM DTT, alkylated with 55 mM iodoacetamide, and digested overnight with 240 ng trypsin. The resulting peptide mixture was visualised on a Voyager DE Pro MALDI-TOF Biospectrometry Workstation, in linear positive ion mode.

	Accession	Mass	Score	Description
1.	gi|7710044	69508	161	kelch-like ECH-associated protein 1 [Mus musculus]
2.	gi|74181739	69492	161	unnamed protein product [Mus musculus]
3.	gi|26337871	69478	161	unnamed protein product [Mus musculus]
4.	gi|37359786	71015	159	mKIAA0132 protein [Mus musculus]
5.	gi|74212473	69482	143	unnamed protein product [Mus musculus]

Match to: **gi|7710044 kelch-like ECH-associated protein 1 [Mus musculus]**
Sequence Coverage: **45%**

```
  1 MQPEPKLSGA PRSSQFLPLW SKCPEGAGDA VMYASTECKA EVTPSQDGNR
 51 TFSYTLEDHT KQAFGVMNEL RLSQQLCDVT LQVKYEDIPA AQFMAHKVVL
101 ASSSPVFKAM FTNGLREQGM EVVSIEGIHP KVMERLIEFA YTASISVGEK
151 CVLHVMNGAV MYQIDSVVRA CSDFLVQQLD PSNAIGIANF AEQIGCTELH
201 QRAREYIYMH FGEVAKQEEF FNLSHCQLAT LISRDDLNVR CESEVFHACI
251 DWVKYDCPQR RFYVQALLRA VRCHALTPRF LQTQLQKCEI LQADARCKDY
301 LVQIFQELTL HKPTQAVPCR APKVGRLIYT AGGYFRQSLS YLEAYNPSNG
351 SWLRLADLQV PRSGLAGCVV GGLLYAVGGR NNSPDGNTDS SALDCYNPMT
401 NQWSPCASMS VPRNRIGVGV IDGHIYAVGG SHGCIHHSSV ERYEPERDEW
451 HLVAPMLTRR IGVGVAVLNR LLYAVGGFDG TNRLNSAECY YPERNEWRMI
501 TPMNTIRSGA GVCVLHNCIY AAGGYDGQDQ LNSVERYDVE TETWTFVAPM
551 RHHRSALGIT VHQGKIYVLG GYDGHTFLDS VECYDPDSDT WSEVTRMTSG
601 RSGVGVAVTM EPCRKQIDQQ NCTC
```

Fig. 3.13 - MASCOT protein database search result for peptide mass fingerprint obtained from the MALDI-TOF MS analysis of protein(s) purified by Ni^{2+} affinity, under non-denaturing conditions, from pET-21a(+)/Keap1 -transformed BL21 (DE3). The peptide mass fingerprint shown in Fig. 3.12 was used in a MASCOT protein database search (http://www.matrixscience.com), which identified mouse Keap1 as the major constituent protein in the tryptic digest. The five proteins identified with the highest degree of confidence are shown (all are variant database entries for mouse Keap1). The amino acid sequence coverage for mouse Keap1 was 45 %. The specific amino acids covered by the MALDI-TOF MS analysis are underlined and in bold.

3.4 DISCUSSION

The Nrf2-ARE pathway represents an inducible defence mechanism that affords protection to mammalian cells against chemical/oxidative stress (for a review, see Kensler *et al.*, 2007). The work presented in this chapter describes the development of a cell-free *in vitro* test system, based on the use of recombinant mouse Keap1 protein in combination with mass spectrometry, that provides an experimental basis to test the hypothesis that NAPQI activates the Nrf2-ARE pathway via the direct chemical modification of cysteine residues within Keap1, the cytosolic repressor of Nrf2. This system may also provide insights into the molecular mechanism that triggers Nrf2 activation in mouse liver following administration of paracetamol *in vivo* (Goldring *et al.*, 2004).

Recombinant DNA technology (Cohen *et al.*, 1973) has contributed greatly to the field of biomedicine. The ability to express recombinant proteins has enabled, for example, the large-scale and reliable production of human insulin for the treatment of diabetes (Crea *et al.*, 1978; Goeddel *et al.*, 1979). The use of recombinant protein technology and mass spectrometry has proved to be a fruitful combination for the detection and characterisation of post-translational modifications, and is now commonplace within the field of biomedical research (see the reviews by Liebler (2002) and Mann *et al.* (2003) for further details). Many groups have used these principles to investigate, for example, the oxidation state of the active site cysteine in human protein tyrosine phosphatase 1B (DeGnore *et al.*, 1998), the inhibition of NF-κB -DNA binding via covalent modification of Cys-62 within the p50 subunit by the anti-inflammatory molecules 15d-PGJ_2 (Cernuda-Morollon *et al.*, 2001), andrographolide (Xia *et al.*, 2004) and kamebakaurin (Lee *et al.*, 2002), and the modification of apolipoprotein B-100, the major protein constituent of low density lipoprotein, by the lipid peroxidation product 4-hydroxy-2-nonenal (Bolgar *et al.*, 1996). These and many other investigations have demonstrated that the use of mass spectrometry coupled with recombinant protein technology is a feasible and accurate means of characterising post-translational modifications at the amino acid level. Increasingly, with the improvement of pre-analytical separation

techniques and the continual evolution and increased sensitivity of mass spectrometers, the principles of these *in vitro* studies are being exploited to enable the characterisation of protein post-translational modifications in cells and *in vivo*, from samples that are inherently much more complex in nature (Ji *et al.*, 2007; Koen *et al.*, 2006; Lemercier *et al.*, 2004; Meier *et al.*, 2007; Meier *et al.*, 2005; Shin *et al.*, 2007)..

The use of recombinant proteins has many advantages for the detection of chemical modification(s) by mass spectrometry. For instance, the purification and enrichment of a protein dramatically reduces the complexity of the sample to be analysed. Such a strategy may eliminate the confounding effects of other proteins on the reaction being studied. Furthermore, given that only a small fraction of the total protein may be modified, protein enrichment effectively increases the sensitivity of the mass spectrometer for the detection of modifications. In addition, the prior characterisation of residue-specific modifications *in vitro*, using recombinant proteins, may better inform *in vivo* analyses, by identifying diagnostic data patterns that help the investigator to detect specific changes within a complex heterogeneous sample. However, there are also limitations to the use of recombinant proteins as biological models. For example, a given protein may not fold into its native form when expressed in bacteria. Such misfolding can particularly affect proteins which in the native state bear disulphide bonds, the formation of which is inhibited in the reducing environment of the *E. coli* cytoplasm (Singh *et al.*, 2005). It is also important to consider that modifications observed *in vitro*, from the reaction between a chemical and purified recombinant protein, may not necessarily occur within a much more complex cellular milieu. Therefore, one should be cautious when attempting to extrapolate data obtained from *in vitro* analyses to a cellular, or even whole organism, context.

Recombinant proteins are routinely expressed with conjoined affinity tags, which can be defined as amino acid sequences with a high affinity for a specific biological or chemical ligand (Arnau *et al.*, 2006). The incorporation of such tags enables the purification and enrichment of the protein of interest from the heterogeneous mixture of proteins present within the host expression system, such as *E. coli*. Polyhistidine tags,

which comprise a short peptide containing (normally six) consecutive histidine residues, are amongst the most widely-used affinity tags for recombinant protein purification. The principle of immobilised metal-affinity chromatography (Porath *et al.*, 1975), i.e. the strong interaction between a transition metal (Ni^{2+}, Co^{2+}, Cu^{2+}, Zn^{2+}) and the side chain of histidine, is central to the use of polyhistidine tags in the process of protein purification. Importantly in this case, the binding specificity of this reaction is robust under both native and denaturing conditions (Porath, 1992). Competition for transition metal binding with imidazole, which contains the same ring structure as the side chain of histidine, enables the elution of affinity-purified proteins (Hochuli, 1990). Many other affinity tags have been developed, including short peptides such as FLAG ('DYKDDDDK') and c-Myc ('EQKLISEEDL'), which enable purification via affinity towards an immobilised antibody, and much longer sequences that have a natural affinity for a biological molecule, such as streptavidin-binding protein (binds to immobilised streptavidin) and GST (binds to immobilised GSH) (Terpe, 2003). However, immobilised antibodies are generally expensive, and the incorporation of a large peptide or protein, in the case of GST, may have significant effects on the structure and/or function of the recombinant protein itself. In this regard, and given its wide-spread application in the purification of recombinant proteins, the polyhistidine tag was chosen as the fusion partner for recombinant Keap1 in this study.

E. coli is one of the most commonly-used systems for the expression of recombinant proteins, due in part to its rapid growth and well-characterised genetics (Baneyx, 1999). However, the use of *E. coli* for the production of recombinant protein is by no means a flawless process; one of the most frequent problems encountered, particularly with expression vectors that contain a strong promoter, is the tendency of highly-expressed proteins to misfold and form insoluble aggregates, known as inclusion bodies (Hartley *et al.*, 1988; Kane *et al.*, 1991). From the results presented in section 3.3.3, it appears that initial attempts at expressing Keap1-His were hindered by aggregation, with a large proportion of the protein being insoluble following disruption of the bacteria. Importantly, proteins aggregated within inclusion bodies tend to lack biological activity (Rudolph *et al.*, 1996). Fortunately, however, methods for the recovery of recombinant

protein from inclusion bodies have been developed, and have classically involved the use of concentrated chemical denaturants, particularly urea and guanidine hydrochloride, which are classified as chaotropes in light of their ability to disrupt non-covalent molecular structures (Rudolph *et al.*, 1996). Reducing agents, such as DTT and β-mercaptoethanol, may also be used to counteract aggregation caused by the misforming of disulphide bonds (Rudolph *et al.*, 1996). To facilitate the refolding of solubilised proteins, denaturants and reductants are gradually removed via dilution or dialysis (Rudolph *et al.*, 1996).

Denaturants and reductants have been used in this study to enable the enhanced recovery of insoluble recombinant Keap1-His. In this case, it is not possible to fully determine whether the recombinant Keap1 protein expressed here and in other work (Dinkova-Kostova *et al.*, 2002) is correctly folded, because there is currently no point of reference, given that a crystal structure has been resolved only for the DGR and C-terminal domains of the mouse protein (Padmanabhan *et al.*, 2005). Until the complete crystal structure of Keap1 is determined, the most suitable method for determining the fidelity of the folding of recombinant Keap1 may be to ensure that the protein is able to associate with its known interaction partners, namely Nrf2, actin, CUL3 and RBX1 (Cullinan *et al.*, 2004; Dhakshinamoorthy *et al.*, 2001; Furukawa *et al.*, 2005; Itoh *et al.*, 1999; Kang *et al.*, 2004; Kobayashi *et al.*, 2004; Zhang *et al.*, 2004; Zhang *et al.*, 2005). However, given that the redox states of the 25 cysteines in mouse Keap1-His were not consistent within or across purifications in section 3.3.4, it was decided that all cysteines would be rendered free for adduction via exposure to the reducing agent DTT. Therefore, studies of Keap1-His modification by Nrf2-activating molecules in chapter 4 will examine the relative reactivities of Keap1 cysteines towards different electrophiles, to explore the possibility that certain residues are preferentially reactive towards all Nrf2 inducers. In light of this, the precise folding state of Keap1-His following denaturation and renaturation was not deemed to be critical, given that all disulphide bonds were subsequently reduced, inhibiting tertiary structure formation. However, in order to examine the consequence(s) of cysteine modification on the structure of Keap1, correctly-folded soluble protein would need to be readily available. To this end, and

towards the latter stages of this PhD, a method for the enhanced recovery of soluble Keap1-His was developed. Although not used for experimental purposes in this thesis, the ability to isolate recombinant Keap1 in a soluble form may facilitate circular dicroism and/or nuclear magnetic resonance-based structural studies to test the hypothesis that modification of one or more cysteines within Keap1 causes a conformational change in the protein. Indeed, this has been postulated as a critical molecular event that leads to the disruption of Nrf2 repression by Keap1, causing the induction of adaptive cell defence processes (for a review, see Tong *et al.*, 2006b). Experiments that test this hypothesis will enhance our understanding of the likely importance of Keap1 cysteine modification in the activation of Nrf2.

In relation to this thesis, the most pertinent example of the use of mass spectrometry to characterise the modification of a recombinant protein is the study by Talalay and colleagues, who reported the residue-selective adduction of mouse Keap1 by the thiol-reactive electrophile dex-mes (Dinkova-Kostova *et al.*, 2002). Although not representative of the physiological conditions within a cell, the procedures employed in this paper enabled the identification of five cysteines, from a total of 25 in the mouse protein, that were preferentially reactive towards dex-mes *in vitro* at a molar ratio of 33:1 dex-mes:Keap1 (Dinkova-Kostova *et al.*, 2002). Specifically, these residues were Cys-257, -273, -288, -297 and -613 (Dinkova-Kostova *et al.*, 2002). Indeed, it has recently been demonstrated that a Keap1 protein in which Cys-257, -273, -288 and -297 are mutated to alanine binds dex-mes at half the rate of the wild-type protein (Wakabayashi *et al.*, 2004). Other investigations have utilised site-directed mutagenesis to demonstrate that the integrities of Cys-273 and -288 in particular are critical for the function of Keap1 (Kobayashi *et al.*, 2006; Levonen *et al.*, 2004; Wakabayashi *et al.*, 2004; Zhang *et al.*, 2003). Therefore, it would appear there is value in determining the relative reactivities of Keap1 cysteine residues towards Nrf2-activating molecules using *in vitro* systems similar to those described by Dinkova-Kostova *et al.* (2002) and in this chapter.

In summary, this chapter describes the development and validation of a cell-free *in vitro* test system for exploring the modification of cysteine residues within Keap1 by Nrf2-activating electrophiles. This system will be employed in chapter 4 to examine the role of Keap1 modification in the activation of Nrf2 by NAPQI, DNCB and 15d-PGJ_2.

CHAPTER 4

Chemical modification of Keap1 *in vitro* by N-acetyl-*p*-benzoquinoneimine and other Nrf2-activating electrophiles

CONTENTS

4.1 INTRODUCTION

The activity of the transcription factor Nrf2 is primarily regulated through its interaction with the cysteine-rich protein Keap1 (Itoh *et al.*, 1999). It has been postulated that the modification of one or more cysteine residues within Keap1 may evoke a conformational change in the protein, rendering it unable to efficiently repress Nrf2, and thus providing a trigger for activation of the transcription factor (Dinkova-Kostova *et al.*, 2002). To date, compelling evidence for the chemical modification of Keap1 has been provided through the use of biotinylated analogues of Nrf2-activating molecules (Itoh *et al.*, 2004; Levonen *et al.*, 2004), spectroscopic binding experiments (Dinkova-Kostova *et al.*, 2002) and mass spectrometry (Dinkova-Kostova *et al.*, 2002).

In the only investigation to date to employ mass spectrometry as an analytical tool to examine the modification of Keap1 cysteines, the thiol-reactive steroid dex-mes was shown to preferentially modify Cys-257, -273, -288 and -297, located within the IVR domain, and the C-terminal Cys-613, of recombinant mouse Keap1 (Dinkova-Kostova *et al.*, 2002). Cys-273, -288, -297 and -613 are amongst the many cysteines (see Fig. 1.9) in the mouse Keap1 protein that have low predicted pKa values, and thus high relative reactivities, as they are flanked by at least one basic amino acid (Snyder *et al.*, 1981). Cys-273, -297 and -613 are immediately flanked by two basic residues, and are thus anticipated to be particularly reactive toward electrophiles. Therefore, further work is required to identify the target residues within Keap1 of other Nrf2-activating molecules, in order to determine whether a defined cysteine, or subset of cysteines, represents a common target for all such molecules.

Insights into the role of specific cysteine residues in the function of Keap1, particularly Cys-151, -273 and -288, have mainly come from studies employing site-directed mutagenesis (Kobayashi *et al.*, 2006; Levonen *et al.*, 2004; Wakabayashi *et al.*, 2004; Zhang *et al.*, 2003). Cys-151, which resides within the BTB domain of Keap1, does not appear to be integral to Keap1 function in the absence of chemical/oxidative stress, but is critical to its ability to respond to such conditions (Zhang *et al.*, 2003; Zhang *et al.*,

2004). In contrast, Cys-273 and -288, both located within the IVR domain of Keap1, are essential for the repressive activity of Keap1 under basal conditions (Kobayashi *et al.*, 2006; Levonen *et al.*, 2004; Wakabayashi *et al.*, 2004; Zhang *et al.*, 2003). Mutation of Cys-273 and/or -288 to serine or alanine renders Keap1 unable to direct ubiquitination of Nrf2, inhibit its nuclear accumulation or repress transactivation of an ARE reporter transgene (Kobayashi *et al.*, 2006; Levonen *et al.*, 2004; Wakabayashi *et al.*, 2004; Zhang *et al.*, 2003). Furthermore, the responsiveness of Nrf2 to known inducers is diminished or abolished by the expression of Keap1 Cys-273/288 mutants (Levonen *et al.*, 2004; Zhang *et al.*, 2003). Notably, the mutation of other cysteines within the IVR, N-terminal and C-terminal domains has essentially no effect on Keap1 function (Wakabayashi *et al.*, 2004; Zhang *et al.*, 2003). Hence, the structural integrities of Cys-151, -273 and -288 are paramount for the function of Keap1. As for Cys-273 and -288, Cys-151 is flanked by basic amino acids (see Fig. 1.9), and is thus anticipated to be highly reactive towards electrophiles (Snyder *et al.*, 1981). Therefore, in light of the evidence discussed, these residues are plausible targets for electrophilic inducers of Nrf2.

The work presented in chapter 3 has described the development of a cell-free *in vitro* system for examining the modification of Keap1 by Nrf2-activating electrophiles, using tandem mass spectrometry to facilitate the identification of specific target residues. Through the use of a panel of structurally distinct molecules (NAPQI, DNCB and 15d-PGJ_2) that were shown to activate Nrf2 in chapter 2, the initial aim of the work presented in this chapter is to use this *in vitro* system to determine the capacity of these molecules to modify cysteine residues within Keap1. Furthermore, this study aims to map the Keap1 adduct patterns associated with different Nrf2-activating electrophiles, to test the hypothesis that all such molecules selectively modify one or more cysteines amongst the subset of Cys-151, -273 and -288, and that this underlies the ability of these molecules to activate Nrf2-dependent cell defence.

4.2 METHODS

4.2.1 Materials and reagents

Recombinant human His-GSTP1-1 was kindly donated by Samantha Dowdall (School of Biomedical Sciences, University of Liverpool, UK). DNFB was from Sigma-Aldrich (Poole, UK). All other reagents were of analytical or molecular grade, and were from Sigma-Aldrich.

4.2.2 Expression and purification of Keap1-His

Expression and purification of Keap1-His was as described in section 3.2.6.

4.2.3 Determination of on-bead Keap1-His content

Determination of on-bead Keap1-His content was as described in section 3.2.9.

4.2.4 Incubation of Keap1-His with electrophiles

To render all cysteines free for modification, Keap1-His -coupled Ni^{2+}-charged agarose beads (50 μL dry volume; ~350 pmol) were resuspended in 0.148 mL phosphate buffer and 2 μL of 0.1 M DTT, and then incubated on a mechanical roller at 4 °C for 15 min. The beads were washed three times in 0.5 mL phosphate buffer to remove residual DTT. The beads were resuspended in 0.149 mL phosphate buffer, and 1 μL of 200X NAPQI, DNCB, 2,4-dinitrofluorobenzene (DNFB), 15d-PGJ_2 or TMA, dissolved in DMSO, was added to give the required molar ratio of Keap1:electrophile. Following incubation on a mechanical roller for 1 h at 4 °C, the beads were washed three times in 0.5 mL phosphate buffer to remove residual electrophile. To cap unmodified cysteines, the

beads were resuspended in 0.13 mL phosphate buffer and 20 μL of 0.55 M iodoacetamide, and incubated on a mechanical roller at 4 °C for 15 min. The beads were washed three times in 0.5 mL phosphate buffer to remove residual iodoacetamide. Tryptic digestion was performed as described in section 3.2.10.

4.2.5 LC-ESI-MS/MS mass spectrometry

Samples were analysed essentially as described in section 3.2.12. Amino acid modifications were detected with ProteinPilot software v2.0, using the Paragon™ algorithm (Shilov *et al.*, 2007) and the most recent version of the SwissProt database. Paracetamol (+149.1 amu), dinitrophenyl (DNP; +166.0 amu), 15d-PGJ_2 (+316.2 amu), TMA (+192.0 amu) or carboxyamidomethyl (+57.0 amu) were selected as variable modifications. All adducts were confirmed by visual inspection of the MS/MS spectra.

4.2.6 Generation of peptide modification maps

Keap1 peptide modification maps were generated using a software package available at http://www.liv.ac.uk/pfg/localtools.html, described previously by Beynon (2005).

4.3 RESULTS

4.3.1 Modification of Keap1-His by Nrf2-activating electrophiles *in vitro*

In order to ascertain the relative reactivities of the 25 cysteines within mouse Keap1 towards a panel of Nrf2-activating electrophiles, a dose-ranging study of the selectivity of Keap1 modifications was conducted *in vitro*, using LC-ESI-MS/MS. In reporting Keap1 adducts, the frequency of adducts detected from a total of three independent experiments has been used as an indicator of the relative reactivities of individual cysteine residues towards the panel of electrophiles. Keap1 protein sequence coverage from MS/MS spectra averaged 89 % across 12 individual experiments. All cysteines were consistently detected, with the exception of Cys-622 and -624, which were not released from the Ni^{2+}-charged agarose beads by tryptic digestion, due to their proximity to the polyhistidine tag of Keap1-His. Compound mutation of the three cysteines (Cys-613, -622, -624) located within the C-terminal domain of Keap1 has no effect on the repressive activity of Keap1 towards Nrf2 (Wakabayashi et al., 2004), implying that Cys-622 and -624 are not essential for Keap1 function.

4.3.2 Modification of Keap1-His by NAPQI *in vitro*

Following incubation of Keap1-His with NAPQI for 1 h, no cysteine adducts were detected at a molar ratio of 0.01:1 NAPQI:Keap1. At a molar ratio of 0.1:1 NAPQI:Keap1, there was evidence for the modification of cysteine residues by NAPQI, albeit in one of three experiments. In this case, the identification of modified residues was based solely on the mass-to-charge ratio (m/z) and retention time of the modified peptide, as MS/MS spectra were not generated due to the relative low abundance of the modified peptide ions. Therefore, it was not possible to unequivocally identify the modified residues by manually sequencing the corresponding MS/MS spectrum. In light of this fact, the cysteine residues that were judged to be the most readily modified by NAPQI *in vitro* were those that were detected following incubation of Keap1 with

NAPQI at a molar ratio of 1:1 NAPQI:Keap1, namely Cys-77, -226, -257, -273, -288, -434, -489, -583 and -613 (Table 4.1 and Fig. 4.1). Through inspection of the corresponding MS/MS spectra, each of these residues were found to be modified at this molar ratio in at least two of three independent experiments. Cys-151, the integrity of which has recently been shown to be critical for the ability of Keap1 to respond to chemical/oxidative stress (Zhang *et al.*, 2003; Zhang *et al.*, 2004), was modified by NAPQI only at a molar ratio of 5:1 and above. Of the 23 Keap1 cysteines that were routinely detected by LC-ESI-MS/MS, only eight residues were not modified by NAPQI at the highest molar ratio of 10:1, namely Cys-241, -249, -297, -319, -395, -406, -513 and -518.

		Molar Ratio NAPQI:Keap1				
Keap1 Domain	**Cysteine #**	**0**	**0.1:1**	**1:1**	**5:1**	**10:1**
N-terminal	23				1/3	2/3
N-terminal	38				1/3	2/3
BTB	77		1/3	3/3	3/3	3/3
BTB	151				2/3	2/3
BTB	171					1/3
IVR	196					1/3
IVR	226			3/3	3/3	3/3
IVR	241					
IVR	249					
IVR	257			2/3	3/3	3/3
IVR	273		1/3	2/3	3/3	3/3
IVR	288		1/3	3/3	3/3	3/3
IVR	297					
IVR	319				1/3	
DGR	368				1/3	2/3
DGR	395					
DGR	406					
DGR	434			2/3	2/3	3/3
DGR	489		1/3	3/3	3/3	3/3
DGR	513			1/3		
DGR	518			1/3		
DGR	583		1/3	3/3	3/3	3/3
C-terminal	613			3/3	3/3	3/3
C-terminal	622	*nd*	*nd*	*nd*	*nd*	*nd*
C-terminal	624	*nd*	*nd*	*nd*	*nd*	*nd*

Table 4.1 - Keap1-His cysteines modified by NAPQI *in vitro*. Ni^{2+} agarose bead-purified mouse Keap1-His (~350 pmol) was reduced on-bead with 1 mM DTT for 15 min and incubated with NAPQI at the indicated molar ratios for 1 h. Free sulphydryls were capped with 55 mM iodoacetamide for 15 min. Keap1-His was digested overnight at 37 °C with 240 ng trypsin and the resulting tryptic peptides were analysed for adducts of interest by LC-ESI-MS/MS. The frequency of adduct detection, from a total of three experiments, is shown. Blank cells indicate that no NAPQI adducts were detected. *nd*; Cys-622 and -624 were not routinely detected as NAPQI-modified or carboxyamidomethylated peptides.

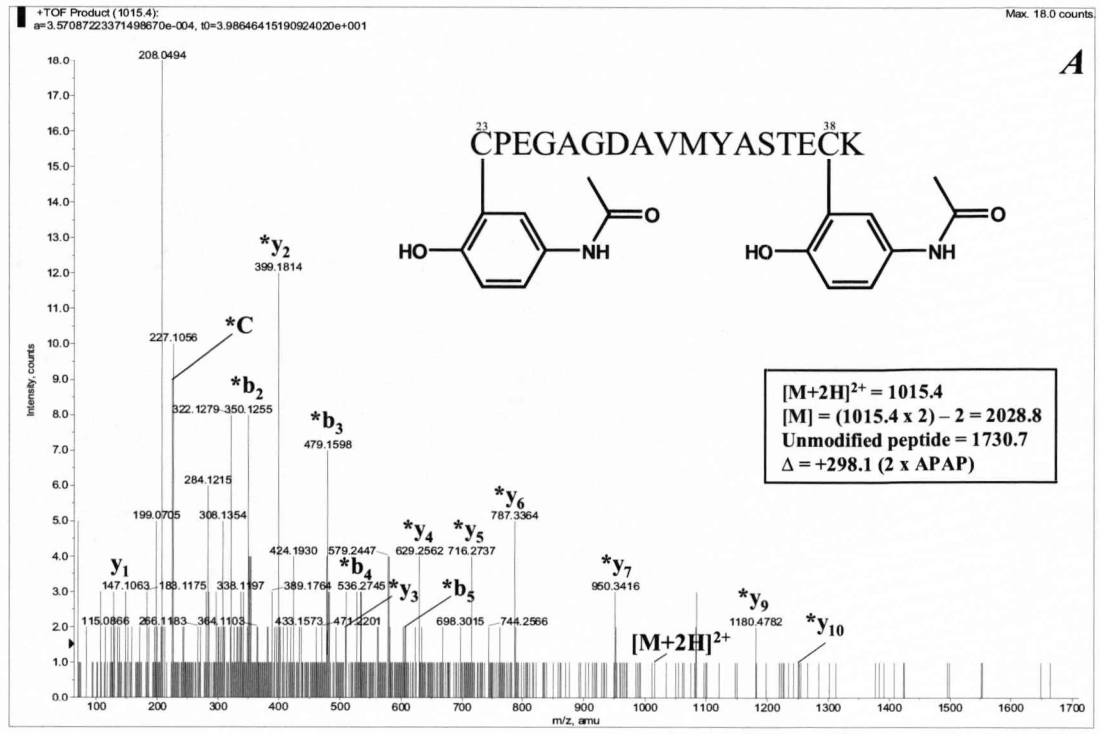

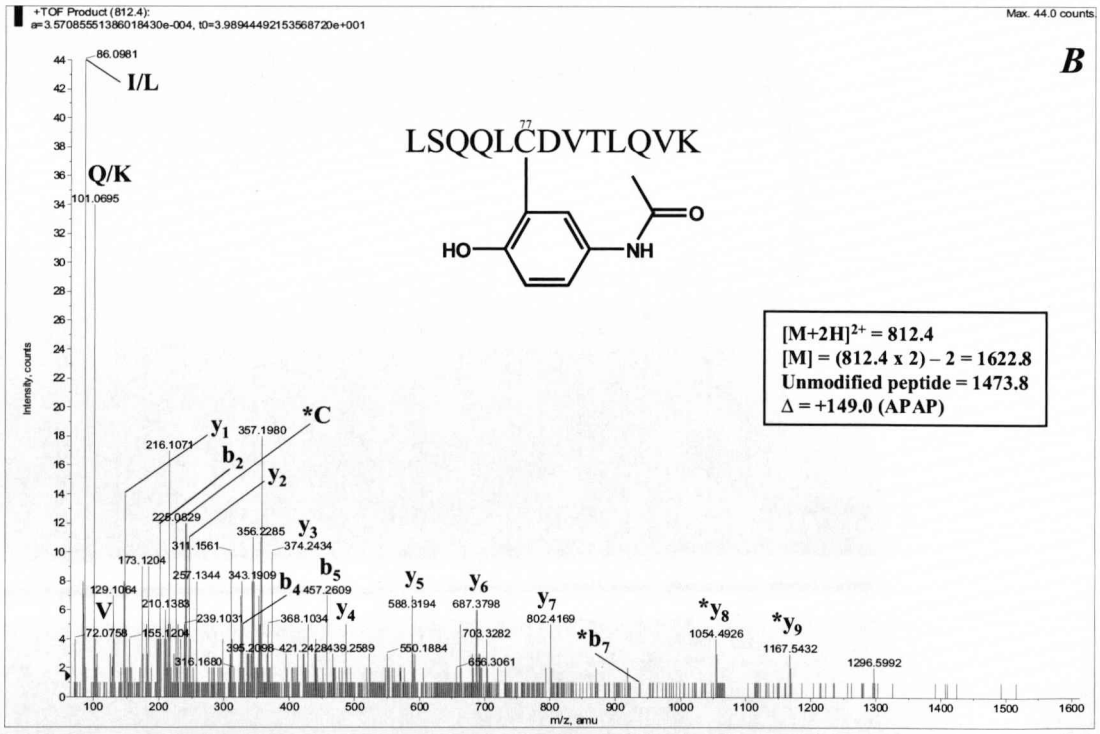

Fig. 4.1 - MS/MS spectrum indicating modification of Keap1-His (A) Cys-23/38 and (B) Cys-77 by NAPQI *in vitro*. y- and b-ions are labelled where present. * denotes ions for which a mass shift of +149.1 amu indicates modification by NAPQI. Immonium ions are labelled with the one-letter code for their corresponding amino acid.

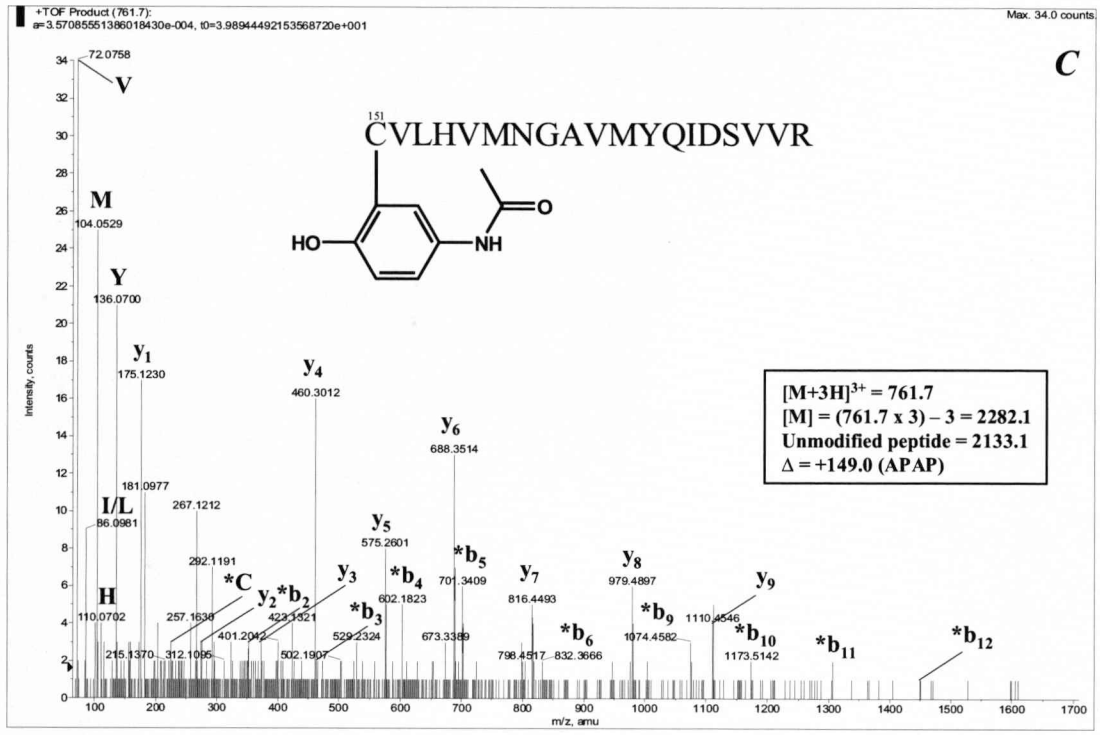

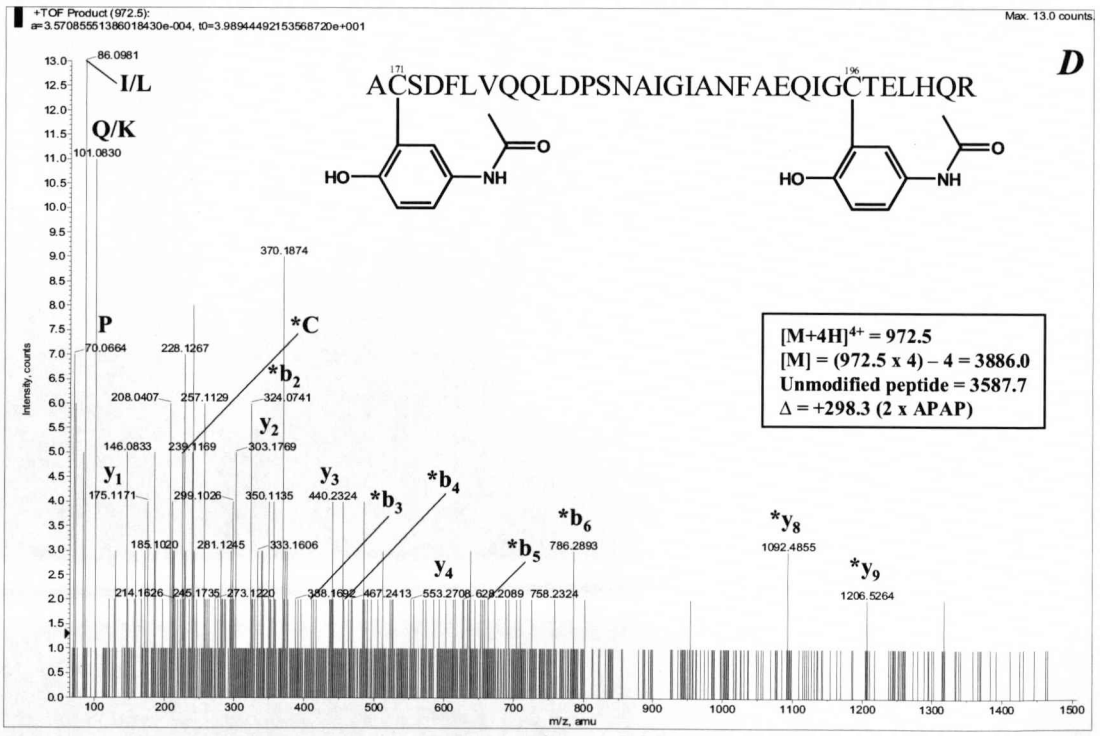

Fig. 4.1 - MS/MS spectrum indicating modification of Keap1-His (C) Cys-151 and (D) Cys-171/196 by NAPQI *in vitro*. y- and b-ions are labelled where present. * denotes ions for which a mass shift of +149.1 amu indicates modification by NAPQI. Immonium ions are labelled with the one-letter code for their corresponding amino acid.

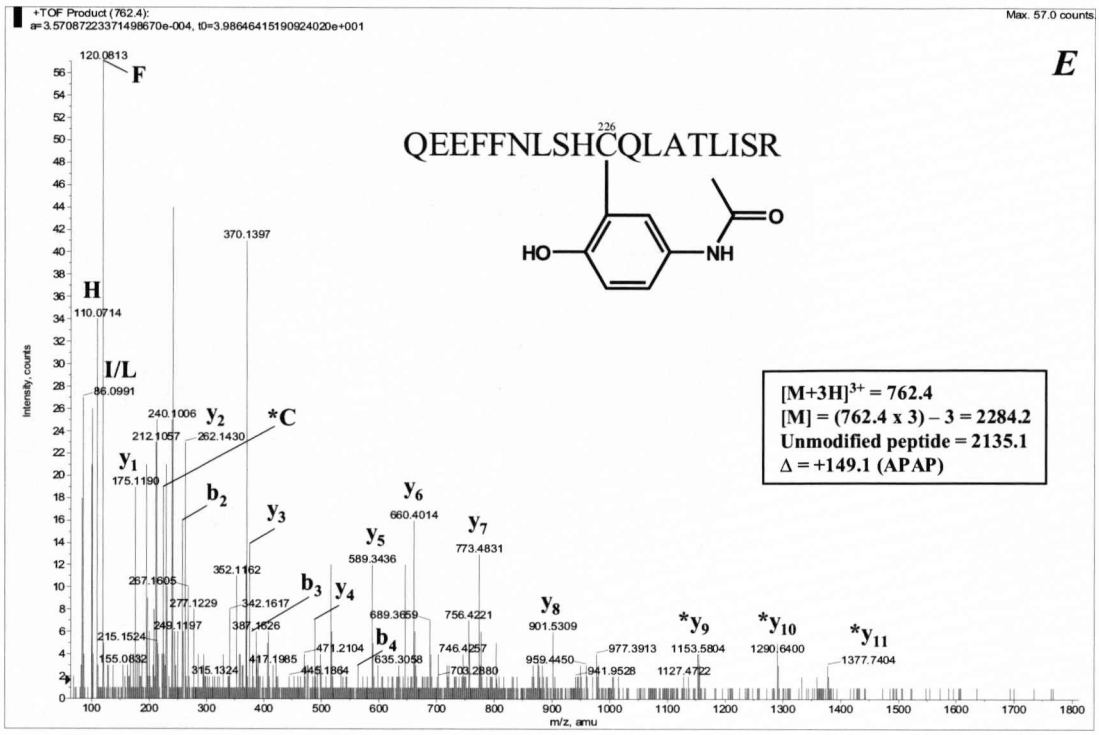

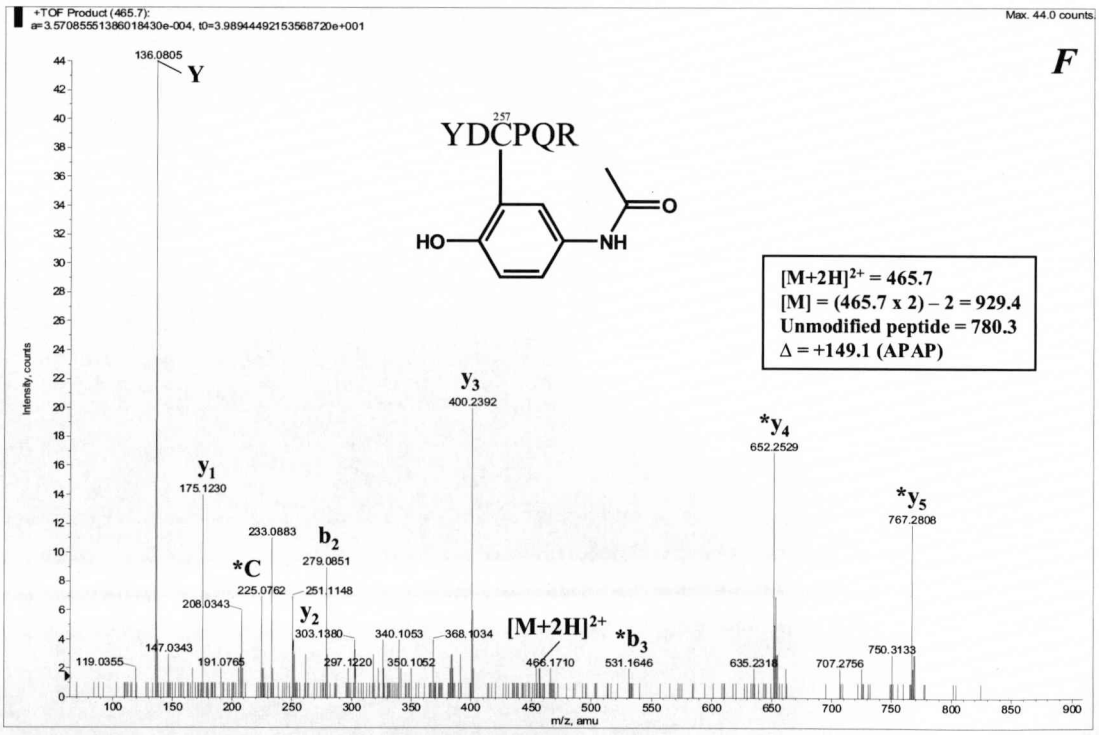

Fig. 4.1 - MS/MS spectrum indicating modification of Keap1-His (E) Cys-226 and (F) Cys-257 by NAPQI *in vitro*. y- and b-ions are labelled where present. * denotes ions for which a mass shift of +149.1 amu indicates modification by NAPQI. Immonium ions are labelled with the one-letter code for their corresponding amino acid.

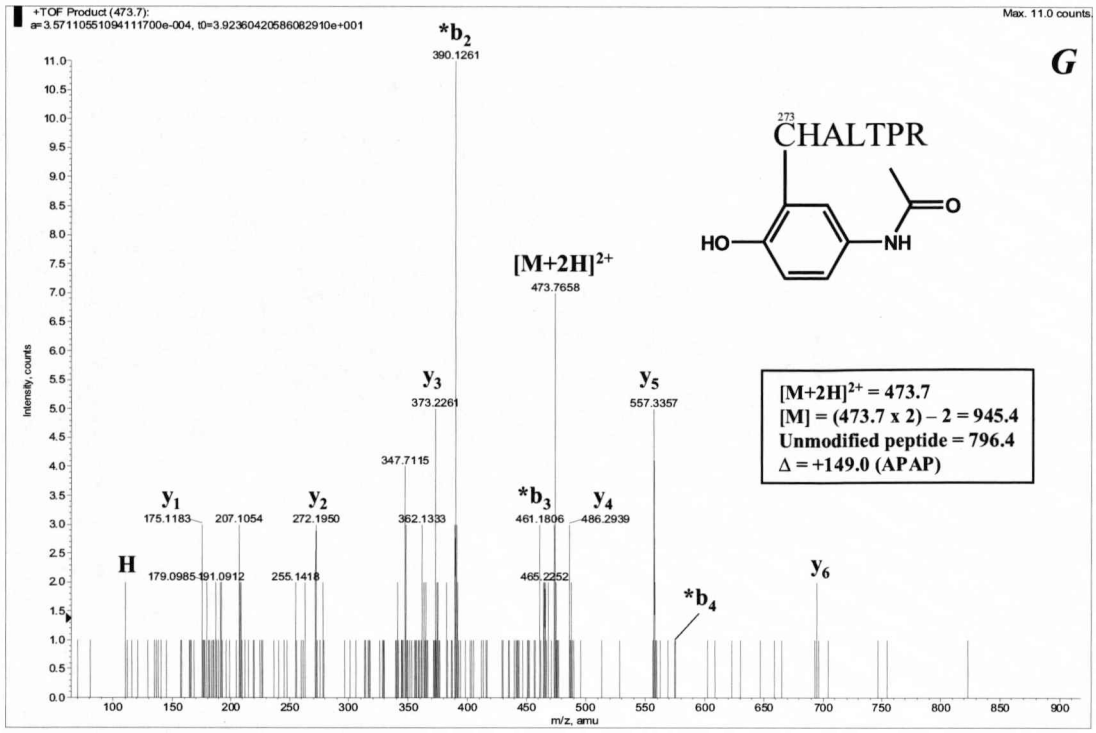

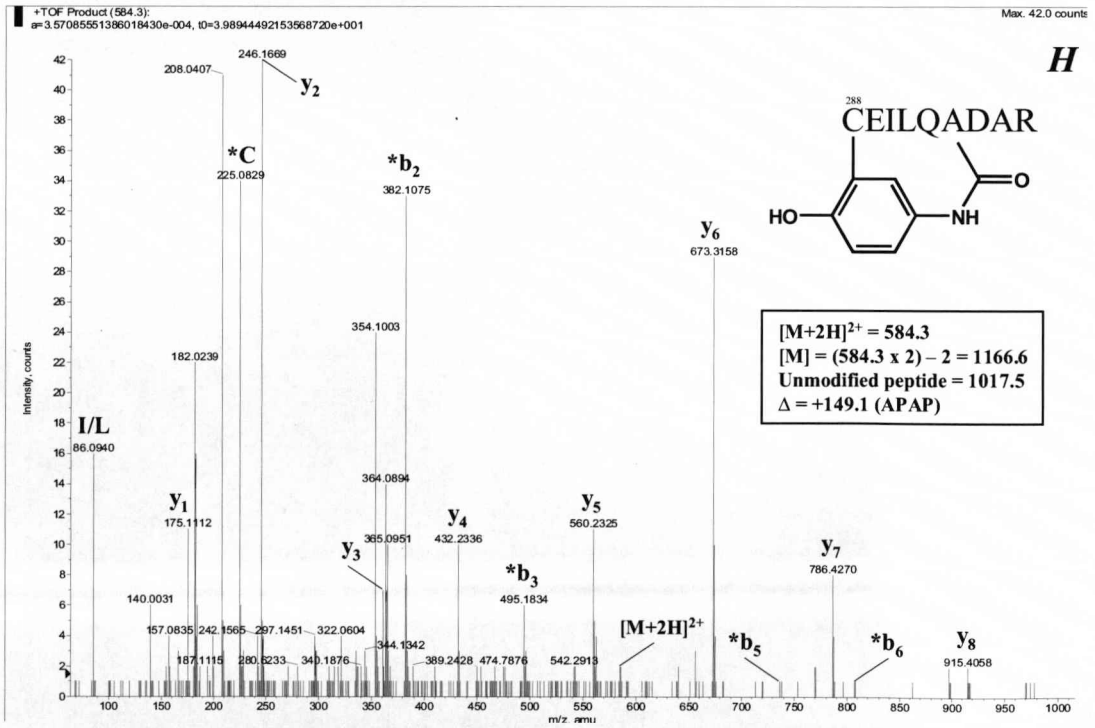

Fig. 4.1 - MS/MS spectrum indicating modification of Keap1-His (G) Cys-273 and (H) Cys-288 by NAPQI *in vitro*. y- and b-ions are labelled where present. * denotes ions for which a mass shift of +149.1 amu indicates modification by NAPQI. Immonium ions are labelled with the one-letter code for their corresponding amino acid.

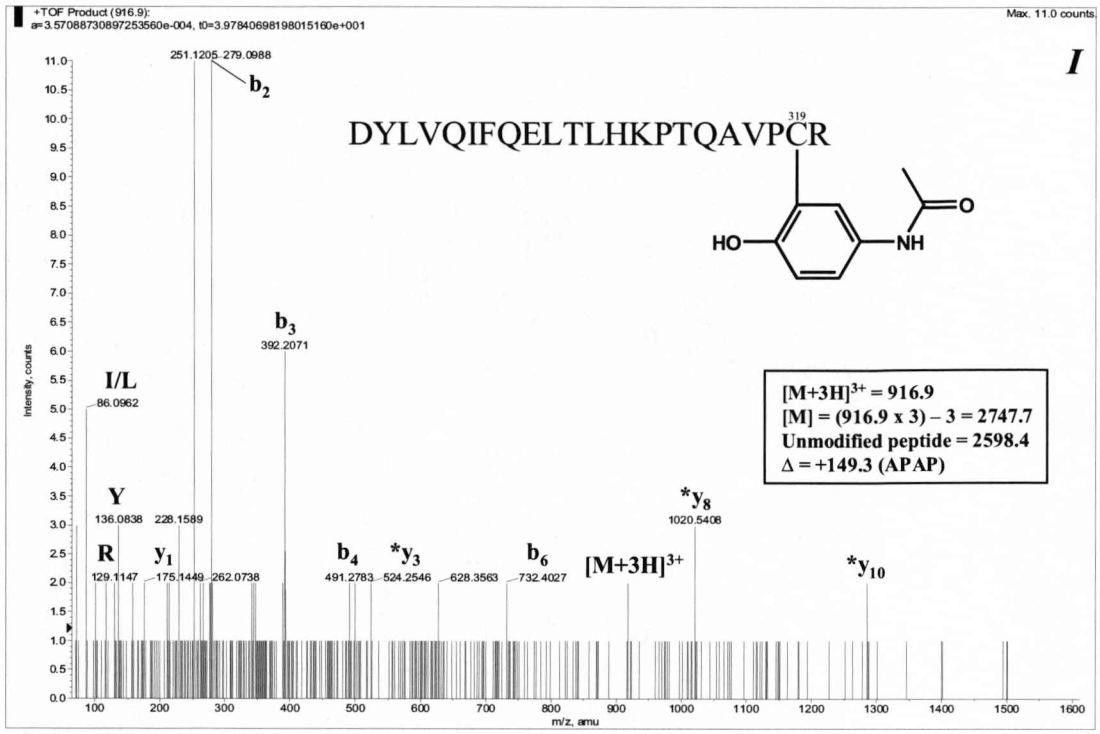

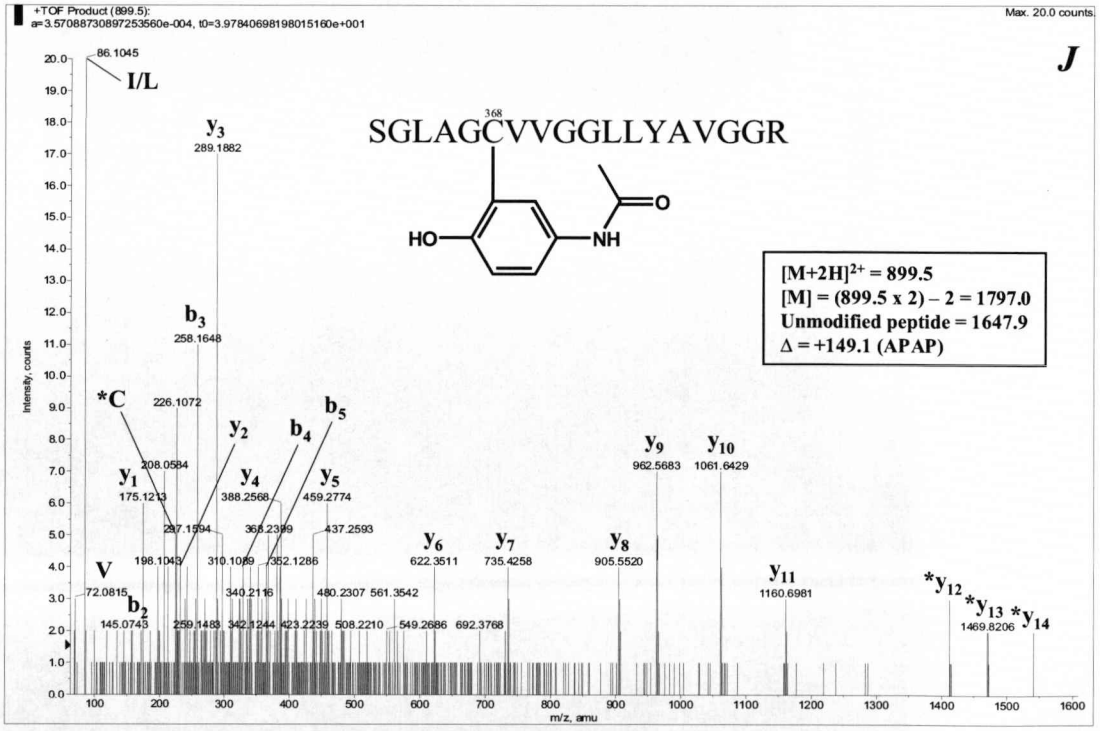

Fig. 4.1 - MS/MS spectrum indicating modification of Keap1-His (I) Cys-319 and (J) Cys-368 by NAPQI *in vitro*. y- and b-ions are labelled where present. * denotes ions for which a mass shift of +149.1 amu indicates modification by NAPQI. Immonium ions are labelled with the one-letter code for their corresponding amino acid.

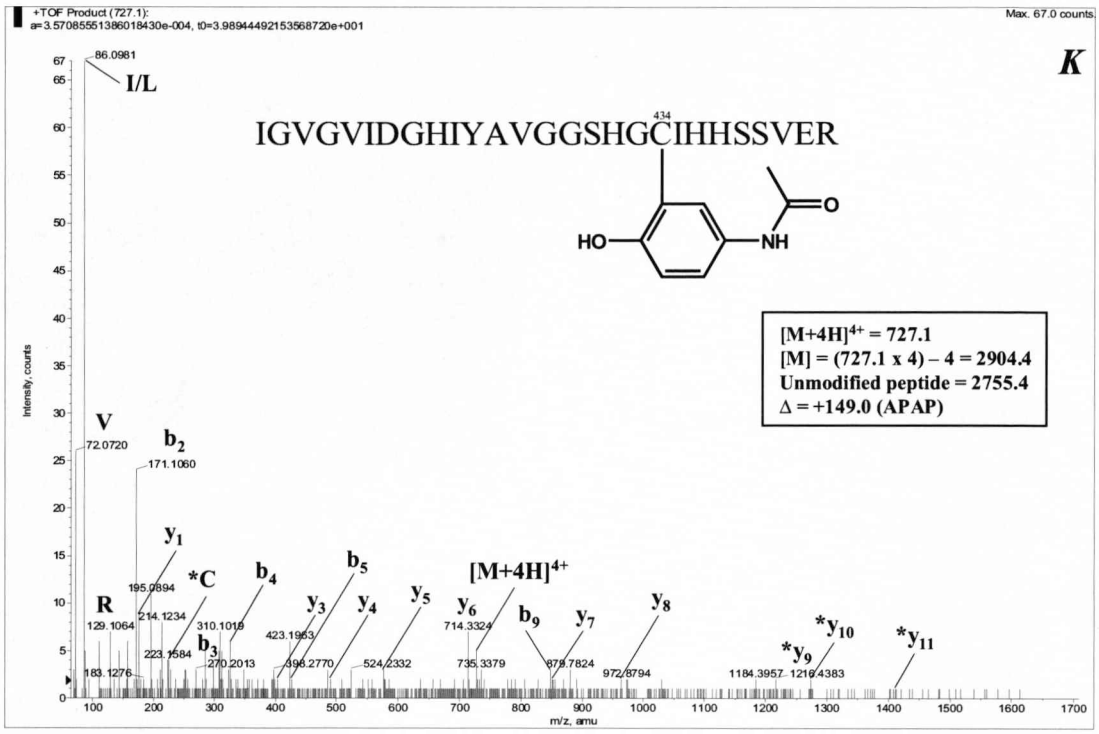

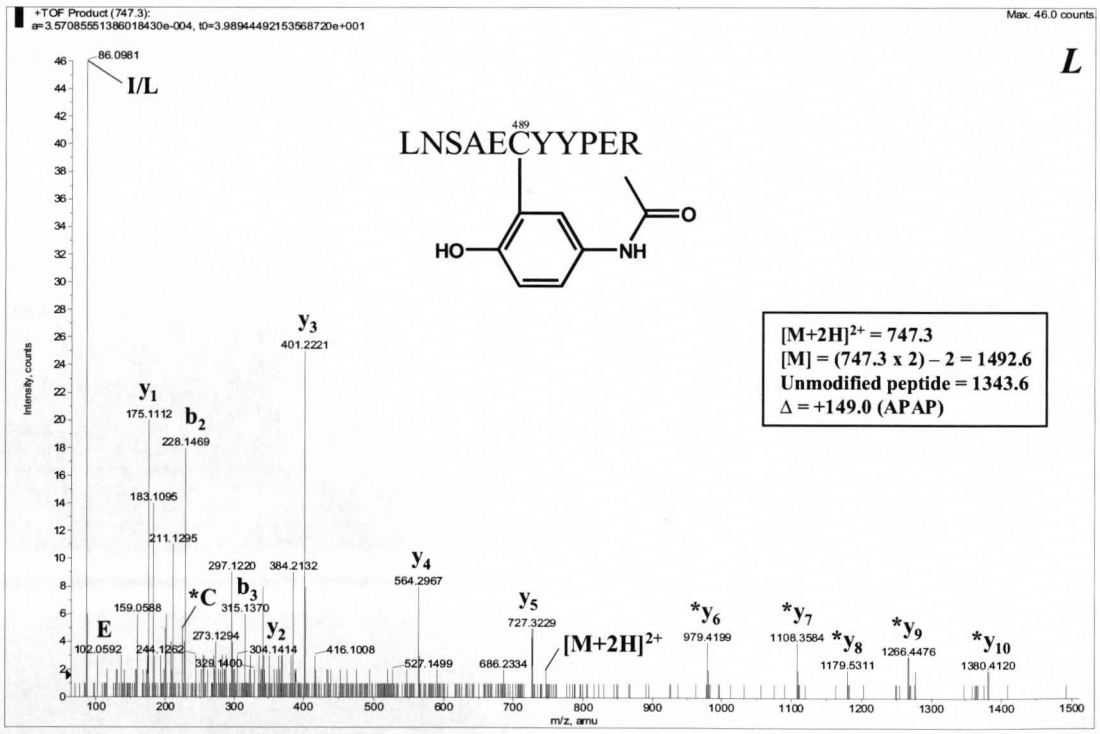

Fig. 4.1 - MS/MS spectrum indicating modification of Keap1-His (K) Cys-434 and (L) Cys-489 by NAPQI *in vitro*. y- and b-ions are labelled where present. * denotes ions for which a mass shift of +149.1 amu indicates modification by NAPQI. Immonium ions are labelled with the one-letter code for their corresponding amino acid.

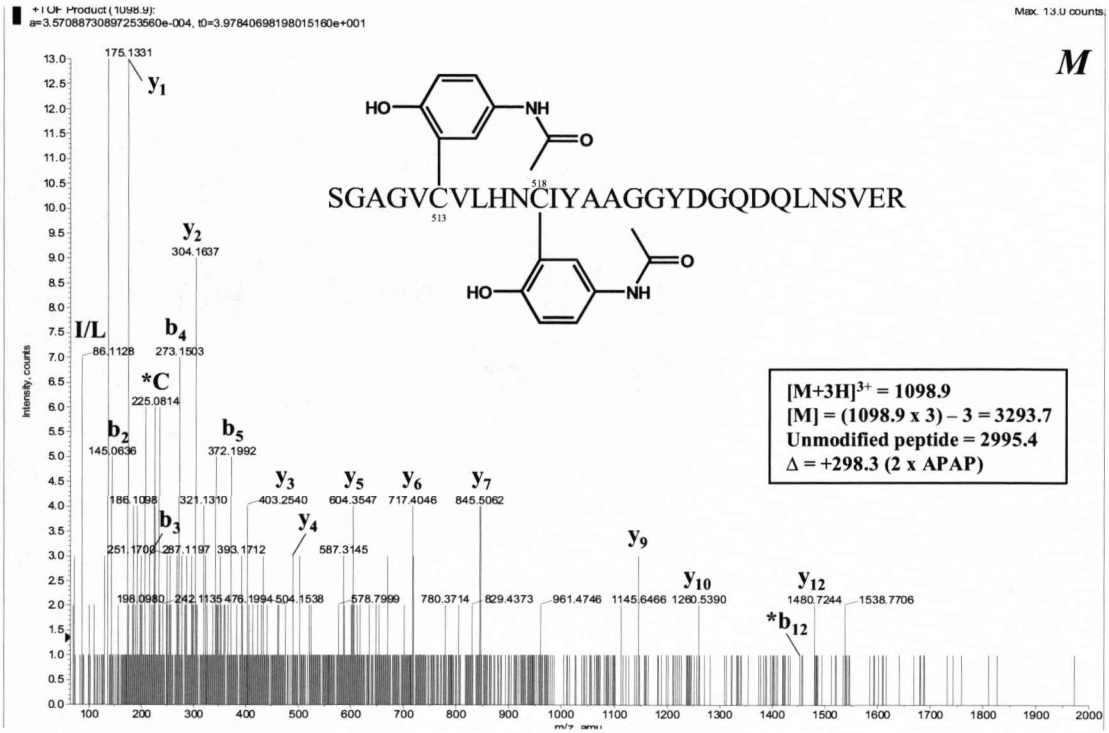

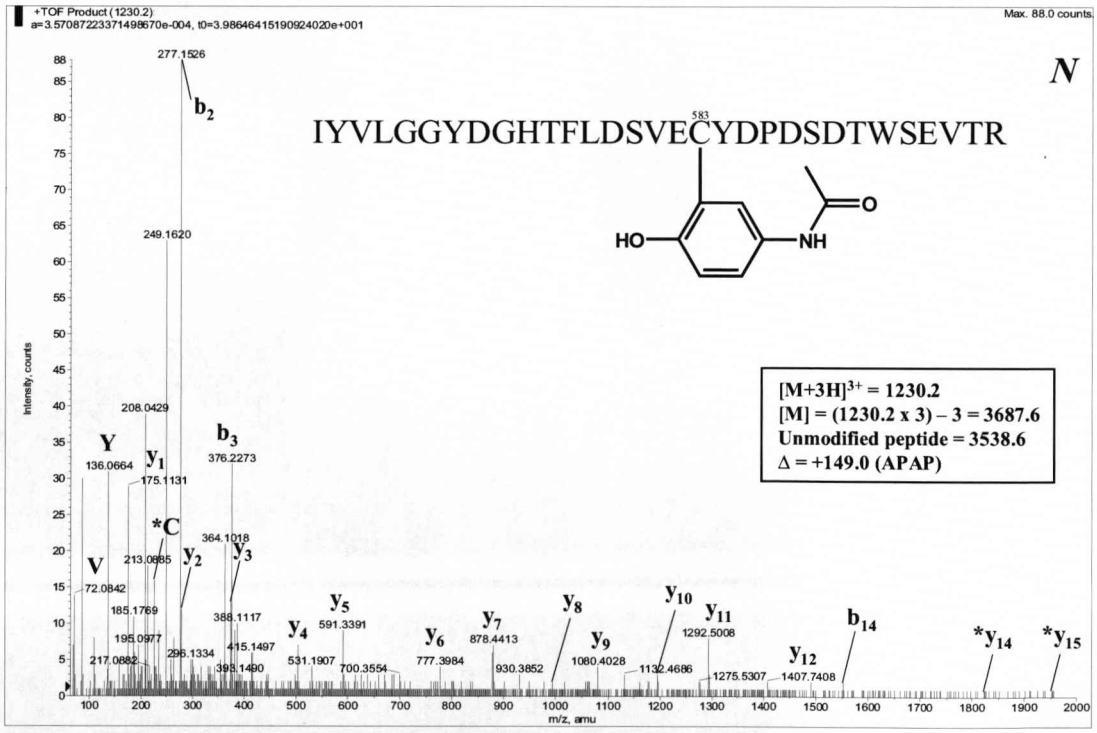

Fig. 4.1 - MS/MS spectrum indicating modification of Keap1-His (M) Cys-513/518 and (N) Cys-583 by NAPQI *in vitro*. y- and b-ions are labelled where present. * denotes ions for which a mass shift of +149.1 amu indicates modification by NAPQI. Immonium ions are labelled with the one-letter code for their corresponding amino acid.

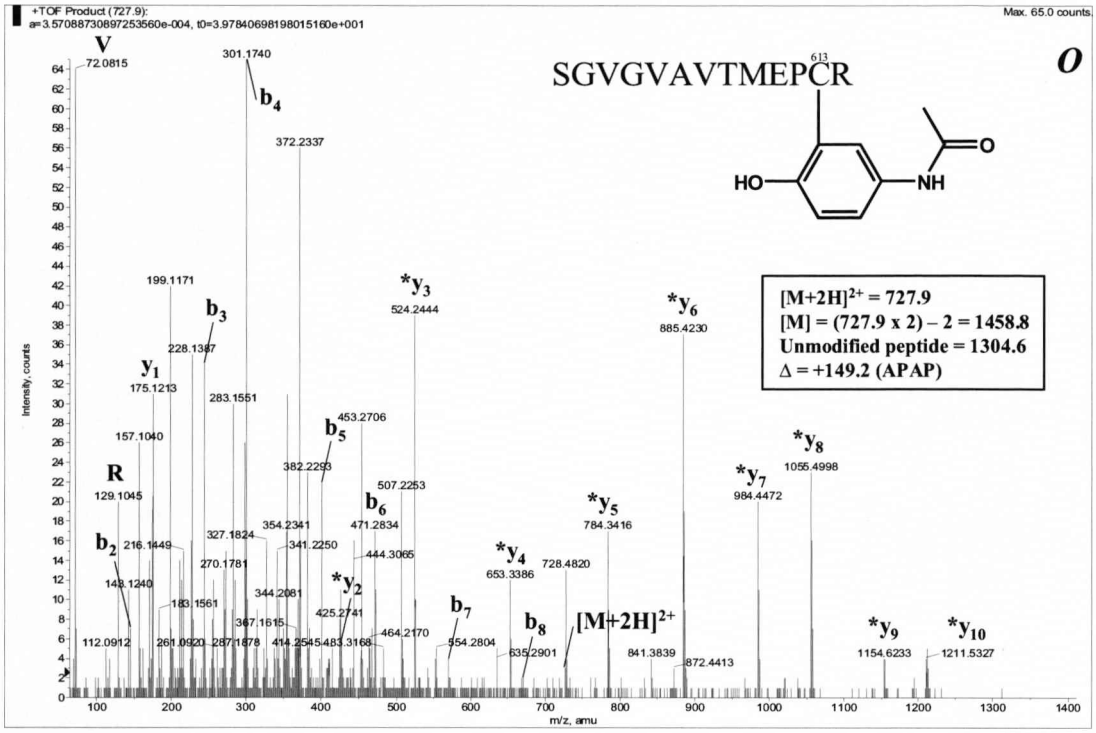

Fig. 4.1 - MS/MS spectrum indicating modification of Keap1-His (O) Cys-613 by NAPQI *in vitro*. y- and b-ions are labelled where present. * denotes ions for which a mass shift of +149.1 amu indicates modification by NAPQI. Immonium ions are labelled with the one-letter code for their corresponding amino acid.

4.3.3 Modification of Keap1-His by DNCB *in vitro*

Following incubation of Keap1-His with DNCB for 1 h, as for NAPQI, no cysteine adducts were detected at a molar ratio of 0.01:1 DNCB:Keap1. Although there was evidence, based on the sequencing of MS/MS spectra, for the modification of Cys-77, -226, -489 and -613 at a molar ratio of 1:1 DNCB:Keap1, this was limited to one of three experiments (Table 4.2 and Fig. 4.2). For this reason, the residues judged to be most readily modified by DNCB were those for which adduction was observed in at least two of three independent experiments at a molar ratio of 5:1, namely Cys-77, -226, -257, -489, -583 and -613. DNCB did not modify any of Cys-151, -273 and -288, residues which have previously been suggested as plausible targets of Nrf2-activating molecules (Dinkova-Kostova *et al.*, 2002; Kobayashi *et al.*, 2006; Levonen *et al.*, 2004; Wakabayashi *et al.*, 2004; Zhang *et al.*, 2003; Zhang *et al.*, 2004), implying that these cysteine residues are not particularly reactive with DNCB under the experimental conditions employed. In order to confirm that DNCB did not form adducts with Cys-151, -273 and/or -288 *in vitro*, the molar ratio was raised to 50:1 DNCB:Keap1; even at this ratio, no ions corresponding to the modified forms of these peptides were detected. In order to ascertain that Cys-151, -273 and -288 were available for adduction in the presence of DNCB, Keap1 was co-incubated simultaneously with NAPQI and DNCB; all three cysteines were modified by NAPQI, but not by DNCB (data not shown). Furthermore, Keap1 was incubated with DNFB, which also stimulates Nrf2 nuclear accumulation in Hepa-1c1c7 cells (Fig. 4.3). DNFB is more reactive than DNCB, as fluorine is a better leaving group than chlorine, thus enhancing bimolecular nucleophilic substitution. Nevertheless, modification of Cys-151, -273 or -288 by DNFB was not detected; indeed, the pattern of cysteine modifications observed matched that of DNCB, with modification of Cys-171, -196 and -434 also detected (Fig. 4.4). Consistent with its known chemical reactivity (Park *et al.*, 1987), DNFB formed adducts with tyrosine and lysine residues in Keap1 at the highest molar ratio of 50:1 (Fig. 4.4). In summary, DNCB does selectively modify cysteines within Keap1 *in vitro*, but at different residues to NAPQI.

		Molar Ratio DNCB:Keap1					
Keap1 Domain	**Cysteine #**	**0**	**0.1:1**	**1:1**	**5:1**	**10:1**	**50:1**
N-terminal	23						
N-terminal	38						
BTB	77			1/3	3/3	3/3	3/3
BTB	151						
BTB	171						
IVR	196						
IVR	226		1/3	1/3	3/3	3/3	3/3
IVR	241						
IVR	249						
IVR	257				3/3	3/3	3/3
IVR	273						
IVR	288						
IVR	297						
IVR	319						
DGR	368				1/3	2/3	2/3
DGR	395						
DGR	406						
DGR	434						
DGR	489			1/3	3/3	3/3	3/3
DGR	513						1/3
DGR	518						1/3
DGR	583				2/3	1/3	1/3
C-terminal	613		1/3	1/3	3/3	3/3	3/3
C-terminal	622	*nd*	*nd*	*nd*	*nd*	*nd*	*nd*
C-terminal	624	*nd*	*nd*	*nd*	*nd*	*nd*	*nd*

Table 4.2 - Keap1-His cysteines modified by DNCB *in vitro*. Ni^{2+} agarose bead-purified mouse Keap1-His (~350 pmol) was reduced on-bead with 1 mM DTT for 15 min and incubated with DNCB at the indicated molar ratios for 1 h. Free sulphydryls were capped with 55 mM iodoacetamide for 15 min. Keap1-His was digested overnight at 37 °C with 240 ng trypsin and the resulting tryptic peptides were analysed for adducts of interest by LC-ESI-MS/MS. The frequency of adduct detection, from a total of three experiments, is shown. Blank cells indicate that no DNCB adducts were detected. *nd*; Cys-622 and -624 were not routinely detected as DNCB-modified or carboxyamidomethylated peptides.

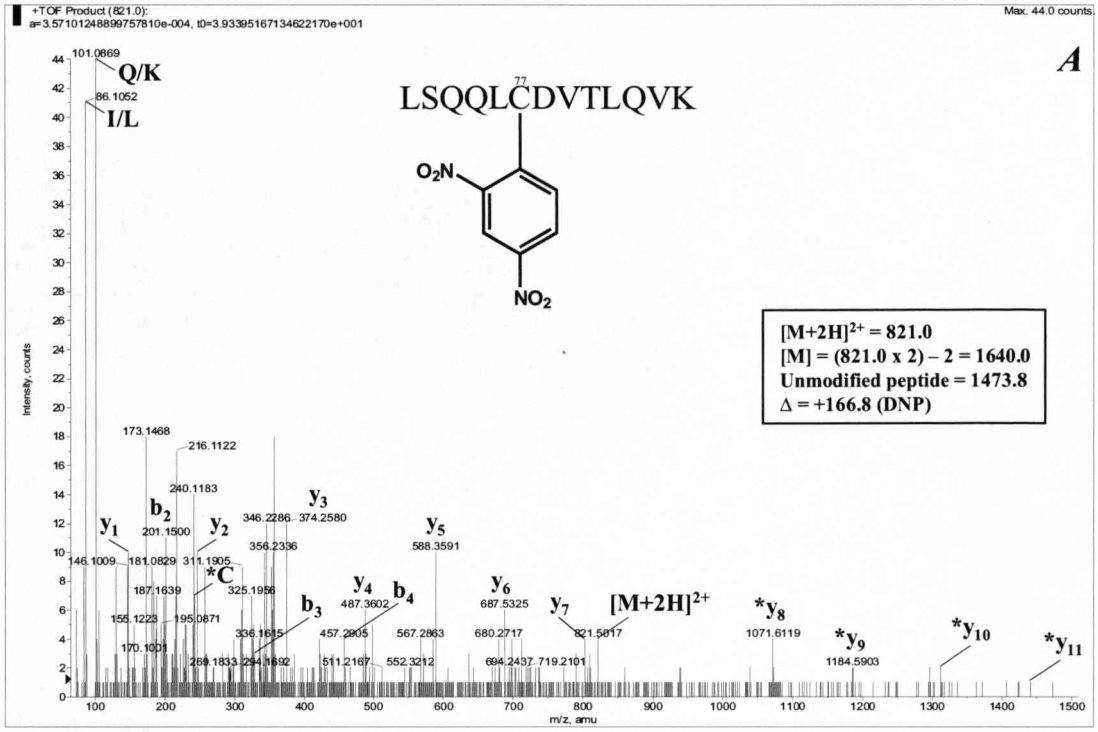

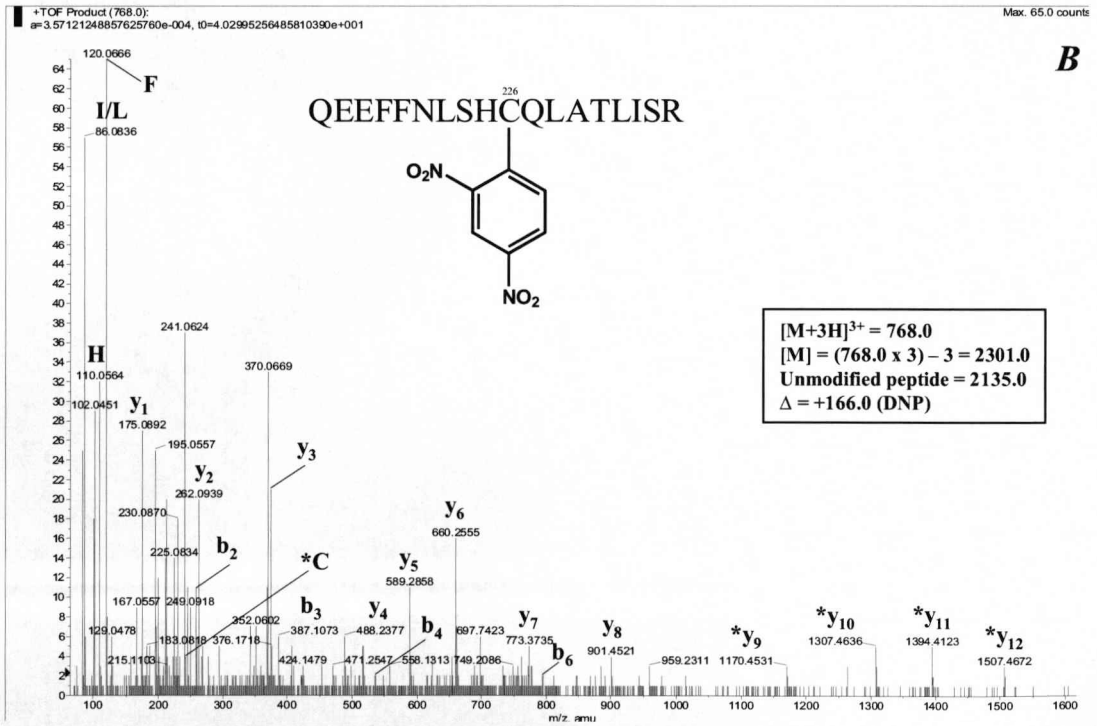

Fig. 4.2 - MS/MS spectrum indicating modification of Keap1-His (A) Cys-77 and (B) Cys-226 by DNCB *in vitro*. y- and b-ions are labelled where present. * denotes ions for which a mass shift of +166.0 amu indicates modification by DNCB. Immonium ions are labelled with the one-letter code for their corresponding amino acid.

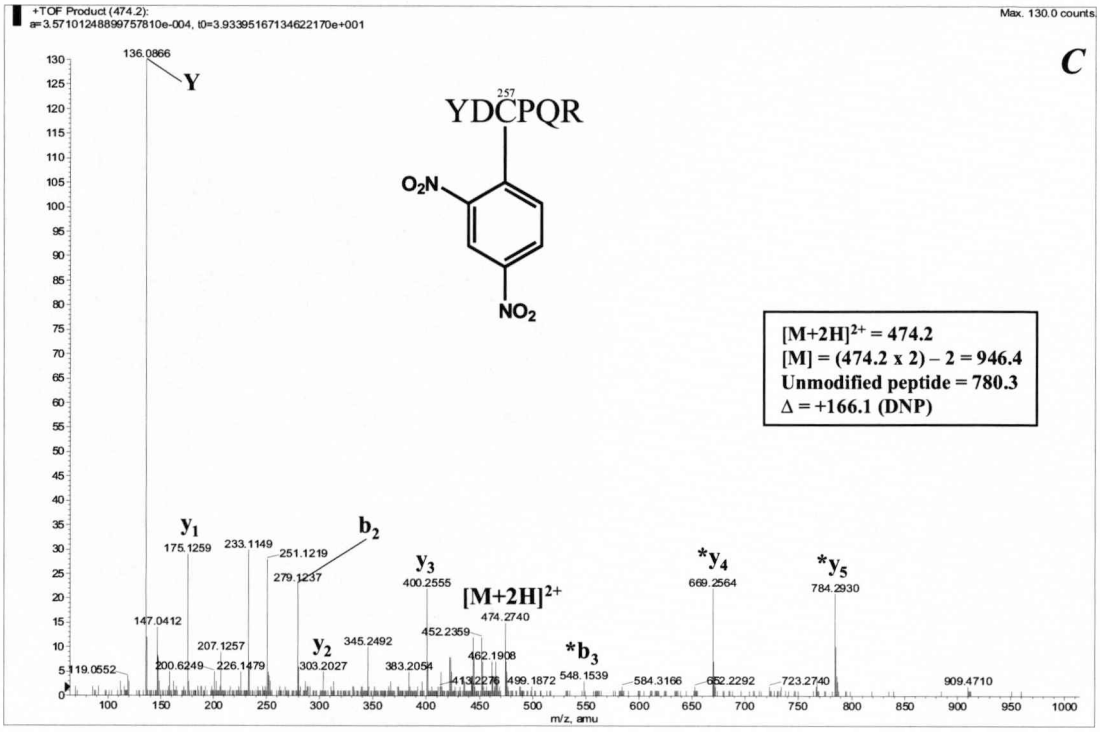

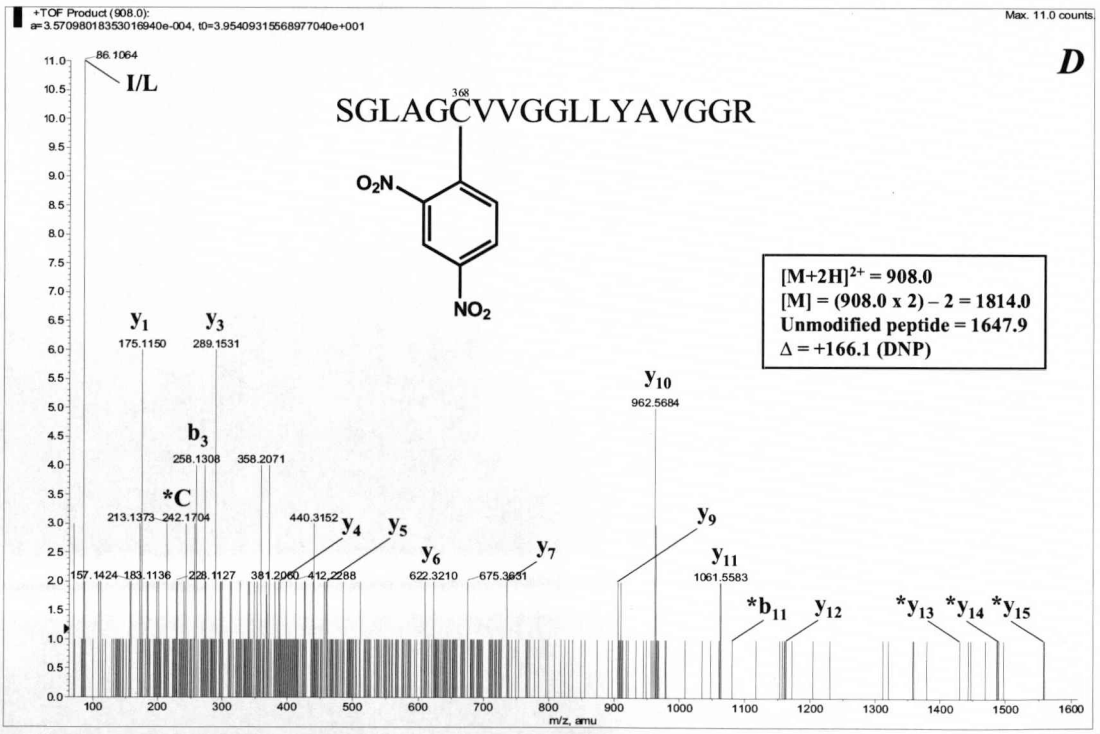

Fig. 4.2 - MS/MS spectrum indicating modification of Keap1-His (C) Cys-257 and (D) Cys-368 by DNCB *in vitro*. y- and b-ions are labelled where present. * denotes ions for which a mass shift of +166.0 amu indicates modification by DNCB. Immonium ions are labelled with the one-letter code for their corresponding amino acid.

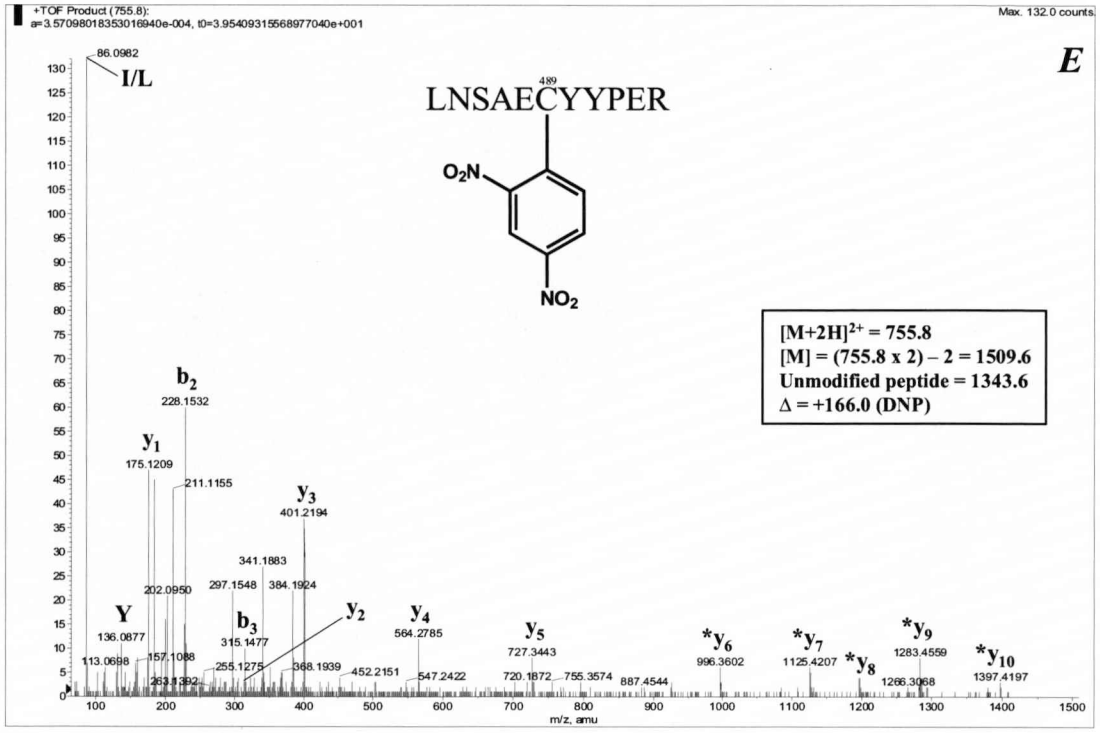

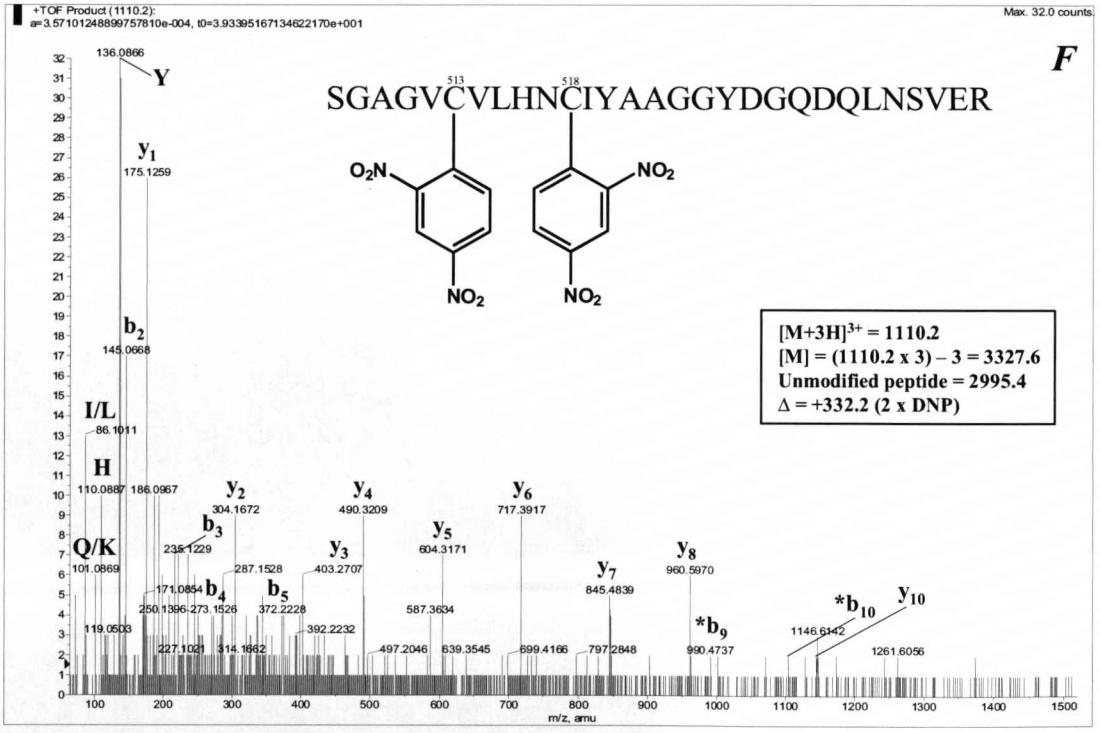

Fig. 4.2 - MS/MS spectrum indicating modification of Keap1-His (E) Cys-489 and (F) Cys-515/518 by DNCB *in vitro*. y- and b-ions are labelled where present. * denotes ions for which a mass shift of +166.0 amu indicates modification by DNCB. Immonium ions are labelled with the one-letter code for their corresponding amino acid.

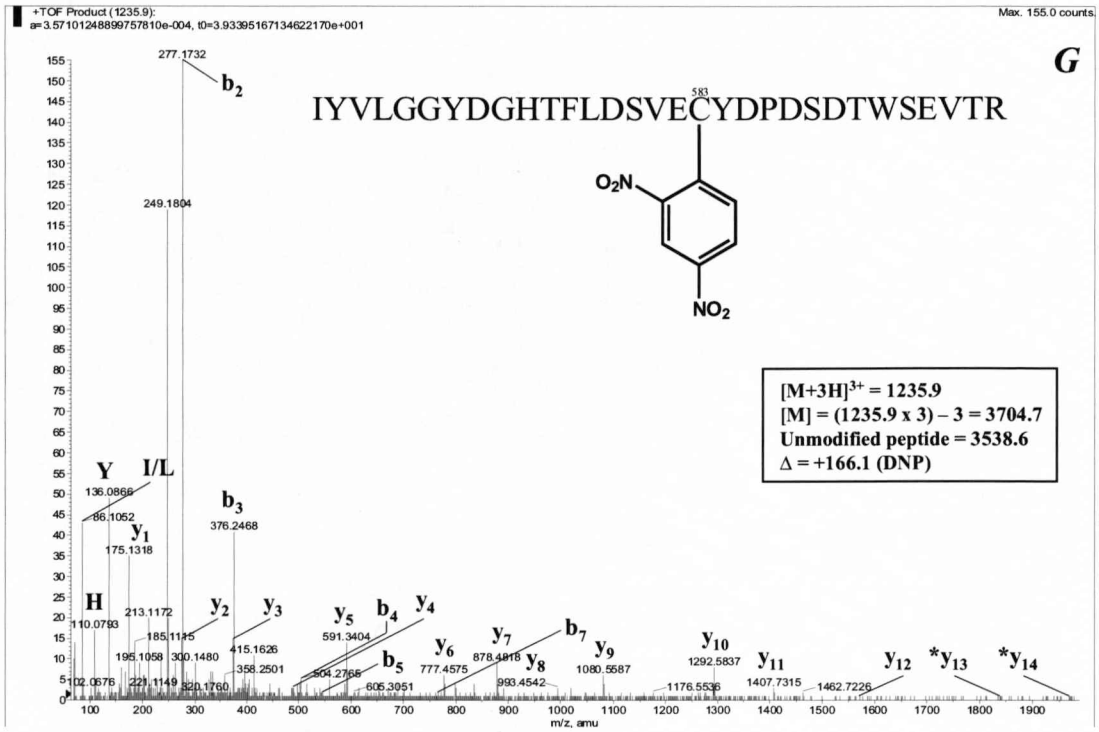

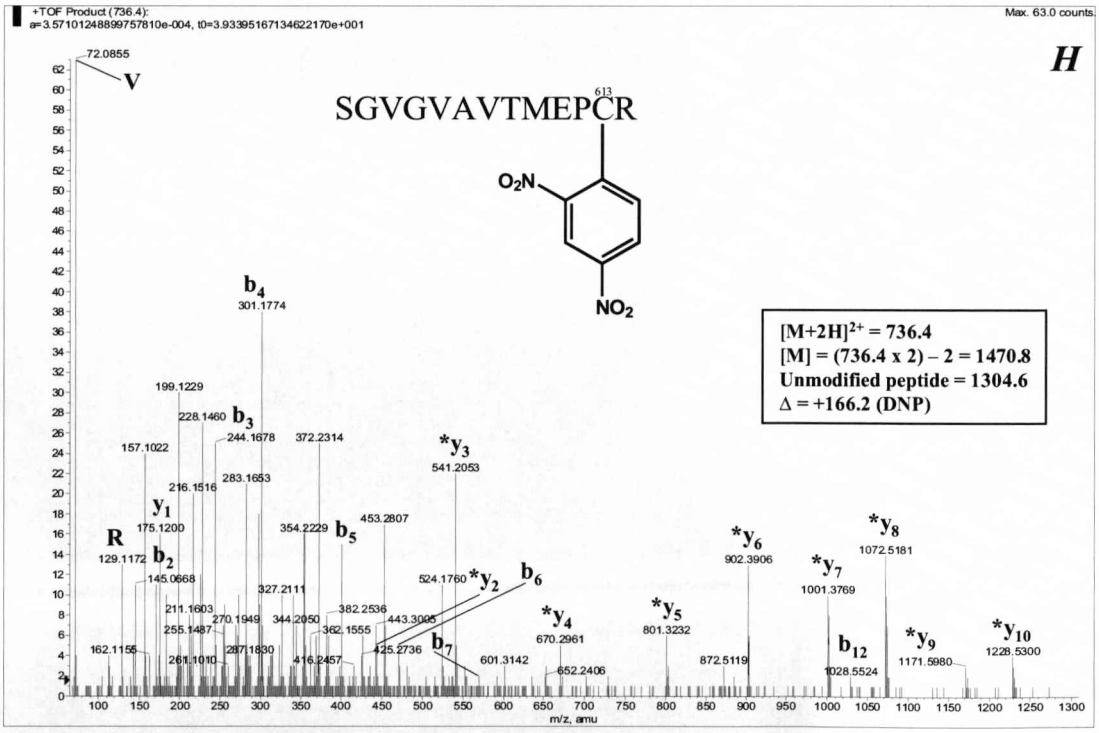

Fig. 4.2 - MS/MS spectrum indicating modification of Keap1-His (G) Cys-583 and (H) Cys-613 by DNCB *in vitro*. y- and b-ions are labelled where present. * denotes ions for which a mass shift of +166.0 amu indicates modification by DNCB. Immonium ions are labelled with the one-letter code for their corresponding amino acid.

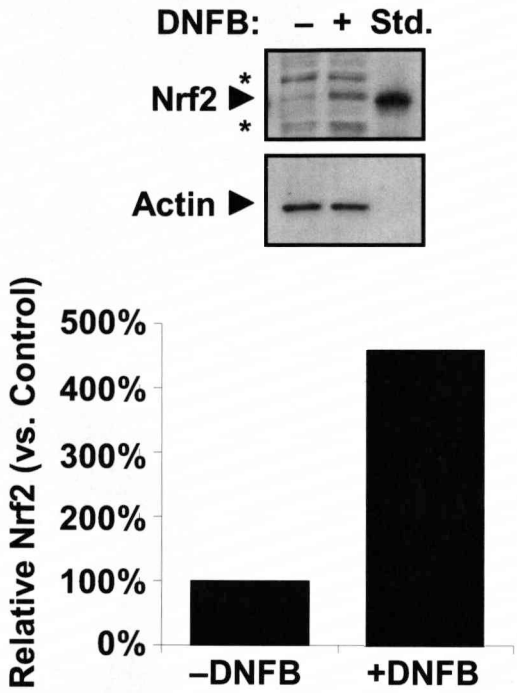

Fig. 4.3 - Activation of Nrf2 by DNFB. Hepa-1c1c7 cells were exposed to vehicle (0.5 % DMSO) or DNFB (100 μM) for 1 h. Nuclear fractions were prepared and the Nrf2 protein level was assessed by Western blot analysis. Nrf2 bands were quantified by densitometry and expressed relative to β-actin, to enable comparison with vehicle-treated control Nrf2 level, which was arbitrarily set at 100 %. Recombinant Nrf2-His was loaded onto the gels as a standard (Std). Non-specific proteins that cross-react with the antibody are labeled *.

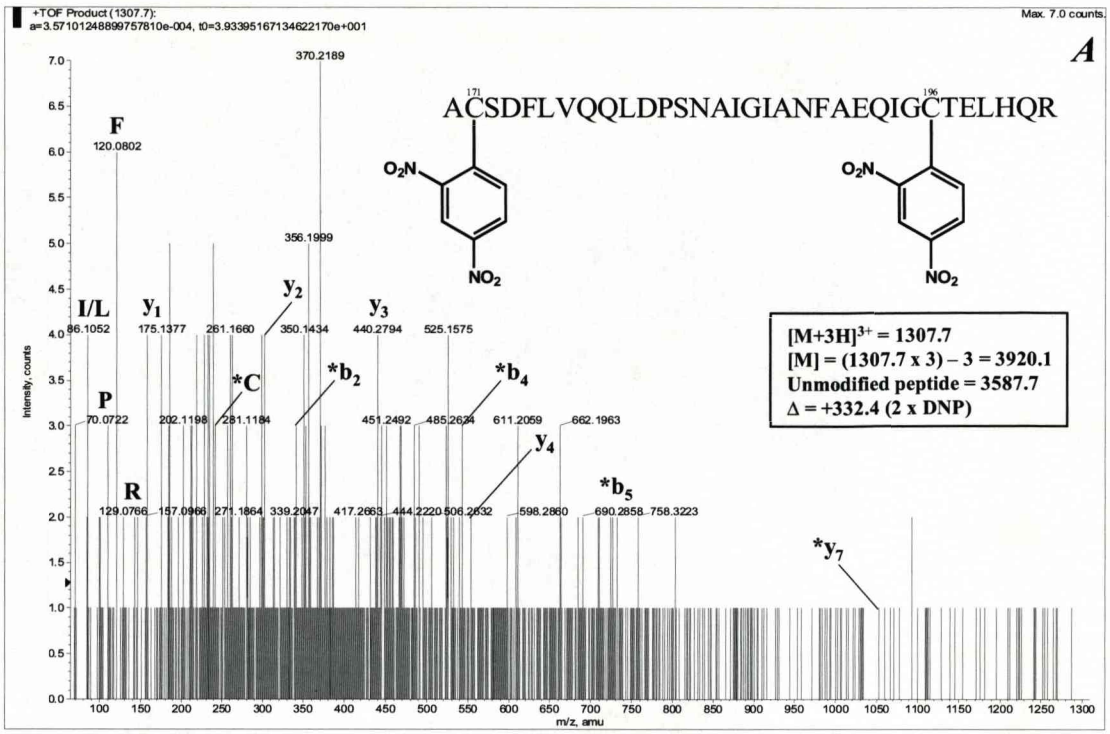

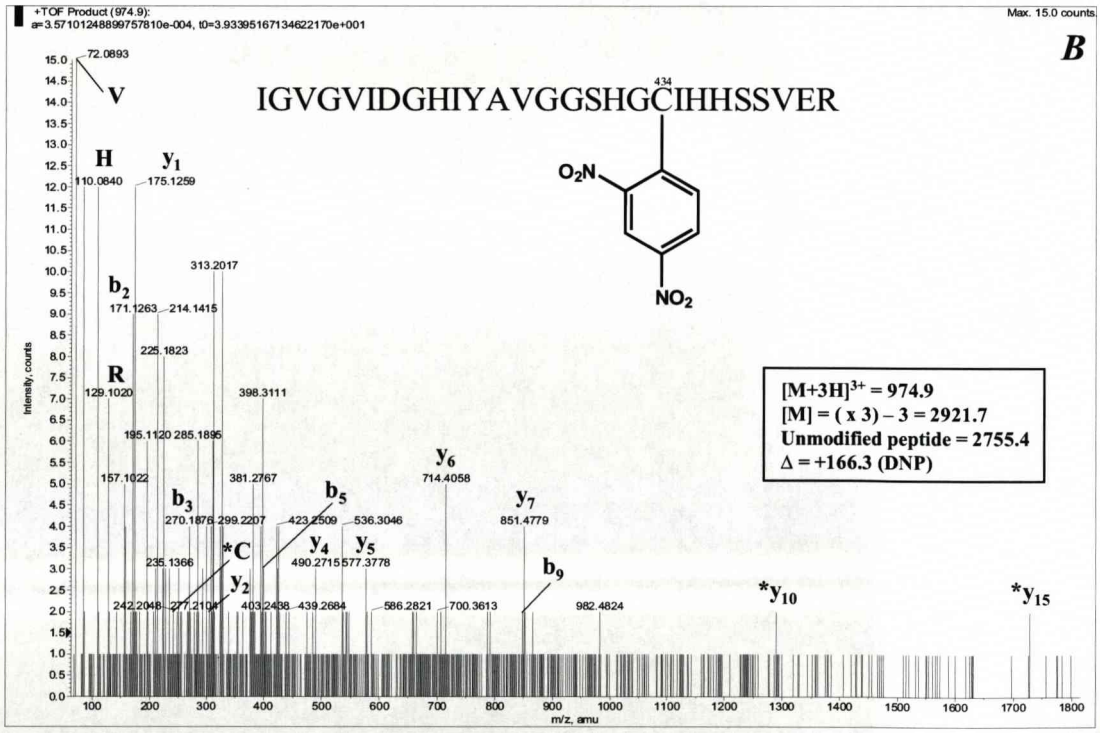

Fig. 4.4 - MS/MS spectrum indicating modification of Keap1-His (A) Cys-171/196 and (B) Cys-434 by DNFB *in vitro*. y- and b-ions are labelled where present. * denotes ions for which a mass shift of +166.0 amu indicates modification by DNFB. Immonium ions are labelled with the one-letter code for their corresponding amino acid.

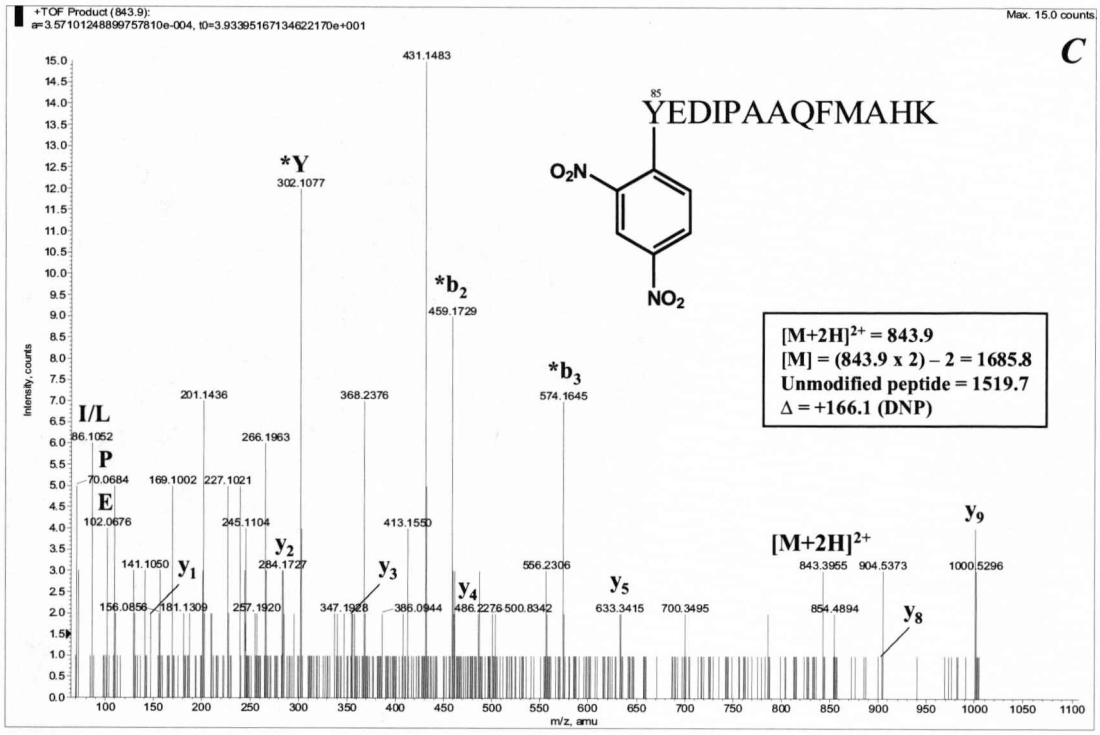

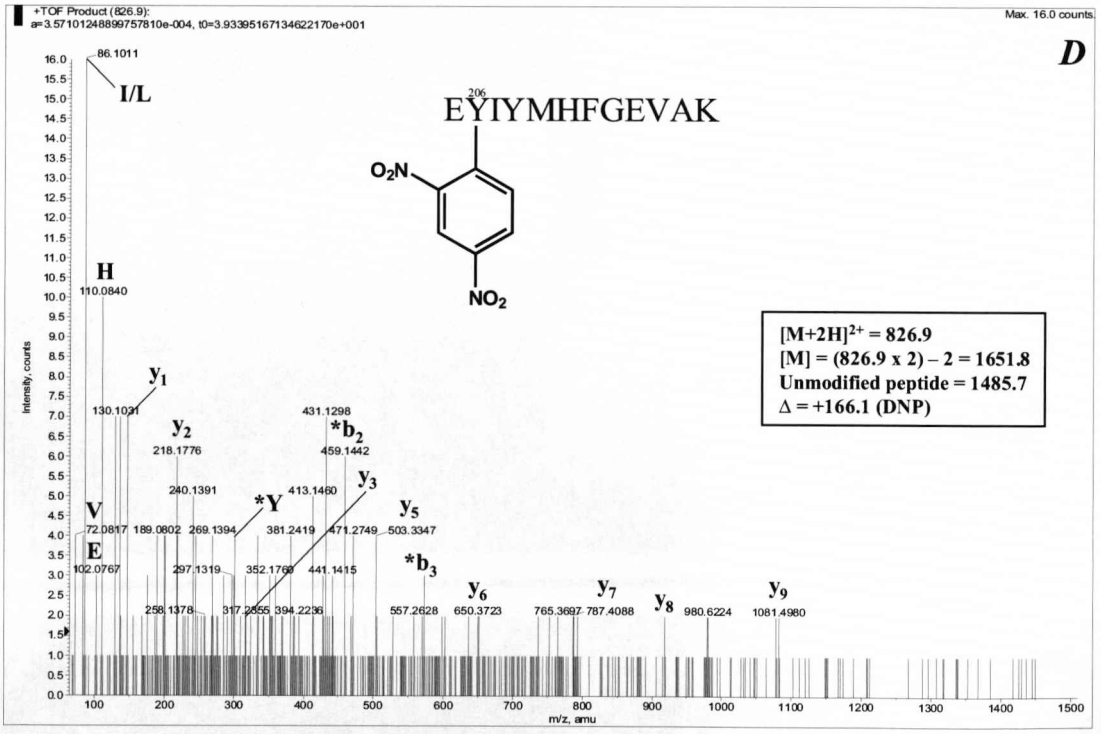

Fig. 4.4 - MS/MS spectrum indicating modification of Keap1-His (C) Tyr-85 and (D) Tyr-206 by DNFB *in vitro*. y- and b-ions are labelled where present. * denotes ions for which a mass shift of +166.0 amu indicates modification by DNFB. Immonium ions are labelled with the one-letter code for their corresponding amino acid.

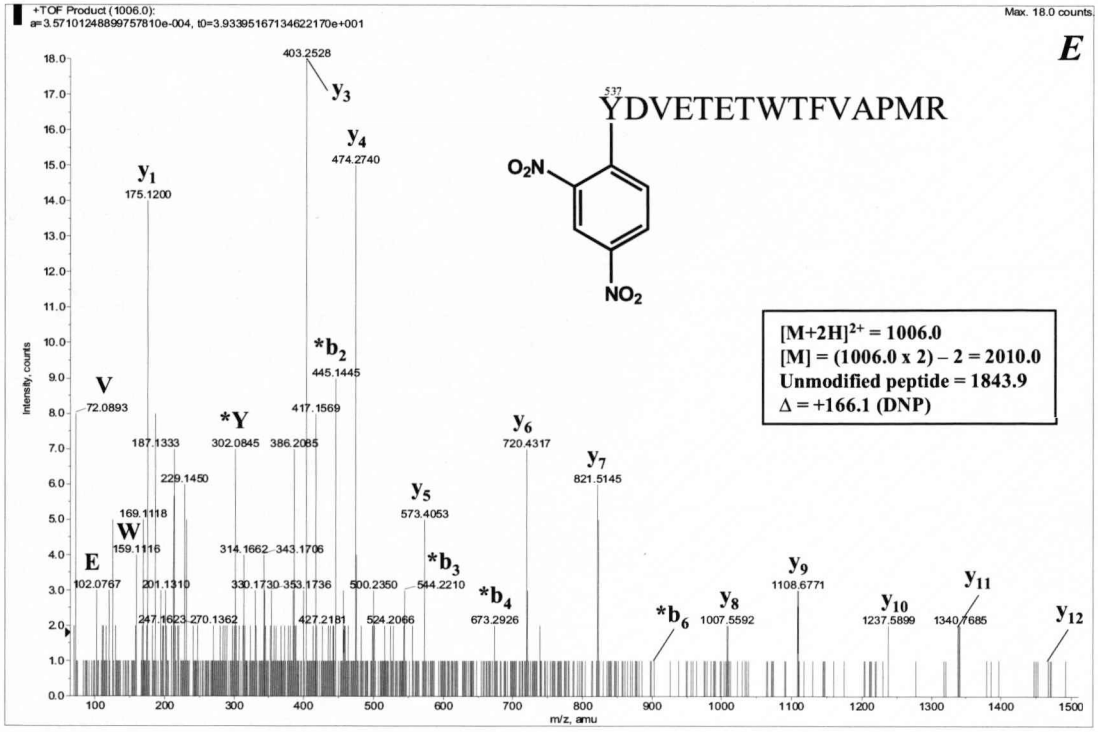

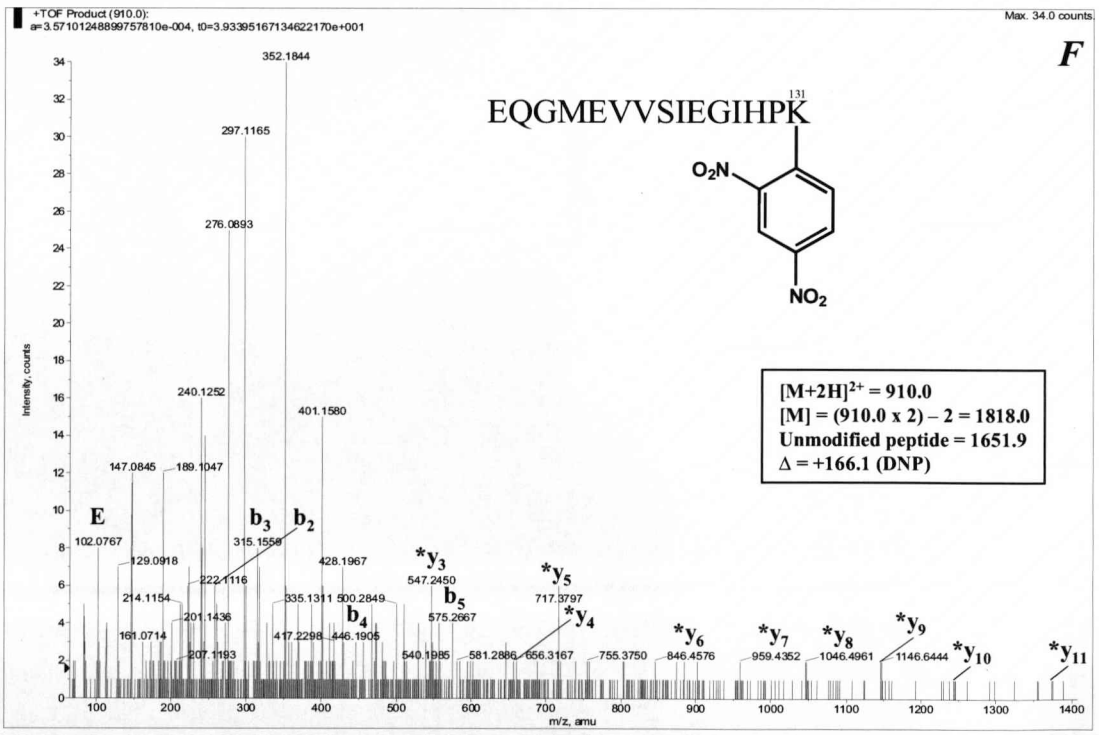

Fig. 4.4 - MS/MS spectrum indicating modification of Keap1-His (E) Tyr-537 and (F) Lys-131 by DNFB *in vitro*. y- and b-ions are labelled where present. * denotes ions for which a mass shift of +166.0 amu indicates modification by DNFB. Immonium ions are labelled with the one-letter code for their corresponding amino acid.

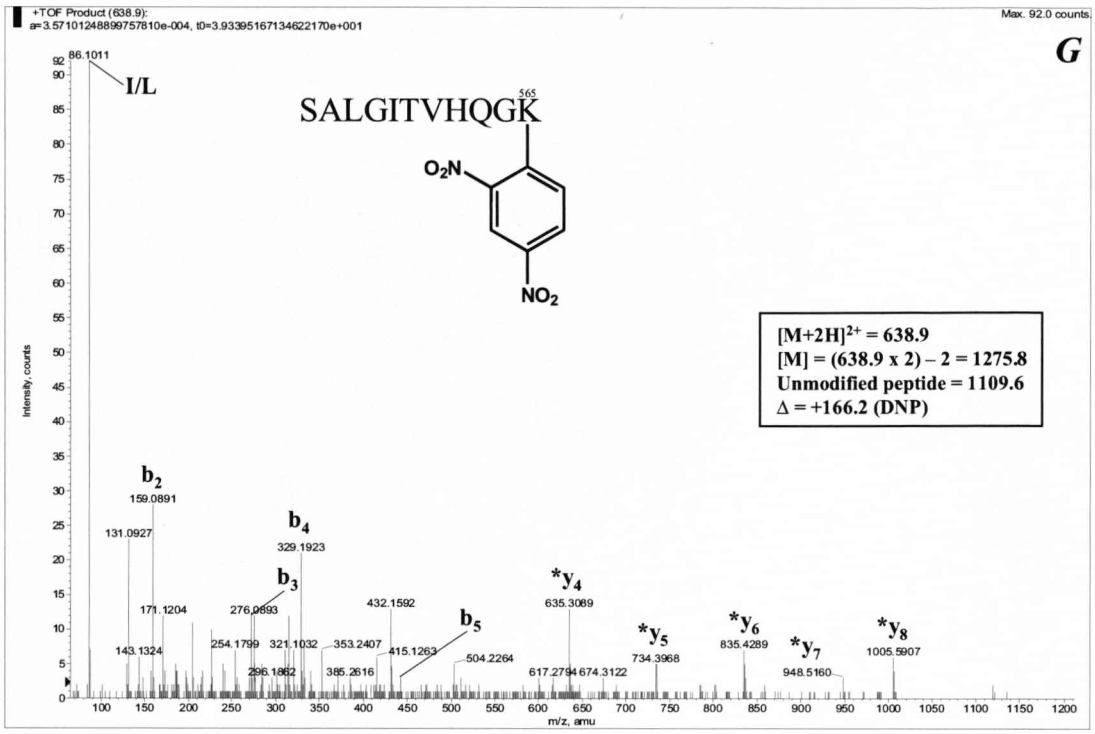

Fig. 4.4 - MS/MS spectrum indicating modification of Keap1-His (G) Lys-565 by DNFB *in vitro*. y- and b-ions are labelled where present. * denotes ions for which a mass shift of +166.0 amu indicates modification by DNFB. Immonium ions are labelled with the one-letter code for their corresponding amino acid.

4.3.4 Modification of Keap1-His by 15d-PGJ$_2$ *in vitro*

Following incubation of Keap1-His with 15d-PGJ$_2$ for 1 h, as for NAPQI and DNCB, no cysteine adducts were detected at a molar ratio of 0.01:1 15d-PGJ$_2$:Keap1. However, in contrast to NAPQI and DNCB, cysteine adducts were not detected at molar ratios of 0.1:1 or 1:1 15d-PGJ$_2$:Keap1 (Table 4.3 and Fig. 4.5). Indeed, detection of 15d-PGJ$_2$-cysteine adducts was limited to low intensity ions, at relatively high molar ratios, in one of three experiments. The adducts detected were Cys-226, -368, -513/518 and -613. There was no evidence for the modification of Cys-151, -273 and/or -288 by 15d-PGJ$_2$, even following incubation of Keap1 with a 100-fold molar excess of the cyclopentenone.

In order to confirm that the conditions used for the detection of 15d-PGJ$_2$-cysteine adducts were robust, the cyclopentenone was incubated with a reference protein with which our research group has extensive experience as a model for chemical modification experiments (Jenkins *et al.*, 2008), namely human GSTP1-1. At an equimolar ratio and greater, 15d-PGJ$_2$ reproducibly modified the reactive Cys-47 of GSTP1-1, as did NAPQI and DNCB (see Appendix). For some Keap1 and GSTP1-1 peptides modified by 15d-PGJ$_2$, although it was clear that the parent ions had undergone an increase in mass consistent with adduction by 15d-PGJ$_2$ (+316.2 amu), it was not possible to identify modified y- and/or b-ions. However, it was noticeable from visual inspection of the MS/MS spectra that the peptide fragmentation process had resulted in the dissociation of 15d-PGJ$_2$ from the cysteine residue; therefore the singly-charged prostaglandin molecule (317.2 amu) was detectable. This characteristic ion was not present when Keap1 or GSTP1-1 was incubated with iodoacetamide alone. Therefore, it appears that cysteines within Keap1 react weakly with the Nrf2-activating cyclopentenone 15d-PGJ$_2$ *in vitro*, although the lability of the adduct formed between 15d-PGJ$_2$ and cysteine residues in Keap1 may hinder the detection of modifications under the experimental conditions employed here.

		Molar Ratio 15d-PGJ$_2$:Keap1				
Keap1 Domain	**Cysteine #**	**0**	**5:1**	**10:1**	**50:1**	**100:1**
N-terminal	23					
N-terminal	38					
BTB	77					
BTB	151					
BTB	171					
IVR	196					
IVR	226		1/3	1/3	1/3	1/3
IVR	241					
IVR	249					
IVR	257					
IVR	273					
IVR	288					
IVR	297					
IVR	319					
DGR	368			1/3	1/3	1/3
DGR	395					
DGR	406					
DGR	434					
DGR	489					
DGR	513		1/3*	1/3	1/3	1/3
DGR	518					
DGR	583					
C-terminal	613		1/3	1/3	1/3	1/3
C-terminal	622	*nd*	*nd*	*nd*	*nd*	*nd*
C-terminal	624	*nd*	*nd*	*nd*	*nd*	*nd*

Table 4.3 - Keap1-His cysteines modified by 15d-PGJ$_2$ in vitro. Ni^{2+} agarose bead-purified mouse Keap1-His (~350 pmol) was reduced on-bead with 1 mM DTT for 15 min and incubated with 15d-PGJ$_2$ at the indicated molar ratios for 1 h. Free sulphydryls were capped with 55 mM iodoacetamide for 15 min. Keap1-His was digested overnight at 37 °C with 240 ng trypsin and the resulting tryptic peptides were analysed for adducts of interest by LC-ESI-MS/MS. The frequency of adduct detection, from a total of three experiments, is shown. Blank cells indicate that no 15d-PGJ$_2$ adducts were detected. No 15d-PGJ$_2$-cysteine adducts were detected at molar ratios of 0.01:1, 0.1:1 or 1:1. *nd*; Cys-622 and -624 were not routinely detected as 15d-PGJ$_2$ -modified or carboxyamidomethylated peptides. *A mass shift equivalent to the addition of one molecule of 15d-PGJ$_2$ was detected on this peptide. Due to the lack of sufficient b-ions, however, it was not possible to determine which of the two cysteines, Cys-513 or Cys-518, was adducted.

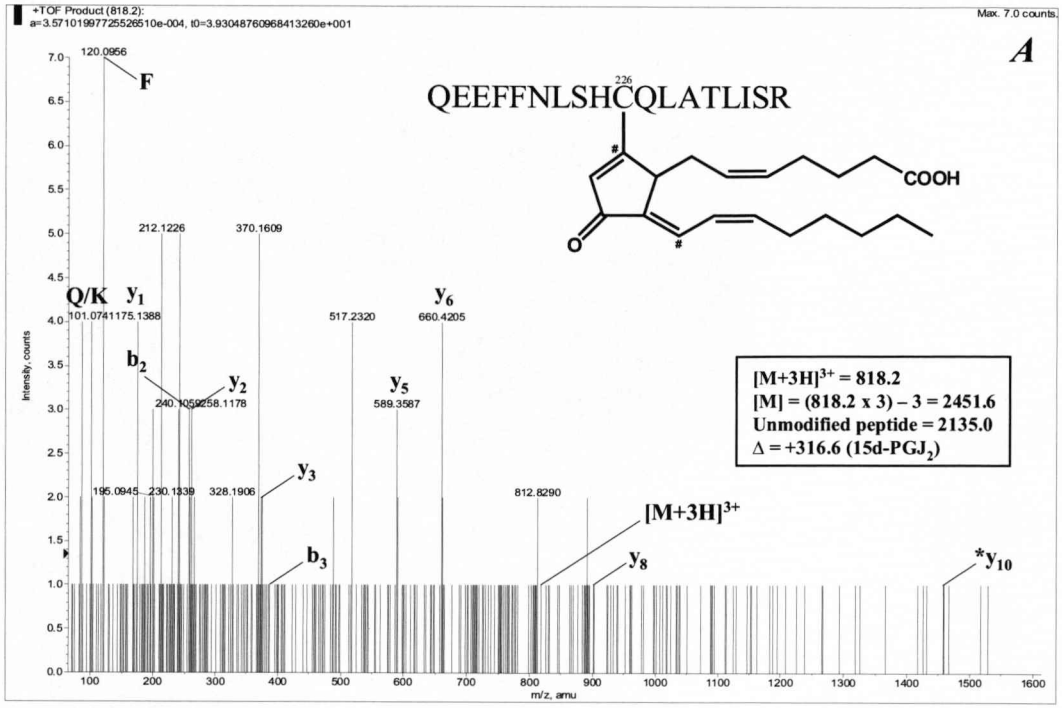

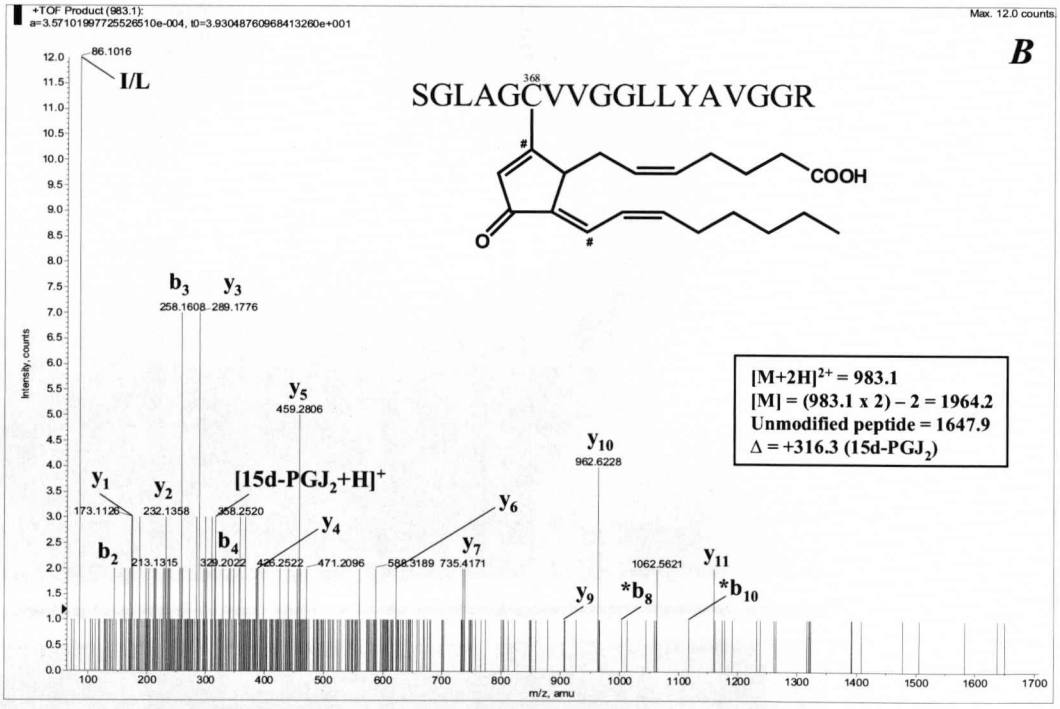

Fig. 4.5 - MS/MS spectrum indicating modification of Keap1-His (A) Cys-226 and (B) Cys-368 by 15d-PGJ$_2$ *in vitro*. y- and b-ions are labelled where present. * denotes ions for which a mass shift of +316.2 amu indicates modification by 15d-PGJ$_2$. Immonium ions are labelled with the one-letter code for their corresponding amino acid. It was not determined via which of the two electrophilic α,β-unsaturated carbonyl moieties (labelled #) adduction occurred.

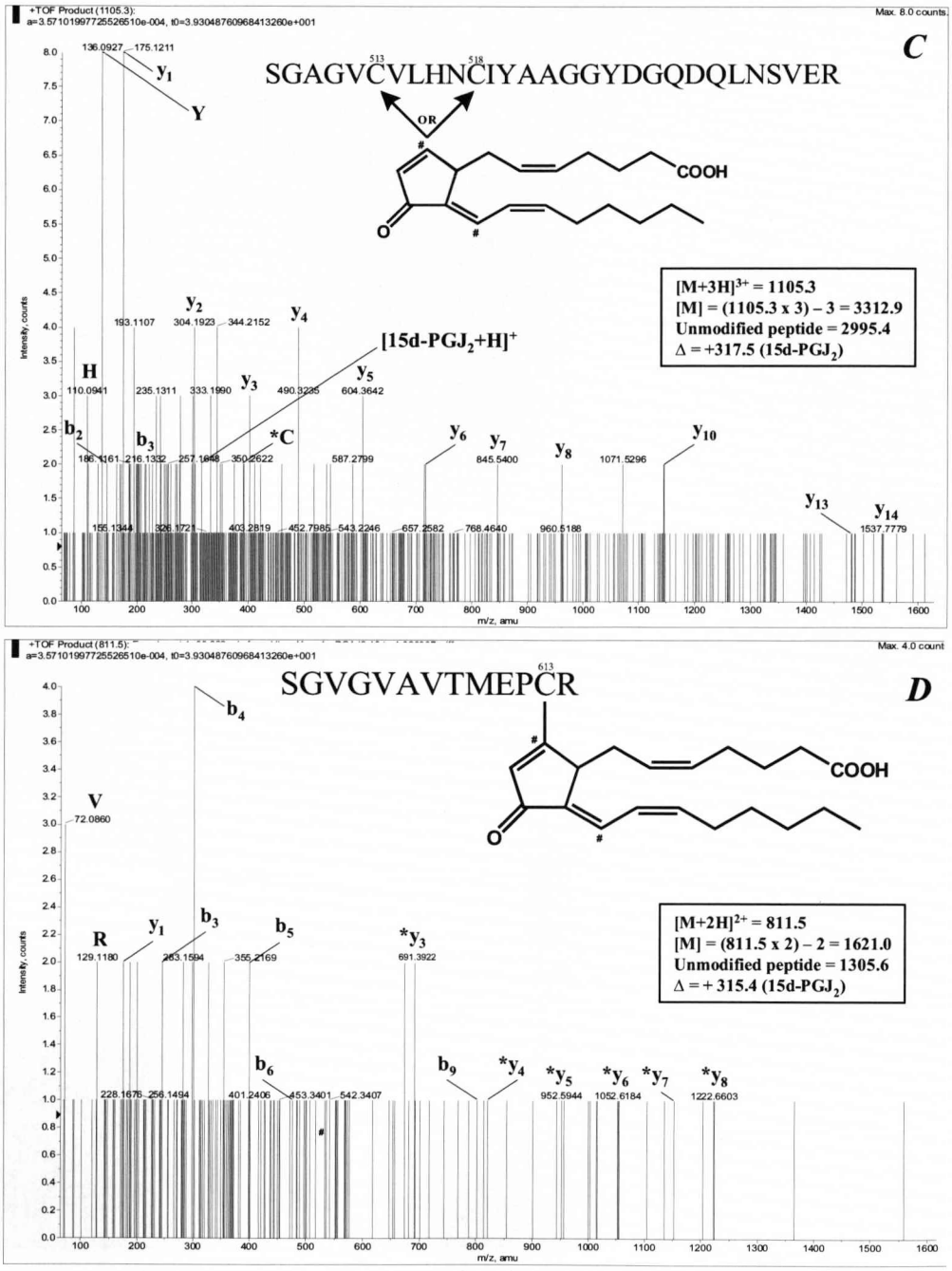

Fig. 4.5 - MS/MS spectrum indicating modification of Keap1-His (C) Cys-513/518 and (D) Cys-613 by 15d-PGJ$_2$ *in vitro*. y- and b-ions are labelled where present. * denotes ions for which a mass shift of +316.2 amu indicates modification by 15d-PGJ$_2$. Immonium ions are labelled with the one-letter code for their corresponding amino acid. It was not determined via which of the two electrophilic α,β-unsaturated carbonyl moieties (labelled #) adduction occurred. C) A mass shift equivalent to the addition of one molecule of 15d-PGJ$_2$ was detected on this peptide. Due to the lack of sufficient b-ions, however, it was not possible to determine which of the two cysteines, Cys-513 or Cys-518, was adducted.

4.3.5 Modification of Keap1-His by TMA *in vitro*

Given that TMA does not activate Nrf2, and is a hard electrophile capable of reacting with the amine group of lysine, but relatively incapable of modifying cysteines, it was anticipated that TMA would not form adducts with cysteine residues within Keap1 *in vitro*. Indeed, no cysteine adducts were detected following incubation of Keap1-His with TMA, to a molar ratio of 50:1, although adduction of Lys-108 was identified (Fig. 4.6).

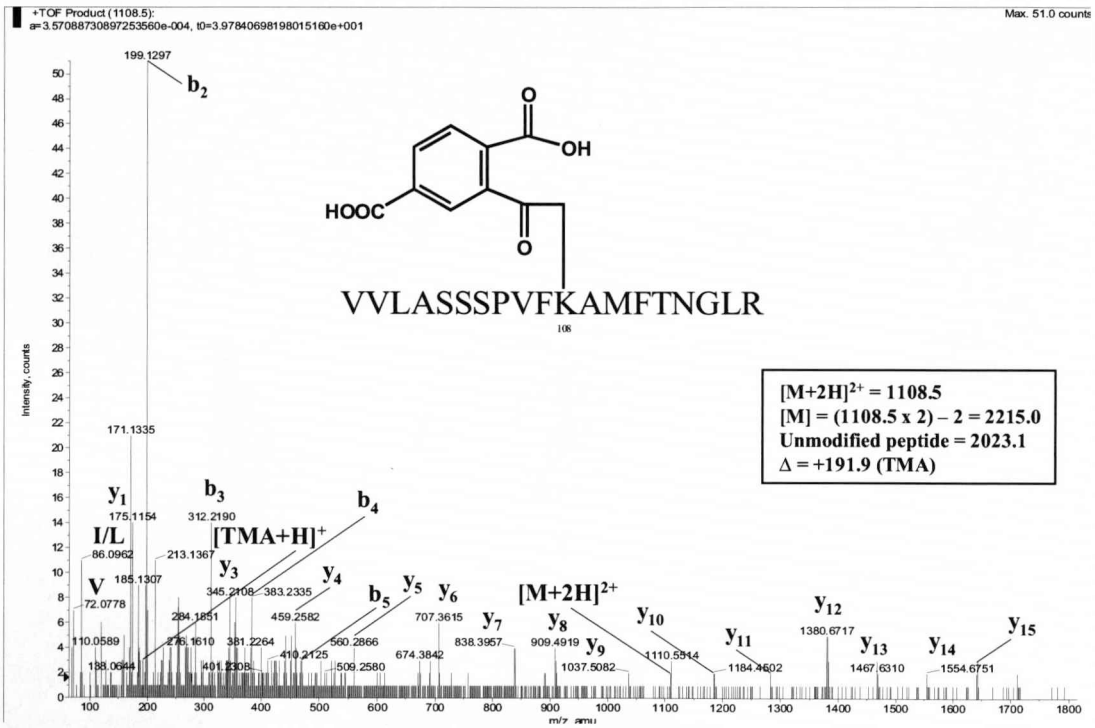

Fig. 4.6 - MS/MS spectrum indicating modification of Keap1-His Lys-108 by TMA *in vitro*. y- and b-ions are labelled where present. * denotes ions for which a mass shift of +192.0 amu indicates modification by TMA. Immonium ions are labelled with the one-letter code for their corresponding amino acid.

4.3.6 Summary of Keap1-His modifications

The only cysteines that were not found to be modified by NAPQI, DNCB and/or 15d-PGJ_2 in this study were Cys-241, -249, -297, -395 and -406. As evidence that these cysteines were available for modification and detectable by LC-ESI-MS/MS analysis, MS/MS spectra for peptides containing Cys-241/249, -297 and -395/406 are presented as iodoacetamide adducts in Fig. 4.7.

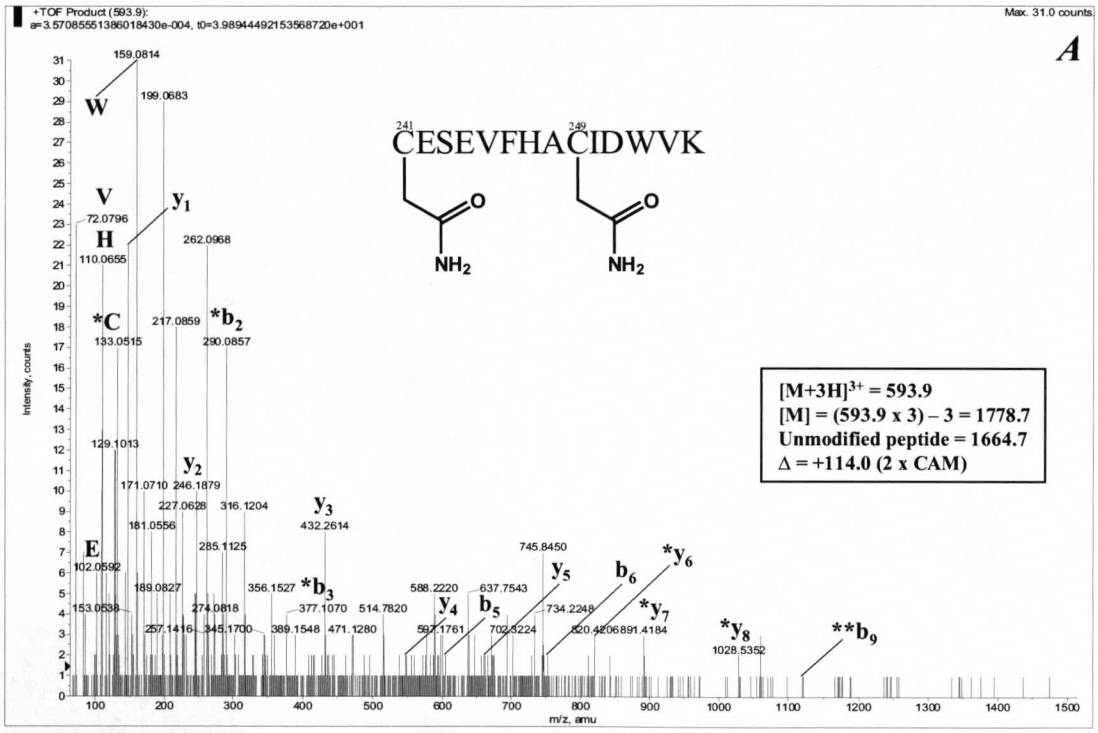

Fig. 4.7 - MS/MS spectrum indicating modification of Keap1-His (A) Cys-241/249 and by iodoacetamide *in vitro*. y- and b-ions are labelled where present. * denotes ions for which a mass shift of +57.1 amu indicates modification by iodoacetamide. Immonium ions are labelled with the one-letter code for their corresponding amino acid.

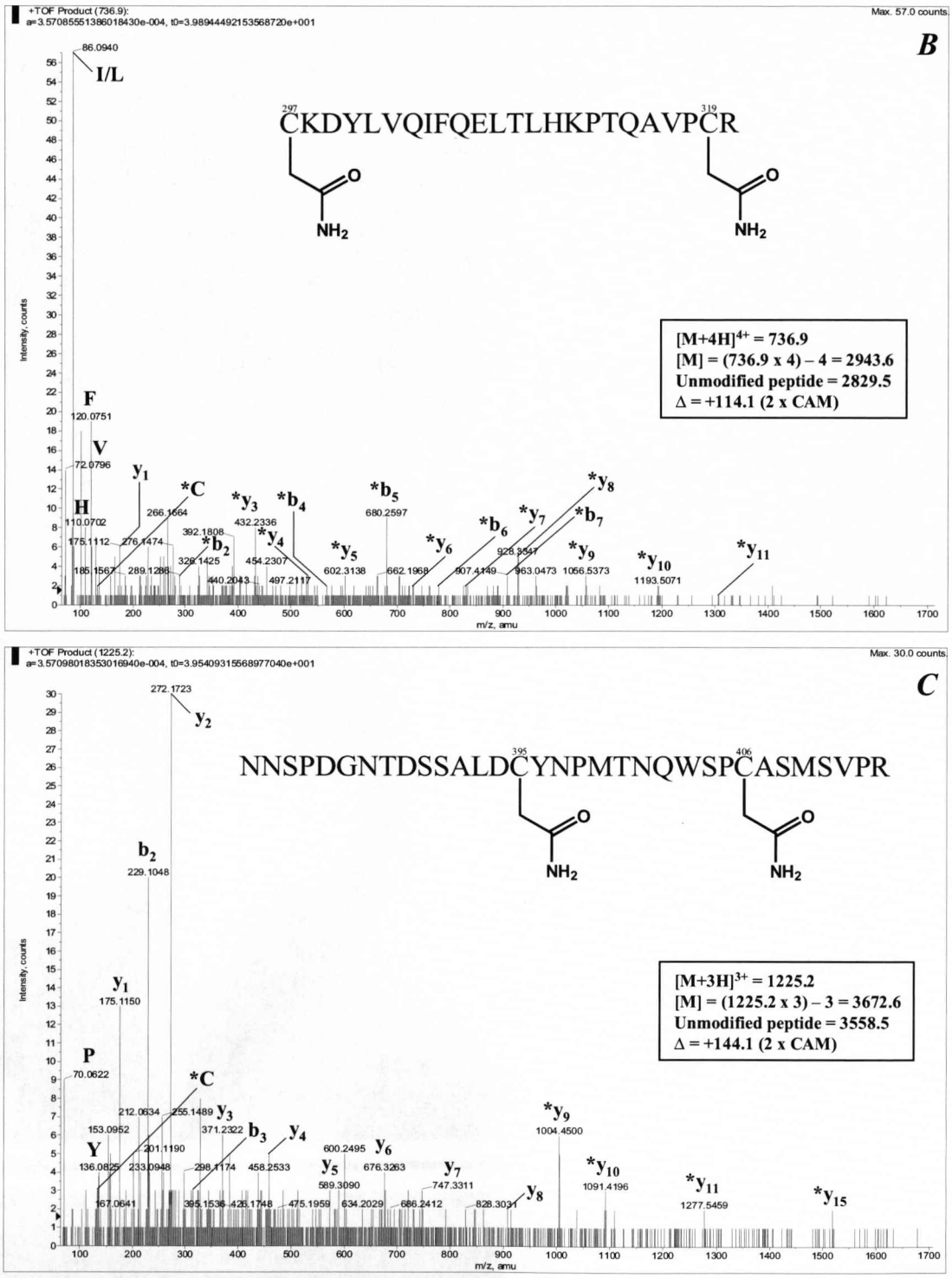

Fig. 4.7 - MS/MS spectrum indicating modification of Keap1-His (B) Cys-297/319 and (C) Cys-395/406 by iodoacetamide *in vitro*. y- and b-ions are labelled where present. * denotes ions for which a mass shift of +57.1 amu indicates modification by iodoacetamide. Immonium ions are labelled with the one-letter code for their corresponding amino acid.

In summary, the results presented in this chapter demonstrate different patterns of Keap1 cysteine modification induced by a panel of chemically distinct, Nrf2-activating electrophiles (Fig. 4.8); the only residues commonly targeted by NAPQI, DNCB and 15d-PGJ_2 *in vitro*, at relatively high molar ratios, were Cys-226, -368 and -613.

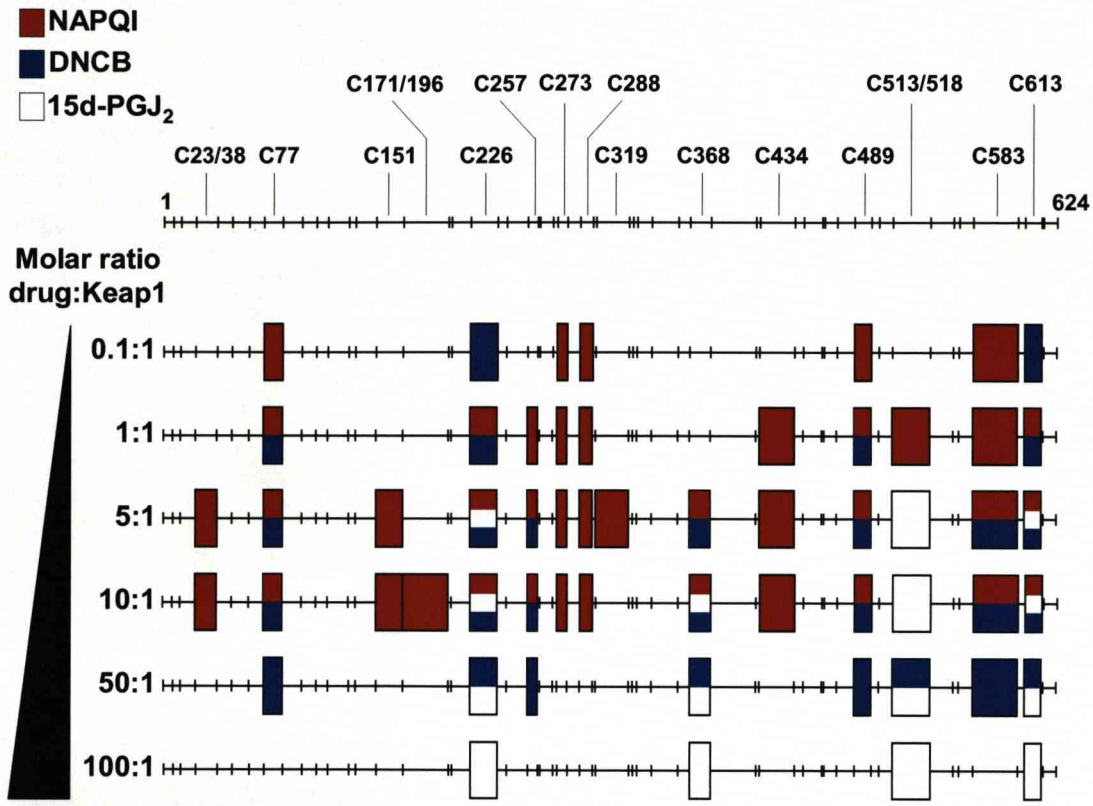

Fig. 4.8 - Summary of *in vitro* Keap1-His cysteine adduct patterns for NAPQI, DNCB and 15d-PGJ_2. Modification maps for cysteine-containing Keap1-His peptides were generated using a software package described previously by Beynon (2005). The horizontal lines represent the full-length Keap1 protein (amino acids 1-624), the vertical lines represent the boundaries between sequential tryptic peptides. Filled boxes represent cysteine-containing peptides found to be modified by NAPQI (■), DNCB (■) or 15d-PGJ_2 (□), at the indicated molar ratios. Multi-shaded boxes represent cysteines modified by more than one of the three molecules. The specific cysteines modified are noted at the top of the figure. Experiments involving a molar ratio of 50:1 were performed with DNCB and 15d-PGJ_2, but not NAPQI. Experiments involving a molar ratio of 100:1 were performed with 15d-PGJ_2 only.

4.4 DISCUSSION

The Nrf2-ARE pathway serves to protect mammalian cells against chemical/oxidative stress, via the inducible expression of cytoprotective enzymes and proteins (for a review, see Kensler *et al.*, 2007). It has been proposed that chemical inducers activate the Nrf2-ARE pathway through the direct modification of critical cysteine residues within Keap1, the cytosolic repressor of Nrf2 (Dinkova-Kostova *et al.*, 2002). The aim of the work presented in this chapter was two-fold, a) to explore the hypothesis that NAPQI activates the Nrf2-ARE pathway through the selective modification of cysteine residues within Keap1, and b) to test, using a panel of structurally-distinct electrophiles, the hypothesis that all Nrf2-activating molecules selectively modify one or more Keap1 cysteines amongst the subset of Cys-151, -273 and -288. In order to test these hypotheses, recombinant mouse Keap1-His (expression and purification described in chapter 3) was exposed to NAPQI, DNCB, 15d-PGJ_2 and TMA *in vitro*, and cysteine adducts were mapped by MS/MS. Importantly, during the course of this work, a number of independent studies have employed a similar methodology to provide compelling evidence for the chemical modification of Keap1 *in vitro* by DNCB (Liu *et al.*, 2005) and the Nrf2-activating molecules menadione (Liu *et al.*, 2005), biotinylated iodoacetamide (BIA) (Eggler *et al.*, 2005; Hong *et al.*, 2005b), sulforaphane (Hong *et al.*, 2005a), xanthohumol (Dietz *et al.*, 2005; Luo *et al.*, 2007), isoliquiritigenin and 10-shogaol (Luo *et al.*, 2007). The results of the work presented in this chapter will be discussed in light of these recent investigations.

This study has demonstrated direct chemical modification of Keap1 by NAPQI, and thereby provides the first evidence for the modification of Keap1 by the metabolite of a widely-used therapeutic drug. At an equimolar ratio of NAPQI:Keap1, 10 cysteine residues were found to be modified, including Cys-257, -273, -288 and -613, i.e. four of the five cysteines in mouse Keap1 originally identified as the most reactive towards dex-mes *in vitro* (Dinkova-Kostova *et al.*, 2002). Indeed, Cys-273 and -288 were amongst five residues found to be the most readily modified by NAPQI at the lowest molar ratio of 0.1:1. Additionally, NAPQI modified the BTB domain residue Cys-151, which has

also been proposed as a target for activators of Nrf2, based on evidence from site-directed mutagenesis experiments (Zhang *et al.*, 2003). Therefore, these findings support the concept that Cys-151, -273 and -288 of Keap1 may be preferential targets of Nrf2-activating molecules, and indirectly support the hypothesis that NAPQI activates the Nrf2-ARE pathway through direct modification of Keap1. Of course, it is necessary to be cautious when attempting to extrapolate data obtained from such *in vitro* analyses to a cellular context. Therefore, a cell-based method is required to further explore, under more biologically-relevant conditions, the association between modification of Keap1 and activation of Nrf2 by NAPQI.

In an attempt to provide a biochemical rationale for the ability of NAPQI and other electrophiles to activate Nrf2-dependent cell defence, the residue-selectivity of Keap1 modification by structurally-distinct Nrf2-activating molecules (DNCB and 15d-PGJ_2) has also been determined. Notably, MALDI-TOF MS has recently been used to show that DNCB forms adducts with human Keap1, following incubation of the protein with a 20-fold molar excess of DNCB for 2 h (Liu *et al.*, 2005). Although the authors of this study did not explicitly identify the cysteine residues that were modified by DNCB, they did note the appearance of new peptide ion signals that correspond to DNCB-modified cysteine-containing peptides (Liu *et al.*, 2005). By comparing the masses of these signals to a theoretical tryptic digest of human Keap1, it can be determined that the specific residues modified by DNCB in the study of Liu *et al.* (2005) were Cys-226, -257, -319, -489 and -613. With the exception of Cys-319, all of these residues were found to be modified in mouse Keap1 by DNCB in section 4.3.3 of this thesis, indicating a degree of agreement between these independent investigations.

In contrast to NAPQI, it was not possible to detect modification by DNCB of Cys-151, -273 or -288, contradicting the notion that these residues are preferentially reactive towards all Nrf2-activating molecules. However, DNCB did preferentially modify the IVR residue Cys-257 and the C-terminal domain residue Cys-613, two of the five cysteines found to be the most reactive towards dex-mes *in vitro* (Dinkova-Kostova *et al.*, 2002), suggesting that modification of reactive Keap1 cysteines in general, and not

of specific residues *per se*, may be critical for the activation of Nrf2-dependent cell defence.

Recently, biotin-tagged analogues of 15d-PGJ_2 have been employed to demonstrate binding of the cyclopentenone to Keap1 in cells (Hosoya *et al.*, 2005; Itoh *et al.*, 2004; Levonen *et al.*, 2004). Although such an approach cannot identify specific residues that are targeted by 15d-PGJ_2, compound mutation of seven cysteines within the IVR domain of Keap1 abolishes this adduct formation (Hosoya *et al.*, 2005), indicating that one or more cysteines within this region are targeted by 15d-PGJ_2 in cells. The present study, in providing the first mass spectrometry-based evidence for the modification of specific Keap1 cysteines by 15d-PGJ_2 *in vitro*, has demonstrated adduction of one of these IVR residues, Cys-226, in addition to Cys-368, -513/518 and -613. Again, it was not possible to detect modification of Cys-151, -273 or -288 by 15d-PGJ_2, confirming that, at least *in vitro*, these residues are not preferential targets for all Nrf2-activating molecules.

Notably, the molar amounts of 15d-PGJ_2 required to detect Keap1 cysteine adducts were relatively high, when compared to NAPQI and DNCB. Furthermore, evidence for modification of Keap1 cysteines by 15d-PGJ_2 was apparent in only one of three experiments. This may be due to the lability of the adducts formed between 15d-PGJ_2 and sulphydryl moieties, which may be susceptible to decomposition during sample preparation or in the course of the MS/MS fragmentation process. Hence, there may be value in optimising workup and/or analysis procedures in order to preserve 15d-PGJ_2-cysteine adducts, in a similar manner to that reported by Hong *et al.* (2005a) in their recent study of Keap1 modification by sulforaphane, which also forms relatively labile adducts with cysteine. Alternatively, it is possible that, in activating Nrf2, the initial point of interaction of 15d-PGJ_2 may be with upstream signalling molecules other than Keap1. Indeed, evidence exists for an inhibitory effect of 15d-PGJ_2 on the ubiquitin-proteasome pathway (Mullally *et al.*, 2001; Shibata *et al.*, 2003), which has a major role in regulating the basal activity of Nrf2 (Kobayashi *et al.*, 2004; McMahon *et al.*, 2003; Nguyen *et al.*, 2003; Stewart *et al.*, 2003; Zhang *et al.*, 2003). Therefore, the ability of 15d-PGJ_2 to activate Nrf2 may be at least partially independent of direct modification of

Keap1. 15d-PGJ_2 has been shown previously to adduct and inhibit the activity of other important cellular proteins including the transcription factors NF-κB (Cernuda-Morollon *et al.*, 2001) and AP-1 (Perez-Sala *et al.*, 2003), and the GSH-conjugating enzyme GSTP1-1 (Sanchez-Gomez *et al.*, 2007); the latter was used in this study as a model cysteine-containing protein to confirm that the method used for detecting 15d-PGJ_2-cysteine adducts was robust. In summary, this work demonstrates that 15d-PGJ_2 selectively modifies Keap1 cysteines *in vitro*, albeit relatively weakly compared to NAPQI and DNCB. It is, therefore, imperative that further work is undertaken to ascertain the importance of Keap1 modification in the activation of Nrf2 by 15d-PGJ_2 in a cellular context.

In contrast to NAPQI, DNCB and 15d-PGJ_2, and in keeping with its known chemical reactivity, it was not possible to detect modification of Keap1 cysteines by the lysine-reactive molecule TMA, which does not activate Nrf2 in Hepa-1c1c7 cells. Taken together, therefore, the findings of this study indicate that reactivity towards cysteine is an important chemical property shared by Nrf2-activating molecules. However, through mapping Keap1 cysteine modifications by three chemically-distinct electrophiles using the same test system, it has been demonstrated that the pattern of adducts associated with different Nrf2-activators may vary, at least *in vitro*, a conclusion that can also be drawn from the recent mass spectrometry-based investigations of Keap1 modification by thiol-reactive, Nrf2-activating electrophiles (Table 4.4) (Dinkova-Kostova *et al.*, 2002; Eggler *et al.*, 2005; Hong *et al.*, 2005a; Hong *et al.*, 2005b; Luo *et al.*, 2007). Indeed, the only residues commonly modified by NAPQI, DNCB and 15d-PGJ_2 in this study, at relatively high molar ratios, were Cys-226, -368 and -613. Given that Cys-226 and -613 are flanked by at least one basic amino acid, which should lower their pKa values and increase their relative reactivities towards electrophiles (Snyder *et al.*, 1981), it is perhaps not surprising that these residues are targeted by all three molecules. Although there are no reports at present whereby mutagenesis of these residues alone has been used to assess their relative importance for Keap1 function, Cys-226 has recently been shown to be preferentially modified *in vitro* by the Nrf2-activating molecules sulforaphane (Hong *et al.*, 2005a) and isoliquiritigenin (Luo *et al.*, 2007), but not by dex

		Mouse Keap1				Human Keap1					
Domain	**Cys #**	**Dex-mes**	**NAPQI**	**DNCB**	**15d-PGJ$_2$**	**BIA[a]**	**BIA[b]**	**SUL**	**XAN**	**ISO**	**SHO**
NT	13	*np*	*np*	*np*	*np*						
NT	14	*np*	*np*	*np*	*np*						
NT	23										
NT	38										
BTB	77										
BTB	151						*nd*				
BTB	171										
IVR	196										
IVR	226										
IVR	241										
IVR	249										
IVR	257										
IVR	273										
IVR	288										
IVR	297										
IVR	319										
DGR	368										
DGR	395						*nd*				
DGR	406						*nd*				
DGR	434										
DGR	489										
DGR	513										
DGR	518										
DGR	583	*nd*									
CT	613										
CT	622		*nd*	*nd*	*nd*						
CT	624		*nd*	*nd*	*nd*						

Table 4.4. Summary of Keap1 cysteine residues modified *in vitro* by Nrf2-activating molecules, as determined in chapter 4 of this thesis and by independent research groups. Shaded cells represent cysteine residues modified at lowest molar ratio of electrophile:Keap1 at which there was reliable evidence for modification. Dex-mes, dexamethasone 21-mesylate (Dinkova-Kostova *et al.*, 2002); NAPQI, DNCB, 15d-PGJ$_2$ (chapter 4 of this thesis); BIA, biotinylated iodoacetamide [a](Eggler *et al.*, 2005) [b](Hong *et al.*, 2005b); SUL, sulforaphane (Hong *et al.*, 2005a); XAN, xanthohumol (Luo *et al.*, 2007); ISO, isoliquiritigenin (Luo *et al.*, 2007); SHO, 10-shogaol (Luo *et al.*, 2007). *np*, residues are not cysteines in the mouse protein. *nd*, peptide not detected during analysis. NT, N-terminal; CT, C-terminal.

-mes (Dinkova-Kostova *et al.*, 2002), xanthohumol and 10-shogaol (Luo *et al.*, 2007). Also, there are conflicting reports regarding the modification of Cys-226 by BIA (Eggler *et al.*, 2005; Hong *et al.*, 2005b). The CT domain, containing Cys-613, is apparently essential for Keap1-mediated repression of Nrf2 activity (Kang *et al.*, 2004), and Cys-613 has been shown to be particularly reactive towards dex-mes (Dinkova-Kostova *et al.*, 2002) and xanthohumol (Luo *et al.*, 2007), but not towards IAB (Eggler *et al.*, 2005; Hong *et al.*, 2005b), sulforaphane (Hong *et al.*, 2005a), 10-shogaol and isoliquiritigenin (Luo *et al.*, 2007). Notably, there are no basic residues flanking Cys-368 in the mouse Keap1 protein. Hence, it is less likely that Cys-368 is stabilised in the thiolate form ($-S^-$) (Snyder *et al.*, 1981), and this residue should not be highly reactive towards electrophiles. It is therefore surprising that Cys-368 is modified by NAPQI, DNCB and 15d-PGJ_2. Cys-368 has also been shown to be a preferential target of sulforaphane (Hong *et al.*, 2005a) and 10-shogaol (Luo *et al.*, 2007), but not of dex-mes (Dinkova-Kostova *et al.*, 2002), IAB (Eggler *et al.*, 2005; Hong *et al.*, 2005b), xanthohumol and isoliquiritigenin (Luo *et al.*, 2007). Therefore, the potential roles of Keap1 Cys-226, -368 and -613 in the regulation of Nrf2 function merit further investigation, but, at least *in vitro*, these residues are not selective targets of all Nrf2-activating molecules.

It was noted that, of the three Nrf2-activating molecules tested in this study, only NAPQI modified the apparently critical subset of Cys-151, -273 and -288. This suggests that, at least within the test system employed, these residues do not react preferentially with all Nrf2-activating molecules. In keeping with this, Cys-151 has been shown to be preferentially modified *in vitro* by xanthohumol, isoliquiritigenin and 10-shogaol (Luo *et al.*, 2007), but not by dex-mes (Dinkova-Kostova *et al.*, 2002) and sulforaphane (Hong *et al.*, 2005a). There is also controversy regarding the preferential reactivity of Cys-151 towards BIA (Eggler *et al.*, 2005; Hong *et al.*, 2005b), although this has recently been attributed to the different procedures used by the two groups for purifying recombinant Keap1 (Eggler *et al.*, 2007). Cys-273 of Keap1 is preferentially adducted *in vitro* by dex-mes (Dinkova-Kostova *et al.*, 2002), but not by sulforaphane (Hong *et al.*, 2005a), BIA (Eggler *et al.*, 2005; Hong *et al.*, 2005b), xanthohumol, isoliquiritigenin and 10-shogaol (Luo *et al.*, 2007). This is somewhat surprising, given that Cys-273 is flanked on either

side by basic amino acids, and thus has a low predicted pKa value, and high relative reactivity towards electrophiles (Snyder *et al.*, 1981). Cys-288 has recently been shown to be selectively targeted *in vitro* by dex-mes (Dinkova-Kostova *et al.*, 2002) and BIA (Eggler *et al.*, 2005; Hong *et al.*, 2005b), but not by sulforaphane (Hong *et al.*, 2005a), xanthohumol, isoliquiritigenin and 10-shogaol (Luo *et al.*, 2007). Therefore, at least in terms of primary structure, the apparently critical subset of Cys-151, -273 and -288 of Keap1 are capable of reacting preferentially with some, but not all, Nrf2-activating molecules (Table 4.4). Further investigations are required to elucidate the importance of direct modification of these residues in the activation of Nrf2.

From the recent mass spectrometry-based investigations of Keap1 modification by Nrf2-activating electrophiles, is it evident that no single cysteine appears to react preferentially with all of the molecules tested, at least *in vitro* (Table 4.4) (Dinkova-Kostova *et al.*, 2002; Eggler *et al.*, 2005; Hong *et al.*, 2005a; Hong *et al.*, 2005b; Luo *et al.*, 2007). The different adduct patterns observed between molecules in these studies may be a function of the inherent reactivity of a given electrophile toward a specific cysteine residue, or may simply reflect slight differences in experimental approaches, or both. Of course, it is plausible that modification of any single residue may in itself be sufficient to trigger the activation of Nrf2. Indeed, such a non-specific triggering mechanism may underlie the chemical versatility of the Nrf2-ARE pathway, in terms of its capacity to 'sense' and respond to a variety of structurally-distinct molecules. More specifically, it is possible that the modification of a single cysteine residue/group of residues within a critical domain of Keap1 provides the molecular trigger for Nrf2 activation. Indeed, it is clear that each of the Nrf2-activating molecules tested to date preferentially modify one or more cysteine residues within the IVR domain of Keap1 *in vitro* (Table 4.4). In keeping with this, it is notable that 1-biotinamido-4-(4'-[maleimidoethyl-cyclohexane]carboxamido)-butane, which does not activate the Nrf2-ARE pathway, modifies human Keap1 *in vitro*, but at cysteine residues outside of the IVR domain (Hong *et al.*, 2005b). Taken together, these findings imply that a number of alternative target sets are present amongst the reactive cysteines of Keap1, but particularly within the IVR domain of the protein (Table 4.4). Further investigations,

particularly within a cellular context, are therefore required to elucidate the importance of modification within the IVR domain in the activation of Nrf2.

CHAPTER 5

Development of a cell-based method for investigating the chemical modification of Keap1 and concomitant activation of Nrf2 by electrophiles

CONTENTS

5.1 INTRODUCTION

It has been postulated that the modification of one or more cysteine residues within Keap1, the major regulator of Nrf2 activity (Itoh *et al.*, 1999), may provide a biochemical trigger for activation of the transcription factor (Dinkova-Kostova *et al.*, 2002). Through the use of a cell-free *in vitro* system, the data presented in chapter 4 demonstrate residue-selective modification of Keap1 by structurally distinct Nrf2-activating electrophiles. However, these results, and the work of others (Dinkova-Kostova *et al.*, 2002; Eggler *et al.*, 2005; Hong *et al.*, 2005a; Hong *et al.*, 2005b; Luo *et al.*, 2007), indicate that no single cysteine appears to react preferentially with all of the molecules tested, at least *in vitro*, perhaps implying that a single common target residue does not exist for all Nrf2-activating molecules. The different Keap1 adduct patterns observed between molecules in the highlighted studies may represent the biochemical versatility of the Nrf2-ARE pathway, in terms of its ability to 'sense' and respond to a variety of structurally distinct molecules. However, these differences may also be the result of the *in vitro* methodologies employed.

It is important to consider that, although bacterially-expressed recombinant proteins are useful tools for assessing the relative reactivities of cysteine residues towards a given molecule *in vitro*, there are inherent limitations in the capacity of these systems to identify the likely targets of a molecule within cells. For instance, such systems may not fully represent the accessibility of specific cysteines for modification in cells, where protein folding, post-translational modification(s) and the interaction with Nrf2, CUL3 and/or other partners may mask certain residues in Keap1. Furthermore, in determining the relative reactivities of Keap1 cysteines towards Nrf2-activating molecules, the work reported in chapter 4 and in other recent mass spectrometry-based investigations (Dinkova-Kostova *et al.*, 2002; Eggler *et al.*, 2005; Hong *et al.*, 2005a; Hong *et al.*, 2005b; Luo *et al.*, 2007) have employed bacterially-expressed, purified Keap1 proteins in which all cysteines are free for adduction, due to prior incubation with reducing agents such as DTT or tris(carboxyethyl)phosphine. However, the physiological relevance of such a method cannot be determined, at least at present, as the native redox

states of the numerous cysteines in Keap1 have yet to be determined, with the exception of the eight residues located within the DGR domain of the human protein (Li *et al.*, 2004). In light of this gap in our current knowledge, and in addition to the limitations of *in vitro* systems, it is particularly difficult to infer that selective modifications of Keap1 observed *in vitro* also occur *in vivo*. Hence, there are several key milestones that need to be achieved to facilitate a better understanding of the contribution of Keap1 modification to the activation of the Nrf2-ARE pathway; a) the determination of the redox states of all of the cysteine residues in the native Keap1 protein, b) the comprehensive analysis of residue-selective Keap1 modification by Nrf2-activating molecules within a cellular and, where bioanalytical techniques permit, *in vivo* context, and c) detailed examination of the effect of cysteine modification on the structure/folding of Keap1 and its interaction with Nrf2. Such studies should greatly enhance our appreciation of the molecular switch that triggers Nrf2-dependent cell defence in response to chemical/oxidative stress.

In considering the evidence for modification of Keap1 in cells, a review of the published literature to date reveals two major issues, a) only two (biotinylated) Nrf2-activating molecules have been shown to modify Keap1 within a cellular context (Hong *et al.*, 2005b; Hosoya *et al.*, 2005; Itoh *et al.*, 2004; Levonen *et al.*, 2004), and b) only one of these studies used mass spectrometry to unequivocally identify the target residues within Keap1 that were modified, in this case, by BIA (Hong *et al.*, 2005b). Therefore, there is a clear need to further determine the role that Keap1 modification plays in the activation of Nrf2 in cells, and to identify the target residues that are modified by Nrf2-activating molecules. In keeping with this, the initial aim of the work presented in this chapter was to develop a cell-based method to enable the characterisation, by MS/MS, of Keap1 modification within a more biologically-relevant cellular setting, in order to test the hypothesis that modification of Keap1 is associated with activation of Nrf2 in cells. Two approaches were taken; immunoprecipitation of endogenous Keap1, and ectopic expression of an epitope-tagged Keap1 protein followed by affinity purification. The latter model system was used to map the Keap1 adduct patterns associated with Nrf2-

activating molecules, in order to test the hypothesis that a common cysteine, or subset of cysteines, is modified by all such molecules within a cellular context.

5.2 METHODS

5.2.1 Materials and reagents

HotStarTaq DNA polymerase and the QIAfilter Plasmid Midi Kit were from Qiagen (Crawley, UK). *Eco47*III and *Taq* DNA polymerase were from Promega (Southampton, UK). *EcoR*I and *Ava*I were from Roche Diagnostics (Burgess Hill, UK). pcDNA3.1/V5-His-TOPO was from Invitrogen (Paisley, UK). *Pme*I was from New England Biolabs (Hitchin, UK). The sonicating water bath was from Decon (Hove, UK). The monoclonal mouse anti-Keap1 primary antibody was from R&D Systems (Abingdon, UK). The mouse monoclonal anti-human Nrf2 antibody was kindly donated by Dr. Paul Hayter (Pfizer Ltd, Sandwich, UK). The Concentrator 5301 was from Eppendorf (Cambridge, UK). RIPA buffer, NP-40, protein-G agarose beads, *BamH*I, *EcoR*V, *Sac*I, anti-V5 agarose beads, Brilliant Blue G colloidal concentrate, the rabbit anti-DNP primary antibody and the rabbit anti-mouse HRP-conjugated secondary antibody were from Sigma-Aldrich (Poole, UK). All other reagents were of analytical or molecular grade, and were from Sigma-Aldrich.

5.2.2 Immunoprecipitation of endogenous Keap1

Eight fully-confluent 75 cm^2 flasks of Hepa-1c1c7 cells were harvested by trypsinisation, as described in section 2.2.2. Following resuspension in growth media, cells were pelleted by centrifugation at 1000 g for 5 min, and the supernatant was discarded. The pellet was washed in 5 mL 1X PBS, divided into two equal aliquots, and centrifuged at 1000 g for 5 min. For denaturing immunoprecipitation, following the method of Tansey (2007a), one of the pellets was resuspended in 0.2 mL TSD buffer (50 mM Tris-Cl (Sigma-Aldrich), 1 % (v/v) SDS, 5 mM DTT, 0.2 % (v/v) protease inhibitor cocktail), heated at 80 °C for 10 min and clarified by centrifugation at 1000 g for 5 min. For non-denaturing immunoprecipitation, following the method of Tansey (2007b), the other pellet was resuspended in 0.2 mL radioimmunoprecipitation assay (RIPA) buffer

(0.15 M NaCl, 1 % (v/v) NP-40, 0.5 % (v/v) sodium deoxycholate, 0.1 % (v/v) SDS, 25 mM Tris-Cl, 0.2 % (v/v) protease inhibitor cocktail) and centrifuged at 1000g for 5 min. The protein content of clarified lysates was determined as described in section 2.2.5. The lysates were split into four aliquots of 1 mg total protein. Each aliquot was diluted to 0.5 mL with TNN buffer (50 mM Tris-Cl, 0.25 M NaCl, 5 mM EDTA, 0.5 % (v/v) NP-40, 0.2 % (v/v) protease inhibitor cocktail) for denaturing immunoprecipitation, or RIPA buffer for non-denaturing immunoprecipitation. Selected aliquots were supplemented with 0.4 mL 1X PBS or a crude lysate from Keap1-His -expressing BL21 (DE3) *E. coli*. The bacterial lysate was prepared by pelleting a 10 mL culture (induced with 1 mM IPTG for 4 h at 37 °C, 250 rpm) at 5000 g for 5 min. The pellet was washed in 10 mL 1X PBS and centrifuged at 5000 g for 5 min. The pellet was resuspended in 1 mL 1X PBS and disrupted by sonication (10 sec, followed by 10 sec recovery, x 4 repeats). Disrupted bacteria were centrifuged at 5000 g for 5 min, and the supernatant retained as a crude lysate. Aliquots were pre-cleared with 20 µL protein-G agarose beads via incubation on a mechanical roller at 4 °C for 1 h. The beads were pelleted by centrifugation at 5000 g for 1 min. The supernatants were transferred to a new tube and supplemented with 5 µg monoclonal mouse anti-Keap1 or polyclonal goat anti-Keap1 antisera. Immunoprecipitation was performed overnight at 4 °C, on a mechanical roller. Antibody conjugates were captured via the addition of 50 µL protein-G agarose beads, and incubation at 4 °C, on a mechanical roller, for 2 h. The beads were pelleted, by centrifugation at 5000 g for 1 min, and washed three times with 0.2 mL 1X PBS. In order to elute immunoprecipitated proteins, the beads were resuspended in an equal volume of NuPAGE loading buffer, heated at 80 °C for 5 min, and centrifuged at 5000 g for 5 min. The supernatants were loaded onto pre-cast 4-12 % NuPAGE Novex bis-tris polyacrylamide gels. Western blot analysis was performed essentially as described in section 2.2.6. For samples in which the monoclonal mouse anti-Keap1 antibody had been used for immunoprecipitation, membranes were probed with the goat anti-Keap1 primary and rabbit anti-goat HRP-conjugated IgG secondary antibodies. For samples in which the polyclonal goat anti-Keap1 antibody had been used for immunoprecipitation, membranes were probed with the monoclonal mouse anti-Keap1 primary (1:1000 in

TBS-Tween containing 2 % (w/v) BSA) and rabbit anti-mouse HRP-conjugated secondary (1:10,000 in TBS-Tween containing 2 % (w/v) BSA) antibodies.

5.2.3 Preparation of mouse *Keap1* coding sequence DNA template

The DNA template for mouse *Keap1* was prepared as described in section 3.2.2.

5.2.4 Polymerase chain reaction

The purified vector, containing the mouse *Keap1* cDNA clone, was used as a template for hot-start PCR amplification of the mouse *Keap1* coding sequence. A forward primer (5'-ATGCAGCCCGAACCCAAG-3') and two reverse primers ('STOP' 5'-TCAGCAG GTACAGTTTTG-3' and 'V5-HIS' 5'-GCAGGTACAGTTTTGTTGAT-3') were designed to enable the amplification of *Keap1* with ('STOP') or without ('V5-HIS') the stop codon (TGA). Hot-start PCR was performed as described in section 3.2.3. The PCR products were resolved by electrophoresis on a 1 % agarose gel, supplemented with 0.5 μg/mL ethidium bromide, and purified using a Perfectprep gel cleanup kit, in accordance with the manufacturer's instructions. The gel-purified PCR products were 3' A-tailed using *Taq* DNA polymerase. Reactions (10 μL) contained 8 μL gel-purified PCR product, 1X *Taq* DNA polymerase buffer containing 1.5 mM $MgCl_2$, 5 μM deoxyadenosine triphosphate (dATP) and 2.5 U *Taq* DNA polymerase. A-tailing was performed at 72 °C for 8 min.

5.2.5 Sub-cloning of *Keap1* into pcDNA3.1/V5-His-TOPO

The A-tailed Keap1 PCR products were ligated into the T-overhangs of the TOPO cloning site of pcDNA3.1/V5-His-TOPO, in accordance with the manufacturer's instructions. XL10-Gold ultracompetent *E. coli* were immediately transformed with the

ligated constructs (3 μL per 30 μL bacteria), via a 30 sec heat-shock at 42 °C, and incubated in 0.25 mL SOC media for 1 h, at 37 °C, 250 rpm. The bacteria were streaked onto a sterile LB-agar plate, containing 50 μg/mL ampicillin, and incubated at 37 °C overnight. Antibiotic-resistant colonies were picked from the plate and used to inoculate 2 mL LB broth containing 50 μg/mL ampicillin; these cultures were incubated for 24 h at 37 °C, 250 rpm. The constructs were purified by mini-prep. Diagnostic restriction digests were performed with *Bam*I/*Eco47*III (5 μL PCR product, 10 U *Bam*I, 10 U *Eco47*III, 1X buffer D, 37 °C, 1 h) and *EcoR*V/*Eco47*III (5 μL PCR product, 10 U *EcoR*V, 10 U *Eco47*III, 1X buffer SB, 37 °C, 1 h). Glycerol stocks of a pcDNA3.1/Keap1-transformed XL10 Gold colony were made by supplementing a mid-log phase culture with 15 % (v/v) glycerol; these stocks were stored at -80 °C until required. For transfections, pcDNA3.1/Keap1 was purified from a 0.6 L culture of XL10 Gold *E. coli*, in LB broth supplemented with 50 μg/mL ampicillin, using a QIAfilter Plasmid Midi Kit. pcDNA3.1/Keap1 was eluted into 1X TE buffer, and the DNA concentration and purity were assessed as described for RNA in section 2.2.13, with the following exception (given that an absorbance of 1 at 260 nm equates to 50 μg/mL DNA):

Absorbance at 260 nm x 100 (to correct for dilution) x 50 = DNA concentration (μg/mL)

5.2.6 DNA two-strand sequencing

XL10 Gold *E. coli* transformed with pcDNA3.1/Keap1, along with primers (3.2 μM), were sent to Geneservice for two-strand sequencing of pcDNA3.1/Keap1. The T7 forward (5'-TAATACGACTCACTATAGGG-3') and BGH reverse (5'-CCTCGACTG TGCCTTCTA-3') priming sites were designated as the external sequencing sites. The internal sequencing primers were custom-synthesised by Sigma-Genosys, in accordance with the requirements of Geneservice; internal forward 5'-CCACCCTAAGGTCATGG AAA-3', internal reverse 5'-GCTAGTTATTGCTCAG CGG-3'. Sequencing results were analysed using ChromasPro software; no mutations were identified.

5.2.7 Cell culture

Hepa-1c1c7 were maintained as described in section 2.2.2. The human embryonic kidney cell line, HEK293T, was maintained in 'growth media' (DMEM supplemented with 584 mg/L L-glutamine, 10 % FBS, 100 U/mL penicillin and 100 μg/mL streptomycin) and cultured as described for Hepa-1c1c7 in section 2.2.2. HEK293T are transformed with the large T antigen of Simian virus 40 (SV40), and this enables episomal replication of transfected vectors that contain the SV40 origin of replication, effectively amplifying the expression of the transfected gene product (DuBridge *et al.*, 1987).

5.2.8 Transfection of cells with Keap1-V5-His

Hepa-1c1c7 or HEK293T cells were seeded onto 56.7 cm^2 Nunclon Δ culture dishes, at 5 x 10^6 cells/dish, 24 h prior to transfection,. At around 80 % confluency, cells were transfected with pcDNA3.1/Keap1-V5-His using Lipofectamine 2000, with slight modifications to the manufacturer's instructions. For each dish of cells, 1 mL DMEM was combined with 16 μg pcDNA3.1/Keap1-V5-His in a sterile 25 mL tube. In a separate 25 mL tube, 1 mL DMEM was combined with 40 μL Lipofectamine 2000. The contents of each tube were combined, mixed gently, and incubated at room temperature for 20 min. The entire mixture was added, dropwise, to the dish of cells. Cells were returned to a humidified incubator, at 37 °C in a 5 % CO_2 atmosphere, for 24 h. The cells from three dishes were combined and lysed, by repeated vigorous pipetting, in 1 mL RIPA buffer. The lysate was clarified by centrifugation at 5000 g for 1 min.

5.2.9 Western blot analysis of whole cell lysates

Whole cell lysates (20 μg) were analysed by Western blot as described in section 2.2.6. Recombinant mouse Keap1-His was loaded as a standard to confirm antibody specificity.

5.2.10 Purification of Keap1-V5-His from cell lysates

The whole cell lysate (1 mL) prepared in section 5.2.8 was aliquoted into two 1.5 mL microcentrifuge tubes (0.5 mL each). The lysates were incubated with 60 μL HIS-Select or anti-V5 agarose beads, on a mechanical roller, for 2 h at 4 °C. The beads were collected by centrifugation at 5000 g for 1 min, and washed three times with 0.5 mL 1X PBS.

5.2.11 Western blot analysis of purified Keap1-V5-His

Keap1-V5-His purification was confirmed by Western blot analysis, essentially as described in section 2.2.6. Proteins were eluted from HIS-Select or anti-V5 agarose beads by resuspending in an equal volume of NuPAGE loading buffer. The slurry was heated at 80 °C for 5 min, the beads were pelleted by centrifugation at 5000 g for 5 min, and the supernatant loaded onto a pre-cast 4-12 % NuPAGE Novex bis-tris polyacrylamide gel.

5.2.12 Coomassie Brilliant Blue staining and in-gel tryptic digestion

Following electrophoresis, as described in section 2.2.6, the gel was fixed for 1 h in 40 % (v/v) methanol containing 7 % (v/v) glacial acetic acid. Coomassie staining solution was prepared by mixing 4 part Coomassie stain (0.1 % (w/v) Coomassie Brilliant Blue

G-250 in 2 % (w/v) phosphoric acid, 16 % (w/v) ammonium sulphate) with 1 part methanol. The gel was stained with Coomassie solution for 1 h, with gentle agitation. The gel was destained, with 25 % (v/v) methanol containing 10 % (v/v) glacial acetic acid, for 1 min. The gel was rinsed with, and then stored at 4 °C in, 25 % (v/v) methanol. The stained gel was placed on top of a light box and bands of interest were carefully excised using a scalpel. The gel pieces were individually destained, in 0.1 mL of 50 mM ammonium bicarbonate in 50 % (v/v) ACN, for 15 min at room temperature, with occasional agitation. The destaining solution was removed and the gel pieces were dried in a Concentrator 5301 over 15 min. The gel pieces were rehydrated in 10 μL of 50 mM ammonium bicarbonate containing 5 ng/μL sequencing-grade modified trypsin, and incubated at 37 °C overnight. Following the addition of 30 μL of 60 % (v/v) ACN, 1 % (v/v) TFA, the samples were placed in a sonicating water bath for 5 min, at room temperature. The gel pieces were pelleted by centrifugation, at 1000 g for 30 sec, and the supernatant transferred to a new tube. A further 30 μL of 60 % (v/v) ACN, 1 % (v/v) TFA was added to the gel pieces, and the samples were placed in a sonicating water bath for 5 min, at room temperature. The gel pieces were pelleted by centrifugation, at 1000 g for 30 sec, and the supernatant combined with that from the previous centrifugation step. The sample was dried in a Concentrator 5301 over 1h, and the solute reconstituted in 10 μL of 5 % (v/v) ACN, 0.05 % (v/v) TFA.

5.2.13 Preparation of Keap1-V5-His for mass spectrometry

Keap1-V5-His, bound to anti-V5 agarose beads, was reduced by resuspending the beads (50 μL dry volume) in 0.148 mL phosphate buffer and 2 μL of 0.1 M DTT. The slurry was incubated on a mechanical roller at 4 °C for 15 min. The beads were washed three times in 0.5 mL phosphate buffer to remove residual DTT. To cap unmodified cysteines, the beads were resuspended in 0.13 mL phosphate buffer and 20 μL of 0.55 M iodoacetamide, and incubated on a mechanical roller at 4 °C for 15 min. The beads were washed three times in 0.5 mL phosphate buffer to remove residual iodoacetamide. Tryptic digestion was performed as described in section 3.2.10. For LC-ESI-MS/MS

analysis, the beads were pelleted by centrifugation at 5000 g for 30 sec. The supernatant, containing tryptic peptides, was transferred to a new tube and dried in a Concentrator 5301 over 45 min. The solute was reconstituted in 65 μL of 5 % (v/v) ACN, 0.05 % (v/v) TFA.

5.2.14 MALDI-TOF mass spectrometry

Samples were analysed as described in section 3.2.11.

5.2.15 LC-ESI-MS/MS mass spectrometry

The reconstituted solute (60 μL) from section 5.2.13 was loaded using a 0.1 mL loop. Samples were analysed essentially as described in section 3.2.12. LC conditions were as follows: 15 min at 5 % (v/v) ACN, 0.05 % (v/v) TFA, a gradient of 5-48 % (v/v) ACN, 0.05 % (v/v) TFA over 60 min, 10 min at 99 % (v/v) ACN, 0.05 % (v/v) TFA and 10 min at 5 % (v/v) ACN, 0.05 % (v/v) TFA, with a flow rate of 0.35 μL/min throughout.

5.2.16 Treatment of Keap1-V5 -expressing cells with electrophiles

Keap1-V5 -expressing HEK293T cells were treated essentially as described for Hepa-1c1c7 cells in section 2.2.3. Three dishes of cells were simultaneously exposed to each electrophile. The cells from these three dishes were combined and lysed, by repeated vigorous pipetting, in 1 mL RIPA buffer. The lysate was clarified by centrifugation at 5000 g for 1 min.

5.2.17 Preparation of nuclear fractions

Nuclear fractions were prepared from HEK293T cells as described for Hepa-1c1c7 cells in section 2.2.4.

5.2.18 Determination of protein content

The total protein content of subcellular fractions was determined as described in section 2.2.5.

5.2.19 Western blot analysis of nuclear fractions

Nuclear fractions (20 μg) were resolved by denaturing electrophoresis and transferred to nitrocellulose membranes, which were then blocked, as described in section 2.2.6. Blocked membranes were probed for 1 h with a monoclonal mouse anti-human Nrf2 antiserum (1:1000 in TBS-Tween containing 2 % (w/v) BSA). Following several washes in TBS-Tween, membranes were probed for 1 h with rabbit anti-mouse HRP-conjugated anti-IgG (1:10,000 in TBS-Tween containing 2 % (w/v) BSA). Recombinant human Nrf2-His was loaded as a standard to confirm antibody specificity.

5.2.20 Immunopurification of Keap1-V5-His

Keap1-V5-His was immunopurified from the whole cell lysate prepared in section 5.2.4. 1 mL lysate was incubated with 80 μL anti-V5 agarose beads, on a mechanical roller, for 2 h at 4 °C. The beads were collected by centrifugation at 5000 g for 1 min, and washed three times with 0.5 mL 1X PBS.

5.2.21 Western blot analysis of immunopurified Keap1-V5-His

Keap1-V5-His immunopurification was confirmed by Western blot analysis, as described in section 5.2.11. To probe for DNCB adducts, a rabbit anti-DNP primary antibody was used (1:20,000 in TBS-Tween containing 2 % (w/v) BSA). To enable additional probing, membranes were stripped by shaking in 0.1 M glycine (pH 3.0), for 2 h, at room temperature.

5.3 RESULTS

5.3.1 Immunoprecipitation of endogenous Keap1

In an effort to examine the modification of Keap1 by Nrf2-activating electrophiles under physiologically relevant cellular conditions, attempts were made to immunoprecipitate endogenous Keap1 from Hepa-1c1c7 cells and analyse the protein by mass spectrometry. At the time at which these investigations were carried out, two commercial anti-Keap1 primary antibodies were available. The first was a monoclonal antibody, produced from a hybridoma resulting from the fusion of a mouse myeloma with B cells obtained from a mouse immunised with a purified recombinant fragment (amino acids 90-250) of human Keap1 (R&D Systems). The fragment of human Keap1 used as the immunogen shares 98 % sequence homology with the equivalent fragment of mouse Keap1. Furthermore, this antibody can detect the mouse protein by Western blot (Fig. 5.1a). The second anti-Keap1 antibody was a polyclonal antibody, raised in goat against a purified recombinant fragment (amino acids 10-60) of human Keap1 (Santa Cruz Biotechnology). The fragment of human Keap1 used as the immunogen for this antibody shares 84 % sequence homology with the equivalent fragment of mouse Keap1. This antibody can also detect the mouse protein by Western blot (Fig. 5.1b).

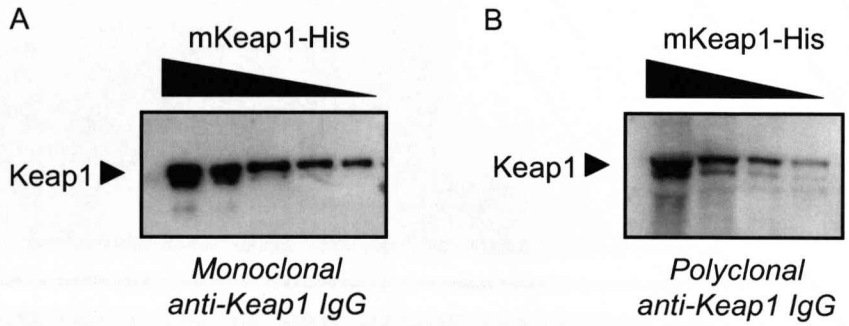

Fig. 5.1 - Detection of mouse Keap1 by monoclonal and polyclonal anti-Keap1 antibodies. Recombinant mouse Keap1-His was purified using Ni^{2+} -charged agarose beads and various amounts were resolved by denaturing electrophoresis. Keap1 was detected by Western blot, using a monoclonal (A) or polyclonal (B) anti-Keap1 antibody. This result demonstrates that each antibody can detect mouse Keap1 by Western blot. Note, the amounts of protein loaded onto each gel are not identical, thus it is not possible to differentiate between the sensitivities of the antibodies from these gels.

Ideally, it would be possible to immunoprecipitate endogenous Keap1 under non-denaturing conditions, so as not to disrupt the structural integrity of the protein and affect the putative modification of Keap1 by Nrf2-activating electrophiles. However, the ability of both anti-Keap1 antibodies to detect mouse Keap1 by Western blot had only been confirmed under denaturing conditions, and hence immunoprecipitations were attempted separately under non-denaturing and denaturing conditions. Protein G sepharose was used to immunopurify antibody conjugates, as both Keap1 antibodies were of the IgG class, which shows high affinity for streptococcal Protein G (Bjorck *et al.*, 1984).

A series of controls demonstrated that the polyclonal anti-Keap1 antibody reacted strongly with Protein G, and non-specifically with some cellular proteins in both non-denatured and denatured lysates (Fig. 5.2). Although endogenous Keap1 was detected in the input and flow-through fractions of the cell lysates, particularly in the non-denatured lysate, immunoprecipitation with the monoclonal anti-Keap1 antibody only resulted in a noticeable recovery of Keap1 when the cell lysates were supplemented with recombinant mouse Keap1-His protein (Fig. 5.3). Even less endogenous Keap1 protein was recovered following immunoprecipitation with the polyclonal anti-Keap1 antibody (Fig. 5.4). Therefore, under the experimental conditions employed, the two available commercial anti-Keap1 antibodies are not suitable for the immunoprecipitation of endogenous Keap1 from Hepa-1c1c7 cells. Although extensive optimisation may enhance the recovery of Keap1 from cells, it is anticipated that the material yielded may still not be sufficient for effective analysis by mass spectrometry.

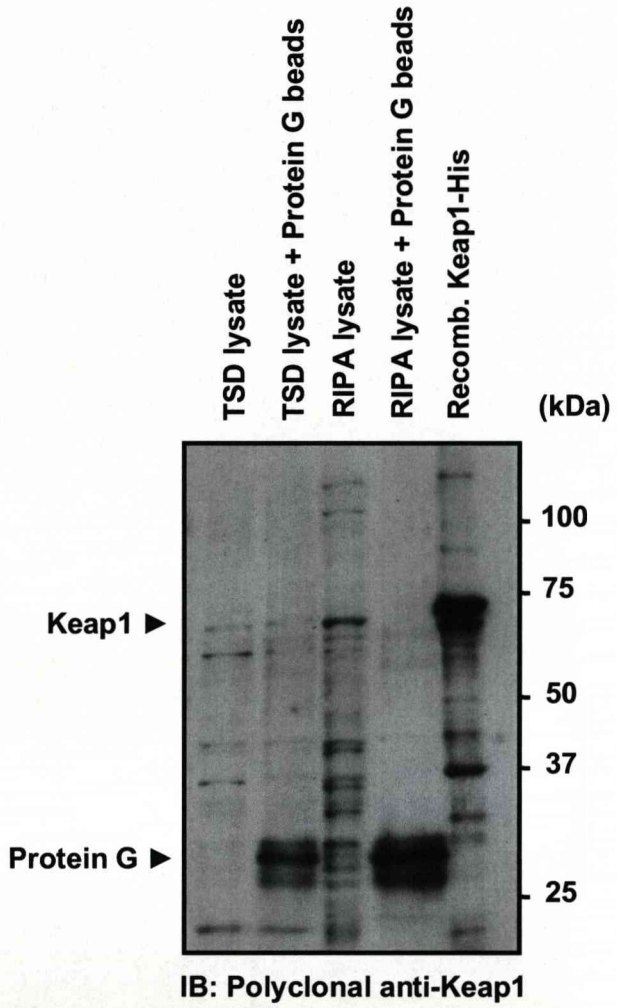

Fig. 5.2 - Non-specific reactivity of polyclonal anti-Keap1 antibody with cellular proteins and Protein G. Hepa-1c1c7 cells were lysed under denaturing (TSD) or non-denaturing (RIPA) conditions. Each lysate (0.2 mg protein) was incubated with Protein G sepharose beads for 1 h at 4 °C. Lysates (20 μg) were resolved, by denaturing electrophoresis, alongside the proteins eluted from the respective Protein G sepharose beads and a crude lysate from Keap1-His -expressing BL21 (DE3) *E. coli*. Proteins reacting with the polyclonal anti-Keap1 antibody were detected by Western blot. IB; immunoblot.

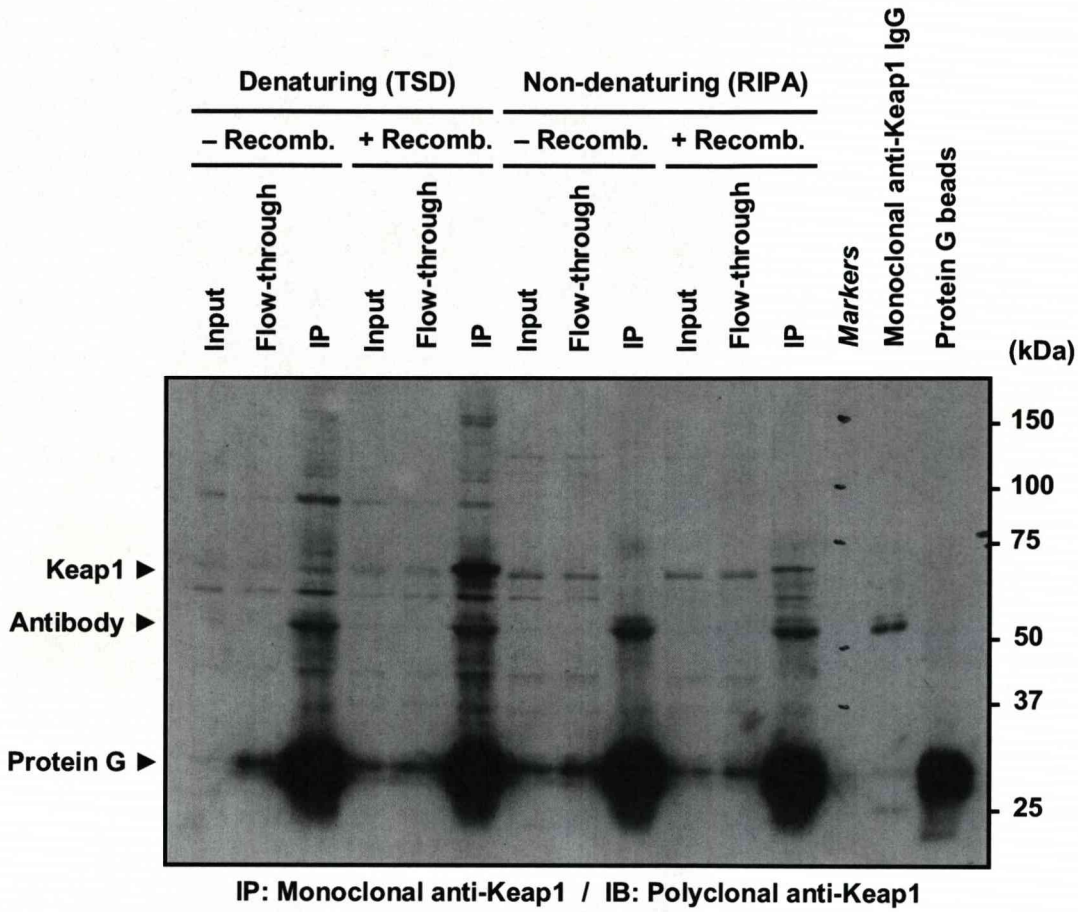

Fig. 5.3 - Attempted immunoprecipitation of Keap1 from Hepa-1c1c7 cells using a monoclonal anti-Keap1 antibody. Hepa-1c1c7 cells were lysed under denaturing (TSD) or non-denaturing (RIPA) conditions. Lysates (1 mg protein) were not supplemented (- recomb.), or supplemented (+ recomb.) with a crude lysate from Keap1-His -expressing BL21 (DE3) *E. coli*, and pre-cleared with Protein G sepharose beads for 1 h at 4 °C. Cleared lysates were incubated at 4 °C, overnight, with 5 μg monoclonal anti-Keap1 antibody, and antibody conjugates were captured via incubation with Protein G sepharose beads for 2 h at 4 °C. Fractions of the lysates pre- (input) and post- (flow-through) immunoprecipitation were resolved by denaturing electrophoresis, alongside the proteins eluted from the respective Protein G sepharose beads and appropriate controls. Keap1 was detected by Western blot, with a polyclonal anti-Keap1 antibody. IP; immunoprecipitation. IB; immunoblot.

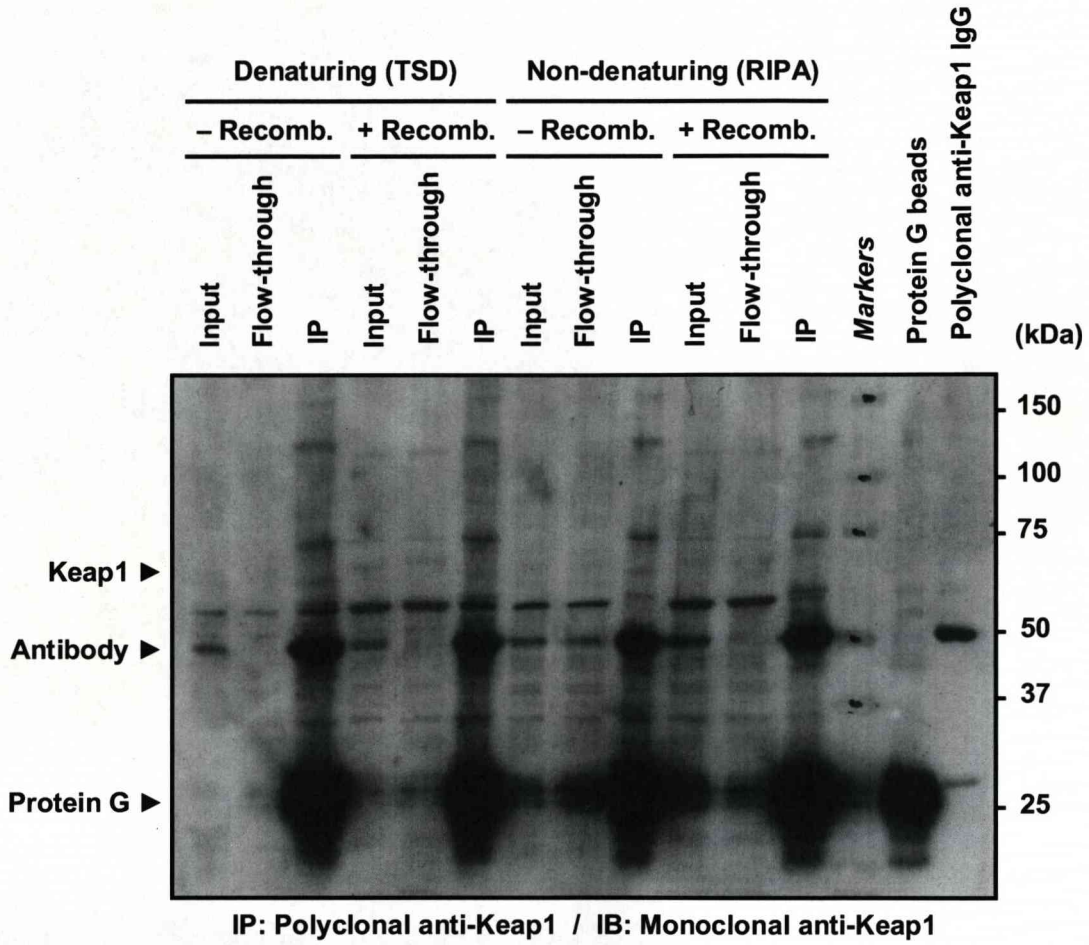

Fig. 5.4 - Attempted immunoprecipitation of Keap1 from Hepa-1c1c7 cells using a polyclonal anti-Keap1 antibody. Hepa-1c1c7 cells were lysed under denaturing (TSD) or non-denaturing (RIPA) conditions. Lysates (1 mg protein) were not supplemented (-recomb.), or supplemented (+ recomb.) with a crude lysate from Keap1-His -expressing BL21 (DE3) *E. coli*, and pre-cleared with Protein G sepharose beads for 1 h at 4 °C. Cleared lysates were incubated at 4 °C, overnight, with 5 μg polyclonal anti-Keap1 antibody, and antibody conjugates were captured via incubation with Protein G sepharose beads for 2 h at 4 °C. Fractions of the lysates pre- (input) and post- (flow-through) immunoprecipitation were resolved by denaturing electrophoresis, alongside the proteins eluted from the respective Protein G sepharose beads and appropriate controls. Keap1 was detected by Western blot, with a monoclonal anti-Keap1 antibody. IP; immunoprecipitation. IB; immunoblot.

5.3.2 PCR amplification of mouse *Keap1* coding sequence

In light of the unsuccessful attempts to immunoprecipitate endogenous Keap1 from Hepa-1c1c7 cells, the ectopic expression of epitope-tagged Keap1 was pursued as an alternative method of detecting in-cell modification of Keap1 by mass spectrometry. The mouse *Keap1* coding sequence (1875 bp) was amplified by PCR. Primers were designed to enable to amplification of the coding sequence with or without the TGA stop codon, to facilitate the eventual translation of a wild-type ('STOP') or V5-His -tagged Keap1 protein, respectively. Both PCR products were 3' A-tailed (Fig. 5.5) in order to enable ligation into the TOPO cloning site of pcDNA3.1/V5-His-TOPO (Fig. 5.6).

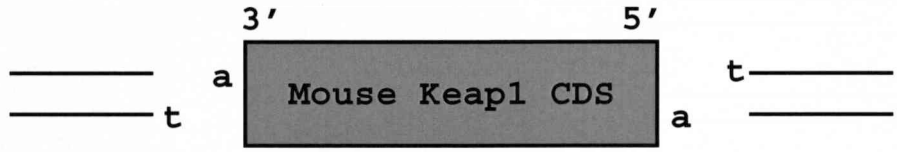

Fig. 5.5 - Schematic diagram showing 3' A-tailing of the mouse *Keap1* coding sequence (CDS) and its ligation into pcDNA3.1/V5-His-TOPO, via the T-overhangs of the TOPO cloning site. The nucleotides immediately flanking the TOPO cloning site of pcDNA3.1/V5-His-TOPO are represented as solid lines.

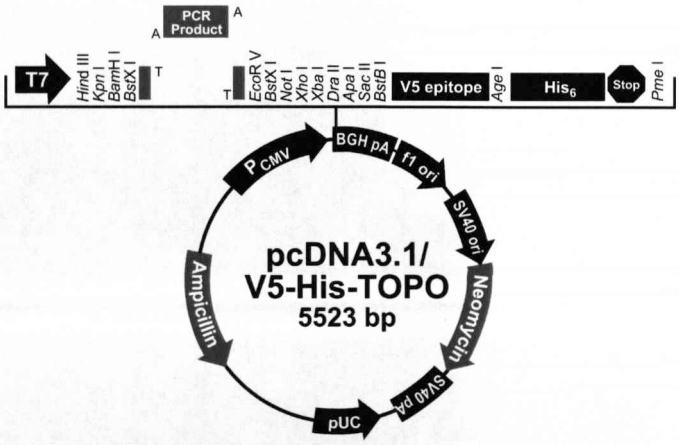

Fig. 5.6 - pcDNA3.1/V5-His-TOPO vector map. The A-tailed *Keap1* coding sequence was ligated into the T-overhangs of pcDNA3.1/V5-His-TOPO. Image taken from the Invitrogen on-line catalogue (http://www.invitrogen.com/content/sfs/vectors/pcdna3.1 v5histopo_map .pdf).

5.3.3 Ligation of mouse *Keap1* coding sequence into pcDNA3.1/V5-His-TOPO

The A-tailed *Keap1* PCR products were ligated into pcDNA3.1/V5-His-TOPO, and XL10-Gold ultracompetent *E. coli* were transformed with one of the two ligated constructs. Successful transformation was confirmed by diagnostic restriction digests of construct DNA purified from selected bacterial colonies (Fig. 5.7). Specifically, fragments of the expected size(s) were visualised following digestion with *BamH*I and *Eco47*III (*BamH*I cuts at -34 of *Keap1*, *Eco47*III cuts at 1606 of *Keap1*; 1640 bp fragment) and *Eco47*III and *EcoR*V (*Eco47*III cuts at 1606 of *Keap1*, *EcoR*V cuts at 1891 of *Keap1*; 285 bp fragment).

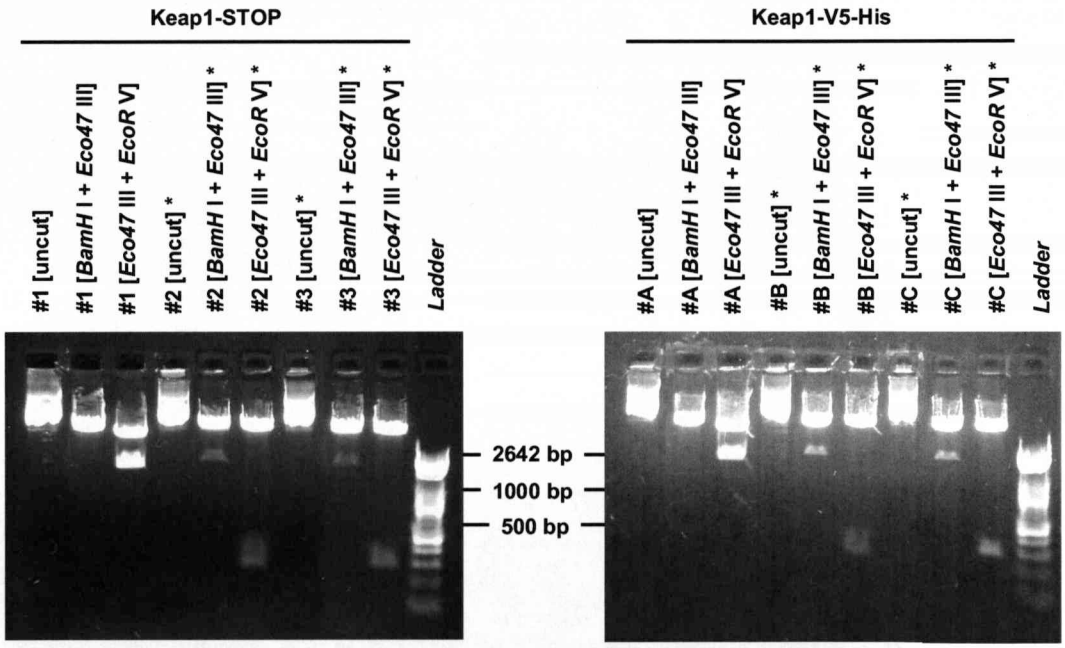

Fig. 5.7 - Diagnostic restriction digests of pcDNA3.1/Keap1 'STOP' and 'V5-His' variants from putative transformed XL10-Gold *E. coli*. Each pcDNA3.1/Keap1 construct was purified from three selected bacterial colonies (#1-3 and #A-C) by mini-prep. The constructs were digested with *BamH*I and *Eco47*III (*BamH*I cuts at -34, *Eco47*III cuts at 1606; 1640 bp fragment) and *Eco47*III and *EcoR*V (*Eco47*III cuts at 1606, *EcoR*V cuts at 1891; 285 bp fragment). The restriction fragments, the undigested constructs, and a 100 bp DNA ladder were resolved by electrophoresis on a 1 % (w/v) agarose gel, containing 0.5 µg/mL ethidium bromide. DNA fragments were visualised under UV illumination. Constructs yielding restriction fragments of expected size, i.e. those from colonies #2, #3, #B and #C, are labeled *.

These diagnostic restriction digests demonstrate that the *Keap1* coding sequences ligated into pcDNA3.1/V5-His-TOPO successfully, and in the correct orientation. In order to confirm that the PCR amplification process had not introduced mutations into the *Keap1* coding sequence, the pcDNA3.1/Keap1 constructs were verified by two-strand sequencing. This process confirmed that no non-synonymous mutations, i.e. those that result in the translation of a different amino acid, were present in either pcDNA3.1/Keap1 construct.

5.3.4 Expression and purification of pcDNA3.1/Keap1

HEK293T, a human embryonic kidney cell line that is widely used as a model for the ectopic expression of proteins, and Hepa-1c1c7, the mouse hepatoma cell line used for investigations into the molecular regulation of the Nrf2-ARE pathway in chapter 2, were transiently transfected with Keap1 -STOP (i.e. wild-type protein) or -V5-His (Keap1 protein proceeded by a 45 amino acid sequence, which contains the V5 epitope and polyhistidine region, but does not contain any cysteines). Both Keap1 variants were expressed in both cell lines, however the level of expression was markedly higher in HEK293T cells (Fig. 5.8). In light of the relatively weak expression of Keap1 -STOP and -V5-His in Hepa-1c1c7 cells, and given that only Keap1-V5-His could be affinity- or immuno-purified from cell lysates, all subsequent experiments were undertaken using HEK293T cells transiently expressing Keap1-V5-His only.

Theoretically, it should be possible to purify Keap1-V5-His by both Ni^{2+} affinity and anti-V5 immunoaffinity, as the protein bears both a V5 epitope and a polyhistidine tag. In order to compare the recovery of Keap1-V5-His achieved with each purification method, cell lysates prepared from Keap1-V5-His -expressing HEK293T cells were incubated with Ni^{2+}-charged agarose beads or anti-V5 agarose beads.

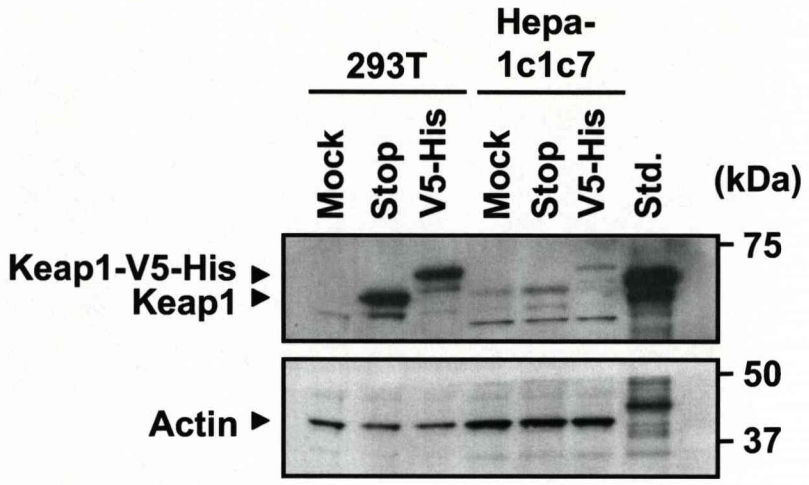

Fig. 5.8 - Transient expression of Keap1-STOP and Keap1-V5-His in HEK293T and Hepa-1c1c7 cells. HEK293T or Hepa-1c1c7 cells were mock transfected or transfected for 24 h with pcDNA3.1/Keap1 -STOP or -V5-His. Whole cell lysates were prepared and resolved by denaturing electrophoresis. Keap1 and β-actin were detected by Western blot. Recombinant mouse Keap1-His was loaded onto the gel as a standard (Std).

Although Ni^{2+} affinity purification did yield a large amount of Keap1, as assessed by Western blot, a substantial number of other proteins were co-purified, as demonstrated by Ponceau Red stain of the pull-down fraction (Fig. 5.9). Such was the abundance of contaminating proteins within the sample, it was not possible to identify Keap1-V5-His by MALDI-TOF MS analysis. Anti-V5 immunopurification yielded a greater amount of Keap1, in a much purer form, than Ni^{2+} affinity purification (Fig. 5.9). In fact, only three prominent protein bands were visible on the Ponceau Red stain of the pull-down fraction (Fig. 5.9). The major constituents of these bands were identified, by LC-ESI-MS/MS analysis of Coomassie Brilliant Blue G-250 -stained, trypsin-digested polyacrylamide gel sections, to be mouse Keap1 and the heavy (gamma) and light (kappa) chains of mouse IgG (Fig. 5.10); the latter were the fragments of anti-V5 IgG released from the anti-V5 agarose beads, along with Keap1-V5-His, during the elution process. MALDI-TOF MS analysis of the total protein fraction bound to the anti-V5 agarose beads, following incubation with Keap1-V5-His -expressing HEK293T cell lysate, identified mouse Keap1 as the major constituent protein (Fig. 5.11 and Fig. 5.12).

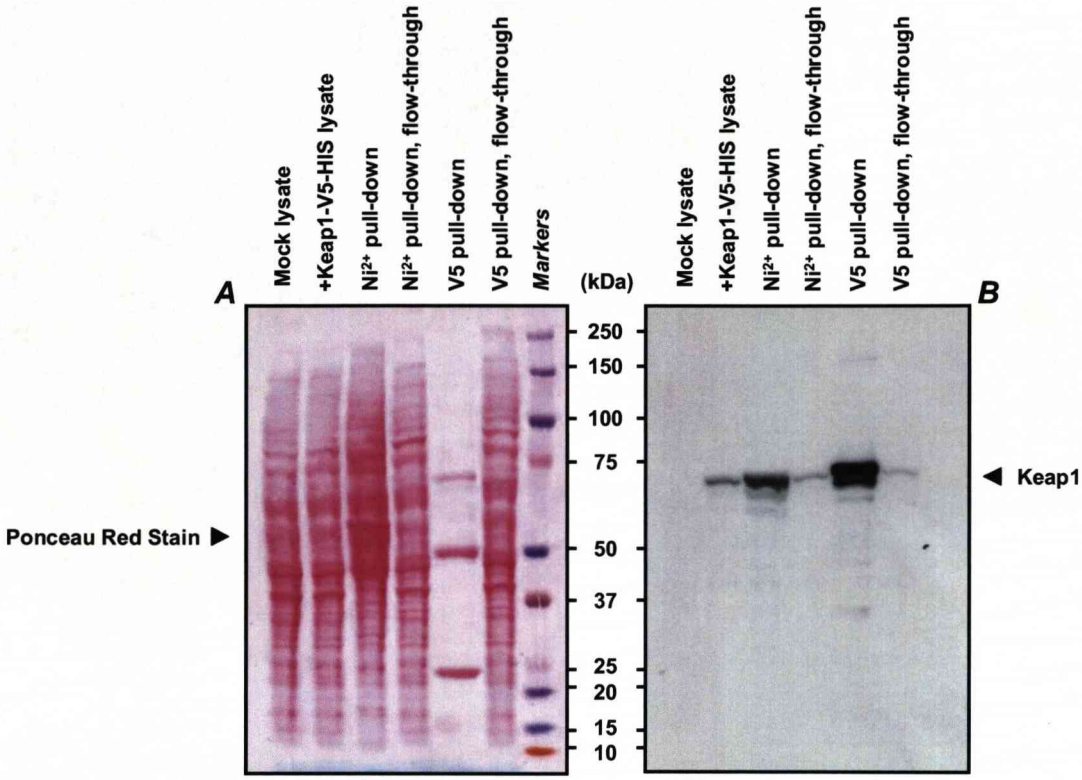

Fig. 5.9 - Purification of Keap1-V5-His from HEK293T cells. HEK293T cells were mock transfected or transfected for 24 h with pcDNA3.1/Keap1-V5-His. Whole cell lysates were prepared and incubated with Ni^{2+}-charged agarose beads or anti-V5 agarose beads for 2 h at 4 °C. The crude lysates, the proteins that eluted from the respective agarose beads (pull-down) and the lysates that remained following the pull-downs (flow-through) were resolved by denaturing electrophoresis, alongside protein molecular weight markers. Resolved proteins were transferred to nitrocellulose and total protein was visualised by Ponceau Red stain (A). Keap1 was detected on the same membrane by Western blot (B).

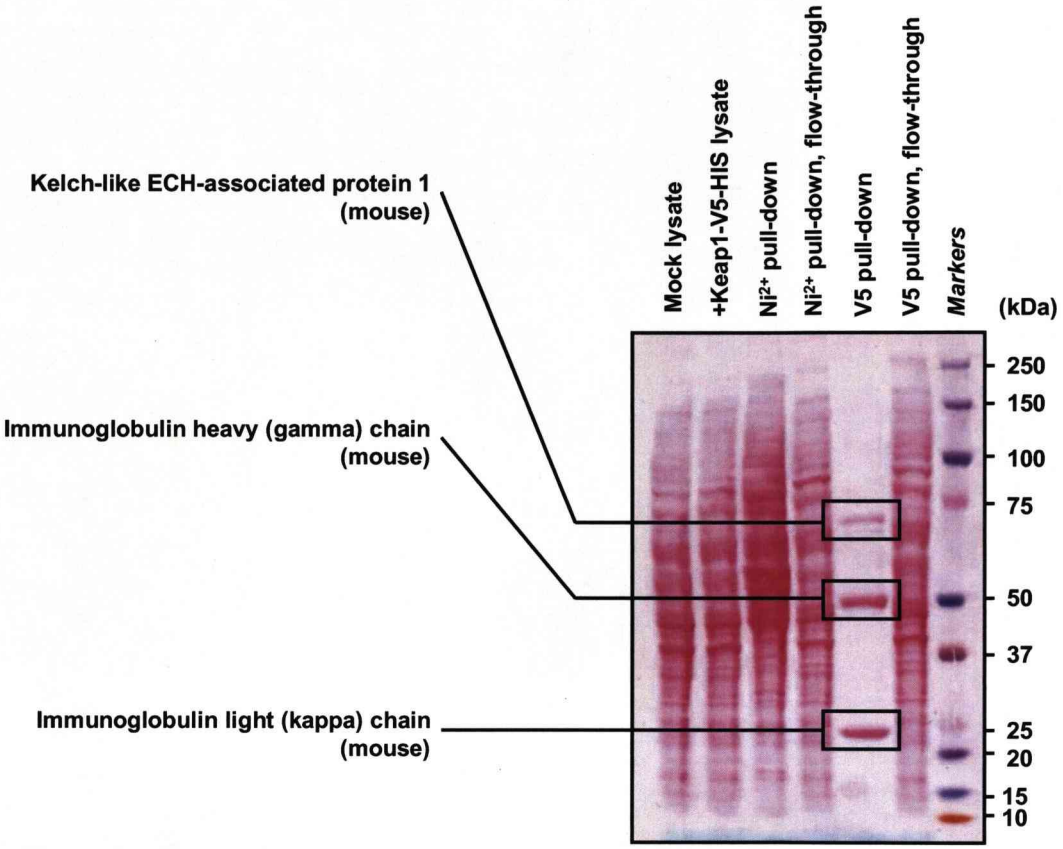

Fig. 5.10 - Identification of prominent proteins eluted from anti-V5 agarose beads. HEK293T cells were mock transfected or transfected for 24 h with pcDNA3.1/Keap1-V5-His and whole cell lysates were prepared. The lysates were incubated with Ni^{2+}-charged agarose beads or anti-V5 agarose beads and all fractions were resolved by denaturing electrophoresis. The Ponceau Red stain of the proteins, following transfer to nitrocellulose, is shown. The equivalent polyacrylamide gel was stained with Coomassie Brilliant Blue G-250 and the bands were excised. The protein(s) present within the bands were digested with trypsin, and the resulting peptide mixtures were analysed by LC-ESI-MS/MS. The data obtained from the MS/MS spectra were used in a ProteinPilot database search to identify the major protein constituent(s) for each band. The protein identified with the highest degree of confidence for each band is shown.

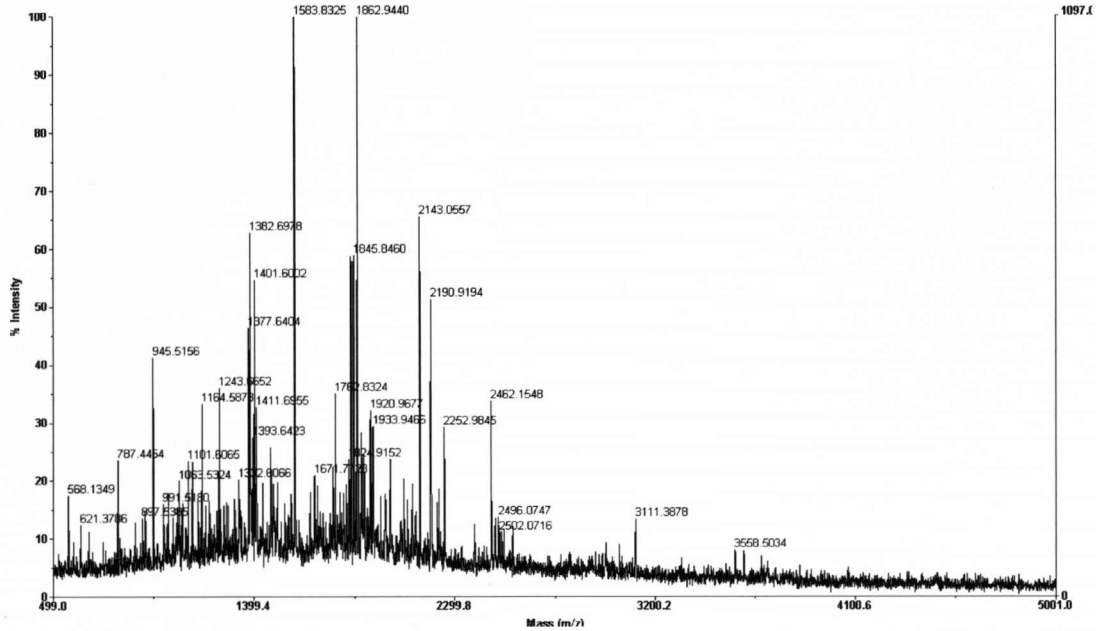

Fig. 5.11 - MALDI-TOF mass spectrum of the tryptic digest of protein(s) purified by anti-V5 immunoaffinity from Keap1-V5-His -expressing HEK23T cells. HEK293T cells were transfected for 24 h with pcDNA3.1/Keap1-V5-His, whole cell lysates were prepared and incubated with anti-V5 agarose beads. Bead-bound protein(s) were reduced with 1 mM DTT, alkylated with 55 mM iodoacetamide, and digested overnight with 240 ng trypsin. The resulting peptide mixture was visualised on a Voyager DE Pro MALDI-TOF Biospectrometry Workstation, in linear positive ion mode.

	Accession	Mass	Score	Description
1.	gi|7710044	69508	101	kelch-like ECH-associated protein 1 [Mus musculus]
2.	gi|74181739	69492	101	unnamed protein product [Mus musculus]
3.	gi|26337871	69478	94	unnamed protein product [Mus musculus]
4.	gi|74212473	69482	93	unnamed protein product [Mus musculus]
5.	gi|37359786	71015	88	mKIAA0132 protein [Mus musculus]

Match to: **gi|7710044 Kelch-like ECH-associated protein 1 [Mus musculus]**
Sequence Coverage: **47%**

```
  1 MQPEPKLSGA PRSSQFLPLW SKCPEGAGDA VMYASTECKA EVTPSQDGNR
 51 TFSYTLEDHT KQAFGVMNEL RLSQQLCDVT LQVKYEDIPA AQFMAHKVVL
101 ASSSPVFKAM FTNGLREQGM EVVSIEGIHP KVMERLIEFA YTASISVGEK
151 CVLHVMNGAV MYQIDSVVRA CSDFLVQQLD PSNAIGIANF AEQIGCTELH
201 QRAREYIYMH FGEVAKQEEF FNLSHCQLAT LISRDDLNVR CESEVFHACI
251 DWVKYDCPQR RFYVQALLRA VRCHALTPRF LQTQLQKCEI LQADARCKDY
301 LVQIFQELTL HKPTQAVPCR APKVGRLIYT AGGYFRQSLS YLEAYNPSNG
351 SWLRLADLQV PRSGLAGCVV GGLLYAVGGR NNSPDGNTDS SALDCYNPMT
401 NQWSPCASMS VPRNRIGVGV IDGHIYAVGG SHGCIHHSSV ERYEPERDEW
451 HLVAPMLTRR IGVGVAVLNR LLYAVGGFDG TNRLNSAECY YPERNEWRMI
501 TPMNTIRSGA GVCVLHNCIY AAGGYDGQDQ LNSVERYDVE TETWTFVAPM
551 RHHRSALGIT VHQGKIYVLG GYDGHTFLDS VECYDPDSDT WSEVTRMTSG
601 RSGVGVAVTM EPCRKQIDQQ NCTC
```

Fig. 5.12 - MASCOT protein database search result for peptide mass fingerprint obtained from the MALDI-TOF MS analysis of protein(s) purified by anti-V5 immunoaffinity from Keap1-V5-His -expressing HEK293T cells. The peptide mass fingerprint shown in Fig. 5.11 was used in a MASCOT protein database search (http://www.matrixscience.com), which identified mouse Keap1 as the major constituent protein in the tryptic digest. The five proteins identified with the highest degree of confidence are shown (all are variant database entries for mouse Keap1). The amino acid sequence coverage for mouse Keap1 was 47 %. The specific amino acids covered by the MALDI-TOF MS analysis are underlined and in bold.

5.3.5 Validation of Keap1-V5 -expressing HEK293T cells as a model for investigating the modification of Keap1 by Nrf2-activating electrophiles in cells

As the results presented in section 5.3.4 demonstrate that the most efficient method of purifying Keap1-V5-His from HEK293T cells was via the V5 epitope, the construct will subsequently be referred to simply as Keap1-V5. HEK293T cells were transiently transfected with Keap1-V5 and exposed to 100 μM DNCB for 1 h. These conditions were shown to induce the nuclear accumulation of Nrf2 in Hepa-1c1c7 in chapter 2, and here (Fig. 5.13a). In response to DNCB exposure, Nrf2 accumulated within the nuclei of both mock transfected HEK293T cells and cells expressing epitope-tagged Keap1 (Fig.

5.13b), findings that are consistent with recent studies by Liebler and colleagues (Hong *et al.*, 2005a; Hong *et al.*, 2005b). Furthermore, Keap1-V5 immunopurified from HEK293T cells was shown to be associated with endogenous Nrf2, and this association was enhanced following exposure of cells to DNCB, in agreement with recent independent observations (He *et al.*, 2006; Kobayashi *et al.*, 2006) (Fig. 5.14). The in-cell modification of Keap1-V5 by DNCB was demonstrated by the reaction of an anti-DNP antibody with Keap1-V5, following its immunoprecipitation from DNCB-exposed, but not vehicle-exposed, cells (Fig. 5.14). Therefore, Keap1-V5 -expressing HEK293T cells represent a functionally valid model system for investigating the modification of Keap1 by Nrf2-activating molecules, and the associated biological effects, in a cellular context.

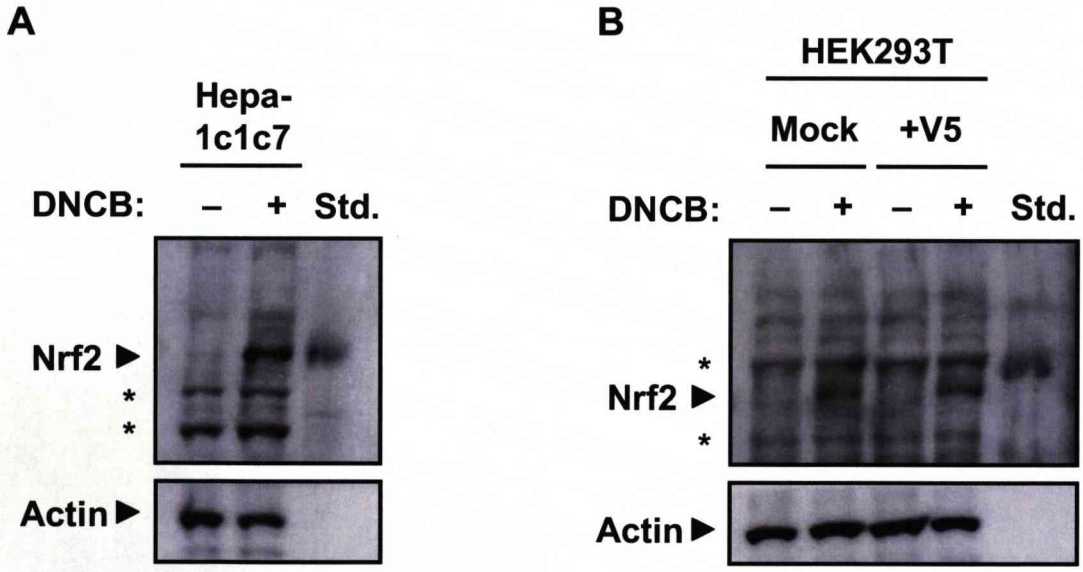

Fig. 5.13 - Ectopic expression of Keap1-V5 in HEK293T cells does not compromise the responsiveness of Nrf2 to DNCB. Hepa-1c1c7 cells or HEK293T cells that were mock transfected or transfected with Keap1-V5 were exposed to 0.5 % (v/v) DMSO (-) or 100 μM DNCB (+) for 1 h. Nuclear fractions were prepared and the Nrf2 protein level was assessed in Hepa-1c1c7 (A) or HEK293T cells (B) by Western blot analysis with an anti-mouse or anti-human Nrf2 antibody, respectively. Recombinant mouse (Hepa-1c1c7) or human (HEK293T) Nrf2-His was loaded onto the appropriate gel as a standard (Std). Non-specific proteins that cross-react with the antibody are labeled *.

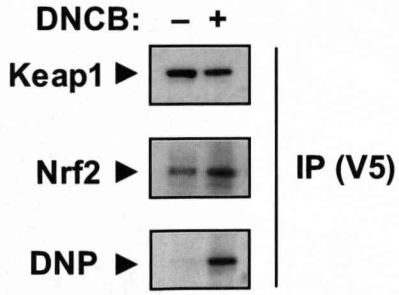

Fig. 5.14 - Association of Keap1-V5 with endogenous Nrf2 and modification by DNCB in HEK293T cells. HEK293T cells expressing Keap1-V5 were exposed to 0.5 % (v/v) DMSO (-) or 100 μM DNCB (+) for 1 h. Keap1-V5 was immunopurified using anti-V5 agarose beads. The proteins eluted from the beads were resolved by denaturing electrophoresis. Keap1-V5, its association with endogenous Nrf2, and its modification by DNCB were assessed by Western blot analysis with anti-Keap1, anti-human Nrf2 and anti-dinitrophenyl (DNP) antibodies, respectively.

5.3.6 Mass spectrometric analysis of Keap1-V5 modification by Nrf2-activating electrophiles in cells

Keap1-V5 -expressing HEK239T cells were exposed to NAPQI, DNCB (both 100 μM) or 15d-PGJ_2 (10 μM) for 1 h, conditions that stimulated the nuclear accumulation of Nrf2 in Hepa-1c1c7 cells in chapter 2. LC-ESI-MS/MS analysis revealed that NAPQI modified Cys-226 (2/2 experiments), -288 (2/2) and -434 (2/2), DNCB modified Cys-257 (2/2), and 15d-PGJ_2 modified Cys-257 (2/2) and -273 (2/2) of Keap1-V5 in HEK293T cells (Fig. 5.15). Careful examination of the MS/MS spectrum indicating modification of Cys-273 by 15d-PGJ_2 revealed that, by coincidence, the unfragmented peptide ion $[M+2H]^{2+}$ (557.3 amu) masked both y_5 (557.4 amu) and $*b_2$ (557.28) fragment ions, resulting in a relatively high intensity peak at this m/z (Fig. 5.15f-g). Overall, although there is residue selectivity amongst this panel of Nrf2-activating molecules, a common theme is apparent, in that the modification of cysteines within the IVR domain of Keap1 (Fig. 5.16) is associated with the activation of Nrf2 by electrophiles in cells. Despite recent suggestions that Keap1 is ubiquitinated under certain conditions of chemical/oxidative (Hong *et al.*, 2005b; Zhang *et al.*, 2005), there was no evidence for the ubiquitination of Keap1-V5 in the experiments reported here.

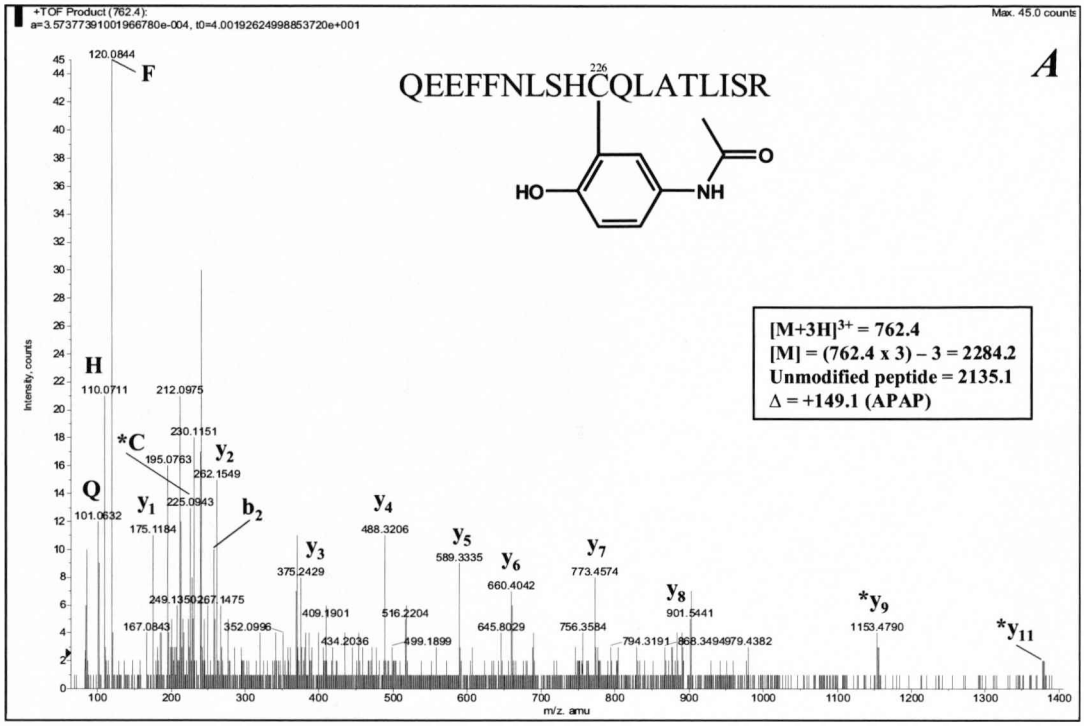

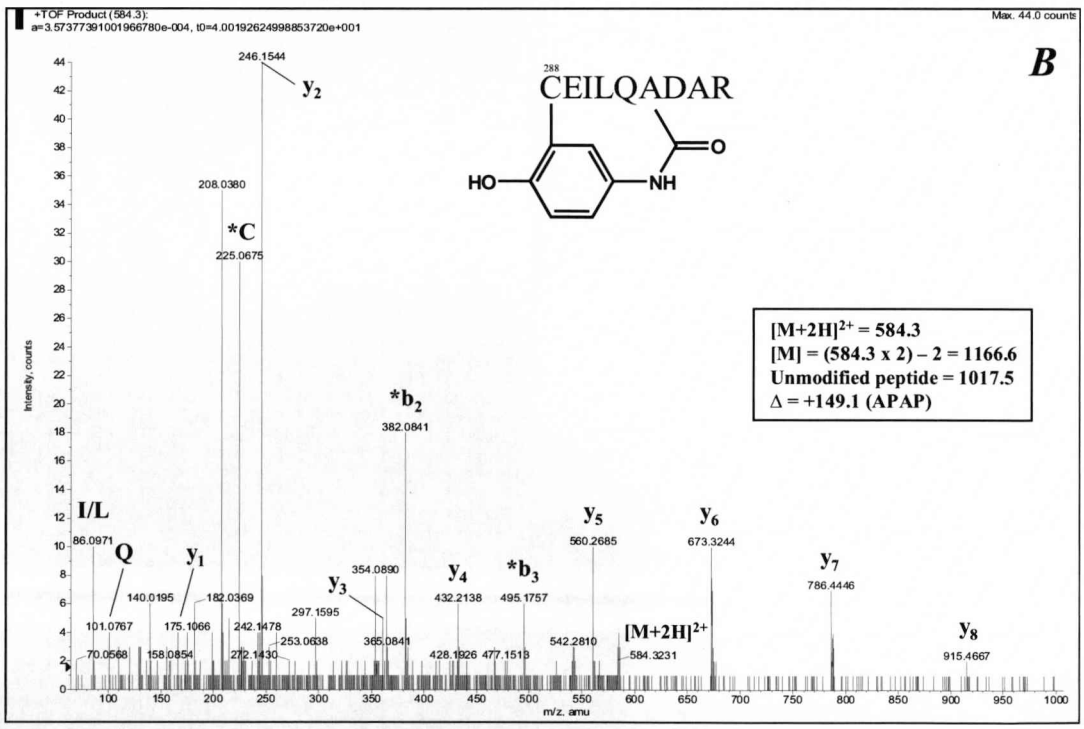

Fig. 5.15 - MS/MS spectrum indicating modification of Keap1-V5 (A) Cys-226 and (B) Cys-288 by NAPQI in HEK293T cells. y- and b-ions are labelled where present. * denotes ions for which a mass shift of +149.1 amu indicates modification by NAPQI. Immonium ions are labelled with the one-letter code for their corresponding amino acid.

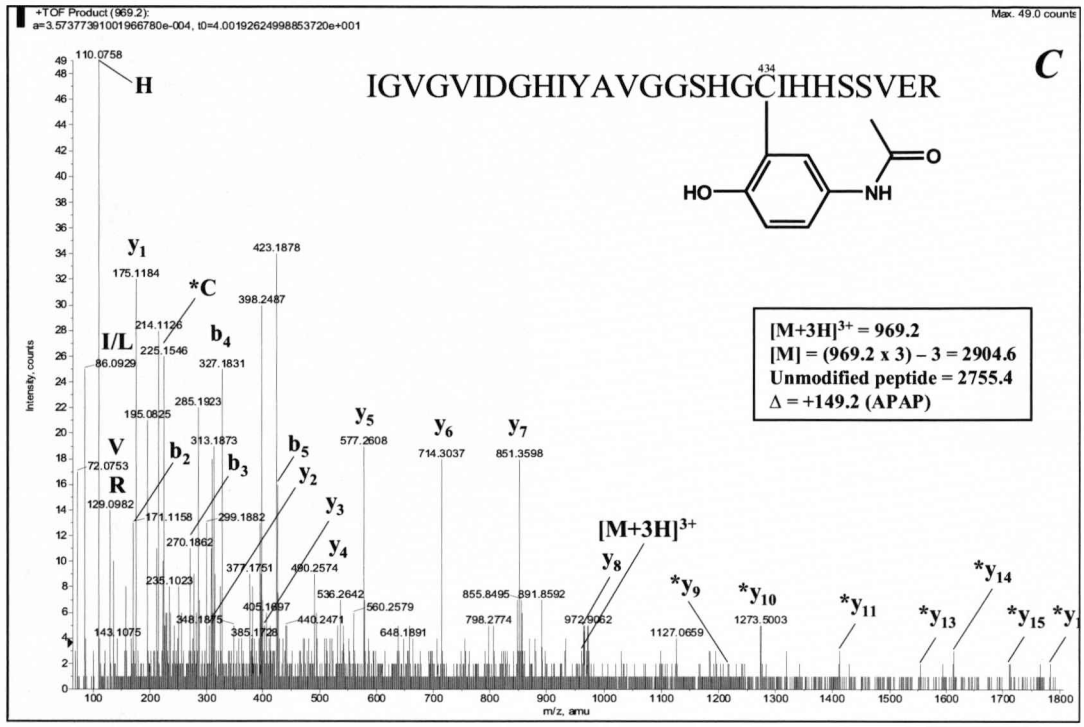

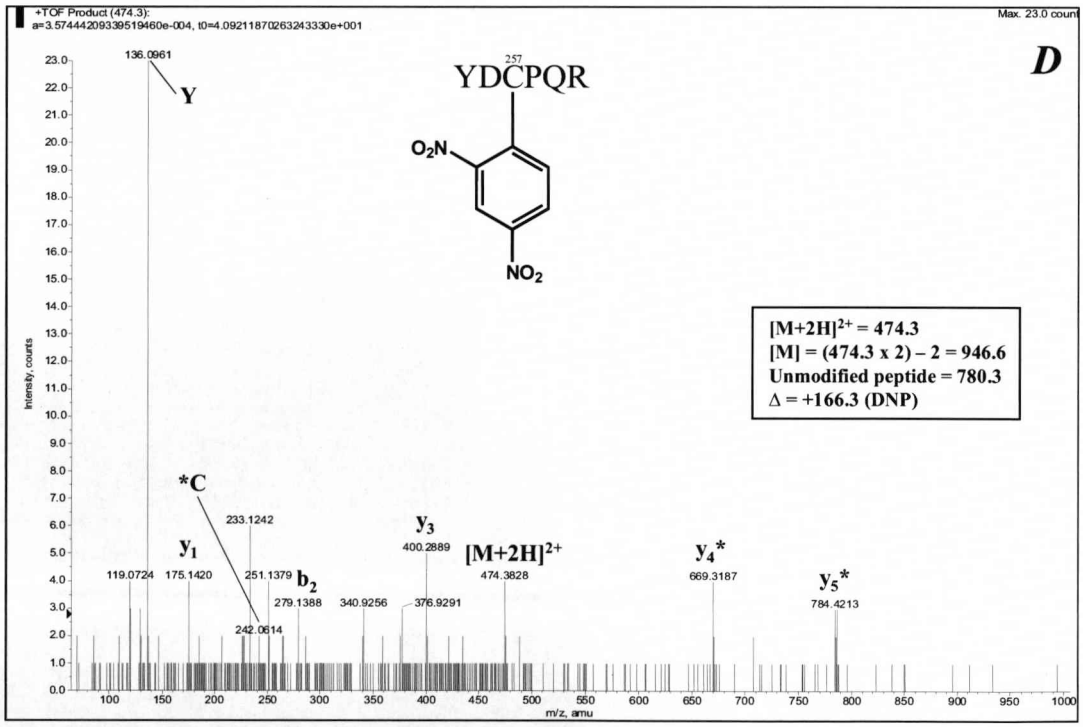

Fig. 5.15 - MS/MS spectrum indicating modification of Keap1-V5 (C) Cys-434 by NAPQI and (D) Cys-257 by DNCB in HEK293T cells. y- and b-ions are labelled where present. * denotes ions for which a mass shift of C) +149.1 amu indicates modification by NAPQI and D) +166.0 amu indicates modifications by DNCB. Immonium ions are labelled with the one-letter code for their corresponding amino acid.

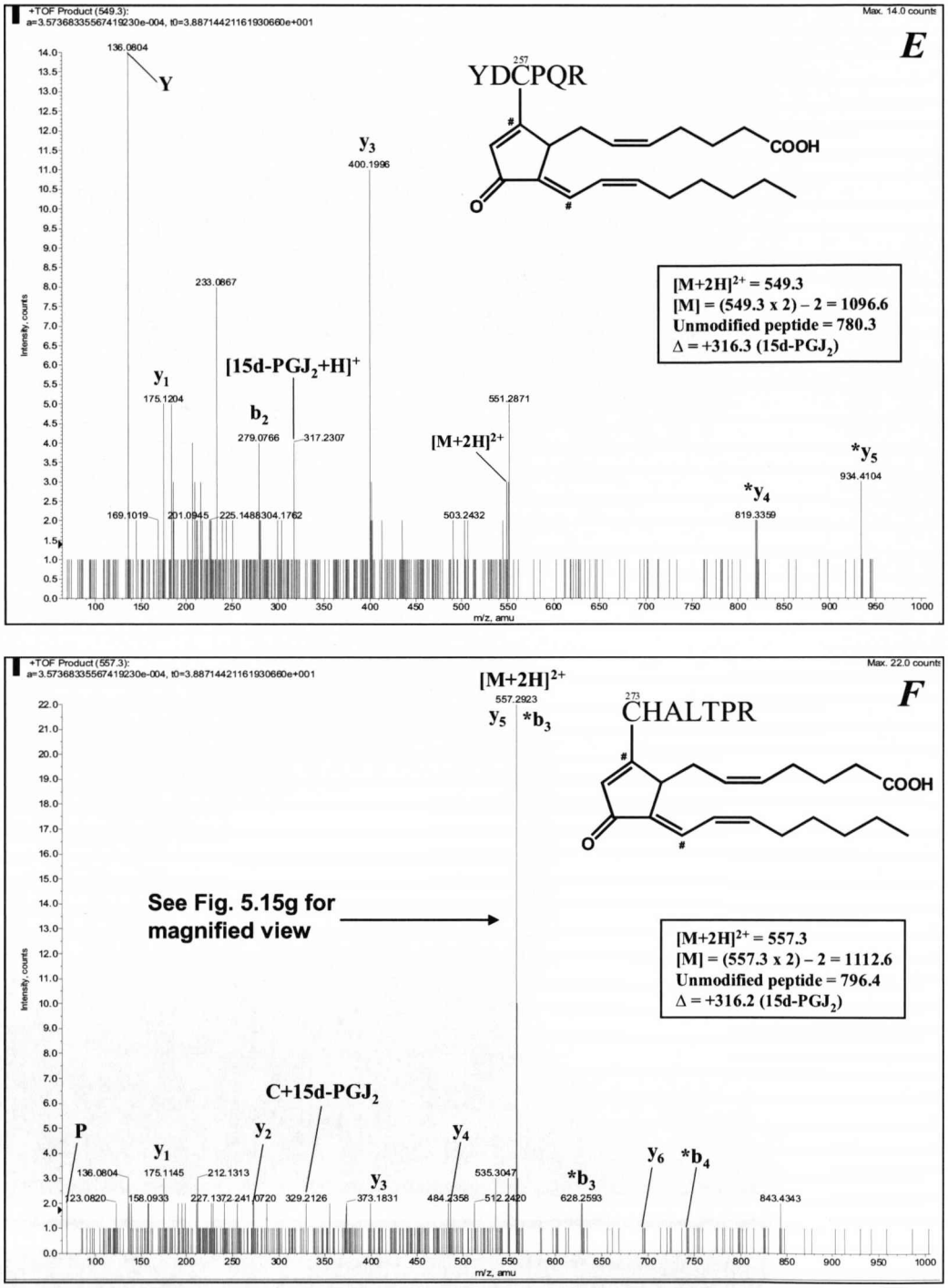

Fig. 5.15 - MS/MS spectrum indicating modification of Keap1-V5 (E) Cys-257 and (F) Cys-273 by 15d-PGJ$_2$ in HEK293T cells. y- and b-ions are labelled where present. It should be noted that adduction of Keap1 cysteines by 15d-PGJ$_2$ may occur via either of the electrophilic α,β-unsaturated carbonyl moieties (labelled #). * denotes ions for which a mass shift of +316.2 amu indicates modification by 15d-PGJ$_2$. Immonium ions are labelled with the one-letter code for their corresponding amino acid.

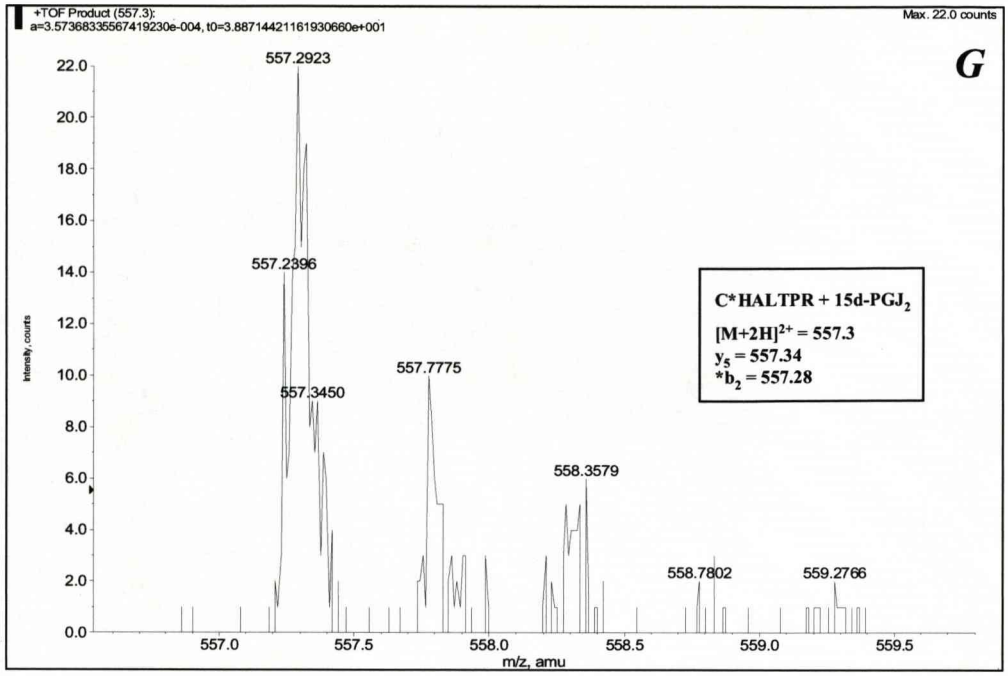

Fig. 5.15 - Magnified view of $[M+2H]^{2+}$ from MS/MS spectrum indicating modification of Keap-V5 (G) Cys-273 by 15d-PGJ$_2$ in HEK293T cells. The unfragmented peptide ion $[M+2H]^{2+}$ (557.3 amu) masks both the y_5 (557.4 amu) and $*b_2$ (557.28) fragment ions in Fig. 5.15f.

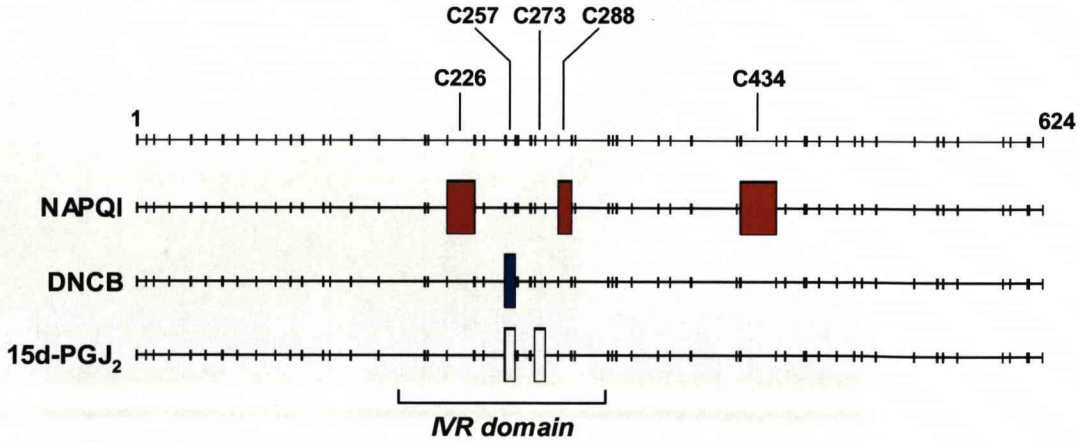

Fig. 5.16 - Summary of Keap1-V5 cysteine adduct patterns for NAPQI, DNCB and 15d-PGJ$_2$ in HEK293T cells. Modification maps for cysteine-containing Keap1-V5 peptides were generated using a software package described previously by Beynon (2005). The horizontal lines represent the full-length Keap1 protein (amino acids 1-624), the vertical lines represent the boundaries between sequential tryptic peptides. Filled boxes represent cysteine-containing peptides found to be modified by NAPQI (■), DNCB (■) or 15d-PGJ$_2$ (□).The specific cysteines modified are noted at the top of the figure. The IVR domain of Keap1 (amino acids 180-314) is highlighted.

5.3.7 Mass spectrometric analysis of putative Keap1-V5 -interacting proteins

Although the primary aim of the experiments described in this chapter was to identify the specific Keap1 cysteine targets of Nrf2-activating electrophiles within a cellular context, the techniques used also enabled the characterisation of other proteins that were immunopurified from HEK293T cells with Keap1-V5. Due to a lack of time at the end of the project, it was not possible to differentiate between proteins that had an intrinsic affinity for the anti-V5 agarose beads and those that were immunopurified in a complex with Keap1-V5. Nevertheless, a subset of nuclear and cytosolic proteins was consistently identified in the immunopurified fractions by LC-ESI-MS/MS (Table 5.1). Four proteins were detected in the immunopurified fraction only when HEK293T cells had been exposed to an Nrf2-activating electrophile, and not vehicle control (Table 5.2). These proteins were identified as dipeptidyl-peptidase 3 (DPP3), eukaryotic peptide chain release factor subunit 1, heat shock protein 90β (HSP-90β), and peroxiredoxin 1 (PRX1).

Protein	Function
40S ribosomal protein S12	Structural constituents of the ribosome
60S ribosomal protein L12	
Actin, cytoplasmic 1	Structural constituent of the cytoskeleton
ATP-dependent RNA helicase A	Transcriptional activator; unwinds double-stranded DNA and RNA
ATP synthase subunit alpha, mitochondrial precursor	Produces ATP from ADP in the presence of a proton gradient across the mitochondrial membrane.
DNA-binding protein A	Translational repressor
Elongation factor 1-alpha 1	Promotes GTP-dependent binding of aminoacyl-tRNA to the A-site of ribosomes during protein biosynthesis

Table 5.1 - Proteins immunopurified alongside Keap1-V5 from HEK293T cells exposed to vehicle or Nrf2 activators. HEK293T cells expressing Keap1-V5 were exposed to vehicle (0.5 % (v/v) DMSO) or Nrf2 activators (100 μM DNCB, 100 μM NAPQI or 10 μM 15d-PGJ_2) for 1 h. Keap1-V5 was immunopurified using anti-V5 agarose beads. Proteins eluted from the beads were analysed by LC-ESI-MS/MS. Proteins identified in at least two samples from cells exposed to vehicle or Nrf2 activators are presented. Protein function descriptions are taken directly from the NCBI Entrez Protein database (http://www.ncbi.nlm.nih.gov/sites/entrez?db=protein).

Heat shock 70 kDa protein 1	Molecular chaperone; stabilises proteins against aggregation and mediates folding of newly translated polypeptides
Heterogeneous nuclear ribonucleoprotein A/B	Binds single-stranded RNA
Histone H1D	Enable condensation of nucleosome chains into higher order structures.
Histone H2B	
Histone H4	
Ig gamma-1 chain C region secreted form	*Fragments of anti-V5 antibody, covalently attached to agarose beads*
Ig heavy chain V region H8	
Interleukin enhancer-binding factor 3	May facilitate double-stranded RNA-regulated gene expression at the level of post-transcription
KH domain-containing, RNA-binding, signal transduction-associated protein 1	Adapter protein in signal transduction cascades; represses CBP-dependent transcriptional activation by binding to CBP; mediates mRNA nuclear export
Non-POU domain-containing octamer-binding protein	DNA- and RNA binding protein; involved in several nuclear processes
Nuclease sensitive element-binding protein 1	Binds to splice sites in pre-mRNA and regulates splice site selection; binds and stabilizes cytoplasmic mRNA
Nucleolysin TIAR	RNA-binding protein; possesses nucleolytic activity against cytotoxic lymphocyte target cells; may be involved in apoptosis
Nucleophosmin	Associated with nucleolar ribonucleoprotein structures; binds single-stranded nucleic acids; may function in the assembly and/or transport of the ribosome
Phosphoglycerate mutase family member 5 precursor	Catalyzes the conversion of 3-phosphoglycerate to 2-phosphoglycerate in the glycolytic cycle
Probable ATP-dependent RNA helicase DDX17	Involved in ATP-dependent RNA unwinding; required in a variety of cellular processes including splicing, ribosome biogenesis and RNA degradation
Protein TFG	Putative component of the NF-κB pathway that interacts with NEMO and TANK, and activates NF-κB in cooperation with other proteins.
Putative Xaa-Pro aminopeptidase 3	Releases any N-terminal amino acid that is linked to proline
RNA-binding protein EWS	Translational repressor

Table 5.1 contd. - Proteins immunopurified alongside Keap1-V5 from HEK293T cells exposed to vehicle or Nrf2 activators.

RNA-binding protein FUS	Promotes ATP-independent annealing of complementary single-stranded DNAs and D-loop formation in superhelical double-stranded DNA
Serine/arginine repetitive matrix protein 2	Component of the active spliceosome; involved in pre-mRNA splicing
Sequestosome-1	Scaffold protein; may regulate the activation of NF-κB by TNF-α, nerve growth factor and IL-1; may regulate signaling cascades through ubiquitination
Splicing factor 3B subunit 1	Involved in RNA splicing
TATA-binding protein-associated factor 2N	RNA and DNA -binding protein; belongs to the RNA polymerase II (Pol II) transcriptional multiprotein complex
Tubulin alpha-1A chain	Structural constituents of microtubules
Tubulin beta-2A chain	
Y-box-binding protein 2	Major constituent of messenger ribonucleoprotein particles (mRNPs); involved in regulating the stability and/or translation of germ cell mRNAs.
Zinc finger protein 503	Transcriptional repressor

Table 5.1 contd. - Proteins immunopurified alongside Keap1-V5 from HEK293T cells exposed to vehicle or Nrf2 activators.

Protein	**Function**
Dipeptidyl-peptidase 3	Cleaves N-terminal Arg-Arg-β-naphthylamide from a peptide comprising four or more residues
Eukaryotic peptide chain release factor subunit 1	Directs the termination of nascent peptide synthesis in response to the stop codons UAA, UAG and UGA.
Heat shock protein 90β	Molecular chaperone; stabilises proteins against aggregation and mediates folding of newly translated polypeptides
Peroxiredoxin 1	Reduces peroxides; involved in redox regulation of the cell

Table 5.2 - Proteins immunopurified alongside Keap1-V5 from HEK293T cells exposed to Nrf2 activators only. HEK293T cells expressing Keap1-V5 were exposed to vehicle (0.5 % (v/v) DMSO) or Nrf2 activators (100 μM DNCB, 100 μM NAPQI or 10 μM 15d-PGJ_2) for 1 h. Keap1-V5 was immunopurified using anti-V5 agarose beads. Proteins eluted from the beads were analysed by LC-ESI-MS/MS. Proteins identified in at least two samples from cells exposed to Nrf2 activators, but not vehicle, are presented. Protein function descriptions are taken directly from the NCBI Entrez Protein database (http://www.ncbi.nlm.nih.gov/sites/entrez?db=protein).

5.4 DISCUSSION

The Nrf2-ARE pathway protects mammalian cells against chemical/oxidative stress, via the inducible expression of cytoprotective enzymes and proteins (for a review, see Kensler *et al.*, 2007). The elucidation of the precise molecular mechanisms that underlie the capacity of the Nrf2-ARE pathway to 'sense' and respond to stress is vital to our understanding of the biochemical pathways that regulate Nrf2-dependent cell defence. It has been proposed that chemical inducers activate the Nrf2-ARE pathway through the direct modification of critical cysteine residues within Keap1, the cytosolic repressor of Nrf2 (Dinkova-Kostova *et al.*, 2002). Although the results presented in chapter 4 and a number of recent studies (Dietz *et al.*, 2005; Dinkova-Kostova *et al.*, 2002; Eggler *et al.*, 2005; Hong *et al.*, 2005a; Hong *et al.*, 2005b; Liu *et al.*, 2005; Luo *et al.*, 2007) have provided compelling evidence for the modification of recombinant Keap1 protein by Nrf2-activating molecules *in vitro*, very little is known regarding the residue-selectivity of Keap1 modification in a cellular context. Therefore, the aim of the work presented in this chapter was to develop a cell-based method to enable the characterisation, by MS/MS, of Keap1 modification within a more biologically-relevant cellular setting, in order to explore the hypothesis that modification of Keap1 is associated with activation of Nrf2 in cells.

Initial attempts to characterise Keap1 modification in cells focused on the immunoprecipitation of the endogenous protein from Hepa-1c1c7 cells. As a general strategy to look at post-translational modification of proteins, immunoprecipitation coupled to mass spectrometry is still in its infancy (for some examples, see Abraham *et al.*, 2000; Walgren *et al.*, 2003; Yang *et al.*, 2006). Unfortunately, it was not possible to immunoprecipitate enough Keap1 for MS/MS analysis, despite employing two different anti-Keap1 antibodies under non-denaturing and denaturing conditions. Further optimisation may enhance the yield of this procedure, but it may be that the low cellular abundance of Keap1, as has recently been reported by McMahon *et al.* (2006), is below the present detection limits of MS/MS analysis, particularly when considering that the non-specific binding of other proteins may mask the Keap1 signal.

In light of the unsuccessful attempts at immunoprecipitation of endogenous Keap1, a cell-based model was developed, in which Keap1-V5 was ectopically expressed in HEK293T cells. Efforts to purify Keap1-V5 from cells using a secondary affinity tag, the polyhistidine epitope that has a high affinity for Ni^{2+}, were not successful, due to the large number of contaminating proteins that co-precipitated with Keap1-V5. However, this can be rationalised in light of the observation that proteins with as little as two adjacent histidines show affinity for the Ni^{2+} nitrilotriacetic acid adsorbent that is typically used for purification of polyhistidine-tagged proteins (Hochuli *et al.*, 1988). A BLAST protein database search reveals at least 91 human proteins that contain four or five adjacent histidines. A much higher number of matches would be anticipated for proteins with two or three adjacent histidines. Conversely, no human proteins contain the complete 14 amino acid V5 epitope (GKPIPNPLLGLDST), which probably accounts for the relatively low complexity of the anti-V5 agarose bead eluate in section 5.3.4. Therefore, use of the polyhistidine tag alone is not sufficient for the highly stringent purification of Keap1-V5 from cells.

The functional validity of Keap1-V5 -expressing HEK293T cells as a model for studying the biochemical regulation of the Nrf2-ARE pathway was confirmed by the following observations; a) Nrf2 nuclear accumulation was detected following exposure of mock-transfected and Keap1-V5 -expressing cells to DNCB, b) Keap1-V5 interacted with endogenous Nrf2, and this interaction was enhanced following exposure of cells to DNCB, and c) Keap1-V5 was modified by DNCB in cells, as shown by its immunoreactivity towards an anti-DNP antibody. It is plausible that the over-expression of Keap1-V5 may alter the dose-response relationship for Nrf2 activation by chemical inducers, through the increased repression of the transcription factor under basal conditions. However, at least at the single concentration of DNCB used to validate this model system in section 5.3.5, this did not appear to be the case, a finding that is consistent with previous studies whereby epitope-tagged Keap1 has been over-expressed in cells (Dhakshinamoorthy *et al.*, 2001; Hong *et al.*, 2005a; Hong *et al.*, 2005b; Zhang *et al.*, 2004). It could be suggested that ectopically-expressed Keap1-V5 may simply be compartmentalised within the cell at some distance from the native site(s) of interaction

with Nrf2. However, this cannot be the case entirely, as endogenous Nrf2 has clearly been shown to associate with Keap1-V5 in section 5.3.5. Thus, although it would appear that over-expression of Keap1-V5 does not compromise the functionality of the Nrf2-ARE pathway, in terms of its ability to respond to chemical inducers, further work is required to fully characterise the nature of the interaction between Keap1-V5 and endogenous Nrf2 under basal conditions and in the presence of chemical/oxidative stress. For example, it would be of interest to examine the effect of Keap1-V5 expression, perhaps with or without co-expression of Nrf2, on the activity of an ARE-driven luciferase reporter transgene, such as that described in section 2.2.8.

Using the functional HEK293T cell model in which modification of Keap1 could be detected concomitantly with activation of Nrf2, residue-selective adduction of Keap1 by NAPQI, DNCB and 15d-PGJ_2 was observed. NAPQI modified Cys-226, -288 and -434, DNCB modified Cys-257, and 15d-PGJ_2 modified Cys-257 and -273 of Keap1-V5. Of these residues, Cys-257, -273 and -288 of mouse Keap1 have previously been shown to be highly reactive towards dex-mes *in vitro* (Dinkova-Kostova *et al.*, 2002). In addition, it has been demonstrated that site-directed mutagenesis of Cys-273 and/or -288 of human and mouse Keap1 causes an increase in the basal activity of Nrf2 (Kobayashi *et al.*, 2006; Levonen *et al.*, 2004; Wakabayashi *et al.*, 2004; Zhang *et al.*, 2003). On the other hand, the single mutation of Cys-257 of human and mouse Keap1 (Levonen *et al.*, 2004; Zhang *et al.*, 2003) or the compound mutation of Cys-226 along with Cys-241 and -249 of mouse Keap1 (Wakabayashi *et al.*, 2004) have no apparent effect on the basal and/or inducible activity of Nrf2.

There are no reports on the functional effect of mutating Cys-434, the one residue outside of the IVR domain that was found to be adducted (by NAPQI) in this study. However, it is notable that this residue lies at the end of strand β2 blade III of the β-propeller structure that is formed by the DGR domain of Keap1 (Padmanabhan *et al.*, 2006). A hydrogen bond between the neighbouring Ser-431 and Asn-414 of Keap1 stabilises the position of Arg-415, which allows it to interact with residues located within the ETGE and DLG motifs of the Neh2 domain of Nrf2 (Padmanabhan *et al.*,

2006). It is possible, therefore, that the modification of Cys-434 may provoke a local conformational change that may disrupt the molecular contacts between Keap1 and Nrf2, leading to a loss of repression of the transcription factor. Hence, further investigations are required to define the biological significance of the direct modification of Cys-434, and the other Keap1 target residues identified here. For instance, there may be value in examining the effect of mutating Cys-434 to a bulky amino acid such as tryptophan or tyrosine, as a means of assessing the likely effect on Nrf2 activity of a substantial chemical modification at Cys-434 of Keap1.

Although no single residue in Keap1-V5 was targeted by all three molecules in cells, the common theme established in chapter 4, i.e. the modification of one or more cysteines within the IVR domain of Keap1, was again apparent. Indeed, the only previous report of residue-selective Keap1 adduction in cells also identified IVR residues (Cys-241, -257 and -273) as targets of BIA (Hong *et al.*, 2005b). Recent work has also shown that binding of biotinylated 15d-PGJ_2 (Hosoya *et al.*, 2005) to Keap1 is attenuated by compound mutation of cysteine residues within this IVR domain, including Cys-257 and -273, which have been shown to be modified by 15d-PGJ_2 in cells in this study. In this regard, it would be interesting to investigate whether the mutation of single or multiple residues that are targets of the panel of electrophiles used here completely abolishes the modification of Keap1 and prevents the activation of Nrf2.

It was notable that, although all three Nrf2-activating molecules did modify cysteine residues within the IVR domain of Keap1-V5 in cells and Keap1-His *in vitro* (chapter 4), the overall pattern of adducts associated with each molecule was more random in the *in vitro* experiments. There are several plausible explanations for this discrepancy. Firstly, the redox states of the numerous cysteines in Keap1 have yet to be determined, with the exception of the eight residues located within the DGR domain of the human protein; these cysteines do not appear to participate in disulphide bonds, at least in the absence of chemical/oxidative stress (Li *et al.*, 2004). Therefore, a recombinant Keap1-His protein in which all cysteines are free for adduction, as used in chapter 4, may not be representative of the physiological state of the protein in cells. It is therefore imperative

that the redox states of the cysteine residues outside of the DGR domain of Keap1 are determined. Secondly, the relative reactivities of Keap1 cysteines in the recombinant protein may differ significantly from the situation in cells, due to protein folding, post-translational modification(s), and/or the interaction with protein partners. These factors may cause some potential binding sites that are free for adduction *in vitro* to be obscured on the protein in cells. Thirdly, in order to modify Keap1 within a cell, an electrophile must bypass various intracellular antioxidants and reductants, such as GSH, as well as other cellular proteins. These obstacles may hinder the modification of some cysteines in Keap1 that may not be as reactive as those which were found to be adducted in cells here. For these reasons, one should be cautious when attempting to extrapolate data obtained from *in vitro* analyses to a cellular or *in vivo* context.

Despite the discrepancies between the two methods, a degree of overlap was observed between some of the target residues identified in cells and those that were found to be the most reactive in recombinant Keap1-His *in vitro*. This suggests that, whilst *in vitro* systems are not fully representative of the physiological conditions within cells, determining the reactivity of cysteines in recombinant Keap1 *in vitro* towards inducers of the Nrf2-ARE pathway is useful. The different reactivities of Keap1 residues in the two model systems used in this thesis may be informative of various cellular factors, such as protein folding, that may influence the nature of the trigger for Nrf2 activation. Future work should focus on utilising the model cell system described here to examine the site-selectivity of Keap1 modification by other electrophiles, in order to further characterise the critical target residues of Nrf2-activating molecules within cells. Furthermore, this system may prove useful in defining the role of Keap1 modifications other than alkylation in triggering Nrf2-dependent cell defence.

HEK293T cells (DuBridge *et al.*, 1987) have been used as a model in many studies whereby the ectopic expression of a protein has been exploited to gain an insight into its biological role. A particularly noteworthy example is the recent work by Macpherson *et al.* (2007), who used mass spectrometry to demonstrate that thiol-reactive, noxious electrophiles activate the transient receptor potential ankyrin 1 ion channel, which is

present in nociceptive neurons, via the covalent modification of reactive cysteine residues. Indeed, HEK293T were used as the cellular expression vehicle in the only previous examination of Keap1 modification by an Nrf2-activating molecule in cells (Hong *et al.*, 2005b). Although HEK293T cells are a suitable model, it would be desirable to examine Keap1 modification in Hepa-1c1c7 cells, to enable a better correlation with the biochemical analyses performed in chapter 2. To this end, transient expression of Keap1-V5 was attempted in Hepa-1c1c7 cells, but, as demonstrated in section 5.3.4, the level of expression was considerably lower than that in HEK293T cells. Indeed, this is not unexpected, given that HEK293T cells, but not Hepa-1c1c7 cells, are transformed with the large T antigen of SV40 (DuBridge *et al.*, 1987), enabling episomal replication of pcDNA3.1/Keap1 and thus effectively increasing the expression of Keap1-V5. In addition, attempts were made to generate Hepa-1c1c7 clones stably-transfected with pcDNA3.1/Keap1, but these attempts were unsuccessful. This may be rationalised in terms of continual over-expression of Keap1 causing a relentless over-repression of Nrf2, lowering cytoprotective barriers, and thus resulting in transfected cells being highly susceptible to background levels of oxidative stress. Therefore, the constant over-expression of Keap1 may be toxic to cells. In keeping with this, there are no reports in the literature in which stably-transfected Keap1-expressing cell lines have been developed. Hence, there may be value in pursuing the generation of stably-transfected Hepa-1c1c7 cells using an inducible expression system, such as the doxycycline-responsive Tet-On system (Gossen *et al.*, 1995). The expression of transgenes through the Tet-On system can be tightly regulated in response to varying concentrations of doxycycline (Gossen *et al.*, 1995), such that it may be possible to express Keap1-V5 at levels equivalent to endogenous Keap1, reducing the confounding effects of protein over-expression, whilst still enabling immunopurification and mass spectrometric analysis.

Whilst a comprehensive analysis was not possible within the timeframe of this thesis, it was noted that some proteins were consistently immunopurified along with Keap1-V5 from HEK293T cells. Interestingly, both cytosolic and nuclear proteins were identified, despite the recent confirmation that endogenous Keap1 is predominantly a cytosolic

protein (Watai *et al.*, 2007). Of course, the disruption of subcellular compartments following cell lysis may expose some proteins that would not normally be accessible to Keap1 under physiological conditions. Therefore, future work should examine the cellular localisation of Keap1-V5 and ensure that appropriate subcellular fractions are isolated prior to its immunopurification. Noteworthy proteins that were identified as putative Keap1-interacting partners include the cytoskeletal protein actin, which is known to associate with Keap1 in the cytosol (Kang *et al.*, 2004), KH domain-containing, RNA-binding, signal transduction-associated protein 1, which is known to repress transcriptional activation through binding to the Nrf2-interacting protein CBP (Babic *et al.*, 2004; Hong *et al.*, 2002; Katoh *et al.*, 2001; Zhu *et al.*, 2001), and phosphoglycerate mutase family member 5, which has recently been shown to be a substrate for Keap1-mediated ubiquitination and proteasomal degradation (Lo *et al.*, 2006). Although the physiological significance of these and other putative interactions with Keap1 warrant further exploration, these particular observations may be important in terms of validating this method for identifying Keap1-interacting proteins. However, perhaps surprisingly, Nrf2 was not identified alongside Keap1-V5 in any of the immunopurified fractions. This conflict may represent the relative low cellular abundance of Nrf2, which may be below the limit of detection of current MS/MS analysis.

Four proteins were consistently identified in the immunopurified fraction only following exposure of HEK293T cells to an Nrf2-activating molecule. One of these proteins, DPP3 is a cytosolic enzyme that cleaves N-terminal Arg-Arg-β-naphthylamide and, to a lesser extent, other dipeptide motifs (Ellis *et al.*, 1967). Such peptidase activity is important in regulating the disposition of enkephalins and angiotensins (Ellis *et al.*, 1967; Lee *et al.*, 1982). Although DPP3 has not previously been shown to associate with Nrf2 or Keap1 directly, the ectopic expression of DPP3 has recently been shown to promote Nrf2 nuclear accumulation and induce Nrf2-dependent cell defence in IMR-32 human neuroblastoma cells (Liu *et al.*, 2007), via a mechanism that is sensitive to inhibition of the PI3K and PKC phosphorylation pathways (Liu *et al.*, 2007). It is notable that, similar to Keap1 (Dinkova-Kostova *et al.*, 2005), DPP3 is a zinc-binding protein, and its activity

is inhibited by thiol-reactive molecules (Fukasawa *et al.*, 1998; Lee *et al.*, 1982). However, it appears unlikely that Nrf2 or Keap1 are substrates of DPP3, as neither protein contains the N-terminal Arg-Arg-β-naphthylamide motif that is favoured by the enzyme. Alternatively, DPP3 may directly associate with Keap1 by some other means under conditions of chemical/oxidative stress and disrupt the interaction with Nrf2, triggering an adaptive defence response. A second protein that was identified as a novel activator of Nrf2 in the study by Liu *et al.* (2007) was the scaffold protein sequestosome 1. This ubiquitin-binding protein, which may have a regulatory role in the NF-κB pathway (Moscat *et al.*, 2007) was shown here, by mass spectrometry, to immunopurify along with Keap1-V5 in cells exposed to either vehicle or Nrf2 inducers. Therefore, the biochemical mechanisms by which DPP3 and sequestosome 1 activate the Nrf2-ARE pathway require further examination.

Of the other proteins that were shown to immunopurify alongside Keap1-V5 from HEK293T cells only following exposure to Nrf2-activating molecules, eukaryotic peptide chain release factor subunit 1 directs the termination of protein translation via recognition of a stop codon and the hydrolysis of the ester bond linking the polypeptide chain with the peptidyl site tRNA (for a review, see Nakamura *et al.*, 1998). Another identified protein, HSP-90β is a molecular chaperone that acts to maintain correct protein folding and regulate the activity of several signaling proteins, including steroid hormone receptors and protein kinases (Pearl *et al.*, 2006; Zhao *et al.*, 2005). PRX1, which catalyses the reduction of peroxides (Ishii *et al.*, 2007; Wood *et al.*, 2003), was also immunopurified alongside Keap1-V5 only from HEK293T cells exposed to Nrf2-activating molecules. In light of the important antioxidant role of the PRX family (Ishii *et al.*, 2007; Wood *et al.*, 2003), it is possible that the putative interaction of PRX1 with Keap1 signifies the involvement of oxidative stress, and more specifically a change in the redox state of Keap1 cysteines, following exposure of cells to Nrf2-activating molecules. Although the 1-Cys PRX6 is known to interact with GSTP1-1, a process that reestablishes the catalytic activity of PRX6 (Manevich *et al.*, 2004; Noguera-Mazon *et al.*, 2006; Ralat *et al.*, 2006), there are no reports documenting an interaction between the 2-Cys PRX1 and another protein. Hence, the identification of PRX1 as a possible

interaction partner of Keap1 is intriguing and, along with the other proteins discussed here, warrants further examination. Of course, in light of the absence of suitable controls, particularly anti-V5 immunopurifications from HEK293T cells that do not express Keap1-V5, it is not possible to differentiate between those proteins which genuinely interact with Keap1-V5 and those which simply have an affinity for the anti-V5 agarose beads. Once these controls are properly established, this model system may prove a valuable tool in identifying novel interaction partners of Keap1 under different cellular conditions.

Although the work presented in this chapter represents the most comprehensive cellular analysis of Keap1 modification by Nrf2-activating molecules to date, there remains a need to further characterise the residue-selectivities of different inducers, particularly those with distinct electrophilic chemistries, in order to gain further insight into the precise chemical nature of the redox switch that controls the activation of Nrf2-dependent cell defence. Mass spectrometry is increasingly being used to characterise the modification of endogenous protein(s) in cells and tissues (Ji *et al.*, 2007; Koen *et al.*, 2006; Lemercier *et al.*, 2004; Meier *et al.*, 2007; Meier *et al.*, 2005; Shin *et al.*, 2007). Ultimately, experimental methods and bioanalytical techniques must evolve to enable the sensitive analysis of endogenous Keap1 modification *in vivo*, in order to step closer to fully understanding the biochemical regulation of the Nrf2-ARE pathway under physiological conditions.

CHAPTER 6

Concluding discussion

CONTENTS

6.1 Introduction

Adverse drug reactions, such as DILI, constitute a major public heath concern. In order to improve patient wellbeing, and to address the issue of drug attrition within the pharmaceutical industry, it is important that the design and development of safer, more efficacious medicines is informed by continued advances in our understanding of the chemical, biochemical and molecular mechanisms that underlie specific adverse drug reactions. The process of drug metabolism can, in some cases, contribute to the onset of toxicity, through the generation of chemically reactive intermediates that can promote oxidative stress and/or inhibit the function of critical cellular macromolecules (for a review, see Park, 1986). Hence, the ability of an organism to withstand the potential toxic effect(s) of a given molecule is often determined by the balance between bioactivation and detoxification. In order to maintain a favourable balance between bioactivation and detoxification, mammalian cells have evolved a multi-faceted, highly regulated cell defence system that affords protection against the deleterious effects of endogenous and exogenous chemical species. The functionality of this defence system is regulated, in part, by the activity of certain transcription factors, particularly Nrf2 (for a review, see Jaiswal, 2004). An appreciation of the molecular mechanisms that underlie the adaptive response to cellular stress is vital to gain insights into the signalling events that determine the progression and outcome of adverse drug reactions, such as DILI. Therefore, the main aims of the studies presented in this thesis were to further our understanding of the means by which the Nrf2-ARE cell defence pathway is regulated, and to elucidate its role in the protection against DILI.

6.2 Activation of Nrf2 by paracetamol – Role of Keap1 modification by NAPQI

The commonly-used analgesic and antipyretic paracetamol is often associated with DILI. Indeed, the hepatotoxicity associated with overdose of paracetamol is the single biggest cause of acute liver failure in both the UK (Davern *et al.*, 2006) and USA (Larson *et al.*, 2005). Research within this laboratory has provided evidence to suggest

that the liver launches an adaptive defence response to paracetamol that is mediated by Nrf2 (Goldring *et al.*, 2004), findings that have recently been confirmed by a separate research group (Aleksunes *et al.*, 2008). Primed with the knowledge that Nrf2-activating molecules are chemically reactive and capable of modifying sulphydryl groups (Dinkova-Kostova *et al.*, 2001), it was hypothesised that the underyling molecular mechanism by which paracetamol activates the Nrf2-ARE pathway was through the modification of Keap1 by the metabolic intermediate NAPQI. Consistent with this hypothesis, the results presented in chapter 2 demonstrate that NAPQI can directly activate the Nrf2-ARE pathway and induce an adaptive defence response in a mouse liver cell line. Furthermore, the results presented in chapters 4 and 5 show that NAPQI can directly modify cysteine residues within Keap1, in a residue-selective manner, both in recombinant Keap1 protein *in vitro* and in cells. Although further work is required, particularly using cells that possess the metabolic competence required to bioactivate paracetamol to NAPQI *in situ*, these findings support the notion that modification of Keap1 by NAPQI underlies the ability of paracetamol to activate the Nrf2-ARE pathway. Through the analysis of Keap1 modifications by the Nrf2-activating molecules DNCB and 15d-PGJ_2, and by reference to several recent *in vitro* investigations of Keap1 modification by structurally-distinct electrophiles (Dinkova-Kostova *et al.*, 2002; Eggler *et al.*, 2005; Hong *et al.*, 2005a; Hong *et al.*, 2005b; Luo *et al.*, 2007), it has become clear that, although no single cysteine residue in Keap1 is preferentially modified by all of the molecules tested, the adduction of residues within the IVR domain represents a possible unifying theme. Indeed, cell-based models have been used to confirm that activation of Nrf2 by NAPQI, DNCB, 15d-PGJ_2 (chapter 5 of this thesis) and BIA (Hong *et al.*, 2005b) is associated with the selective modification of cysteines within the IVR domain of Keap1. Therefore, although further work is required to characterise the residue-selectivity of Keap1 modification by other Nrf2-activating molecules in cells, and ultimately *in vivo*, it would appear that the modification of cysteine residues within the IVR domain is associated with the activation of Nrf2, and is therefore a possible triggering mechanism for the induction of Nrf2-dependent cell defence.

6.3 The importance of Keap1 modification in the activation of Nrf2

Although it is well-established that Nrf2-activating molecules can modify Keap1, it is important to consider the fate of Keap1 following modification, and the means by which modification may contribute to the activation of Nrf2-dependent cell defence. The formation of high molecular weight forms of Keap1 has been observed following exposure of cells to tBHQ (Zhang *et al.*, 2003) and ebselen (Sakurai *et al.*, 2006), and this phenomenon is prevented through mutation of Cys-151 (Sakurai *et al.*, 2006; Zhang *et al.*, 2003), implying that Cys-151 plays an important role in 'sensing' molecules that promote the formation of high molecular weight Keap1 complexes. It has been postulated that the incorporation of multiple ubiquitin molecules accounts for the increase in molecular weight of Keap1 in response to tBHQ and ebselen. The ubiquitination and degradation of Keap1, via a proteasome-independent pathway, may contribute to the diminished repression of Nrf2 under certain conditions of chemical/oxidative stress (Hong *et al.*, 2005b; Zhang *et al.*, 2005). Molecular deletion of the IVR domain attenuates the ubiquitination of Keap1 following exposure to tBHQ (Zhang *et al.*, 2005), and MS/MS analysis has provided evidence for the ubiquitination of IVR residue Lys-298 (Hong *et al.*, 2005b), further implicating the IVR domain as an important regulatory region of the Keap1 protein. However, it appears that not all Nrf2-activating molecules induce the formation of high molecular weight forms of Keap1 (Hong *et al.*, 2005b; Sakurai *et al.*, 2006; Zhang *et al.*, 2005). Indeed, from the results presented in chapter 5, there was no evidence for the ubiquitination of Keap1-V5 in HEK293T cells following exposure to NAPQI, DNCB or 15d-PGJ_2. Hence, the general importance of Keap1 ubiquitination in the response to chemical/oxidative stress is yet to be fully determined.

When considering the biological consequence(s) of Keap1 modification, it has yet to be demonstrated conclusively that direct modification of Keap1 antagonises its interaction with the ETGE and/or DLG motifs of Nrf2. However, support for this concept has come from recent observations that the reaction of Nrf2-activating molecules with recombinant Keap1 results in a conformational change in the protein, as demonstrated

by alterations in its circular dichroism spectrum (Gao *et al.*, 2007) and tryptophan fluorescence (Dinkova-Kostova *et al.*, 2005b). Recently, Keap1 has been shown to contain thiol-bound zinc, which is displaced following exposure of the protein to Nrf2-activating molecules, and Cys-273 and -288 of Keap1 are important for zinc coordination (Dinkova-Kostova *et al.*, 2005a). Amongst other E3 ubiquitin ligase complexes, MDM2, for example, requires integrity of its protein structure for its ligase activity towards the cell cycle regulator p53, via the coordination of zinc with cysteine residues (Fang *et al.*, 2000). Hence, it is possible that chemical/oxidative stress may promote modification of critical cysteine residues within Keap1, resulting in the displacement of zinc and rendering Keap1 unable to serve as an efficient substrate adaptor for Nrf2 ubiquitination. It has also been suggested that Nrf2-activating molecules can disrupt the ubiquitination of Nrf2 by attenuating the association between Keap1 and CUL3, possibly through induction of conformational changes in the structure of Keap1 (Gao *et al.*, 2007). However, single/multiple mutations of cysteine residues within the IVR domain of Keap1 do not affect its association with CUL3 (Kobayashi *et al.*, 2004), and thus further evidence is required to support this notion.

The S-guanylation of Keap1 by 8-nitroguanosine 3',5'-cyclic monophosphate, a nitrated derivative of cyclic GMP, has recently been demonstrated in cultured cells (Sawa *et al.*, 2007), implying that putative endogenous ligands may interact with Keap1 to activate Nrf2-dependent cell defence in response to oxidative/nitrosative stress. In addition to the concept of direct modification of Keap1 by Nrf2-activating molecules, it has also been suggested that the oxidation of one or more cysteines may lead to the formation of a disulfide-linked Keap1 homodimer, via the intermediate formation of a sulphenic acid (Wakabayashi *et al.*, 2004). Should the oxidation of Keap1 cysteines be confirmed as a mechanism of Nrf2 activation, it is possible that the induction of antioxidant defences (TRX, TRX-R, GR, GSH etc.) by Nrf2 may provide a means of regenerating functional Keap1, through the reduction of oxidised residues, and may therefore represent a feedback loop that limits the extent of Nrf2-ARE pathway activation over time.

6.4 Activation of Nrf2 via mechanisms other than the modification of Keap1

It is important to consider that signaling events other than the modification of Keap1 may contribute to the activation of the Nrf2-ARE pathway. Indeed, it is possible that multiple activation mechanisms have evolved to enable this cytoprotective pathway to respond to a variety of stimuli under diverse cellular conditions. The activation of Nrf2 has been associated with the direct phosphorylation of the transcription factor by PKC (Bloom *et al.*, 2003; Huang *et al.*, 2002; Nguyen *et al.*, 2000), ERK-1 (Papaiahgari *et al.*, 2006) and PERK (Cullinan *et al.*, 2003). Furthermore, the chemical inhibition of phosphatases, which serve to remove phosphate groups from the substrates of protein kinases (for a review, see Hunter, 1995), stimulates activation of the Nrf2-ARE pathway (Nguyen *et al.*, 2003). Therefore, it is possible that the phosphorylation of Nrf2 enables it to evade Keap1-mediated repression. In this regard, Nrf2 may be regulated by a mechanism similar to that of the transcription factor p53 (Nguyen *et al.*, 2004). Under physiological conditions, p53 is directed for ubiquitin-dependent proteasomal degradation via its association with the E3 ligase MDM2, but is phosphorylated in response to DNA damage, weakening its interaction with MDM2 and enabling its stabilisation (Chehab *et al.*, 1999; Unger *et al.*, 1999). Therefore, as with many other cellular processes, the activity of Nrf2 may be regulated by phosphorylation.

The pharmacological inhibition of protein kinase pathways has been used extensively to demonstrate a role for the PKC (Liby *et al.*, 2005; Numazawa *et al.*, 2003), MAPK (Papaiahgari *et al.*, 2004; Yeh *et al.*, 2006; Yuan *et al.*, 2006; Zipper *et al.*, 2003) and PI3K (Kang *et al.*, 2007; Martin *et al.*, 2004; Nakaso *et al.*, 2003; Reichard *et al.*, 2006; Wielandt *et al.*, 2006) pathways in the activation of Nrf2 by specific inducers. It is important to consider that inhibition of a protein kinase pathway will undoubtedly have significant effects on multiple cell signaling processes, which themselves may have an impact upon the integrity of the Nrf2 system. Furthermore, the specificity of some of the small-molecule inhibitors that are commonly used to dissect the involvement of certain protein kinases in a biological process has been questioned (Bain *et al.*, 2003; Bain *et al.*, 2007; Davies *et al.*, 2000). The p38 MAPK inhibitor SB203580 (Alam *et al.*, 2000;

Balogun *et al.*, 2003; Yeh *et al.*, 2006), the ERK MAPK inhibitor PD98059 (Yao *et al.*, 2007; Zipper *et al.*, 2003; Zipper *et al.*, 2000), and the PI3K inhibitor LY294002 (Kang *et al.*, 2002; Lee *et al.*, 2001; Li *et al.*, 2006) have all been used to demonstrate the role of protein kinase cascades in the activation of Nrf2 by certain inducers, despite recent concerns regarding their specificity. Therefore, there are still some questions surrounding the importance of phosphorylation in the activation of Nrf2. What is clear is that no single protein kinase cascade is involved in the activation of Nrf2 by all inducers. Hence, in light of the conflicting evidence regarding the relative contributions of distinct protein kinases to the activation of Nrf2, the importance of phosphorylation in the stimulation of Nrf2 may be chemical, cell or species -dependent in nature. In any case, further work is required to fully define the role of phosphorylation in regulating the activation state of Nrf2. It is possible that the modification of cysteines within Keap1 and the phosphorylation of Nrf2 represent cooperative mechanisms of triggering Nrf2-dependent cell defence. Certain protein kinases are known to be activated in response to oxidative stress, whereas cysteine-based phosphatases are inactivated under such conditions (for reviews, see Nakashima *et al.*, 2002; Salmeen *et al.*, 2005). Therefore, it is plausible that the onset of chemical/oxidative stress may trigger the activation of the Nrf2-ARE pathway via the modification of Keap1, the activation of Nrf2-targeting protein kinases, the inhibition of phosphatases, or indeed a combination of these mechanisms. It will be important to determine the relative contributions of these and other signals in driving the Nrf2 response.

Aside from the concept of post-translational modification, a novel mechanism of Nrf2 activation has been proposed by Karapetian and colleagues (2005), who identified the nuclear protein prothymosin α as a partner for Keap1, an interaction that may displace Nrf2 via competition for Keap1 binding. Although predominantly documented as a cytoplasmic protein (Watai *et al.*, 2007), individual studies have described the nuclear translocation of Keap1 in response to the nuclear export inhibitor leptomycin B and following the molecular mutation of a nuclear export signal (NES) found within the IVR domain of Keap1 (Karapetian *et al.*, 2005; Nguyen *et al.*, 2005; Velichkova *et al.*, 2005). However, conflicting evidence exists regarding the nuclear accumulation of Keap1

following exposure to chemical/oxidative stress (He *et al.*, 2007; Nguyen *et al.*, 2005; Velichkova *et al.*, 2005). Notably, no nuclear localisation signal (NLS) has been identified in Keap1. Therefore, with the exception of experimental conditions under which the NES of Keap1 is repressed, it is not clear under what physiological circumstances Keap1 may localise to the nucleus, although it has been suggested that sub-cellular redistribution may be possible via association with Nrf2, which does possess at least two NLS (Velichkova *et al.*, 2005). Hence, the likelihood of an interaction between Keap1 and prothymosin α requires clarification.

It is notable that investigations into the modification of the components of the Nrf2-ARE pathway by inducers have focused almost exclusively on Keap1, with apparently very little interest in the possibility that Nrf2 itself is directly modified by inducers. It is known that Nrf2 contains a redox-sensitive cysteine (Cys-506) in the Neh1 DNA-binding domain (Bloom *et al.*, 2002). Mutation or oxidation of this residue inhibits the ability of Nrf2 to drive ARE-regulated gene expression (Bloom *et al.*, 2002). Hence, given that Nrf2-activating molecules clearly augment the transactivation of ARE-driven genes, it should be assumed that these molecules do not directly modify Cys-506 of Nrf2, at least under more physiological conditions. Further work is required to determine whether the modification of Cys-506 represents a toxic effect that perturbs the cytoprotective activity of Nrf2 following exposure of cells to very high levels of a xenobiotic. The human and mouse Keap1 proteins contain 27 and 25 cysteines respectively, representing 4.3 and 4.0 % of the 624 total amino acids. In contrast, the human and mouse Nrf2 proteins contain six and seven cysteine residues, respectively, representing 1.0 % and 1.2 % of the 605 and 597 total amino acids. Given that the average cysteine content across all human and mouse proteins is 2.3 % (Miseta *et al.*, 2000), it is apparent that the cysteine content of Keap1 is almost double, whereas that of Nrf2 is almost half, that of most proteins. Notwithstanding the many other cellular proteins that are cysteine-rich, it is possible that, within the confines of the Nrf2-ARE pathway, Keap1 and Nrf2 have evolved with marked differences in cysteine content in order to provide a degree of selectivity for the modification of Keap1 over that of Nrf2,

such that cells can 'sense' and respond to chemical/oxidative stress without the disruption of Nrf2-DNA binding.

6.5 Contribution of the Nrf2-ARE pathway to the physiology of the liver

The Nrf2-ARE cell defence pathway appears to have an important role in the physiology and pathophysiology of the liver (for a review, see Aleksunes *et al.*, 2007). For instance, studies on the effects of model hepatotoxins and hepatocarcinogens in *Nrf2*$^{-/-}$ animals have shown that the integrity of the Nrf2-ARE pathway is vital to enable organisms to withstand exposure to paracetamol (Chan *et al.*, 2001; Enomoto *et al.*, 2001; Okawa *et al.*, 2006), 2-amino-3-methylimidazo[4,5-f]quinoline (Kitamura *et al.*, 2007) and pentachlorophenol (Umemura *et al.*, 2006). Furthermore, the liver appears to launch an adaptive, Nrf2-driven defence response following exposure to model hepatotoxins such as paracetamol and carbon tetrachloride (Fukushima *et al.*, 2006; Goldring *et al.*, 2004; Randle *et al.*, 2008). Evidence has recently emerged to suggest that activation of the Nrf2-ARE pathway represents an early adaptive response to combat alcohol-induced liver injury, following the increase in oxidative stress that is associated with the induction of CYP2E1 by ethanol (Gong *et al.*, 2006). Loss of Nrf2 is also associated with an increase in levels of lipid peroxidation and DNA damage in the liver, probably due to a compromised ability to nullify oxidative stress (Li *et al.*, 2004). Therefore, the Nrf2-ARE pathway appears to serve a vital protective role against toxic insult in the liver, as indeed it does in many other tissues within the body.

For some drugs, including isoniazid, halothane and allyl alcohol, there is a well-established increase in the risk of DILI with age (Banks *et al.*, 1995; Dalu *et al.*, 1995; Maddrey, 2005; Mitchell *et al.*, 1976; Mooney *et al.*, 1985; Rikans, 1984; Schenker *et al.*, 1994; Tarazi *et al.*, 1993). The process of aging is also associated with a decline in the cytoprotective activity of Nrf2 (Shih *et al.*, 2007; Suh *et al.*, 2004; Zaman *et al.*, 2007). It is possible, therefore, that a gradual reduction in the protective capacity of the Nrf2-ARE pathway may contribute to the link between age and susceptibility to the

DILI caused by some drugs. The age-related decline in Nrf2 activity may also be an important consideration in the transplantation of organs, as low levels of *Nrf2* mRNA in the livers of older donors have been linked to reduced organ function following transplantation (Zaman *et al.*, 2007). Nrf2 may serve an important role in the process of tissue repair, as liver regeneration is impaired, following partial hepatectomy, in mice lacking Nrf2 (Beyer *et al.*, 2008). It appears that accumulation of ROS in the injured Nrf2-deficient liver reduces tyrosine phosphorylation of insulin receptor substrates 1 and 2, preventing stimulation of insulin-like growth factor 1 receptor (Beyer *et al.*, 2008). As a result, PI3K-mediated phosphorylation, and thus activation, of the protein kinase AKT and its downstream targets is reduced (Beyer *et al.*, 2008), therefore inhibiting cell proliferation and survival (Lawlor *et al.*, 2001). Hence, it would appear that the Nrf2-ARE pathway has several important roles in maintaining the physiological integrity of the liver, and in protecting it against deleterious toxic insults, such as those which may cause DILI. As such, the therapeutic targeting of the Nrf2-ARE pathway, either prophylactically or immediately following exposure to a hepatotoxin/carcinogen, may prove to be a worthwhile strategy for the prevention and/or treatment of DILI. Consistent with this notion, the synthetic triterpenoid CDDO-imidazolide, which is a potent inducer of the Nrf2-ARE pathway, has recently been shown to protect against aflatoxin-induced hepatocarcinogenesis in rats (Yates *et al.*, 2006). Furthermore, pharmacological manipulation of Nrf2 by the isothiocyanate sulforaphane, a derivative of glucoraphanin, which is present at high concentrations in broccoli, Brussels sprouts and cabbage (Zhang *et al.*, 1992), is currently being trialed as a means of preventing breast cancer (Cornblatt *et al.*, 2007; Dinkova-Kostova *et al.*, 2007; Dinkova-Kostova *et al.*, 2006; Shapiro *et al.*, 2006).

6.6 Future directions

Since Nrf2 was first characterised by Moi *et al.* (1994), there have been huge advances in our understanding of the chemical, biochemical and molecular means by which the Nrf2-ARE pathway is regulated. This thesis has sought to further define the importance

of direct modification of Keap1 in the activation of Nrf2. Future research should consider the relative importance of different post-translational modifications (direct adduction, oxidation, phosphorylation) in triggering Nrf2 activation, and the precise means by which these modifications are translated into biological effect. However, before further studies are undertaken in this area, it is vital that the native redox states of the cysteine residues in Keap1 are fully defined. In this regard, there may be value in developing a differential chemical capping approach, similar to that used in section 3.3.4 of this thesis, to define those cysteines that are free for modification and those that participate in disulphide bonds in the correctly-folded protein. The recombinant Keap1 protein expressed and purified under non-denaturing conditions, described in section 3.3.5, may be suitable for such an application. It will also be important to determine which cysteine residues are located on the solvent-accessible surfaces of Keap1, as it is these residues which are likely to be the most susceptible to modification. Of course, it should be considered that interactions with protein partners, including Nrf2, CUL3 and actin, may conceal otherwise accessible cysteines in Keap1. Therefore, it may be useful to create an *in vitro* reconstruction of the Nrf2-CUL3-Keap1-actin complex, and to identify the cysteine residues that are labelled. It is important that these experiments are performed promptly, so that a more representative *in vitro* test system can be designed, and so as to gain a better understanding of the value of extrapolating recent *in vitro* findings (Dinkova-Kostova *et al.*, 2002; Eggler *et al.*, 2005; Hong *et al.*, 2005a; Luo *et al.*, 2007) to a cellular and *in vivo* context.

Although there is strong evidence to suggest that Nrf2-activating molecules selectively modify cysteine residues in Keap1 (Dinkova-Kostova *et al.*, 2002; Eggler *et al.*, 2005; Hong *et al.*, 2005a; Hong *et al.*, 2005b; Luo *et al.*, 2007), it has yet to be demonstrated unequivocally that modification of Keap1 triggers the activation of Nrf2 in cells or *in vivo*. The major bioanalytical constraint that hampers the investigation of protein modification and function in parallel is that modifications are often substoichiometric in nature, with only as much as 1-2 % of the total amount of a given protein modified under physiological conditions. This problem can be further compounded by the fact that modifications are often lost through the processes of protein turnover and repair

(Schoneich *et al.*, 2006). This makes it particularly difficult to detect a modified protein, and even more difficult to identify the site of modification, from a cell/tissue lysate containing thousands of proteins with different levels of abundance. In a recent review on this subject, Liebler (2008) likened this problem to "looking for dozens of needles in thousand of haystacks". It is for this reason that many investigators seeking to define the impact of post-translational modification(s) on the activity of a given protein have opted initially to conduct experiments using recombinant protein, which can be expressed at relatively high levels and purified to near homogeneity via an incorporated epitope tag. Although useful for gaining a chemical insight into the modification of a protein in isolation, the *in vitro* reaction of a large amount of protein with a high concentration of electrophile is not indicative of the situation in cells and *in vivo*. Therefore, the enrichment of endogenous proteins is required in order to facilitate the reliable and sensitive analysis of relatively low-abundance post-translational modifications. Such enrichment strategies can be as simple as decreasing the overall complexity of the sample through biochemical purification of subcellular compartments and organelles. In addition, chemically-adapted model electrophiles, such as biotinylated analogues of iodoacetamide and N-ethylmaleimide (Dennehy *et al.*, 2006; Shin *et al.*, 2007), have been developed that enable affinity enrichment of modified proteins. However, such an approach may not be particularly valuable for investigations of protein modification by xenobiotics and intracellular signalling molecules, as these would also need to be chemically tagged. This may prove practically difficult, and it is not clear what effect the presence of such a tag has on the reactivity of an electrophile.

In light of the unsuitability of some pre-analytical enrichment strategies for examining the modification of native proteins in cells and tissues, advances have been made in the field of mass spectrometry that have effectively increased the specificity and the sensitivity of this already powerful analytical tool. One such advance is the process of multiple reaction monitoring (MRM), whereby predefined target ions, such as those that represent modified peptides, are selected and enriched within the mass spectrometer during the analytical run. Because only ions of a predefined mass-to-charge ratio are filtered into the collision cell of the mass spectrometer, and fragmented product ions can

be trapped and ejected towards the mass detector at a given threshold, background signals are lowered significantly, and thus signal-to-noise ratios are increased, allowing more sensitive detection of modified peptides (Unwin *et al.*, 2005). In this regard, the prior characterisation of residue-specific modifications *in vitro* using recombinant proteins may better inform cellular and *in vivo* analyses, by identifying diagnostic data patterns that help to define specific ions to be selected during the MRM process. Research within our group has recently demonstrated the potential of MRM as a means of detecting post-translational modifications *in vivo*, using mouse GSTP1-1 as a model protein (Jenkins *et al.*, 2008). Although the feasibility of using MRM to detect modification of proteins that are much lower in abundance than GSTP1-1, such as Keap1, is still unclear, advances in the sampling rate, sensitivity and resolution of mass spectrometers are now beginning to enable the characterisation of endogenous protein modification in cells and tissues (Ji *et al.*, 2007; Koen *et al.*, 2006; Lemercier *et al.*, 2004; Meier *et al.*, 2007; Meier *et al.*, 2005; Shin *et al.*, 2007).

In addition to correlating the activation of Nrf2 with the occurrence of a particular modification *per se*, it will also be important to understand how the extent of modification influences the biological response. It is possible that Keap1 functions as a redox rheostat, in that the modification of a single highly reactive 'sensor' cysteine within the IVR domain is sufficient to trigger the activation of Nrf2, with additional modifications of other cysteine residues augmenting this response. In this regard, it is vital to obtain quantitative measurements of the ratio of modified versus unmodified residues in Keap1, and to relate this to biological outcome. This may be possible through the use of stable isotope labelling of Keap1 cysteines by isotope-coded affinity tagging (ICAT), in which heavy and light -tagged model electrophiles are applied to the protein or cell extract under different conditions (i.e. unmodified control sample = light-tagged, modified sample = heavy-tagged). Both samples are mixed and the mass differences resolved by mass spectrometry, in order to quantify their relative abundance (Sethuraman *et al.*, 2004a; Sethuraman *et al.*, 2004b). If a particular cysteine residue in Keap1 is modified, it will not be available for ICAT labelling, and the abundance of the modified peptide ion will decrease relative to that of the unmodified ion.

As discussed in section 6.4, it is important to consider that signaling events other than the direct modification of Keap1 may contribute to the activation of the Nrf2-ARE pathway by some inducers. Recently, much attention has focused on the importance of reversible oxidation of thiols (to sulphenic acid; -SOH) as a signalling mechanism within cells (for a review, see Biswas *et al.*, 2006). In fact, there is evidence to suggest that pro-oxidants can activate Nrf2 (Gong *et al.*, 2006; Lee-Hilz *et al.*, 2006; Purdom-Dickinson *et al.*, 2007), and oxidation of protein thiols has been proposed as a means by which NAPQI induces hepatocellular dysfunction (for a review, see Jaeschke *et al.*, 2003). Therefore, it is possible that both direct adduction and oxidation of Keap1 are important in the activation of Nrf2 by NAPQI. The *in vitro* and cell-based assays developed during this thesis to study direct adduction of Keap1 may be suitable tools for investigating the role of oxidation in the activation of Nrf2. Residue-specific oxidation can be detected by mass spectrometric measurement of the relevant mass shifts (+16 Da for -SOH, +32 Da for $-SO_2H$, +48 Da for $-SO_3H$), although the detection of reversible -SOH formation is complicated by the lability of this modification. However, -SOH trapping agents are available, such as 5,5-dimethyl-1,3-cyclohexanedione, which reacts with -SOH to form a stable thioether (Allison, 1976) that can be detected by mass spectrometry (+138 Da). In addition, -SOH can be detected following reaction with arsenite, which does not affect disulphides, but reduces -SOH back to -SH, which can then be labelled for detection (Torchinsky, 1981). These and other tools may facilitate investigations into the role of Keap1 oxidation in the activation of Nrf2.

A switch in the ubiquitination of Nrf2 to that of Keap1 has been suggested as a means by which some molecules antagonise Keap1-mediated repression of the transcription factor (Hong *et al.*, 2005b; Zhang *et al.*, 2005). However, the general importance of this mechanism is not yet clear. Ubiquitination can be detected by way of a Gly-Gly dipeptide tag (+114 Da) that remains attached to the modified lysine residue following tryptic digestion (Peng *et al.*, 2003). This principle of diagnostic mass shifts also enables the mass spectrometric detection of residue-specific phosphorylation (HPO_3; +80 Da), and this is important because there is much ambiguity surrounding the importance of direct phosphorylation of Nrf2 in the activation of the transcription factor by some

inducers. Therefore, much work remains to be done in defining the relative contributions of these and other post-translational modifications in the activation of Nrf2. These important questions may be addressed, in order to advance our appreciation of the means by which the Nrf2-ARE pathway is regulated, once the relevant bioanalytical constraints are surmounted.

6.7 Concluding remarks

In summary, the main aims of the studies presented in this thesis were to further our understanding of the means by which the Nrf2-ARE pathway is regulated, and to elucidate its role in the protection against DILI. Specifically, investigations have been undertaken in an attempt to elucidate the molecular mechanisms by which paracetamol, which causes DILI in overdose, activates the Nrf2-ARE pathway in mouse liver. The results presented in this thesis have demonstrated that NAPQI, the hepatotoxic metabolite of paracetamol, can directly activate the Nrf2-ARE cell defence pathway in mouse liver cells, and selectively modifies cysteines residues within Keap1, both in the recombinant protein *in vitro* and in a cell-based model. In determining the residue-selectivity of Keap1 modification in cells by NAPQI and other Nrf2-activating molecules, and taking into account the recent work of Hong *et al.* (2005b), a unifying theme has been observed, in that all of the molecules tested modify one or more cysteines within the IVR domain of Keap1. The identification of a universal triggering mechanism may better facilitate the targeting of the Nrf2-ARE pathway for the prevention and/or treatment of diseases, such as DILI, in the near future. Furthermore, a better understanding of the molecular mechanisms that govern the activity of the Nrf2-ARE pathway may facilitate its incorporation into pre-clinical screens for novel xenobiotics that are likely to cause chemical/oxidative stress and thus pose a risk of toxicity in patients.

In light of the important role of the Nrf2-ARE pathway in regulating inducible, and perhaps basal, cell defence, genetic variation in this pathway may have important

consequences for human health. Research in this laboratory has identified several novel, albeit synonymous, polymorphisms in the genes encoding *Nrf2* and *Keap1*, through the screening of a cohort of healthy human volunteers (Wang *et al.*, 2006). Single nucleotide polymorphisms have been identified within the promoter region of the human (Arisawa *et al.*, 2007; Marzec *et al.*, 2007; Yamamoto *et al.*, 2004) and mouse (Cho *et al.*, 2002) *Nrf2* genes, and these mutations are associated with an increase in susceptibility to certain diseases (Arisawa *et al.*, 2007; Arisawa *et al.*, 2008; Cho *et al.*, 2002; Marzec *et al.*, 2007). Furthermore, two non-synonymous mutations in *Nrf2* have recently been identified in Japanese type II diabetes patients (Fukushima-Uesaka et al., 2007), and somatic loss-of-function mutations in *Keap1* have been identified in lung and breast carcinoma cell lines and in lung cancer patients (Nioi *et al.*, 2007; Padmanabhan *et al.*, 2006; Singh *et al.*, 2006). It will be important to determine whether there is variability in the competence of the Nrf2-ARE pathway amongst the general population, and whether such variability influences an individual's susceptibility to an adverse drug reaction. The design of safe and effective treatment regimens is critically dependent on our understanding of the chemical, biochemical and molecular mechanisms that underlie physiological processes and the actions of specific drugs. Therefore, if future work does reveal a degree of inter-individual variability in the competence of the Nrf2-ARE pathway, the development of a diagnostic screen, perhaps based on the establishment of a biomarker for the functionality of the Nrf2-ARE pathway, may contribute to the advancement of 'personalised medicine', by allowing clinicians to identify susceptible patients before, and not after, the onset of an adverse drug reaction.

APPENDIX

MS/MS spectra depicting modification of GSTP1-1 Cys-47 by 15d-PGJ$_2$, iodoacetamide, NAPQI and DNCB

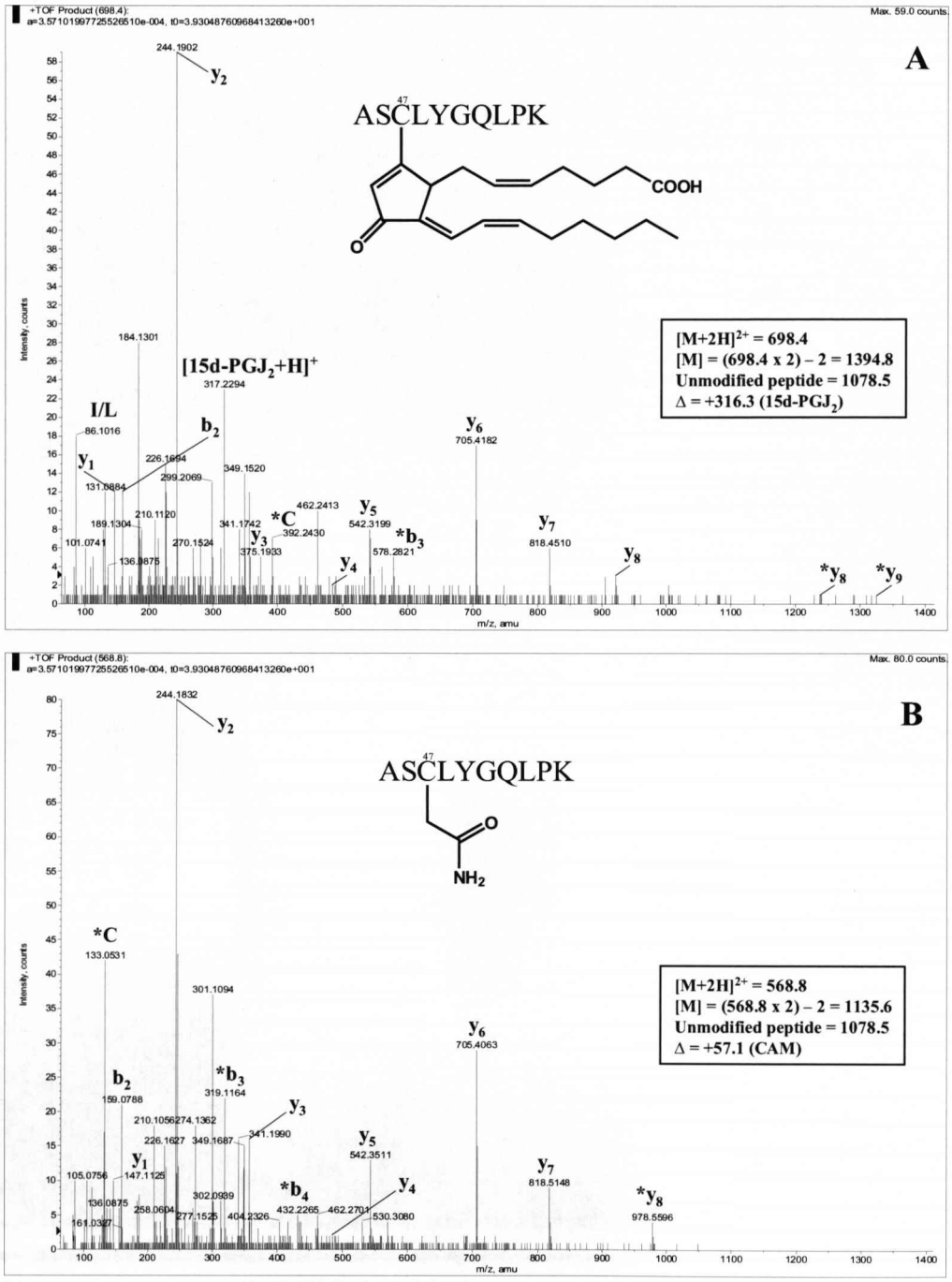

Appendix Fig. 1 - MS/MS spectrum indicating modification of GSTP1-1 Cys-47 by 15d-PGJ$_2$ (A) or iodoacetamide (B) *in vitro*. y- and b-ions are labelled where present. * denotes ions for which a mass shift of +316.2 amu indicates modification by 15d-PGJ$_2$ (A) or +57.1 amu indicates modification by iodoacetamide (B). Immonium ions are labelled with the one-letter code for their corresponding amino acid. Note: both the singly-charged 15d-PGJ$_2$ ion (317.2 amu), characteristic of adduct cleavage during MS/MS peptide fragmentation, and the cysteine-15d-PGJ$_2$ immonium ion (392.2 amu) are absent following incubation of GSTP1-1 with iodoacetamide alone.

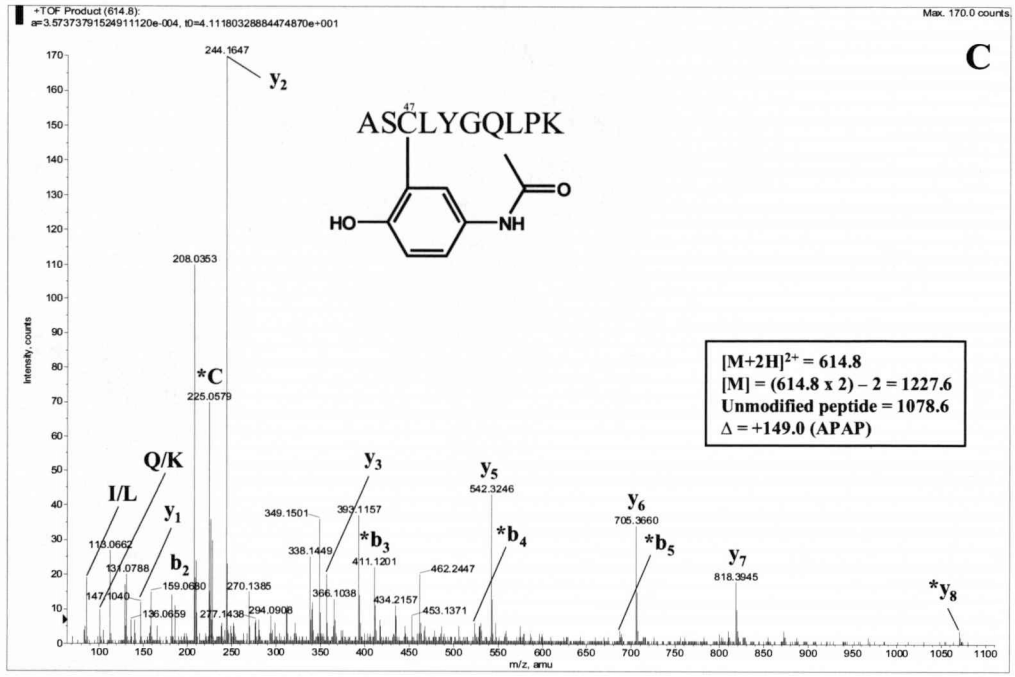

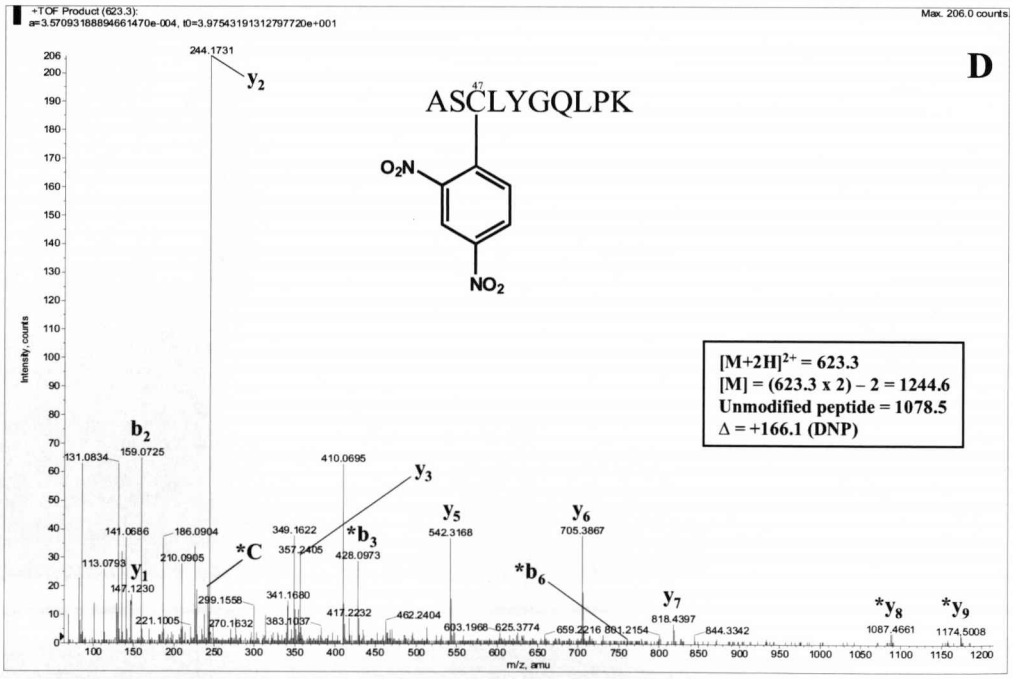

Appendix Fig. 1 - MS/MS spectrum indicating modification of GSTP1-1 Cys-47 by NAPQI (C) or DNCB (D) *in vitro*. y- and b-ions are labelled where present. * denotes ions for which a mass shift of +149.1 amu indicates modification by NAPQI (C) or +166.0 amu indicates modification by DNCB (D). Immonium ions are labelled with the one-letter code for their corresponding amino acid.

BIBLIOGRAPHY

Abate, C, Patel, L, Rauscher, FJ, 3rd, Curran, T (1990). Redox regulation of fos and jun DNA-binding activity in vitro. *Science* **249:** 1157-61.

Abraham, J, Kelly, J, Thibault, P, Benchimol, S (2000). Post-translational modification of p53 protein in response to ionizing radiation analyzed by mass spectrometry. *J Mol Biol* **295:** 853-64.

Ahlfors, SR, Kristiansson, MH, Lindh, CH, Jonsson, BA, Hansson, C (2005). Adducts between nucleophilic amino acids and hexahydrophthalic anhydride, a structure inducing both types I and IV allergy. *Biomarkers* **10:** 321-35.

Alam, J, Killeen, E, Gong, P, Naquin, R, Hu, B, Stewart, D, Ingelfinger, JR, Nath, KA (2003). Heme activates the heme oxygenase-1 gene in renal epithelial cells by stabilizing Nrf2. *Am J Physiol Renal Physiol* **284:** F743-52.

Alam, J, Stewart, D, Touchard, C, Boinapally, S, Choi, AM, Cook, JL (1999). Nrf2, a Cap'n'Collar transcription factor, regulates induction of the heme oxygenase-1 gene. *J Biol Chem* **274:** 26071-8.

Alam, J, Wicks, C, Stewart, D, Gong, P, Touchard, C, Otterbein, S, Choi, AM, Burow, ME, Tou, J (2000). Mechanism of heme oxygenase-1 gene activation by cadmium in MCF-7 mammary epithelial cells. Role of p38 kinase and Nrf2 transcription factor. *J Biol Chem* **275:** 27694-702.

Albano, E, Rundgren, M, Harvison, PJ, Nelson, SD, Moldeus, P (1985). Mechanisms of N-acetyl-p-benzoquinone imine cytotoxicity. *Mol Pharmacol* **28:** 306-11.

Aleksunes, LM, Manautou, JE (2007). Emerging role of Nrf2 in protecting against hepatic and gastrointestinal disease. *Toxicol Pathol* **35:** 459-73.

Aleksunes, LM, Slitt, AL, Maher, JM, Augustine, LM, Goedken, MJ, Chan, JY, Cherrington, NJ, Klaassen, CD, Manautou, JE (2008). Induction of Mrp3 and Mrp4 transporters during acetaminophen hepatotoxicity is dependent on Nrf2. *Toxicol Appl Pharmacol* **226:** 74-83.

Allison, WS (1976). Formation and reactions of sulfenic acids in proteins. *Acc Chem Res* **9:** 293-299.

Andersson, BS, Rundgren, M, Nelson, SD, Harder, S (1990). N-acetyl-p-benzoquinone imine-induced changes in the energy metabolism in hepatocytes. *Chem Biol Interact* **75:** 201-11.

Aono, J, Yanagawa, T, Itoh, K, Li, B, Yoshida, H, Kumagai, Y, Yamamoto, M, Ishii, T (2003). Activation of Nrf2 and accumulation of ubiquitinated A170 by arsenic in osteoblasts. *Biochem Biophys Res Commun* **305:** 271-7.

Arisawa, T, Tahara, T, Shibata, T, Nagasaka, M, Nakamura, M, Kamiya, Y, Fujita, H, Yoshioka, D, Arima, Y, Okubo, M, Hirata, I, Nakano, H (2007). Association between promoter polymorphisms of nuclear factor-erythroid 2-related factor 2 gene and peptic ulcer diseases. *Int J Mol Med* **20:** 849-53.

Arisawa, T, Tahara, T, Shibata, T, Nagasaka, M, Nakamura, M, Kamiya, Y, Fujita, H, Yoshioka, D, Arima, Y, Okubo, M, Hirata, I, Nakano, H (2008). The influence of promoter polymorphism of nuclear factor-erythroid 2-related factor 2 gene on the aberrant DNA methylation in gastric epithelium. *Oncol Rep* **19:** 211-6.

Arnau, J, Lauritzen, C, Petersen, GE, Pedersen, J (2006). Current strategies for the use of affinity tags and tag removal for the purification of recombinant proteins. *Protein Expr Purif* **48:** 1-13.

Babic, I, Jakymiw, A, Fujita, DJ (2004). The RNA binding protein Sam68 is acetylated in tumor cell lines, and its acetylation correlates with enhanced RNA binding activity. *Oncogene* **23:** 3781-9.

Bain, J, McLauchlan, H, Elliott, M, Cohen, P (2003). The specificities of protein kinase inhibitors: an update. *Biochem J* **371:** 199-204.

Bain, J, Plater, L, Elliott, M, Shpiro, N, Hastie, J, McLauchlan, H, Klevernic, I, Arthur, S, Alessi, D, Cohen, P (2007). The selectivity of protein kinase inhibitors; a further update. *Biochem J*: Sep 13 [Epub ahead of print].

Balogun, E, Hoque, M, Gong, P, Killeen, E, Green, CJ, Foresti, R, Alam, J, Motterlini, R (2003). Curcumin activates the haem oxygenase-1 gene via regulation of Nrf2 and the antioxidant-responsive element. *Biochem J* **371:** 887-95.

Baneyx, F (1999). Recombinant protein expression in Escherichia coli. *Curr Opin Biotechnol* **10:** 411-21.

Banks, AT, Zimmerman, HJ, Ishak, KG, Harter, JG (1995). Diclofenac-associated hepatotoxicity: analysis of 180 cases reported to the Food and Drug Administration as adverse reactions. *Hepatology* **22:** 820-7.

Banning, A, Deubel, S, Kluth, D, Zhou, Z, Brigelius-Flohe, R (2005). The GI-GPx gene is a target for Nrf2. *Mol Cell Biol* **25:** 4914-23.

Bannister, AJ, Kouzarides, T (1996). The CBP co-activator is a histone acetyltransferase. *Nature* **384:** 641-3.

Bender, RP, Lindsey, RH, Jr., Burden, DA, Osheroff, N (2004). N-acetyl-p-benzoquinone imine, the toxic metabolite of acetaminophen, is a topoisomerase II poison. *Biochemistry* **43:** 3731-9.

Bernstein, E, Caudy, AA, Hammond, SM, Hannon, GJ (2001). Role for a bidentate ribonuclease in the initiation step of RNA interference. *Nature* **409:** 363-6.

Bessems, JG, Vermeulen, NP (2001). Paracetamol (acetaminophen)-induced toxicity: molecular and biochemical mechanisms, analogues and protective approaches. *Crit Rev Toxicol* **31:** 55-138.

Beyer, TA, Xu, W, Teupser, D, auf dem Keller, U, Bugnon, P, Hildt, E, Thiery, J, Kan, YW, Werner, S (2008). Impaired liver regeneration in Nrf2 knockout mice: role of ROS-mediated insulin/IGF-1 resistance. *Embo J* **27:** 212-23.

Beynon, RJ (2005). A simple tool for drawing proteolytic peptide maps. *Bioinformatics* **21:** 674-5.

Birge, RB, Bartolone, JB, Nishanian, EV, Bruno, MK, Mangold, JB, Cohen, SD, Khairallah, EA (1988). Dissociation of covalent binding from the oxidative effects of acetaminophen. Studies using dimethylated acetaminophen derivatives. *Biochem Pharmacol* **37:** 3383-93.

Biswal, S, Acquaah-Mensah, G, Datta, K, Wu, X, Kehrer, JP (2002). Inhibition of cell proliferation and AP-1 activity by acrolein in human A549 lung adenocarcinoma cells due to thiol imbalance and covalent modifications. *Chem Res Toxicol* **15:** 180-6.

Biswas, S, Chida, AS, Rahman, I (2006). Redox modifications of protein-thiols: Emerging roles in cell signaling. *Biochem Pharmacol* **71:** 551-564.

Bjorck, L, Kronvall, G (1984). Purification and some properties of streptococcal protein G, a novel IgG-binding reagent. *J Immunol* **133:** 969-74.

Blank, M, Shiloh, Y (2007). Programs for cell death: apoptosis is only one way to go. *Cell Cycle* **6:** 686-95.

Bloom, D, Dhakshinamoorthy, S, Jaiswal, AK (2002). Site-directed mutagenesis of cysteine to serine in the DNA binding region of Nrf2 decreases its capacity to upregulate antioxidant response element-mediated expression and antioxidant induction of NAD(P)H:quinone oxidoreductase1 gene. *Oncogene* **21:** 2191-200.

Bloom, DA, Jaiswal, AK (2003). Phosphorylation of Nrf2 at Ser40 by protein kinase C in response to antioxidants leads to the release of Nrf2 from INrf2, but is not required for Nrf2 stabilization/accumulation in the nucleus and transcriptional activation of antioxidant response element-mediated NAD(P)H:quinone oxidoreductase-1 gene expression. *J Biol Chem* **278:** 44675-82.

Boelsterli, UA (2003). Diclofenac-induced liver injury: a paradigm of idiosyncratic drug toxicity. *Toxicol Appl Pharmacol* **192:** 307-22.

Bolgar, MS, Yang, CY, Gaskell, SJ (1996). First direct evidence for lipid/protein conjugation in oxidized human low density lipoprotein. *J Biol Chem* **271:** 27999-8001.

Botting, R (2000a). Paracetamol-inhibitable COX-2. *J Physiol Pharmacol* **51:** 609-18.

Botting, RM (2000b). Mechanism of action of acetaminophen: is there a cyclooxygenase 3? *Clin Infect Dis* **31 Suppl 5:** S202-10.

Boulares, HA, Giardina, C, Navarro, CL, Khairallah, EA, Cohen, SD (1999). Modulation of serum growth factor signal transduction in Hepa 1-6 cells by acetaminophen: an inhibition of c-myc expression, NF-kappaB activation, and Raf-1 kinase activity. *Toxicol Sci* **48:** 264-74.

Boutaud, O, Aronoff, DM, Richardson, JH, Marnett, LJ, Oates, JA (2002). Determinants of the cellular specificity of acetaminophen as an inhibitor of prostaglandin H(2) synthases. *Proc Natl Acad Sci U S A* **99:** 7130-5.

Bradford, MM (1976). A rapid and sensitive method for the quantitation of microgram quantities of protein utilizing the principle of protein-dye binding. *Anal Biochem* **72:** 248-54.

Brady, JT, Montelius, DA, Beierschmitt, WP, Wyand, DS, Khairallah, EA, Cohen, SD (1988). Effect of piperonyl butoxide post-treatment on acetaminophen hepatotoxicity. *Biochem Pharmacol* **37:** 2097-9.

Bridge, AJ, Pebernard, S, Ducraux, A, Nicoulaz, AL, Iggo, R (2003). Induction of an interferon response by RNAi vectors in mammalian cells. *Nat Genet* **34:** 263-4.

Brinegar, AC, Kinsella, JE (1981). Reversible modification of lysine in beta-lactoglobulin using citraconic anhydride. Effects on the sulfhydryl groups. *Int J Pept Protein Res* **18:** 18-25.

Buckley, BJ, Marshall, ZM, Whorton, AR (2003). Nitric oxide stimulates Nrf2 nuclear translocation in vascular endothelium. *Biochem Biophys Res Commun* **307:** 973-9.

Budihardjo, I, Oliver, H, Lutter, M, Luo, X, Wang, X (1999). Biochemical pathways of caspase activation during apoptosis. *Annu Rev Cell Dev Biol* **15:** 269-90.

Burk, RF, Hill, KE, Hunt, RW, Jr., Martin, AE (1990). Isoniazid potentiation of acetaminophen hepatotoxicity in the rat and 4-methylpyrazole inhibition of it. *Res Commun Chem Pathol Pharmacol* **69:** 115-8.

Cao, TT, Ma, L, Kandpal, G, Warren, L, Hess, JF, Seabrook, GR (2005). Increased nuclear factor-erythroid 2 p45-related factor 2 activity protects SH-SY5Y cells against oxidative damage. *J Neurochem* **95:** 406-17.

Cernuda-Morollon, E, Pineda-Molina, E, Canada, FJ, Perez-Sala, D (2001). 15-Deoxy-Delta 12,14-prostaglandin J2 inhibition of NF-kappaB-DNA binding through covalent modification of the p50 subunit. *J Biol Chem* **276:** 35530-6.

Chan, JY, Kwong, M (2000). Impaired expression of glutathione synthetic enzyme genes in mice with targeted deletion of the Nrf2 basic-leucine zipper protein. *Biochim Biophys Acta* **1517:** 19-26.

Chan, JY, Kwong, M, Lu, R, Chang, J, Wang, B, Yen, TS, Kan, YW (1998). Targeted disruption of the ubiquitous CNC-bZIP transcription factor, Nrf-1, results in anemia and embryonic lethality in mice. *EMBO J* **17:** 1779-87.

Chan, K, Han, XD, Kan, YW (2001). An important function of Nrf2 in combating oxidative stress: detoxification of acetaminophen. *Proc Natl Acad Sci U S A* **98:** 4611-6.

Chan, K, Kan, YW (1999). Nrf2 is essential for protection against acute pulmonary injury in mice. *Proc Natl Acad Sci U S A* **96:** 12731-6.

Chan, K, Lu, R, Chang, JC, Kan, YW (1996). NRF2, a member of the NFE2 family of transcription factors, is not essential for murine erythropoiesis, growth, and development. *Proc Natl Acad Sci U S A* **93:** 13943-8.

Chanas, SA, Jiang, Q, McMahon, M, McWalter, GK, McLellan, LI, Elcombe, CR, Henderson, CJ, Wolf, CR, Moffat, GJ, Itoh, K, Yamamoto, M, Hayes, JD (2002). Loss of the Nrf2 transcription factor causes a marked reduction in constitutive and inducible expression of the glutathione S-transferase Gsta1, Gsta2, Gstm1, Gstm2, Gstm3 and Gstm4 genes in the livers of male and female mice. *Biochem J* **365:** 405-16.

Chandra, J, Samali, A, Orrenius, S (2000). Triggering and modulation of apoptosis by oxidative stress. *Free Radic Biol Med* **29:** 323-33.

Chehab, NH, Malikzay, A, Stavridi, ES, Halazonetis, TD (1999). Phosphorylation of Ser-20 mediates stabilization of human p53 in response to DNA damage. *Proc Natl Acad Sci U S A* **96:** 13777-82.

Chen, C, Pung, D, Leong, V, Hebbar, V, Shen, G, Nair, S, Li, W, Kong, AN (2004). Induction of detoxifying enzymes by garlic organosulfur compounds through transcription factor Nrf2: effect of chemical structure and stress signals. *Free Radic Biol Med* **37:** 1578-90.

Chen, J, Regan, RF (2005a). Increasing expression of heme oxygenase-1 by proteasome inhibition protects astrocytes from heme-mediated oxidative injury. *Curr Neurovasc Res* **2:** 189-96.

Chen, ZH, Saito, Y, Yoshida, Y, Sekine, A, Noguchi, N, Niki, E (2005b). 4-Hydroxynonenal induces adaptive response and enhances PC12 cell tolerance primarily through induction of thioredoxin reductase 1 via activation of Nrf2. *J Biol Chem* **280:** 41921-7.

Chen, ZH, Yoshida, Y, Saito, Y, Sekine, A, Noguchi, N, Niki, E (2006). Induction of adaptive response and enhancement of PC12 cell tolerance by 7-hydroxycholesterol and 15-deoxy-delta(12,14)-prostaglandin J2 through up-regulation of cellular glutathione via different mechanisms. *J Biol Chem* **281:** 14440-5.

Chien, JY, Thummel, KE, Slattery, JT (1997). Pharmacokinetic consequences of induction of CYP2E1 by ligand stabilization. *Drug Metab Dispos* **25:** 1165-75.

Cho, HY, Jedlicka, AE, Reddy, SP, Kensler, TW, Yamamoto, M, Zhang, LY, Kleeberger, SR (2002a). Role of NRF2 in protection against hyperoxic lung injury in mice. *Am J Respir Cell Mol Biol* **26:** 175-82.

Cho, HY, Jedlicka, AE, Reddy, SP, Zhang, LY, Kensler, TW, Kleeberger, SR (2002b). Linkage analysis of susceptibility to hyperoxia. Nrf2 is a candidate gene. *Am J Respir Cell Mol Biol* **26:** 42-51.

Choi, H, Kim, S, Mukhopadhyay, P, Cho, S, Woo, J, Storz, G, Ryu, S (2001). Structural basis of the redox switch in the OxyR transcription factor. *Cell* **105:** 103-13.

Chojkier, M (2005). Troglitazone and liver injury: in search of answers. *Hepatology* **41:** 237-46.

Chomczynski, P, Sacchi, N (1987). Single-step method of RNA isolation by acid guanidinium thiocyanate-phenol-chloroform extraction. *Anal Biochem* **162:** 156-9.

Cohen, P, Holmes, CF, Tsukitani, Y (1990). Okadaic acid: a new probe for the study of cellular regulation. *Trends Biochem Sci* **15:** 98-102.

Coles, B, Wilson, I, Wardman, P, Hinson, JA, Nelson, SD, Ketterer, B (1988). The spontaneous and enzymatic reaction of N-acetyl-p-benzoquinonimine with glutathione: a stopped-flow kinetic study. *Arch Biochem Biophys* **264:** 253-60.

Cooper, CE, Patel, RP, Brookes, PS, Darley-Usmar, VM (2002). Nanotransducers in cellular redox signaling: modification of thiols by reactive oxygen and nitrogen species. *Trends Biochem Sci* **27:** 489-92.

Copple, IM, Goldring, CE, Kitteringham, NR, Park, BK (2008). The Nrf2-Keap1 defence pathway: Role in protection against drug-induced toxicity. *Toxicology* **246:** 24-33.

Cornblatt, BS, Ye, L, Dinkova-Kostova, AT, Erb, M, Fahey, JW, Singh, NK, Chen, MS, Stierer, T, Garrett-Mayer, E, Argani, P, Davidson, NE, Talalay, P, Kensler, TW, Visvanathan, K (2007). Preclinical and clinical evaluation of sulforaphane for chemoprevention in the breast. *Carcinogenesis* **28:** 1485-90.

Cullinan, SB, Gordan, JD, Jin, J, Harper, JW, Diehl, JA (2004). The Keap1-BTB protein is an adaptor that bridges Nrf2 to a Cul3-based E3 ligase: oxidative stress sensing by a Cul3-Keap1 ligase. *Mol Cell Biol* **24:** 8477-86.

Cullinan, SB, Zhang, D, Hannink, M, Arvisais, E, Kaufman, RJ, Diehl, JA (2003). Nrf2 is a direct PERK substrate and effector of PERK-dependent cell survival. *Mol Cell Biol* **23:** 7198-209.

Dahlin, DC, Miwa, GT, Lu, AY, Nelson, SD (1984). N-acetyl-p-benzoquinone imine: a cytochrome P-450-mediated oxidation product of acetaminophen. *Proc Natl Acad Sci U S A* **81:** 1327-31.

Dalu, A, Warbritton, A, Bucci, TJ, Mehendale, HM (1995). Age-related susceptibility to chlordecone-potentiated carbon tetrachloride hepatotoxicity and lethality is due to hepatic quiescence. *Pediatr Res* **38:** 140-8.

Dambach, DM, Durham, SK, Laskin, JD, Laskin, DL (2006). Distinct roles of NF-kappaB p50 in the regulation of acetaminophen-induced inflammatory mediator production and hepatotoxicity. *Toxicol Appl Pharmacol* **211:** 157-65.

Davern, TJ, 2nd, James, LP, Hinson, JA, Polson, J, Larson, AM, Fontana, RJ, Lalani, E, Munoz, S, Shakil, AO, Lee, WM (2006). Measurement of serum acetaminophen-protein adducts in patients with acute liver failure. *Gastroenterology* **130:** 687-94.

Davies, KJ (2000). Oxidative stress, antioxidant defenses, and damage removal, repair, and replacement systems. *IUBMB Life* **50:** 279-89.

Davies, SP, Reddy, H, Caivano, M, Cohen, P (2000). Specificity and mechanism of action of some commonly used protein kinase inhibitors. *Biochem J* **351:** 95-105.

Davis, DC, Potter, WZ, Jollow, DJ, Mitchell, JR (1974). Species differences in hepatic glutathione depletion, covalent binding and hepatic necrosis after acetaminophen. *Life Sci* **14:** 2099-109.

Davis, W, Jr., Ronai, Z, Tew, KD (2001). Cellular thiols and reactive oxygen species in drug-induced apoptosis. *J Pharmacol Exp Ther* **296:** 1-6.

de la Escalera, S, Palacian, E (1989). Dimethylmaleic anhydride, a specific reagent for protein amino groups. *Biochem Cell Biol* **67:** 63-6.

DeGnore, JP, Konig, S, Barrett, WC, Chock, PB, Fales, HM (1998). Identification of the oxidation states of the active site cysteine in a recombinant protein tyrosine phosphatase by electrospray mass spectrometry using on-line desalting. *Rapid Commun Mass Spectrom* **12:** 1457-62.

DeLeve, LD, Kaplowitz, N (1991). Glutathione metabolism and its role in hepatotoxicity. *Pharmacol Ther* **52:** 287-305.

Dennehy, MK, Richards, KA, Wernke, GR, Shyr, Y, Liebler, DC (2006). Cytosolic and nuclear protein targets of thiol-reactive electrophiles. *Chem Res Toxicol* **19:** 20-9.

Dhakshinamoorthy, S, Jain, AK, Bloom, DA, Jaiswal, AK (2005). Bach1 competes with Nrf2 leading to negative regulation of the antioxidant response element (ARE)-mediated NAD(P)H:quinone oxidoreductase 1 gene expression and induction in response to antioxidants. *J Biol Chem* **280:** 16891-900.

Dhakshinamoorthy, S, Jaiswal, AK (2002). c-Maf negatively regulates ARE-mediated detoxifying enzyme genes expression and anti-oxidant induction. *Oncogene* **21:** 5301-12.

Dhakshinamoorthy, S, Jaiswal, AK (2001). Functional characterization and role of INrf2 in antioxidant response element-mediated expression and antioxidant induction of NAD(P)H:quinone oxidoreductase1 gene. *Oncogene* **20:** 3906-17.

Dhakshinamoorthy, S, Jaiswal, AK (2000). Small maf (MafG and MafK) proteins negatively regulate antioxidant response element-mediated expression and antioxidant induction of the NAD(P)H:Quinone oxidoreductase1 gene. *J Biol Chem* **275:** 40134-41.

Dhakshinamoorthy, S, Porter, AG (2004). Nitric oxide-induced transcriptional up-regulation of protective genes by Nrf2 via the antioxidant response element counteracts apoptosis of neuroblastoma cells. *J Biol Chem* **279:** 20096-107.

Dickinson, DA, Forman, HJ (2002). Glutathione in defense and signaling: lessons from a small thiol. *Ann N Y Acad Sci* **973:** 488-504.

Dietz, BM, Kang, YH, Liu, G, Eggler, AL, Yao, P, Chadwick, LR, Pauli, GF, Farnsworth, NR, Mesecar, AD, van Breemen, RB, Bolton, JL (2005). Xanthohumol isolated from Humulus lupulus Inhibits menadione-induced DNA damage through induction of quinone reductase. *Chem Res Toxicol* **18:** 1296-305.

Dietze, EC, Schafer, A, Omichinski, JG, Nelson, SD (1997). Inactivation of glyceraldehyde-3-phosphate dehydrogenase by a reactive metabolite of acetaminophen and mass spectral characterization of an arylated active site peptide. *Chem Res Toxicol* **10:** 1097-103.

Dinkova-Kostova, AT, Fahey, JW, Wade, KL, Jenkins, SN, Shapiro, TA, Fuchs, EJ, Kerns, ML, Talalay, P (2007). Induction of the phase 2 response in mouse and human skin by sulforaphane-containing broccoli sprout extracts. *Cancer Epidemiol Biomarkers Prev* **16:** 847-51.

Dinkova-Kostova, AT, Holtzclaw, WD, Cole, RN, Itoh, K, Wakabayashi, N, Katoh, Y, Yamamoto, M, Talalay, P (2002). Direct evidence that sulfhydryl groups of Keap1 are the sensors regulating induction of phase 2 enzymes that protect against carcinogens and oxidants. *Proc Natl Acad Sci U S A* **99:** 11908-13.

Dinkova-Kostova, AT, Holtzclaw, WD, Wakabayashi, N (2005a). Keap1, the sensor for electrophiles and oxidants that regulates the phase 2 response, is a zinc metalloprotein. *Biochemistry* **44:** 6889-99.

Dinkova-Kostova, AT, Jenkins, SN, Fahey, JW, Ye, L, Wehage, SL, Liby, KT, Stephenson, KK, Wade, KL, Talalay, P (2006). Protection against UV-light-induced skin carcinogenesis in SKH-1 high-risk mice by sulforaphane-containing broccoli sprout extracts. *Cancer Lett* **240:** 243-52.

Dinkova-Kostova, AT, Liby, KT, Stephenson, KK, Holtzclaw, WD, Gao, X, Suh, N, Williams, C, Risingsong, R, Honda, T, Gribble, GW, Sporn, MB, Talalay, P (2005b). Extremely potent triterpenoid inducers of the phase 2 response: correlations of protection against oxidant and inflammatory stress. *Proc Natl Acad Sci U S A* **102:** 4584-9.

Dinkova-Kostova, AT, Massiah, MA, Bozak, RE, Hicks, RJ, Talalay, P (2001). Potency of Michael reaction acceptors as inducers of enzymes that protect against carcinogenesis depends on their reactivity with sulfhydryl groups. *Proc Natl Acad Sci U S A* **98:** 3404-9.

Dubendorff, JW, Studier, FW (1991). Controlling basal expression in an inducible T7 expression system by blocking the target T7 promoter with lac repressor. *J Mol Biol* **219:** 45-59.

DuBridge, RB, Tang, P, Hsia, HC, Leong, PM, Miller, JH, Calos, MP (1987). Analysis of mutation in human cells by using an Epstein-Barr virus shuttle system. *Mol Cell Biol* **7:** 379-87.

Eggler, AL, Liu, G, Pezzuto, JM, van Breemen, RB, Mesecar, AD (2005). Modifying specific cysteines of the electrophile-sensing human Keap1 protein is insufficient to disrupt binding to the Nrf2 domain Neh2. *Proc Natl Acad Sci U S A* **102:** 10070-5.

Eggler, AL, Luo, Y, van Breemen, RB, Mesecar, AD (2007). Identification of the Highly Reactive Cysteine 151 in the Chemopreventive Agent-Sensor Keap1 Protein is Method-Dependent. *Chem Res Toxicol*: Oct 13 [Epub ahead of print].

Elbashir, SM, Harborth, J, Lendeckel, W, Yalcin, A, Weber, K, Tuschl, T (2001a). Duplexes of 21-nucleotide RNAs mediate RNA interference in cultured mammalian cells. *Nature* **411:** 494-8.

Elbashir, SM, Lendeckel, W, Tuschl, T (2001b). RNA interference is mediated by 21- and 22-nucleotide RNAs. *Genes Dev* **15:** 188-200.

Ellis, S, Nuenke, JM (1967). Dipeptidyl arylamidase III of the pituitary. Purification and characterization. *J Biol Chem* **242:** 4623-9.

Enari, M, Sakahira, H, Yokoyama, H, Okawa, K, Iwamatsu, A, Nagata, S (1998). A caspase-activated DNase that degrades DNA during apoptosis, and its inhibitor ICAD. *Nature* **391:** 43-50.

Enomoto, A, Itoh, K, Nagayoshi, E, Haruta, J, Kimura, T, O'Connor, T, Harada, T, Yamamoto, M (2001). High sensitivity of Nrf2 knockout mice to acetaminophen hepatotoxicity associated with decreased expression of ARE-regulated drug metabolizing enzymes and antioxidant genes. *Toxicol Sci* **59:** 169-77.

Evans, AR, Limp-Foster, M, Kelley, MR (2000). Going APE over ref-1. *Mutat Res* **461:** 83-108.

Fahey, JW, Haristoy, X, Dolan, PM, Kensler, TW, Scholtus, I, Stephenson, KK, Talalay, P, Lozniewski, A (2002). Sulforaphane inhibits extracellular, intracellular, and antibiotic-resistant strains of Helicobacter pylori and prevents benzo[a]pyrene-induced stomach tumors. *Proc Natl Acad Sci U S A* **99:** 7610-5.

Fang, S, Jensen, JP, Ludwig, RL, Vousden, KH, Weissman, AM (2000). Mdm2 is a RING finger-dependent ubiquitin protein ligase for itself and p53. *J Biol Chem* **275:** 8945-51.

Fire, A, Xu, S, Montgomery, MK, Kostas, SA, Driver, SE, Mello, CC (1998). Potent and specific genetic interference by double-stranded RNA in Caenorhabditis elegans. *Nature* **391:** 806-11.

Fisher, CD, Augustine, LM, Maher, JM, Nelson, DM, Slitt, AL, Klaassen, CD, Lehman-McKeeman, LD, Cherrington, NJ (2007). Induction of drug-metabolizing enzymes by garlic and allyl sulfide compounds via activation of constitutive androstane receptor and nuclear factor E2-related factor 2. *Drug Metab Dispos* **35:** 995-1000.

Fukasawa, K, Fukasawa, KM, Kanai, M, Fujii, S, Hirose, J, Harada, M (1998). Dipeptidyl peptidase III is a zinc metallo-exopeptidase. Molecular cloning and expression. *Biochem J* **329 (Pt 2):** 275-82.

Fukushima-Uesaka, H, Saito, Y, Maekawa, K, Kamatani, N, Kajio, H, Kuzuya, N, Noda, M, Yasuda, K, Sawada, J (2007). Genetic variations and haplotype structures of transcriptional factor Nrf2 and its cytosolic reservoir protein Keap1 in Japanese. *Drug Metab Pharmacokinet* **22:** 212-9.

Fukushima, T, Kikkawa, R, Hamada, Y, Horii, I (2006). Genomic cluster and network analysis for predictive screening for hepatotoxicity. *J Toxicol Sci* **31:** 419-32.

Furukawa, M, Xiong, Y (2005). BTB protein Keap1 targets antioxidant transcription factor Nrf2 for ubiquitination by the Cullin 3-Roc1 ligase. *Mol Cell Biol* **25:** 162-71.

Gao, L, Wang, J, Sekhar, KR, Yin, H, Yared, NF, Schneider, SN, Sasi, S, Dalton, TP, Anderson, ME, Chan, JY, Morrow, JD, Freeman, ML (2007). Novel n-3 fatty acid oxidation products activate Nrf2 by destabilizing the association between Keap1 and Cullin3. *J Biol Chem* **282:** 2529-37.

Gayarre, J, Sanchez, D, Sanchez-Gomez, FJ, Terron, MC, Llorca, O, Perez-Sala, D (2006). Addition of electrophilic lipids to actin alters filament structure. *Biochem Biophys Res Commun* **349:** 1387-93.

Gibson, GG, Skett, P (2001). *Introduction to Drug Metabolism*. Third edn. Nelson Thornes: Cheltenham.

Goldring, CE, Kitteringham, NR, Elsby, R, Randle, LE, Clement, YN, Williams, DP, McMahon, M, Hayes, JD, Itoh, K, Yamamoto, M, Park, BK (2004). Activation of hepatic Nrf2 in vivo by acetaminophen in CD-1 mice. *Hepatology* **39:** 1267-76.

Gong, P, Cederbaum, AI (2006a). Nrf2 is increased by CYP2E1 in rodent liver and HepG2 cells and protects against oxidative stress caused by CYP2E1. *Hepatology* **43:** 144-53.

Gong, P, Cederbaum, AI (2006b). Transcription factor Nrf2 protects HepG2 cells against CYP2E1 plus arachidonic acid-dependent toxicity. *J Biol Chem* **281:** 14573-9.

Gong, P, Stewart, D, Hu, B, Vinson, C, Alam, J (2002). Multiple basic-leucine zipper proteins regulate induction of the mouse heme oxygenase-1 gene by arsenite. *Arch Biochem Biophys* **405:** 265-74.

Gonzalez, FJ, Gelboin, HV (1994). Role of human cytochromes P450 in the metabolic activation of chemical carcinogens and toxins. *Drug Metab Rev* **26:** 165-83.

Gossen, M, Freundlieb, S, Bender, G, Muller, G, Hillen, W, Bujard, H (1995). Transcriptional activation by tetracyclines in mammalian cells. *Science* **268:** 1766-9.

Greco, A, Ajmone-Cat, MA, Nicolini, A, Sciulli, MG, Minghetti, L (2003). Paracetamol effectively reduces prostaglandin E2 synthesis in brain macrophages by inhibiting enzymatic activity of cyclooxygenase but not phospholipase and prostaglandin E synthase. *J Neurosci Res* **71:** 844-52.

Gregus, Z, Madhu, C, Klaassen, CD (1988). Species variation in toxication and detoxication of acetaminophen in vivo: a comparative study of biliary and urinary excretion of acetaminophen metabolites. *J Pharmacol Exp Ther* **244:** 91-9.

Grunstein, M (1990). Histone function in transcription. *Annu Rev Cell Biol* **6:** 643-78.

Guengerich, FP (1990). Enzymatic oxidation of xenobiotic chemicals. *Crit Rev Biochem Mol Biol* **25:** 97-153.

Hammond, SM, Bernstein, E, Beach, D, Hannon, GJ (2000). An RNA-directed nuclease mediates post-transcriptional gene silencing in Drosophila cells. *Nature* **404:** 293-6.

Harman, AW, Kyle, ME, Serroni, A, Farber, JL (1991). The killing of cultured hepatocytes by N-acetyl-p-benzoquinone imine (NAPQI) as a model of the cytotoxicity of acetaminophen. *Biochem Pharmacol* **41:** 1111-7.

Hartley, DL, Kane, JF (1988). Properties of inclusion bodies from recombinant Escherichia coli. *Biochem Soc Trans* **16:** 101-2.

Hayden, MS, Ghosh, S (2004). Signaling to NF-kappaB. *Genes Dev* **18:** 2195-224.

Hayes, JD, Chanas, SA, Henderson, CJ, McMahon, M, Sun, C, Moffat, GJ, Wolf, CR, Yamamoto, M (2000). The Nrf2 transcription factor contributes both to the basal expression of glutathione S-transferases in mouse liver and to their induction by the chemopreventive synthetic antioxidants, butylated hydroxyanisole and ethoxyquin. *Biochem Soc Trans* **28:** 33-41.

Hazelton, GA, Hjelle, JJ, Klaassen, CD (1986). Effects of cysteine pro-drugs on acetaminophen-induced hepatotoxicity. *J Pharmacol Exp Ther* **237:** 341-9.

He, X, Chen, MG, Lin, GX, Ma, Q (2006). Arsenic induces NAD(P)H-quinone oxidoreductase I by disrupting the Nrf2 x Keap1 x Cul3 complex and recruiting Nrf2 x Maf to the antioxidant response element enhancer. *J Biol Chem* **281:** 23620-31.

He, X, Lin, GX, Chen, MG, Zhang, JX, Ma, Q (2007). Protection against chromium (VI)-induced oxidative stress and apoptosis by Nrf2. Recruiting Nrf2 into the nucleus and disrupting the nuclear Nrf2/Keap1 association. *Toxicol Sci* **98:** 298-309.

Hengartner, MO (2000). The biochemistry of apoptosis. *Nature* **407:** 770-6.

Hinz, B, Cheremina, O, Brune, K (2008). Acetaminophen (paracetamol) is a selective cyclooxygenase-2 inhibitor in man. *Faseb J* **22:** 383-90.

Hiramoto, M, Shimizu, N, Sugimoto, K, Tang, J, Kawakami, Y, Ito, M, Aizawa, S, Tanaka, H, Makino, I, Handa, H (1998). Nuclear targeted suppression of NF-kappa B activity by the novel quinone derivative E3330. *J Immunol* **160:** 810-9.

Hirota, K, Murata, M, Sachi, Y, Nakamura, H, Takeuchi, J, Mori, K, Yodoi, J (1999). Distinct roles of thioredoxin in the cytoplasm and in the nucleus. A two-step mechanism of redox regulation of transcription factor NF-kappaB. *J Biol Chem* **274:** 27891-7.

Hochuli, E (1990). Purification of recombinant proteins with metal chelate adsorbent. *Genet Eng (N Y)* **12:** 87-98.

Hochuli, E, Bannwarth, W, Dobeli, H, Gentz, R, Stuber, D (1988). Genetic Approach to Facilitate Purification of Recombinant Proteins with a Novel Metal Chelate Adsorbent *Nat Biotechnol* **6:** 1321-1325.

Hodgson, E, Goldstein, JA (2001). Metabolism of Toxicants: Phase I Reactions and Pharmacogenomics. In: Hodgson, E, Smart, RC (eds). *Introduction to Biochemical Toxicology*. Third edn. Wiley Interscience: New York. pp 67-113.

Hoffmann, KJ, Streeter, AJ, Axworthy, DB, Baillie, TA (1985a). Identification of the major covalent adduct formed in vitro and in vivo between acetaminophen and mouse liver proteins. *Mol Pharmacol* **27:** 566-73.

Hoffmann, KJ, Streeter, AJ, Axworthy, DB, Baillie, TA (1985b). Structural characterization of the major covalent adduct formed in vitro between acetaminophen and bovine serum albumin. *Chem Biol Interact* **53:** 155-72.

Holme, JA, Dahlin, DC, Nelson, SD, Dybing, E (1984). Cytotoxic effects of N-acetyl-p-benzoquinone imine, a common arylating intermediate of paracetamol and N-hydroxyparacetamol. *Biochem Pharmacol* **33:** 401-6.

Holme, JA, Wirth, PJ, Dybing, E, Thorgeirsson, SS (1982a). Cytotoxic effects of N-hydroxyparacetamol in suspsensions of isolated rat hepatocytes. *Acta Pharmacol Toxicol (Copenh)* **51:** 87-95.

Holme, JA, Wirth, PJ, Dybing, E, Thorgeirsson, SS (1982b). Modulation of N-hydroxyparacetamol cytotoxicity in suspensions of isolated rat hepatocytes. *Acta Pharmacol Toxicol (Copenh)* **51:** 96-102.

Hong, F, Freeman, ML, Liebler, DC (2005a). Identification of sensor cysteines in human Keap1 modified by the cancer chemopreventive agent sulforaphane. *Chem Res Toxicol* **18:** 1917-26.

Hong, F, Sekhar, KR, Freeman, ML, Liebler, DC (2005b). Specific patterns of electrophile adduction trigger Keap1 ubiquitination and Nrf2 activation. *J Biol Chem* **280:** 31768-75.

Hong, W, Resnick, RJ, Rakowski, C, Shalloway, D, Taylor, SJ, Blobel, GA (2002). Physical and functional interaction between the transcriptional cofactor CBP and the KH domain protein Sam68. *Mol Cancer Res* **1:** 48-55.

Hosoya, T, Maruyama, A, Kang, MI, Kawatani, Y, Shibata, T, Uchida, K, Warabi, E, Noguchi, N, Itoh, K, Yamamoto, M (2005). Differential responses of the Nrf2-Keap1 system to laminar and oscillatory shear stresses in endothelial cells. *J Biol Chem* **280:** 27244-50.

Howie, D, Adriaenssens, PI, Prescott, LF (1977). Paracetamol metabolism following overdosage: application of high performance liquid chromatography. *J Pharm Pharmacol* **29:** 235-7.

Huang, HC, Nguyen, T, Pickett, CB (2002). Phosphorylation of Nrf2 at Ser-40 by protein kinase C regulates antioxidant response element-mediated transcription. *J Biol Chem* **277:** 42769-74.

Hubbs, AF, Benkovic, SA, Miller, DB, O'Callaghan, JP, Battelli, L, Schwegler-Berry, D, Ma, Q (2007). Vacuolar leukoencephalopathy with widespread astrogliosis in mice lacking transcription factor nrf2. *Am J Pathol* **170:** 2068-76.

Hunter, T (1995). Protein kinases and phosphatases: the yin and yang of protein phosphorylation and signaling. *Cell* **80:** 225-36.

Igarashi, K, Kataoka, K, Itoh, K, Hayashi, N, Nishizawa, M, Yamamoto, M (1994). Regulation of transcription by dimerization of erythroid factor NF-E2 p45 with small Maf proteins. *Nature* **367:** 568-72.

Iida, K, Itoh, K, Kumagai, Y, Oyasu, R, Hattori, K, Kawai, K, Shimazui, T, Akaza, H, Yamamoto, M (2004). Nrf2 is essential for the chemopreventive efficacy of oltipraz against urinary bladder carcinogenesis. *Cancer Res* **64:** 6424-31.

Ioannides, C, Steele, CM, Parke, DV (1983). Species variation in the metabolic activation of paracetamol to toxic intermediates: role of cytochromes p-450 and p-448. *Toxicol Lett* **16:** 55-61.

Ishii, T, Itoh, K, Ruiz, E, Leake, DS, Unoki, H, Yamamoto, M, Mann, GE (2004). Role of Nrf2 in the regulation of CD36 and stress protein expression in murine macrophages: activation by oxidatively modified LDL and 4-hydroxynonenal. *Circ Res* **94:** 609-16.

Ishii, T, Itoh, K, Takahashi, S, Sato, H, Yanagawa, T, Katoh, Y, Bannai, S, Yamamoto, M (2000). Transcription factor Nrf2 coordinately regulates a group of oxidative stress-inducible genes in macrophages. *J Biol Chem* **275:** 16023-9.

Ishii, T, Sakurai, T, Usami, H, Uchida, K (2005a). Oxidative modification of proteasome: identification of an oxidation-sensitive subunit in 26 S proteasome. *Biochemistry* **44:** 13893-901.

Ishii, T, Yanagawa, T (2007). Stress-induced peroxiredoxins. *Subcell Biochem* **44:** 375-84.

Ishii, Y, Itoh, K, Morishima, Y, Kimura, T, Kiwamoto, T, Iizuka, T, Hegab, AE, Hosoya, T, Nomura, A, Sakamoto, T, Yamamoto, M, Sekizawa, K (2005b). Transcription factor Nrf2 plays a pivotal role in protection against elastase-induced pulmonary inflammation and emphysema. *J Immunol* **175:** 6968-75.

Itoh, K, Chiba, T, Takahashi, S, Ishii, T, Igarashi, K, Katoh, Y, Oyake, T, Hayashi, N, Satoh, K, Hatayama, I, Yamamoto, M, Nabeshima, Y (1997). An Nrf2/small Maf heterodimer mediates the induction of phase II detoxifying enzyme genes through antioxidant response elements. *Biochem Biophys Res Commun* **236:** 313-22.

Itoh, K, Igarashi, K, Hayashi, N, Nishizawa, M, Yamamoto, M (1995). Cloning and characterization of a novel erythroid cell-derived CNC family transcription factor heterodimerizing with the small Maf family proteins. *Mol Cell Biol* **15:** 4184-93.

Itoh, K, Mochizuki, M, Ishii, Y, Ishii, T, Shibata, T, Kawamoto, Y, Kelly, V, Sekizawa, K, Uchida, K, Yamamoto, M (2004). Transcription factor Nrf2 regulates inflammation by mediating the effect of 15-deoxy-Delta(12,14)-prostaglandin j(2). *Mol Cell Biol* **24:** 36-45.

Itoh, K, Wakabayashi, N, Katoh, Y, Ishii, T, Igarashi, K, Engel, JD, Yamamoto, M (1999). Keap1 represses nuclear activation of antioxidant responsive elements by Nrf2 through binding to the amino-terminal Neh2 domain. *Genes Dev* **13:** 76-86.

Itoh, K, Wakabayashi, N, Katoh, Y, Ishii, T, O'Connor, T, Yamamoto, M (2003). Keap1 regulates both cytoplasmic-nuclear shuttling and degradation of Nrf2 in response to electrophiles. *Genes Cells* **8:** 379-91.

Jaeschke, H, Knight, TR, Bajt, ML (2003). The role of oxidant stress and reactive nitrogen species in acetaminophen hepatotoxicity. *Toxicol Lett* **144:** 279-88.

Jahngen-Hodge, J, Obin, MS, Gong, X, Shang, F, Nowell, TR, Jr., Gong, J, Abasi, H, Blumberg, J, Taylor, A (1997). Regulation of ubiquitin-conjugating enzymes by glutathione following oxidative stress. *J Biol Chem* **272:** 28218-26.

Jain, AK, Bloom, DA, Jaiswal, AK (2005). Nuclear import and export signals in control of Nrf2. *J Biol Chem* **280:** 29158-68.

Jain, AK, Jaiswal, AK (2007). GSK-3beta acts upstream of Fyn kinase in regulation of nuclear export and degradation of NF-E2 related factor 2. *J Biol Chem* **282:** 16502-10.

Jain, AK, Jaiswal, AK (2006). Phosphorylation of tyrosine 568 controls nuclear export of Nrf2. *J Biol Chem* **281:** 12132-42.

Jaiswal, AK (2004). Nrf2 signaling in coordinated activation of antioxidant gene expression. *Free Radic Biol Med* **36:** 1199-207.

Jakubikova, J, Sedlak, J, Bod'o, J, Bao, Y (2006). Effect of isothiocyanates on nuclear accumulation of NF-kappaB, Nrf2, and thioredoxin in caco-2 cells. *J Agric Food Chem* **54:** 1656-62.

Jefferys, DB, Leakey, D, Lewis, JA, Payne, S, Rawlins, MD (1998). New active substances authorized in the United Kingdom between 1972 and 1994. *Br J Clin Pharmacol* **45:** 151-6.

Jenkins, RE, Kitteringham, NR, Goldring, CE, Dowdall, SM, Hamlett, J, Lane, CS, Boerma, JS, Vermeulen, NP, Park, BK (2008). Glutathione-S-transferase pi as a model protein for the characterisation of chemically reactive metabolites. *Proteomics* **8:** 301-15.

Jeyapaul, J, Jaiswal, AK (2000). Nrf2 and c-Jun regulation of antioxidant response element (ARE)-mediated expression and induction of gamma-glutamylcysteine synthetase heavy subunit gene. *Biochem Pharmacol* **59:** 1433-9.

Ji, C, Kozak, KR, Marnett, LJ (2001). IkappaB kinase, a molecular target for inhibition by 4-hydroxy-2-nonenal. *J Biol Chem* **276:** 18223-8.

Ji, T, Ikehata, K, Koen, YM, Esch, SW, Williams, TD, Hanzlik, RP (2007). Covalent modification of microsomal lipids by thiobenzamide metabolites in vivo. *Chem Res Toxicol* **20:** 701-8.

Johnson, DA, Andrews, GK, Xu, W, Johnson, JA (2002). Activation of the antioxidant response element in primary cortical neuronal cultures derived from transgenic reporter mice. *J Neurochem* **81:** 1233-41.

Jowsey, IR, Jiang, Q, Itoh, K, Yamamoto, M, Hayes, JD (2003). Expression of the aflatoxin B1-8,9-epoxide-metabolizing murine glutathione S-transferase A3 subunit is regulated by the Nrf2 transcription factor through an antioxidant response element. *Mol Pharmacol* **64:** 1018-28.

Jung, G, Breitmaier, E, Voelter, W (1972). Dissociation equilibrium of glutathione. A Fourier transform-13C-NMR spectroscopic study of pH-dependence and of charge densities. *Eur J Biochem* **24:** 438-45.

Kabe, Y, Ando, K, Hirao, S, Yoshida, M, Handa, H (2005). Redox regulation of NF-kappa-B activation: Distinct redox regulation between the cytoplasm and the nucleus. *Antioxid Redox Signal* **7:** 395-403.

Kalkhoven, E (2004). CBP and p300: HATs for different occasions. *Biochem Pharmacol* **68:** 1145-55.

Kallio, PJ, Wilson, WJ, O'Brien, S, Makino, Y, Poellinger, L (1999). Regulation of the hypoxia-inducible transcription factor 1alpha by the ubiquitin-proteasome pathway. *J Biol Chem* **274:** 6519-25.

Kane, JF, Hartley, DL (1991). Properties of recombinant protein-containing inclusion bodies in Escherichia coli. *Bioprocess Technol* **12:** 121-45.

Kang, ES, Woo, IS, Kim, HJ, Eun, SY, Paek, KS, Kim, HJ, Chang, KC, Lee, JH, Lee, HT, Kim, JH, Nishinaka, T, Yabe-Nishimura, C, Seo, HG (2007). Up-regulation of aldose reductase expression mediated by phosphatidylinositol 3-kinase/Akt and Nrf2 is involved in the protective effect of curcumin against oxidative damage. *Free Radic Biol Med* **43:** 535-45.

Kang, KW, Lee, SJ, Park, JW, Kim, SG (2002). Phosphatidylinositol 3-kinase regulates nuclear translocation of NF-E2-related factor 2 through actin rearrangement in response to oxidative stress. *Mol Pharmacol* **62:** 1001-10.

Kang, MI, Kobayashi, A, Wakabayashi, N, Kim, SG, Yamamoto, M (2004). Scaffolding of Keap1 to the actin cytoskeleton controls the function of Nrf2 as key regulator of cytoprotective phase 2 genes. *Proc Natl Acad Sci U S A* **101:** 2046-51.

Kannan, S, Jaiswal, AK (2006). Low and High Dose UVB Regulation of Transcription Factor NF-E2-Related Factor 2. *Cancer Res* **66:** 8421-9.

Kaplowitz, N, Aw, TY, Ookhtens, M (1985). The regulation of hepatic glutathione. *Annu Rev Pharmacol Toxicol* **25:** 715-44.

Karapetian, RN, Evstafieva, AG, Abaeva, IS, Chichkova, NV, Filonov, GS, Rubtsov, YP, Sukhacheva, EA, Melnikov, SV, Schneider, U, Wanker, EE, Vartapetian, AB (2005). Nuclear oncoprotein prothymosin alpha is a partner of Keap1: implications for expression of oxidative stress-protecting genes. *Mol Cell Biol* **25:** 1089-99.

Karin, M, Liu, Z, Zandi, E (1997). AP-1 function and regulation. *Curr Opin Cell Biol* **9:** 240-6.

Kataoka, K, Nishizawa, M, Kawai, S (1993). Structure-function analysis of the maf oncogene product, a member of the b-Zip protein family. *J Virol* **67:** 2133-41.

Katoh, Y, Iida, K, Kang, MI, Kobayashi, A, Mizukami, M, Tong, KI, McMahon, M, Hayes, JD, Itoh, K, Yamamoto, M (2005). Evolutionary conserved N-terminal domain of Nrf2 is essential for the Keap1-mediated degradation of the protein by proteasome. *Arch Biochem Biophys* **433:** 342-50.

Katoh, Y, Itoh, K, Yoshida, E, Miyagishi, M, Fukamizu, A, Yamamoto, M (2001). Two domains of Nrf2 cooperatively bind CBP, a CREB binding protein, and synergistically activate transcription. *Genes Cells* **6:** 857-68.

Kenna, JG (1997). Immunoallergic drug-induced hepatitis: lessons from halothane. *J Hepatol* **26 Suppl 1:** 5-12.

Kensler, TW, Wakabayashi, N, Biswal, S (2007). Cell survival responses to environmental stresses via the Keap1-Nrf2-ARE pathway. *Annu Rev Pharmacol Toxicol* **47:** 89-116.

Khor, TO, Huang, MT, Kwon, KH, Chan, JY, Reddy, BS, Kong, AN (2006). Nrf2-deficient mice have an increased susceptibility to dextran sulfate sodium-induced colitis. *Cancer Res* **66:** 11580-4.

Kiang, JG, Tsokos, GC (1998). Heat shock protein 70 kDa: molecular biology, biochemistry, and physiology. *Pharmacol Ther* **80:** 183-201.

Kim, SO, Merchant, K, Nudelman, R, Beyer, WF, Jr., Keng, T, DeAngelo, J, Hausladen, A, Stamler, JS (2002). OxyR: a molecular code for redox-related signaling. *Cell* **109:** 383-96.

Kim, YC, Masutani, H, Yamaguchi, Y, Itoh, K, Yamamoto, M, Yodoi, J (2001). Hemin-induced activation of the thioredoxin gene by Nrf2. A differential regulation of the antioxidant responsive element by a switch of its binding factors. *J Biol Chem* **276:** 18399-406.

Kim, YC, Yamaguchi, Y, Kondo, N, Masutani, H, Yodoi, J (2003). Thioredoxin-dependent redox regulation of the antioxidant responsive element (ARE) in electrophile response. *Oncogene* **22:** 1860-5.

Kim, YJ, Ahn, JY, Liang, P, Ip, C, Zhang, Y, Park, YM (2007). Human prx1 gene is a target of Nrf2 and is up-regulated by hypoxia/reoxygenation: implication to tumor biology. *Cancer Res* **67:** 546-54.

Kitamura, Y, Umemura, T, Kanki, K, Kodama, Y, Kitamoto, S, Saito, K, Itoh, K, Yamamoto, M, Masegi, T, Nishikawa, A, Hirose, M (2007). Increased susceptibility to hepatocarcinogenicity of Nrf2-deficient mice exposed to 2-amino-3-methylimidazo[4,5-f]quinoline. *Cancer Sci* **98:** 19-24.

Kitteringham, NR, Powell, H, Clement, YN, Dodd, CC, Tettey, JN, Pirmohamed, M, Smith, DA, McLellan, LI, Kevin Park, B (2000). Hepatocellular response to chemical stress in CD-1 mice: induction of early genes and gamma-glutamylcysteine synthetase. *Hepatology* **32:** 321-33.

Kobayashi, A, Ito, E, Toki, T, Kogame, K, Takahashi, S, Igarashi, K, Hayashi, N, Yamamoto, M (1999). Molecular cloning and functional characterization of a new Cap'n' collar family transcription factor Nrf3. *J Biol Chem* **274:** 6443-52.

Kobayashi, A, Kang, MI, Okawa, H, Ohtsuji, M, Zenke, Y, Chiba, T, Igarashi, K, Yamamoto, M (2004). Oxidative stress sensor Keap1 functions as an adaptor for Cul3-based E3 ligase to regulate proteasomal degradation of Nrf2. *Mol Cell Biol* **24:** 7130-9.

Kobayashi, A, Kang, MI, Watai, Y, Tong, KI, Shibata, T, Uchida, K, Yamamoto, M (2006). Oxidative and electrophilic stresses activate Nrf2 through inhibition of ubiquitination activity of Keap1. *Mol Cell Biol* **26:** 221-9.

Kobayashi, M, Itoh, K, Suzuki, T, Osanai, H, Nishikawa, K, Katoh, Y, Takagi, Y, Yamamoto, M (2002). Identification of the interactive interface and phylogenic conservation of the Nrf2-Keap1 system. *Genes Cells* **7:** 807-20.

Koen, YM, Yue, W, Galeva, NA, Williams, TD, Hanzlik, RP (2006). Site-specific arylation of rat glutathione s-transferase A1 and A2 by bromobenzene metabolites in vivo. *Chem Res Toxicol* **19:** 1426-34.

Kraft, AD, Johnson, DA, Johnson, JA (2004). Nuclear factor E2-related factor 2-dependent antioxidant response element activation by tert-butylhydroquinone and sulforaphane occurring preferentially in astrocytes conditions neurons against oxidative insult. *J Neurosci* **24:** 1101-12.

Kraft, AD, Lee, JM, Johnson, DA, Kan, YW, Johnson, JA (2006). Neuronal sensitivity to kainic acid is dependent on the Nrf2-mediated actions of the antioxidant response element. *J Neurochem* **98:** 1852-65.

Kuo, MH, Allis, CD (1998). Roles of histone acetyltransferases and deacetylases in gene regulation. *Bioessays* **20:** 615-26.

Kwak, MK, Itoh, K, Yamamoto, M, Sutter, TR, Kensler, TW (2001). Role of transcription factor Nrf2 in the induction of hepatic phase 2 and antioxidative enzymes in vivo by the cancer chemoprotective agent, 3H-1, 2-dimethiole-3-thione. *Mol Med* **7:** 135-45.

Kwak, MK, Kensler, TW, Casero, RA, Jr. (2003). Induction of phase 2 enzymes by serum oxidized polyamines through activation of Nrf2: effect of the polyamine metabolite acrolein. *Biochem Biophys Res Commun* **305:** 662-70.

Kwong, M, Kan, YW, Chan, JY (1999). The CNC basic leucine zipper factor, Nrf1, is essential for cell survival in response to oxidative stress-inducing agents. Role for Nrf1 in gamma-gcs(l) and gss expression in mouse fibroblasts. *J Biol Chem* **274:** 37491-8.

Landin, JS, Cohen, SD, Khairallah, EA (1996). Identification of a 54-kDa mitochondrial acetaminophen-binding protein as aldehyde dehydrogenase. *Toxicol Appl Pharmacol* **141:** 299-307.

Larson, AM, Polson, J, Fontana, RJ, Davern, TJ, Lalani, E, Hynan, LS, Reisch, JS, Schiodt, FV, Ostapowicz, G, Shakil, AO, Lee, WM (2005). Acetaminophen-induced acute liver failure: results of a United States multicenter, prospective study. *Hepatology* **42:** 1364-72.

Latchman, DS (1997). Transcription factors: an overview. *Int J Biochem Cell Biol* **29:** 1305-12.

Lawlor, MA, Alessi, DR (2001). PKB/Akt: a key mediator of cell proliferation, survival and insulin responses? *J Cell Sci* **114:** 2903-10.

Lazebnik, YA, Kaufmann, SH, Desnoyers, S, Poirier, GG, Earnshaw, WC (1994). Cleavage of poly(ADP-ribose) polymerase by a proteinase with properties like ICE. *Nature* **371:** 346-7.

Lee-Hilz, YY, Boerboom, AM, Westphal, AH, Berkel, WJ, Aarts, JM, Rietjens, IM (2006). Pro-oxidant activity of flavonoids induces EpRE-mediated gene expression. *Chem Res Toxicol* **19:** 1499-505.

Lee, CM, Snyder, SH (1982). Dipeptidyl-aminopeptidase III of rat brain. Selective affinity for enkephalin and angiotensin. *J Biol Chem* **257:** 12043-50.

Lee, JH, Koo, TH, Hwang, BY, Lee, JJ (2002). Kaurane diterpene, kamebakaurin, inhibits NF-kappa B by directly targeting the DNA-binding activity of p50 and blocks the expression of antiapoptotic NF-kappa B target genes. *J Biol Chem* **277:** 18411-20.

Lee, JM, Calkins, MJ, Chan, K, Kan, YW, Johnson, JA (2003). Identification of the NF-E2-related factor-2-dependent genes conferring protection against oxidative stress in primary cortical astrocytes using oligonucleotide microarray analysis. *J Biol Chem* **278:** 12029-38.

Lee, JM, Hanson, JM, Chu, WA, Johnson, JA (2001a). Phosphatidylinositol 3-kinase, not extracellular signal-regulated kinase, regulates activation of the antioxidant-responsive element in IMR-32 human neuroblastoma cells. *J Biol Chem* **276:** 20011-6.

Lee, JM, Moehlenkamp, JD, Hanson, JM, Johnson, JA (2001b). Nrf2-dependent activation of the antioxidant responsive element by tert-butylhydroquinone is independent of oxidative stress in IMR-32 human neuroblastoma cells. *Biochem Biophys Res Commun* **280:** 286-92.

Lee, OH, Jain, AK, Papusha, V, Jaiswal, AK (2007). An Auto-regulatory Loop between Stress Sensors INrf2 and Nrf2 Controls Their Cellular Abundance. *J Biol Chem* **282:** 36412-20.

Lee, SS, Buters, JT, Pineau, T, Fernandez-Salguero, P, Gonzalez, FJ (1996). Role of CYP2E1 in the hepatotoxicity of acetaminophen. *J Biol Chem* **271:** 12063-7.

Lee, TD, Yang, H, Whang, J, Lu, SC (2005). Cloning and characterization of the human glutathione synthetase 5'-flanking region. *Biochem J* **390:** 521-8.

Lee, WM (2003). Drug-induced hepatotoxicity. *N Engl J Med* **349:** 474-85.

Lemercier, JN, Meier, BW, Gomez, JD, Thompson, JA (2004). Inhibition of glutathione S-transferase P1-1 in mouse lung epithelial cells by the tumor promoter 2,6-di-tert-butyl-4-methylene-2,5-cyclohexadienone (BHT-quinone methide): protein adducts investigated by electrospray mass spectrometry. *Chem Res Toxicol* **17:** 1675-83.

Levonen, AL, Landar, A, Ramachandran, A, Ceaser, EK, Dickinson, DA, Zanoni, G, Morrow, JD, Darley-Usmar, VM (2004). Cellular mechanisms of redox cell signalling: role of cysteine modification in controlling antioxidant defences in response to electrophilic lipid oxidation products. *Biochem J* **378:** 373-82.

Li, J, Johnson, D, Calkins, M, Wright, L, Svendsen, C, Johnson, J (2005). Stabilization of Nrf2 by tBHQ confers protection against oxidative stress-induced cell death in human neural stem cells. *Toxicol Sci* **83:** 313-28.

Li, J, Stein, TD, Johnson, JA (2004a). Genetic dissection of systemic autoimmune disease in Nrf2-deficient mice. *Physiol Genomics* **18:** 261-72.

Li, MH, Cha, YN, Surh, YJ (2006a). Peroxynitrite induces HO-1 expression via PI3K/Akt-dependent activation of NF-E2-related factor 2 in PC12 cells. *Free Radic Biol Med* **41:** 1079-91.

Li, W, Yu, SW, Kong, AN (2006b). Nrf2 possesses a redox-sensitive nuclear exporting signal in the Neh5 transactivation domain. *J Biol Chem* **281:** 27251-63.

Li, X, Zhang, D, Hannink, M, Beamer, LJ (2004b). Crystal structure of the Kelch domain of human Keap1. *J Biol Chem* **279:** 54750-8.

Liby, K, Hock, T, Yore, MM, Suh, N, Place, AE, Risingsong, R, Williams, CR, Royce, DB, Honda, T, Honda, Y, Gribble, GW, Hill-Kapturczak, N, Agarwal, A, Sporn, MB (2005). The synthetic triterpenoids, CDDO and CDDO-imidazolide, are potent inducers of heme oxygenase-1 and Nrf2/ARE signaling. *Cancer Res* **65:** 4789-98.

Liebler, DC (2008). Protein damage by reactive electrophiles: targets and consequences. *Chem Res Toxicol* **21:** 117-28.

Liebler, DC (2002). Proteomic approaches to characterize protein modifications: new tools to study the effects of environmental exposures. *Environ Health Perspect* **110 Suppl 1:** 3-9.

Liebler, DC, Guengerich, FP (2005). Elucidating mechanisms of drug-induced toxicity. *Nat Rev Drug Discov* **4:** 410-20.

Lin, W, Shen, G, Yuan, X, Jain, MR, Yu, S, Zhang, A, Chen, JD, Kong, AN (2006). Regulation of Nrf2 transactivation domain activity by p160 RAC3/SRC3 and other nuclear co-regulators. *J Biochem Mol Biol* **39:** 304-10.

Liu, G, Eggler, AL, Dietz, BM, Mesecar, AD, Bolton, JL, Pezzuto, JM, van Breemen, RB (2005). Screening method for the discovery of potential cancer chemoprevention agents based on mass spectrometric detection of alkylated Keap1. *Anal Chem* **77:** 6407-14.

Liu, XM, Peyton, KJ, Ensenat, D, Wang, H, Hannink, M, Alam, J, Durante, W (2007a). Nitric oxide stimulates heme oxygenase-1 gene transcription via the Nrf2/ARE complex to promote vascular smooth muscle cell survival. *Cardiovasc Res* **75:** 381-9.

Liu, Y, Kern, JT, Walker, JR, Johnson, JA, Schultz, PG, Luesch, H (2007b). A genomic screen for activators of the antioxidant response element. *Proc Natl Acad Sci U S A* **104:** 5205-10.

Lo, SC, Hannink, M (2006a). PGAM5, a Bcl-XL-interacting protein, is a novel substrate for the redox-regulated Keap1-dependent ubiquitin ligase complex. *J Biol Chem* **281:** 37893-903.

Lo, SC, Li, X, Henzl, MT, Beamer, LJ, Hannink, M (2006b). Structure of the Keap1:Nrf2 interface provides mechanistic insight into Nrf2 signaling. *EMBO J* **25:** 3605-17.

Lou, H, Du, S, Ji, Q, Stolz, A (2006). Induction of AKR1C2 by phase II inducers: identification of a distal consensus antioxidant response element regulated by NRF2. *Mol Pharmacol* **69:** 1662-72.

Lu, SC (1999). Regulation of hepatic glutathione synthesis: current concepts and controversies. *FASEB J* **13:** 1169-83.

Luo, Y, Eggler, AL, Liu, D, Liu, G, Mesecar, AD, van Breemen, RB (2007). Sites of alkylation of human Keap1 by natural chemoprevention agents. *J Am Soc Mass Spectrom* **18:** 2226-32.

Macpherson, LJ, Dubin, AE, Evans, MJ, Marr, F, Schultz, PG, Cravatt, BF, Patapoutian, A (2007). Noxious compounds activate TRPA1 ion channels through covalent modification of cysteines. *Nature* **445:** 541-5.

Maddrey, WC (2005). Drug-induced hepatotoxicity: 2005. *J Clin Gastroenterol* **39:** S83-9.

Mahon, TM, O'Neill, LA (1995). Studies into the effect of the tyrosine kinase inhibitor herbimycin A on NF-kappa B activation in T lymphocytes. Evidence for covalent modification of the p50 subunit. *J Biol Chem* **270:** 28557-64.

Manevich, Y, Feinstein, SI, Fisher, AB (2004). Activation of the antioxidant enzyme 1-CYS peroxiredoxin requires glutathionylation mediated by heterodimerization with pi GST. *Proc Natl Acad Sci U S A* **101:** 3780-5.

Mann, M, Jensen, ON (2003). Proteomic analysis of post-translational modifications. *Nat Biotechnol* **21:** 255-61.

Manyike, PT, Kharasch, ED, Kalhorn, TF, Slattery, JT (2000). Contribution of CYP2E1 and CYP3A to acetaminophen reactive metabolite formation. *Clin Pharmacol Ther* **67:** 275-82.

Martin, D, Rojo, AI, Salinas, M, Diaz, R, Gallardo, G, Alam, J, De Galarreta, CM, Cuadrado, A (2004). Regulation of heme oxygenase-1 expression through the phosphatidylinositol 3-kinase/Akt pathway and the Nrf2 transcription factor in response to the antioxidant phytochemical carnosol. *J Biol Chem* **279:** 8919-29.

Marzec, JM, Christie, JD, Reddy, SP, Jedlicka, AE, Vuong, H, Lanken, PN, Aplenc, R, Yamamoto, T, Yamamoto, M, Cho, HY, Kleeberger, SR (2007). Functional polymorphisms in the transcription factor NRF2 in humans increase the risk of acute lung injury. *FASEB J* **21:** 2237-46.

Mashima, T, Naito, M, Tsuruo, T (1999). Caspase-mediated cleavage of cytoskeletal actin plays a positive role in the process of morphological apoptosis. *Oncogene* **18:** 2423-30.

McJunkin, B, Barwick, KW, Little, WC, Winfield, JB (1976). Fatal massive hepatic necrosis following acetaminophen overdose. *JAMA* **236:** 1874-5.

McMahon, M, Itoh, K, Yamamoto, M, Chanas, SA, Henderson, CJ, McLellan, LI, Wolf, CR, Cavin, C, Hayes, JD (2001). The Cap'n'Collar basic leucine zipper transcription factor Nrf2 (NF-E2 p45-related factor 2) controls both constitutive and inducible expression of intestinal detoxification and glutathione biosynthetic enzymes. *Cancer Res* **61:** 3299-307.

McMahon, M, Itoh, K, Yamamoto, M, Hayes, JD (2003). Keap1-dependent proteasomal degradation of transcription factor Nrf2 contributes to the negative regulation of antioxidant response element-driven gene expression. *J Biol Chem* **278:** 21592-600.

McMahon, M, Thomas, N, Itoh, K, Yamamoto, M, Hayes, JD (2006). Dimerization of substrate adaptors can facilitate cullin-mediated ubiquitylation of proteins by a "tethering" mechanism: a two-site interaction model for the Nrf2-Keap1 complex. *J Biol Chem* **281:** 24756-68.

McMahon, M, Thomas, N, Itoh, K, Yamamoto, M, Hayes, JD (2004). Redox-regulated turnover of Nrf2 is determined by at least two separate protein domains, the redox-sensitive Neh2 degron and the redox-insensitive Neh6 degron. *J Biol Chem* **279:** 31556-67.

McWalter, GK, Higgins, LG, McLellan, LI, Henderson, CJ, Song, L, Thornalley, PJ, Itoh, K, Yamamoto, M, Hayes, JD (2004). Transcription factor Nrf2 is essential for induction of NAD(P)H:quinone oxidoreductase 1, glutathione S-transferases, and glutamate cysteine ligase by broccoli seeds and isothiocyanates. *J Nutr* **134:** 3499S-3506S.

Meier, BW, Gomez, JD, Kirichenko, OV, Thompson, JA (2007). Mechanistic basis for inflammation and tumor promotion in lungs of 2,6-di-tert-butyl-4-methylphenol-treated mice: electrophilic metabolites alkylate and inactivate antioxidant enzymes. *Chem Res Toxicol* **20:** 199-207.

Meier, BW, Gomez, JD, Zhou, A, Thompson, JA (2005). Immunochemical and proteomic analysis of covalent adducts formed by quinone methide tumor promoters in mouse lung epithelial cell lines. *Chem Res Toxicol* **18:** 1575-85.

Meyer, M, Schreck, R, Baeuerle, PA (1993). H2O2 and antioxidants have opposite effects on activation of NF-kappa B and AP-1 in intact cells: AP-1 as secondary antioxidant-responsive factor. *EMBO J* **12:** 2005-15.

Mihm, S, Galter, D, Droge, W (1995). Modulation of transcription factor NF kappa B activity by intracellular glutathione levels and by variations of the extracellular cysteine supply. *FASEB J* **9:** 246-52.

Miner, DJ, Kissinger, PT (1979). Evidence for the involvement of N-acetyl-p-quinoneimine in acetaminophen metabolism. *Biochem Pharmacol* **28:** 3285-90.

Miseta, A, Csutora, P (2000). Relationship between the occurrence of cysteine in proteins and the complexity of organisms. *Mol Biol Evol* **17:** 1232-9.

Mitchell, JR, Jollow, DJ, Potter, WZ, Davis, DC, Gillette, JR, Brodie, BB (1973). Acetaminophen-induced hepatic necrosis. I. Role of drug metabolism. *J Pharmacol Exp Ther* **187:** 185-94.

Mitchell, JR, Thorgeirsson, SS, Potter, WZ, Jollow, DJ, Keiser, H (1974). Acetaminophen-induced hepatic injury: protective role of glutathione in man and rationale for therapy. *Clin Pharmacol Ther* **16:** 676-84.

Mitchell, JR, Zimmerman, HJ, Ishak, KG, Thorgeirsson, UP, Timbrell, JA, Snodgrass, WR, Nelson, SD (1976). Isoniazid liver injury: clinical spectrum, pathology, and probable pathogenesis. *Ann Intern Med* **84:** 181-92.

Moi, P, Chan, K, Asunis, I, Cao, A, Kan, YW (1994). Isolation of NF-E2-related factor 2 (Nrf2), a NF-E2-like basic leucine zipper transcriptional activator that binds to the tandem NF-E2/AP1 repeat of the beta-globin locus control region. *Proc Natl Acad Sci U S A* **91:** 9926-30.

Moinova, HR, Mulcahy, RT (1999). Up-regulation of the human gamma-glutamylcysteine synthetase regulatory subunit gene involves binding of Nrf-2 to an electrophile responsive element. *Biochem Biophys Res Commun* **261:** 661-8.

Mooney, H, Roberts, R, Cooksley, WG, Halliday, JW, Powell, LW (1985). Alterations in the liver with ageing. *Clin Gastroenterol* **14:** 757-71.

Moscat, J, Diaz-Meco, MT, Wooten, MW (2007). Signal integration and diversification through the p62 scaffold protein. *Trends Biochem Sci* **32:** 95-100.

Motohashi, H, O'Connor, T, Katsuoka, F, Engel, JD, Yamamoto, M (2002). Integration and diversity of the regulatory network composed of Maf and CNC families of transcription factors. *Gene* **294:** 1-12.

Mullally, JE, Moos, PJ, Edes, K, Fitzpatrick, FA (2001). Cyclopentenone prostaglandins of the J series inhibit the ubiquitin isopeptidase activity of the proteasome pathway. *J Biol Chem* **276:** 30366-73.

Muto, A, Tashiro, S, Tsuchiya, H, Kume, A, Kanno, M, Ito, E, Yamamoto, M, Igarashi, K (2002). Activation of Maf/AP-1 repressor Bach2 by oxidative stress promotes apoptosis and its interaction with promyelocytic leukemia nuclear bodies. *J Biol Chem* **277:** 20724-33.

Myers, TG, Dietz, EC, Anderson, NL, Khairallah, EA, Cohen, SD, Nelson, SD (1995). A comparative study of mouse liver proteins arylated by reactive metabolites of acetaminophen and its nonhepatotoxic regioisomer, 3'-hydroxyacetanilide. *Chem Res Toxicol* **8:** 403-13.

Myhrstad, MC, Husberg, C, Murphy, P, Nordstrom, O, Blomhoff, R, Moskaug, JO, Kolsto, AB (2001). TCF11/Nrf1 overexpression increases the intracellular glutathione level and can transactivate the gamma-glutamylcysteine synthetase (GCS) heavy subunit promoter. *Biochim Biophys Acta* **1517:** 212-9.

Nagy, A (2000). Cre recombinase: the universal reagent for genome tailoring. *Genesis* **26:** 99-109.

Nakamura, Y, Ito, K (1998). How protein reads the stop codon and terminates translation. *Genes Cells* **3:** 265-78.

Nakashima, I, Kato, M, Akhand, AA, Suzuki, H, Takeda, K, Hossain, K, Kawamoto, Y (2002). Redox-linked signal transduction pathways for protein tyrosine kinase activation. *Antioxid Redox Signal* **4:** 517-31.

Nakaso, K, Yano, H, Fukuhara, Y, Takeshima, T, Wada-Isoe, K, Nakashima, K (2003). PI3K is a key molecule in the Nrf2-mediated regulation of antioxidative proteins by hemin in human neuroblastoma cells. *FEBS Lett* **546:** 181-4.

Natsch, A, Emter, R (2007). Skin sensitizers induce antioxidant response element dependent genes: Application to the in vitro testing of the sensitization potential of chemicals. *Toxicol Sci*: Oct 11 [Epub ahead of print].

Nel, A, Xia, T, Madler, L, Li, N (2006). Toxic potential of materials at the nanolevel. *Science* **311:** 622-7.

Netto, LE, de Oliveira, MA, Monteiro, G, Demasi, AP, Cussiol, JR, Discola, KF, Demasi, M, Silva, GM, Alves, SV, Faria, VG, Horta, BB (2007). Reactive cysteine in proteins: Protein folding, antioxidant defense, redox signaling and more. *Comp Biochem Physiol C Toxicol Pharmacol* **146:** 180-93.

Newsome, PN, Plevris, JN, Nelson, LJ, Hayes, PC (2000). Animal models of fulminant hepatic failure: a critical evaluation. *Liver Transpl* **6:** 21-31.

Nguyen, T, Huang, HC, Pickett, CB (2000). Transcriptional regulation of the antioxidant response element. Activation by Nrf2 and repression by MafK. *J Biol Chem* **275:** 15466-73.

Nguyen, T, Sherratt, PJ, Huang, HC, Yang, CS, Pickett, CB (2003). Increased protein stability as a mechanism that enhances Nrf2-mediated transcriptional activation of the antioxidant response element. Degradation of Nrf2 by the 26 S proteasome. *J Biol Chem* **278:** 4536-41.

Nguyen, T, Sherratt, PJ, Nioi, P, Yang, CS, Pickett, CB (2005). Nrf2 controls constitutive and inducible expression of ARE-driven genes through a dynamic pathway involving nucleocytoplasmic shuttling by Keap1. *J Biol Chem* **280:** 32485-92.

Nguyen, T, Yang, CS, Pickett, CB (2004). The pathways and molecular mechanisms regulating Nrf2 activation in response to chemical stress. *Free Radic Biol Med* **37:** 433-41.

Nicotera, P, Melino, G (2004). Regulation of the apoptosis-necrosis switch. *Oncogene* **23:** 2757-65.

Nioi, P, Nguyen, T (2007). A mutation of Keap1 found in breast cancer impairs its ability to repress Nrf2 activity. *Biochem Biophys Res Commun* **362:** 816-21.

Nioi, P, Nguyen, T, Sherratt, PJ, Pickett, CB (2005). The carboxy-terminal Neh3 domain of Nrf2 is required for transcriptional activation. *Mol Cell Biol* **25:** 10895-906.

Nishi, T, Shimizu, N, Hiramoto, M, Sato, I, Yamaguchi, Y, Hasegawa, M, Aizawa, S, Tanaka, H, Kataoka, K, Watanabe, H, Handa, H (2002). Spatial redox regulation of a critical cysteine residue of NF-kappa B in vivo. *J Biol Chem* **277:** 44548-56.

Nishinaka, T, Yabe-Nishimura, C (2005). Transcription factor Nrf2 regulates promoter activity of mouse aldose reductase (AKR1B3) gene. *J Pharmacol Sci* **97:** 43-51.

Noguera-Mazon, V, Lemoine, J, Walker, O, Rouhier, N, Salvador, A, Jacquot, JP, Lancelin, JM, Krimm, I (2006). Glutathionylation induces the dissociation of 1-Cys D-peroxiredoxin non-covalent homodimer. *J Biol Chem* **281:** 31736-42.

Nordberg, J, Arner, ES (2001). Reactive oxygen species, antioxidants, and the mammalian thioredoxin system. *Free Radic Biol Med* **31:** 1287-312.

Novina, CD, Sharp, PA (2004). The RNAi revolution. *Nature* **430:** 161-4.

Numazawa, S, Ishikawa, M, Yoshida, A, Tanaka, S, Yoshida, T (2003). Atypical protein kinase C mediates activation of NF-E2-related factor 2 in response to oxidative stress. *Am J Physiol Cell Physiol* **285:** C334-42.

Obin, M, Shang, F, Gong, X, Handelman, G, Blumberg, J, Taylor, A (1998). Redox regulation of ubiquitin-conjugating enzymes: mechanistic insights using the thiol-specific oxidant diamide. *FASEB J* **12:** 561-9.

Oinonen, T, Lindros, KO (1998). Zonation of hepatic cytochrome P-450 expression and regulation. *Biochem J* **329 (Pt 1):** 17-35.

Okawa, H, Motohashi, H, Kobayashi, A, Aburatani, H, Kensler, TW, Yamamoto, M (2006). Hepatocyte-specific deletion of the keap1 gene activates Nrf2 and confers potent resistance against acute drug toxicity. *Biochem Biophys Res Commun* **339:** 79-88.

Osburn, WO, Kensler, TW (2007). Nrf2 signaling: An adaptive response pathway for protection against environmental toxic insults. *Mutat Res*: Nov 23 [Epub ahead of print].

Padmanabhan, B, Scharlock, M, Tong, KI, Nakamura, Y, Kang, MI, Kobayashi, A, Matsumoto, T, Tanaka, A, Yamamoto, M, Yokoyama, S (2005). Purification, crystallization and preliminary X-ray diffraction analysis of the Kelch-like motif region of mouse Keap1. *Acta Crystallogr Sect F Struct Biol Cryst Commun* **61:** 153-155.

Padmanabhan, B, Tong, KI, Ohta, T, Nakamura, Y, Scharlock, M, Ohtsuji, M, Kang, MI, Kobayashi, A, Yokoyama, S, Yamamoto, M (2006). Structural basis for defects of Keap1 activity provoked by its point mutations in lung cancer. *Mol Cell* **21:** 689-700.

Paget, MSB, Buttner, MJ (2003). Thiol-Based Regulatory Switches. *Annu Rev Genetics* **37:** 91-121.

Pahl, HL (1999). Activators and target genes of Rel/NF-kappaB transcription factors. *Oncogene* **18:** 6853-66.

Palacian, E, Gonzalez, PJ, Pineiro, M, Hernandez, F (1990). Dicarboxylic acid anhydrides as dissociating agents of protein-containing structures. *Mol Cell Biochem* **97:** 101-11.

Pantano, C, Reynaert, NL, Van Der Vliet, A, Janssen-Heininger, YMW (2006). Redox-sensitive kinases of the nuclear factor-kappa-B signaling pathway. *Antioxid Redox Signal* **8:** 1791-1806.

Papaiahgari, S, Kleeberger, SR, Cho, HY, Kalvakolanu, DV, Reddy, SP (2004). NADPH oxidase and ERK signaling regulates hyperoxia-induced Nrf2-ARE transcriptional response in pulmonary epithelial cells. *J Biol Chem* **279:** 42302-12.

Papaiahgari, S, Zhang, Q, Kleeberger, SR, Cho, HY, Reddy, SP (2006). Hyperoxia stimulates an Nrf2-ARE transcriptional response via ROS-EGFR-PI3K-Akt/ERK MAP kinase signaling in pulmonary epithelial cells. *Antioxid Redox Signal* **8:** 43-52.

Park, BK (1986). Metabolic basis of adverse drug reactions. *J R Coll Physicians Lond* **20:** 195-200.

Park, BK, Kitteringham, NR, Maggs, JL, Pirmohamed, M, Williams, DP (2005a). The role of metabolic activation in drug-induced hepatotoxicity. *Annu Rev Pharmacol Toxicol* **45:** 177-202.

Park, BK, Williams, DP, Naisbitt, DJ, Kitteringham, NR, Pirmohamed, M (2005b). Investigation of toxic metabolites during drug development. *Toxicol Appl Pharmacol* **207:** 425-34.

Park, BK, Pirmohamed, M, Kitteringham, NR (1995). The role of cytochrome P450 enzymes in hepatic and extrahepatic human drug toxicity. *Pharmacol Ther* **68:** 385-424.

Park, BK, Pirmohamed, M, Kitteringham, NR (1998). Role of drug disposition in drug hypersensitivity: a chemical, molecular, and clinical perspective. *Chem Res Toxicol* **11:** 969-88.

Park, BK, Tingle, MD, Grabowski, PS, Coleman, JW, Kitteringham, NR (1987). Drug-protein conjugates--XI. Disposition and immunogenicity of dinitrofluorobenzene, a model compound for the investigation of drugs as haptens. *Biochem Pharmacol* **36:** 591-9.

Park, EY, Rho, HM (2002). The transcriptional activation of the human copper/zinc superoxide dismutase gene by 2,3,7,8-tetrachlorodibenzo-p-dioxin through two different regulator sites, the antioxidant responsive element and xenobiotic responsive element. *Mol Cell Biochem* **240:** 47-55.

Pearl, LH, Prodromou, C (2006). Structure and mechanism of the Hsp90 molecular chaperone machinery. *Annu Rev Biochem* **75:** 271-94.

Peng, J, Schwartz, D, Elias, JE, Thoreen, CC, Cheng, D, Marsischky, G, Roelofs, J, Finley, D, Gygi, SP (2003). A proteomics approach to understanding protein ubiquitination. *Nat Biotechnol* **21:** 921-6.

Perez-Sala, D, Cernuda-Morollon, E, Canada, FJ (2003). Molecular basis for the direct inhibition of AP-1 DNA binding by 15-deoxy-Delta 12,14-prostaglandin J2. *J Biol Chem* **278:** 51251-60.

Persengiev, SP, Zhu, X, Green, MR (2004). Nonspecific, concentration-dependent stimulation and repression of mammalian gene expression by small interfering RNAs (siRNAs). *Rna* **10:** 12-8.

Petzer, JP, Navamal, M, Johnson, JK, Kwak, MK, Kensler, TW, Fishbein, JC (2003). Phase 2 enzyme induction by the major metabolite of oltipraz. *Chem Res Toxicol* **16:** 1463-9.

Pickart, CM (2001). Mechanisms underlying ubiquitination. *Annu Rev Biochem* **70:** 503-33.

Pietsch, EC, Chan, JY, Torti, FM, Torti, SV (2003). Nrf2 mediates the induction of ferritin H in response to xenobiotics and cancer chemopreventive dithiolethiones. *J Biol Chem* **278:** 2361-9.

Pintard, L, Willems, A, Peter, M (2004). Cullin-based ubiquitin ligases: Cul3-BTB complexes join the family. *EMBO J* **23:** 1681-7.

Pirmohamed, M, Breckenridge, AM, Kitteringham, NR, Park, BK (1998). Adverse drug reactions. *Br Med J* **316:** 1295-8.

Pirmohamed, M, James, S, Meakin, S, Green, C, Scott, AK, Walley, TJ, Farrar, K, Park, BK, Breckenridge, AM (2004). Adverse drug reactions as cause of admission to hospital: prospective analysis of 18 820 patients. *Br Med J* **329:** 15-9.

Porath, J (1992). Immobilized metal ion affinity chromatography. *Protein Expr Purif* **3:** 263-81.

Porath, J, Carlsson, J, Olsson, I, Belfrage, G (1975). Metal chelate affinity chromatography, a new approach to protein fractionation. *Nature* **258:** 598-9.

Potter, DW, Hinson, JA (1986). Reactions of glutathione with oxidative intermediates of acetaminophen. *Adv Exp Med Biol* **197:** 763-72.

Potter, WZ, Thorgeirsson, SS, Jollow, DJ, Mitchell, JR (1974). Acetaminophen-induced hepatic necrosis. V. Correlation of hepatic necrosis, covalent binding and glutathione depletion in hamsters. *Pharmacology* **12:** 129-43.

Prescott, LF (1980). Kinetics and metabolism of paracetamol and phenacetin. *Br J Clin Pharmacol* **10 Suppl 2:** 291S-298S.

Prestera, T, Holtzclaw, WD, Zhang, Y, Talalay, P (1993a). Chemical and molecular regulation of enzymes that detoxify carcinogens. *Proc Natl Acad Sci U S A* **90:** 2965-9.

Prestera, T, Zhang, Y, Spencer, SR, Wilczak, CA, Talalay, P (1993b). The electrophile counterattack response: protection against neoplasia and toxicity. *Adv Enzyme Regul* **33:** 281-96.

Primiano, T, Sutter, TR, Kensler, TW (1997). Antioxidant-inducible genes. *Adv Pharmacol* **38:** 293-328.

Purdom-Dickinson, SE, Lin, Y, Dedek, M, Morrissy, S, Johnson, J, Chen, QM (2007). Induction of antioxidant and detoxification response by oxidants in cardiomyocytes: evidence from gene expression profiling and activation of Nrf2 transcription factor. *J Mol Cell Cardiol* **42:** 159-76.

Qiu, Y, Benet, LZ, Burlingame, AL (2001). Identification of hepatic protein targets of the reactive metabolites of the non-hepatotoxic regioisomer of acetaminophen, 3'-hydroxyacetanilide, in the mouse in vivo using two-dimensional gel electrophoresis and mass spectrometry. *Adv Exp Med Biol* **500:** 663-73.

Rafeiro, E, Barr, SG, Harrison, JJ, Racz, WJ (1994). Effects of N-acetylcysteine and dithiothreitol on glutathione and protein thiol replenishment during acetaminophen-induced toxicity in isolated mouse hepatocytes. *Toxicology* **93:** 209-24.

Raffray, M, Cohen, GM (1997). Apoptosis and necrosis in toxicology: a continuum or distinct modes of cell death? *Pharmacol Ther* **75:** 153-77.

Ralat, LA, Manevich, Y, Fisher, AB, Colman, RF (2006). Direct evidence for the formation of a complex between 1-cysteine peroxiredoxin and glutathione S-transferase pi with activity changes in both enzymes. *Biochemistry* **45:** 360-72.

Ramos-Gomez, M, Dolan, PM, Itoh, K, Yamamoto, M, Kensler, TW (2003). Interactive effects of nrf2 genotype and oltipraz on benzo[a]pyrene-DNA adducts and tumor yield in mice. *Carcinogenesis* **24:** 461-7.

Ramos-Gomez, M, Kwak, MK, Dolan, PM, Itoh, K, Yamamoto, M, Talalay, P, Kensler, TW (2001). Sensitivity to carcinogenesis is increased and chemoprotective efficacy of enzyme inducers is lost in nrf2 transcription factor-deficient mice. *Proc Natl Acad Sci U S A* **98:** 3410-5.

Randle, LE, Goldring, CE, Benson, CA, Metcalfe, PN, Kitteringham, NR, Park, BK, Williams, DP (2008). Investigation of the effect of a panel of model hepatotoxins on the Nrf2-Keap1 defence response pathway in CD-1 mice. *Toxicology* **243:** 249-60.

Rangasamy, T, Guo, J, Mitzner, WA, Roman, J, Singh, A, Fryer, AD, Yamamoto, M, Kensler, TW, Tuder, RM, Georas, SN, Biswal, S (2005). Disruption of Nrf2 enhances susceptibility to severe airway inflammation and asthma in mice. *J Exp Med* **202:** 47-59.

Rao, L, Perez, D, White, E (1996). Lamin proteolysis facilitates nuclear events during apoptosis. *J Cell Biol* **135:** 1441-55.

Raucy, JL, Lasker, JM, Lieber, CS, Black, M (1989). Acetaminophen activation by human liver cytochromes P450IIE1 and P450IA2. *Arch Biochem Biophys* **271:** 270-83.

Reichard, JF, Motz, GT, Puga, A (2007). Heme oxygenase-1 induction by NRF2 requires inactivation of the transcriptional repressor BACH1. *Nucleic Acids Res* **35:** 7074-86.

Reichard, JF, Petersen, DR (2006). Involvement of phosphatidylinositol 3-kinase and extracellular-regulated kinase in hepatic stellate cell antioxidant response and myofibroblastic transdifferentiation. *Arch Biochem Biophys* **446:** 111-8.

Riedl, SJ, Salvesen, GS (2007). The apoptosome: signalling platform of cell death. *Nat Rev Mol Cell Biol* **8:** 405-13.

Rikans, LE (1984). Influence of aging on the susceptibility of rats to hepatotoxic injury. *Toxicol Appl Pharmacol* **73:** 243-9.

Ritter, JK (2000). Roles of glucuronidation and UDP-glucuronosyltransferases in xenobiotic bioactivation reactions. *Chem Biol Interact* **129:** 171-93.

Rivero, A, Mira, JA, Pineda, JA (2007). Liver toxicity induced by non-nucleoside reverse transcriptase inhibitors. *J Antimicrob Chemother* **59:** 342-6.

Roberts, SA, Price, VF, Jollow, DJ (1986). The mechanisms of cobalt chloride-induced protection against acetaminophen hepatotoxicity. *Drug Metab Dispos* **14:** 25-33.

Robertson, JD, Orrenius, S (2000). Molecular mechanisms of apoptosis induced by cytotoxic chemicals. *Crit Rev Toxicol* **30:** 609-27.

Rosen, GM, Rauckman, EJ, Ellington, SP, Dahlin, DC, Christie, JL, Nelson, SD (1984). Reduction and glutathione conjugation reactions of N-acetyl-p-benzoquinone imine and two dimethylated analogues. *Mol Pharmacol* **25:** 151-7.

Rossi, A, Kapahi, P, Natoli, G, Takahashi, T, Chen, Y, Karin, M, Santoro, MG (2000). Anti-inflammatory cyclopentenone prostaglandins are direct inhibitors of IkappaB kinase. *Nature* **403:** 103-8.

Rudolph, R, Lilie, H (1996). In vitro folding of inclusion body proteins. *Faseb J* **10:** 49-56.

Rumack, BH (2002). Acetaminophen hepatotoxicity: the first 35 years. *J Toxicol Clin Toxicol* **40:** 3-20.

Rundgren, M, Porubek, DJ, Harvison, PJ, Cotgreave, IA, Moldeus, P, Nelson, SD (1988). Comparative cytotoxic effects of N-acetyl-p-benzoquinone imine and two dimethylated analogues. *Mol Pharmacol* **34:** 566-72.

Rushmore, TH, Pickett, CB (1990). Transcriptional regulation of the rat glutathione S-transferase Ya subunit gene. Characterization of a xenobiotic-responsive element controlling inducible expression by phenolic antioxidants. *J Biol Chem* **265:** 14648-53.

Sakurai, T, Kanayama, M, Shibata, T, Itoh, K, Kobayashi, A, Yamamoto, M, Uchida, K (2006). Ebselen, a seleno-organic antioxidant, as an electrophile. *Chem Res Toxicol* **19:** 1196-204.

Salazar, M, Rojo, AI, Velasco, D, de Sagarra, RM, Cuadrado, A (2006). Glycogen synthase kinase-3beta inhibits the xenobiotic and antioxidant cell response by direct phosphorylation and nuclear exclusion of the transcription factor Nrf2. *J Biol Chem* **281:** 14841-51.

Salmeen, A, Barford, D (2005). Functions and mechanisms of redox regulation of cysteine-based phosphatases. *Antioxid Redox Signal* **7:** 560-77.

Sanchez-Gomez, FJ, Gayarre, J, Avellano, MI, Perez-Sala, D (2007). Direct evidence for the covalent modification of glutathione-S-transferase P1-1 by electrophilic prostaglandins: implications for enzyme inactivation and cell survival. *Arch Biochem Biophys* **457:** 150-9.

Sankaranarayanan, K, Jaiswal, AK (2004). Nrf3 negatively regulates antioxidant-response element-mediated expression and antioxidant induction of NAD(P)H:quinone oxidoreductase1 gene. *J Biol Chem* **279:** 50810-7.

Sawa, T, Zaki, MH, Okamoto, T, Akuta, T, Tokutomi, Y, Kim-Mitsuyama, S, Ihara, H, Kobayashi, A, Yamamoto, M, Fujii, S, Arimoto, H, Akaike, T (2007). Protein S-guanylation by the biological signal 8-nitroguanosine 3',5'-cyclic monophosphate. *Nat Chem Biol* **3:** 727-35.

Schenk, H, Klein, M, Erdbrugger, W, Droge, W, Schulze-Osthoff, K (1994). Distinct effects of thioredoxin and antioxidants on the activation of transcription factors NF-kappa B and AP-1. *Proc Natl Acad Sci U S A* **91:** 1672-6.

Schenker, S, Bay, M (1994). Drug disposition and hepatotoxicity in the elderly. *J Clin Gastroenterol* **18:** 232-7.

Schoneich, C, Sharov, VS (2006). Mass spectrometry of protein modifications by reactive oxygen and nitrogen species. *Free Radic Biol Med* **41:** 1507-20.

Sciulli, MG, Seta, F, Tacconelli, S, Capone, ML, Ricciotti, E, Pistritto, G, Patrignani, P (2003). Effects of acetaminophen on constitutive and inducible prostanoid biosynthesis in human blood cells. *Br J Pharmacol* **138:** 634-41.

Sekhar, KR, Crooks, PA, Sonar, VN, Friedman, DB, Chan, JY, Meredith, MJ, Starnes, JH, Kelton, KR, Summar, SR, Sasi, S, Freeman, ML (2003). NADPH oxidase activity is essential for Keap1/Nrf2-mediated induction of GCLC in response to 2-indol-3-yl-methylenequinuclidin-3-ols. *Cancer Res* **63:** 5636-45.

Sekhar, KR, Soltaninassab, SR, Borrelli, MJ, Xu, ZQ, Meredith, MJ, Domann, FE, Freeman, ML (2000). Inhibition of the 26S proteasome induces expression of GLCLC, the catalytic subunit for gamma-glutamylcysteine synthetase. *Biochem Biophys Res Commun* **270:** 311-7.

Semenza, GL (2003). Targeting HIF-1 for cancer therapy. *Nat Rev Cancer* **3:** 721-32.

Semizarov, D, Frost, L, Sarthy, A, Kroeger, P, Halbert, DN, Fesik, SW (2003). Specificity of short interfering RNA determined through gene expression signatures. *Proc Natl Acad Sci U S A* **100:** 6347-52.

Sethuraman, M, McComb, ME, Heibeck, T, Costello, CE, Cohen, RA (2004a). Isotope-coded affinity tag approach to identify and quantify oxidant-sensitive protein thiols. *Mol Cell Proteomics* **3:** 273-8.

Sethuraman, M, McComb, ME, Huang, H, Huang, S, Heibeck, T, Costello, CE, Cohen, RA (2004b). Isotope-coded affinity tag (ICAT) approach to redox proteomics: identification and quantitation of oxidant-sensitive cysteine thiols in complex protein mixtures. *J Proteome Res* **3:** 1228-33.

Shapiro, TA, Fahey, JW, Dinkova-Kostova, AT, Holtzclaw, WD, Stephenson, KK, Wade, KL, Ye, L, Talalay, P (2006). Safety, tolerance, and metabolism of broccoli sprout glucosinolates and isothiocyanates: a clinical phase I study. *Nutr Cancer* **55:** 53-62.

Shaulian, E, Karin, M (2002). AP-1 as a regulator of cell life and death. *Nat Cell Biol* **4:** E131-6.

Shelby, MK, Klaassen, CD (2006). Induction of rat UDP-glucuronosyltransferases in liver and duodenum by microsomal enzyme inducers that activate various transcriptional pathways. *Drug Metab Dispos* **34:** 1772-8.

Shibata, T, Yamada, T, Kondo, M, Tanahashi, N, Tanaka, K, Nakamura, H, Masutani, H, Yodoi, J, Uchida, K (2003). An endogenous electrophile that modulates the regulatory mechanism of protein turnover: inhibitory effects of 15-deoxy-Delta 12,14-prostaglandin J2 on proteasome. *Biochemistry* **42:** 13960-8.

Shih, AY, Imbeault, S, Barakauskas, V, Erb, H, Jiang, L, Li, P, Murphy, TH (2005). Induction of the Nrf2-driven antioxidant response confers neuroprotection during mitochondrial stress in vivo. *J Biol Chem* **280:** 22925-36.

Shih, PH, Yen, GC (2007). Differential expressions of antioxidant status in aging rats: the role of transcriptional factor Nrf2 and MAPK signaling pathway. *Biogerontology* **8:** 71-80.

Shilov, IV, Seymour, SL, Patel, AA, Loboda, A, Tang, WH, Keating, SP, Hunter, CL, Nuwaysir, LM, Schaeffer, DA (2007). The Paragon Algorithm, a next generation search engine that uses sequence temperature values and feature probabilities to identify peptides from tandem mass spectra. *Mol Cell Proteomics* **6:** 1638-55.

Shin, NY, Liu, Q, Stamer, SL, Liebler, DC (2007). Protein targets of reactive electrophiles in human liver microsomes. *Chem Res Toxicol* **20:** 859-67.

Shinkai, Y, Sumi, D, Fukami, I, Ishii, T, Kumagai, Y (2006). Sulforaphane, an activator of Nrf2, suppresses cellular accumulation of arsenic and its cytotoxicity in primary mouse hepatocytes. *FEBS Lett* **580:** 1771-4.

Singh, A, Misra, V, Thimmulappa, RK, Lee, H, Ames, S, Hoque, MO, Herman, JG, Baylin, SB, Sidransky, D, Gabrielson, E, Brock, MV, Biswal, S (2006a). Dysfunctional KEAP1-NRF2 interaction in non-small-cell lung cancer. *PLoS Med* **3:** e420.

Singh, A, Rangasamy, T, Thimmulappa, RK, Lee, H, Osburn, WO, Brigelius-Flohe, R, Kensler, TW, Yamamoto, M, Biswal, S (2006b). Glutathione peroxidase 2, the major cigarette smoke-inducible isoform of GPX in lungs, is regulated by Nrf2. *Am J Respir Cell Mol Biol* **35:** 639-50.

Singh, SM, Panda, AK (2005). Solubilization and refolding of bacterial inclusion body proteins. *J Biosci Bioeng* **99:** 303-10.

Sledz, CA, Holko, M, de Veer, MJ, Silverman, RH, Williams, BR (2003). Activation of the interferon system by short-interfering RNAs. *Nat Cell Biol* **5:** 834-9.

Slitt, AL, Cherrington, NJ, Dieter, MZ, Aleksunes, LM, Scheffer, GL, Huang, W, Moore, DD, Klaassen, CD (2006). trans-Stilbene oxide induces expression of genes involved in metabolism and transport in mouse liver via CAR and Nrf2 transcription factors. *Mol Pharmacol* **69:** 1554-63.

Smilkstein, MJ, Bronstein, AC, Linden, C, Augenstein, WL, Kulig, KW, Rumack, BH (1991). Acetaminophen overdose: a 48-hour intravenous N-acetylcysteine treatment protocol. *Ann Emerg Med* **20:** 1058-63.

Smith, PK, Krohn, RI, Hermanson, GT, Mallia, AK, Gartner, FH, Provenzano, MD, Fujimoto, EK, Goeke, NM, Olson, BJ, Klenk, DC (1985). Measurement of protein using bicinchoninic acid. *Anal Biochem* **150:** 76-85.

Snyder, GH, Cennerazzo, MJ, Karalis, AJ, Field, D (1981). Electrostatic influence of local cysteine environments on disulfide exchange kinetics. *Biochemistry* **20:** 6509-19.

So, HS, Kim, HJ, Lee, JH, Lee, JH, Park, SY, Park, C, Kim, YH, Kim, JK, Lee, KM, Kim, KS, Chung, SY, Jang, WC, Moon, SK, Chung, HT, Park, RK (2006). Flunarizine induces Nrf2-mediated transcriptional activation of heme oxygenase-1 in protection of auditory cells from cisplatin. *Cell Death Differ* **13:** 1763-75.

Stewart, D, Killeen, E, Naquin, R, Alam, S, Alam, J (2003). Degradation of transcription factor Nrf2 via the ubiquitin-proteasome pathway and stabilization by cadmium. *J Biol Chem* **278:** 2396-402.

Stich, TM (1990). Determination of protein covalently bound to agarose supports using bicinchoninic acid. *Anal Biochem* **191:** 343-6.

Storz, G, Tartaglia, LA, Ames, BN (1990). Transcriptional regulator of oxidative stress-inducible genes: direct activation by oxidation. *Science* **248:** 189-94.

Streeter, AJ, Dahlin, DC, Nelson, SD, Baillie, TA (1984). The covalent binding of acetaminophen to protein. Evidence for cysteine residues as major sites of arylation in vitro. *Chem Biol Interact* **48:** 349-66.

Studier, FW, Moffatt, BA (1986). Use of bacteriophage T7 RNA polymerase to direct selective high-level expression of cloned genes. *J Mol Biol* **189:** 113-30.

Suh, JH, Shenvi, SV, Dixon, BM, Liu, H, Jaiswal, AK, Liu, RM, Hagen, TM (2004). Decline in transcriptional activity of Nrf2 causes age-related loss of glutathione synthesis, which is reversible with lipoic acid. *Proc Natl Acad Sci U S A* **101:** 3381-6.

Sun, J, Hoshino, H, Takaku, K, Nakajima, O, Muto, A, Suzuki, H, Tashiro, S, Takahashi, S, Shibahara, S, Alam, J, Taketo, MM, Yamamoto, M, Igarashi, K (2002). Hemoprotein Bach1 regulates enhancer availability of heme oxygenase-1 gene. *EMBO J* **21:** 5216-24.

Talalay, P, De Long, MJ, Prochaska, HJ (1988). Identification of a common chemical signal regulating the induction of enzymes that protect against chemical carcinogenesis. *Proc Natl Acad Sci U S A* **85:** 8261-5.

Tansey, WP (2007a). Denaturing Protein Immunoprecipitation from Mammalian Cells. *CSH Protocols*: doi:10.1101/pdb.prot4619.

Tansey, WP (2007b). Nondenaturing Protein Immunoprecipitation from Mammalian Cells. *CSH Protocols*: doi:10.1101/pdb.prot4620.

Tarazi, EM, Harter, JG, Zimmerman, HJ, Ishak, KG, Eaton, RA (1993). Sulindac-associated hepatic injury: analysis of 91 cases reported to the Food and Drug Administration. *Gastroenterology* **104:** 569-74.

Tee, LB, Boobis, AR, Huggett, AC, Davies, DS (1986). Reversal of acetaminophen toxicity in isolated hamster hepatocytes by dithiothreitol. *Toxicol Appl Pharmacol* **83:** 294-314.

Tee, LB, Davies, DS, Seddon, CE, Boobis, AR (1987). Species differences in the hepatotoxicity of paracetamol are due to differences in the rate of conversion to its cytotoxic metabolite. *Biochem Pharmacol* **36:** 1041-52.

Temple, RJ, Himmel, MH (2002). Safety of newly approved drugs: implications for prescribing. *JAMA* **287:** 2273-5.

Thimmulappa, RK, Mai, KH, Srisuma, S, Kensler, TW, Yamamoto, M, Biswal, S (2002). Identification of Nrf2-regulated genes induced by the chemopreventive agent sulforaphane by oligonucleotide microarray. *Cancer Res* **62:** 5196-203.

Thomas, SH (1993). Paracetamol (acetaminophen) poisoning. *Pharmacol Ther* **60:** 91-120.

Thornberry, NA, Lazebnik, Y (1998). Caspases: enemies within. *Science* **281:** 1312-6.

Thummel, KE, Lee, CA, Kunze, KL, Nelson, SD, Slattery, JT (1993). Oxidation of acetaminophen to N-acetyl-p-aminobenzoquinone imine by human CYP3A4. *Biochem Pharmacol* **45:** 1563-9.

Thummel, KE, Slattery, JT, Ro, H, Chien, JY, Nelson, SD, Lown, KE, Watkins, PB (2000). Ethanol and production of the hepatotoxic metabolite of acetaminophen in healthy adults. *Clin Pharmacol Ther* **67:** 591-9.

Timbrell, J (2002). *Principles of Biochemical Toxicology*. Third edn. Taylor & Francis: London.

Tirmenstein, MA, Nelson, SD (1990). Acetaminophen-induced oxidation of protein thiols. Contribution of impaired thiol-metabolizing enzymes and the breakdown of adenine nucleotides. *J Biol Chem* **265:** 3059-65.

Tirmenstein, MA, Nelson, SD (1989). Subcellular binding and effects on calcium homeostasis produced by acetaminophen and a nonhepatotoxic regioisomer, 3'-hydroxyacetanilide, in mouse liver. *J Biol Chem* **264:** 9814-9.

Tirumalai, R, Rajesh Kumar, T, Mai, KH, Biswal, S (2002). Acrolein causes transcriptional induction of phase II genes by activation of Nrf2 in human lung type II epithelial (A549) cells. *Toxicol Lett* **132:** 27-36.

Tone, Y, Kawamata, K, Murakami, T, Higashi, Y, Yata, N (1990). Dose-dependent pharmacokinetics and first-pass metabolism of acetaminophen in rats. *J Pharmacobiodyn* **13:** 327-35.

Tong, KI, Katoh, Y, Kusunoki, H, Itoh, K, Tanaka, T, Yamamoto, M (2006a). Keap1 recruits Neh2 through binding to ETGE and DLG motifs: characterization of the two-site molecular recognition model. *Mol Cell Biol* **26:** 2887-900.

Tong, KI, Kobayashi, A, Katsuoka, F, Yamamoto, M (2006b). Two-site substrate recognition model for the Keap1-Nrf2 system: a hinge and latch mechanism. *Biol Chem* **387:** 1311-20.

Torchinsky, YM (1981). *Sulfur in proteins*. Pergamon Press: Oxford.

Tsokos-Kuhn, JO, Hughes, H, Smith, CV, Mitchell, JR (1988). Alkylation of the liver plasma membrane and inhibition of the Ca2+ ATPase by acetaminophen. *Biochem Pharmacol* **37:** 2125-31.

Umemura, T, Kuroiwa, Y, Kitamura, Y, Ishii, Y, Kanki, K, Kodama, Y, Itoh, K, Yamamoto, M, Nishikawa, A, Hirose, M (2006). A crucial role of Nrf2 in in vivo defense against oxidative damage by an environmental pollutant, pentachlorophenol. *Toxicol Sci* **90:** 111-9.

Unger, T, Juven-Gershon, T, Moallem, E, Berger, M, Vogt Sionov, R, Lozano, G, Oren, M, Haupt, Y (1999). Critical role for Ser20 of human p53 in the negative regulation of p53 by Mdm2. *EMBO J* **18:** 1805-14.

Unwin, RD, Griffiths, JR, Leverentz, MK, Grallert, A, Hagan, IM, Whetton, AD (2005). Multiple reaction monitoring to identify sites of protein phosphorylation with high sensitivity. *Mol Cell Proteomics* **4:** 1134-44.

Usami, H, Kusano, Y, Kumagai, T, Osada, S, Itoh, K, Kobayashi, A, Yamamoto, M, Uchida, K (2005). Selective induction of the tumor marker glutathione S-transferase P1 by proteasome inhibitors. *J Biol Chem* **280:** 25267-76.

Valacchi, G, Pagnin, E, Phung, A, Nardini, M, Schock, BC, Cross, CE, van der Vliet, A (2005). Inhibition of NFkappaB activation and IL-8 expression in human bronchial epithelial cells by acrolein. *Antioxid Redox Signal* **7:** 25-31.

Vandeputte, C, Guizon, I, Genestie-Denis, I, Vannier, B, Lorenzon, G (1994). A microtiter plate assay for total glutathione and glutathione disulfide contents in cultured/isolated cells: performance study of a new miniaturized protocol. *Cell Biol Toxicol* **10:** 415-21.

Vargas, MR, Pehar, M, Cassina, P, Beckman, JS, Barbeito, L (2006). Increased glutathione biosynthesis by Nrf2 activation in astrocytes prevents p75NTR-dependent motor neuron apoptosis. *J Neurochem* **97:** 687-96.

Velichkova, M, Hasson, T (2005). Keap1 regulates the oxidation-sensitive shuttling of Nrf2 into and out of the nucleus via a Crm1-dependent nuclear export mechanism. *Mol Cell Biol* **25:** 4501-13.

Venugopal, R, Jaiswal, AK (1996). Nrf1 and Nrf2 positively and c-Fos and Fra1 negatively regulate the human antioxidant response element-mediated expression of NAD(P)H:quinone oxidoreductase1 gene. *Proc Natl Acad Sci U S A* **93:** 14960-5.

Wadelius, M, Pirmohamed, M (2007). Pharmacogenetics of warfarin: current status and future challenges. *Pharmacogenomics J* **7:** 99-111.

Wakabayashi, N, Dinkova-Kostova, AT, Holtzclaw, WD, Kang, MI, Kobayashi, A, Yamamoto, M, Kensler, TW, Talalay, P (2004). Protection against electrophile and oxidant stress by induction of the phase 2 response: fate of cysteines of the Keap1 sensor modified by inducers. *Proc Natl Acad Sci U S A* **101:** 2040-5.

Wakabayashi, N, Itoh, K, Wakabayashi, J, Motohashi, H, Noda, S, Takahashi, S, Imakado, S, Kotsuji, T, Otsuka, F, Roop, DR, Harada, T, Engel, JD, Yamamoto, M (2003). Keap1-null mutation leads to postnatal lethality due to constitutive Nrf2 activation. *Nat Genet* **35:** 238-45.

Walgren, JL, Vincent, TS, Schey, KL, Buse, MG (2003). High glucose and insulin promote O-GlcNAc modification of proteins, including alpha-tubulin. *Am J Physiol Endocrinol Metab* **284:** E424-34.

Wang, H, Goldring, CE, Kitteringham, NR, Park, BK (2006a). Analysis of inter-individual variation in the Nrf2/Keap1 genes responsible for induction of the antioxidant response. *Drug Metab Rev* **38 (Suppl 1):** 84-85.

Wang, W, Jaiswal, AK (2006b). Nuclear factor Nrf2 and antioxidant response element regulate NRH:quinone oxidoreductase 2 (NQO2) gene expression and antioxidant induction. *Free Radic Biol Med* **40:** 1119-30.

Wang, W, Kwok, AM, Chan, JY (2007). The p65 isoform of Nrf1 is a dominant negative inhibitor of ARE-mediated transcription. *J Biol Chem.*

Wang, XJ, Hayes, JD, Wolf, CR (2006c). Generation of a stable antioxidant response element-driven reporter gene cell line and its use to show redox-dependent activation of nrf2 by cancer chemotherapeutic agents. *Cancer Res* **66:** 10983-94.

Warabi, E, Takabe, W, Minami, T, Inoue, K, Itoh, K, Yamamoto, M, Ishii, T, Kodama, T, Noguchi, N (2007). Shear stress stabilizes NF-E2-related factor 2 and induces antioxidant genes in endothelial cells: role of reactive oxygen/nitrogen species. *Free Radic Biol Med* **42:** 260-9.

Wasserman, WW, Fahl, WE (1997). Functional antioxidant responsive elements. *Proc Natl Acad Sci U S A* **94:** 5361-6.

Watai, Y, Kobayashi, A, Nagase, H, Mizukami, M, McEvoy, J, Singer, JD, Itoh, K, Yamamoto, M (2007). Subcellular localization and cytoplasmic complex status of endogenous Keap1. *Genes Cells* **12:** 1163-78.

Wielandt, AM, Vollrath, V, Farias, M, Chianale, J (2006). Bucillamine induces glutathione biosynthesis via activation of the transcription factor Nrf2. *Biochem Pharmacol* **72:** 455-62.

Wild, AC, Moinova, HR, Mulcahy, RT (1999). Regulation of gamma-glutamylcysteine synthetase subunit gene expression by the transcription factor Nrf2. *J Biol Chem* **274:** 33627-36.

Williams, RT (1959). *Detoxication Mechanisms: The Metabolism and Detoxication of Drugs, Toxic Substances and Other Organic Compounds* Chapman & Hall: London.

Wood, ZA, Schroder, E, Robin Harris, J, Poole, LB (2003). Structure, mechanism and regulation of peroxiredoxins. *Trends Biochem Sci* **28:** 32-40.

Wu, C (1995). Heat shock transcription factors: structure and regulation. *Annu Rev Cell Dev Biol* **11:** 441-69.

Xanthoudakis, S, Curran, T (1992). Identification and characterization of Ref-1, a nuclear protein that facilitates AP-1 DNA-binding activity. *EMBO J* **11:** 653-65.

Xia, YF, Ye, BQ, Li, YD, Wang, JG, He, XJ, Lin, X, Yao, X, Ma, D, Slungaard, A, Hebbel, RP, Key, NS, Geng, JG (2004). Andrographolide attenuates inflammation by inhibition of NF-kappa B activation through covalent modification of reduced cysteine 62 of p50. *J Immunol* **173:** 4207-17.

Xu, C, Huang, MT, Shen, G, Yuan, X, Lin, W, Khor, TO, Conney, AH, Tony Kong, AN (2006). Inhibition of 7,12-Dimethylbenz(a)anthracene-Induced Skin Tumorigenesis in C57BL/6 Mice by Sulforaphane Is Mediated by Nuclear Factor E2-Related Factor 2. *Cancer Res* **66:** 8293-8296.

Xu, Z, Chen, L, Leung, L, Yen, TS, Lee, C, Chan, JY (2005). Liver-specific inactivation of the Nrf1 gene in adult mouse leads to nonalcoholic steatohepatitis and hepatic neoplasia. *Proc Natl Acad Sci U S A* **102:** 4120-5.

Xue, F, Cooley, L (1993). kelch encodes a component of intercellular bridges in Drosophila egg chambers. *Cell* **72:** 681-93.

Yamamoto, N, Sawada, H, Izumi, Y, Kume, T, Katsuki, H, Shimohama, S, Akaike, A (2007). Proteasome inhibition induces glutathione synthesis and protects cells from oxidative stress: relevance to Parkinson disease. *J Biol Chem* **282:** 4364-72.

Yamamoto, T, Yoh, K, Kobayashi, A, Ishii, Y, Kure, S, Koyama, A, Sakamoto, T, Sekizawa, K, Motohashi, H, Yamamoto, M (2004). Identification of polymorphisms in the promoter region of the human NRF2 gene. *Biochem Biophys Res Commun* **321:** 72-9.

Yang, WH, Kim, JE, Nam, HW, Ju, JW, Kim, HS, Kim, YS, Cho, JW (2006). Modification of p53 with O-linked N-acetylglucosamine regulates p53 activity and stability. *Nat Cell Biol* **8:** 1074-83.

Yao, P, Nussler, A, Liu, L, Hao, L, Song, F, Schirmeier, A, Nussler, N (2007). Quercetin protects human hepatocytes from ethanol-derived oxidative stress by inducing heme oxygenase-1 via the MAPK/Nrf2 pathways. *J Hepatol* **47:** 253-61.

Yates, MS, Kwak, MK, Egner, PA, Groopman, JD, Bodreddigari, S, Sutter, TR, Baumgartner, KJ, Roebuck, BD, Liby, KT, Yore, MM, Honda, T, Gribble, GW, Sporn, MB, Kensler, TW (2006). Potent protection against aflatoxin-induced tumorigenesis through induction of Nrf2-regulated pathways by the triterpenoid 1-[2-cyano-3-,12-dioxooleana-1,9(11)-dien-28-oyl]imidazole. *Cancer Res* **66:** 2488-94.

Yeh, CT, Yen, GC (2006). Involvement of p38 MAPK and Nrf2 in phenolic acid-induced P-form phenol sulfotransferase expression in human hepatoma HepG2 cells. *Carcinogenesis* **27:** 1008-17.

Yew, WW, Leung, CC (2006). Antituberculosis drugs and hepatotoxicity. *Respirology* **11:** 699-707.

Yoh, K, Itoh, K, Enomoto, A, Hirayama, A, Yamaguchi, N, Kobayashi, M, Morito, N, Koyama, A, Yamamoto, M, Takahashi, S (2001). Nrf2-deficient female mice develop lupus-like autoimmune nephritis. *Kidney Int* **60:** 1343-53.

Yu, BP (1994). Cellular defenses against damage from reactive oxygen species. *Physiol Rev* **74:** 139-62.

Yu, X, Egner, PA, Wakabayashi, J, Wakabayashi, N, Yamamoto, M, Kensler, TW (2006). Nrf2-mediated induction of cytoprotective enzymes by 15-deoxy-Delta12,14-prostaglandin J2 is attenuated by alkenal/one oxidoreductase. *J Biol Chem* **281:** 26245-52.

Yuan, X, Xu, C, Pan, Z, Keum, YS, Kim, JH, Shen, G, Yu, S, Oo, KT, Ma, J, Kong, AN (2006). Butylated hydroxyanisole regulates ARE-mediated gene expression via Nrf2 coupled with ERK and JNK signaling pathway in HepG2 cells. *Mol Carcinog* **45:** 841-50.

Yueh, MF, Tukey, RH (2007). Nrf2-Keap1 signaling pathway regulates human UGT1A1 expression in vitro and in transgenic UGT1 mice. *J Biol Chem* **282:** 8749-58.

Zaman, MB, Leonard, MO, Ryan, EJ, Nolan, NP, Hoti, E, Maguire, D, Mulcahy, H, Traynor, O, Taylor, CT, Hegarty, JE, Geoghegan, JG, O'Farrelly, C (2007). Lower expression of Nrf2 mRNA in older donor livers: a possible contributor to increased ischemia-reperfusion injury? *Transplantation* **84:** 1272-8.

Zhang, DD, Hannink, M (2003a). Distinct cysteine residues in Keap1 are required for Keap1-dependent ubiquitination of Nrf2 and for stabilization of Nrf2 by chemopreventive agents and oxidative stress. *Mol Cell Biol* **23:** 8137-51.

Zhang, DD, Lo, SC, Cross, JV, Templeton, DJ, Hannink, M (2004). Keap1 is a redox-regulated substrate adaptor protein for a Cul3-dependent ubiquitin ligase complex. *Mol Cell Biol* **24:** 10941-53.

Zhang, DD, Lo, SC, Sun, Z, Habib, GM, Lieberman, MW, Hannink, M (2005). Ubiquitination of Keap1, a BTB-Kelch substrate adaptor protein for Cul3, targets Keap1 for degradation by a proteasome-independent pathway. *J Biol Chem* **280:** 30091-9.

Zhang, H, Court, N, Forman, HJ (2007a). Submicromolar concentrations of 4-hydroxynonenal induce glutamate cysteine ligase expression in HBE1 cells. *Redox Rep* **12:** 101-6.

Zhang, H, Liu, H, Dickinson, DA, Liu, RM, Postlethwait, EM, Laperche, Y, Forman, HJ (2006a). gamma-Glutamyl transpeptidase is induced by 4-hydroxynonenal via EpRE/Nrf2 signaling in rat epithelial type II cells. *Free Radic Biol Med* **40:** 1281-92.

Zhang, J, Hosoya, T, Maruyama, A, Nishikawa, K, Maher, JM, Ohta, T, Motohashi, H, Fukamizu, A, Shibahara, S, Itoh, K, Yamamoto, M (2007b). Nrf2 Neh5 domain is differentially utilized in the transactivation of cytoprotective genes. *Biochem J* **404:** 459-66.

Zhang, J, Ohta, T, Maruyama, A, Hosoya, T, Nishikawa, K, Maher, JM, Shibahara, S, Itoh, K, Yamamoto, M (2006b). BRG1 interacts with Nrf2 to selectively mediate HO-1 induction in response to oxidative stress. *Mol Cell Biol* **26:** 7942-52.

Zhang, X, Garfinkel, M, Ruden, D (2003b). Phylogenetic conservation of the Nrf2-Keap1 signaling system. In: Forman, HJ (ed). *Signal Transduction by Reactive Oxygen and Nitrogen Species: Pathways and Chemical Principles.* Kluwer Academic Publishers: Secaucus, NJ, USA. pp 256-274.

Zhang, Y (2001). Molecular mechanism of rapid cellular accumulation of anticarcinogenic isothiocyanates. *Carcinogenesis* **22:** 425-31.

Zhang, Y, Talalay, P, Cho, CG, Posner, GH (1992). A major inducer of anticarcinogenic protective enzymes from broccoli: isolation and elucidation of structure. *Proc Natl Acad Sci U S A* **89:** 2399-403.

Zhao, R, Houry, WA (2005). Hsp90: a chaperone for protein folding and gene regulation. *Biochem Cell Biol* **83:** 703-10.

Zhou, S, Chan, E, Duan, W, Huang, M, Chen, YZ (2005). Drug bioactivation, covalent binding to target proteins and toxicity relevance. *Drug Metab Rev* **37:** 41-213.

Zhu, M, Fahl, WE (2001). Functional characterization of transcription regulators that interact with the electrophile response element. *Biochem Biophys Res Commun* **289:** 212-9.

Zipper, LM, Mulcahy, RT (2003). Erk activation is required for Nrf2 nuclear localization during pyrrolidine dithiocarbamate induction of glutamate cysteine ligase modulatory gene expression in HepG2 cells. *Toxicol Sci* **73:** 124-34.

Zipper, LM, Mulcahy, RT (2000). Inhibition of ERK and p38 MAP kinases inhibits binding of Nrf2 and induction of GCS genes. *Biochem Biophys Res Commun* **278:** 484-92.

Zipper, LM, Mulcahy, RT (2002). The Keap1 BTB/POZ dimerization function is required to sequester Nrf2 in cytoplasm. *J Biol Chem* **277:** 36544-52.